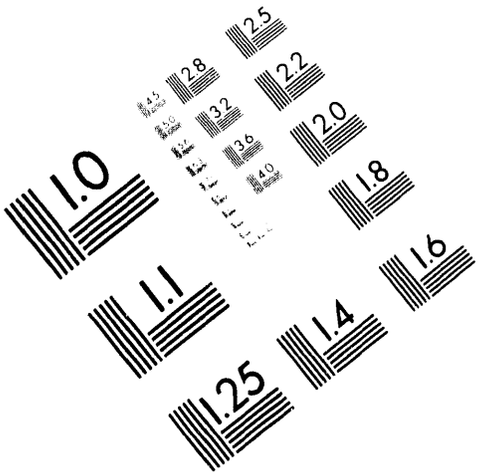
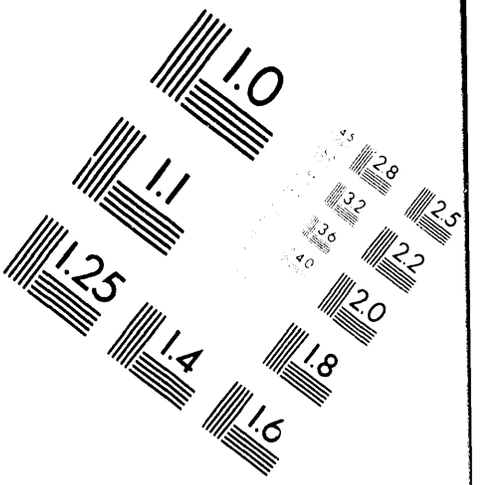


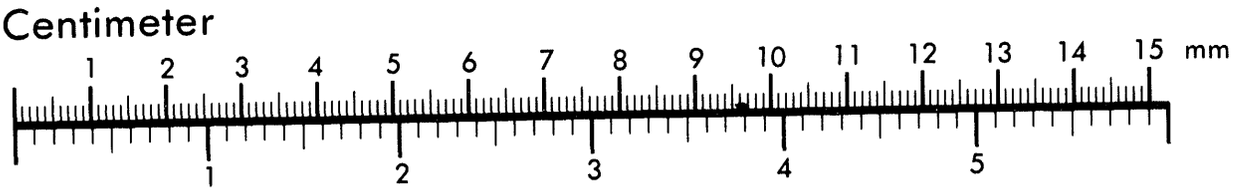


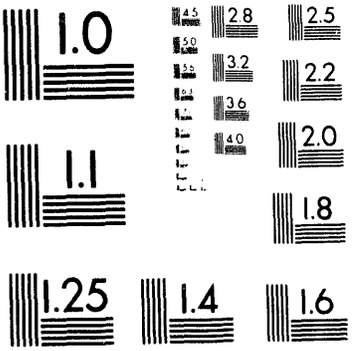
Association for Information and Image Management

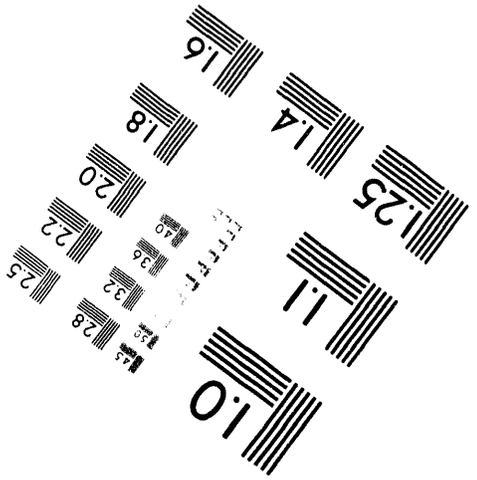
1100 Wayne Avenue, Suite 1100
Silver Spring, Maryland 20910

301/587-8202

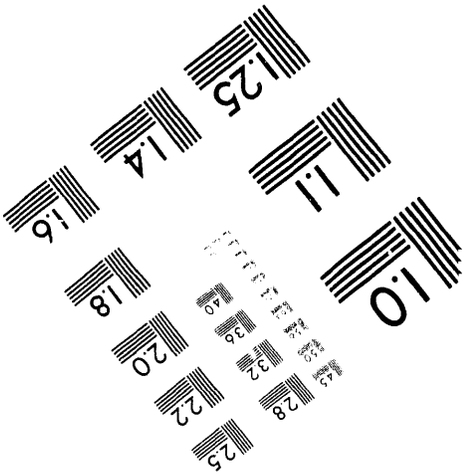








MANUFACTURED TO AIIM STANDARDS
BY APPLIED IMAGE, INC.



1 of 3

DOE/METC-94/1008, Vol. 2
(CONF-9406131)--Vol.2
(DE94012253)
Distribution Category UC-103
UC-106
UC-111

Proceedings of the Coal-Fired Power Systems 94 -- Advances in IGCC and PFBC Review Meeting Volume II

Editors
Heather M. McDaniel
Ronald K. Staubly
Venkat K. Venkataraman

Sponsored by
U.S. Department of Energy
Office of Fossil Energy
Morgantown Energy Technology Center
P.O. Box 880
Morgantown, West Virginia 26507-0880
(304) 291-4764
FAX (304) 291-4403/4469

June 21-23, 1994

MASTER

Contents

Volume I

Session 1 -- Opening Commentaries

1.1 The Role of Advanced Technology in the Future of the Power Generation Industry -- Thomas F. Bechtel 3

1.2 Evolving Utility Business Structure and Impact on New Technology Application -- J. Wayne Leonard 12

Session 2 -- Changes in the Market and Technology Drivers

2.1 Overview of Global Utility Market for Advanced Coal Fired Systems -- Ronald H. Wolk and Neville A. Holt 27

2.2 Overview of the Independent Power Producer (IPP) Market for Advanced Coal-Fired Systems -- Dale R. Simbeck, Stan Vejtasa, and Alan Karp 48

2.3 The Search for Innovative Technology -- C. Lowell Miller 58

Session 3 -- Advanced IGCC Systems

Integrated Gasification Combined Cycle - A View to the Future -- Dale K. Schmidt 61

3.1 IGCC System Studies -- Lawrence K. Rath, George T. Lee, and Patrick H. Le 65

3.2 Transport Reactor Development Status -- Randall E. Rush, Martin O. Fankhanel, and William M. Campbell 73

3.3 Gasification Product Improvement Facility Status -- R. Don Carson, Vijay B. Dixit, Richard S. Sadowski, William H. Skinner, Robert A. Lisauskas, and Stephen A. Johnson 83

Session 4 -- Advanced PFBC Systems

4.1 PFBC System Studies -- Michael E. Reed 93

Contents
(Continued)

4.2 Second-Generation PFBC Systems Research and Development - Phase 2: Circulating PFBC Test Results -- Archie Robertson, James Van Hook, Frank Burkhard, Giovanni Carli, Rich Conn, Paul Crooker, Dave Kulcsar, Chongqing Lu, Anthony Mack, Aydemir Nehrozoglu, Mark Torpey, and Frank Zoldak 104

4.3 Status of the Advanced PFBC at the Power Systems Development Facility -- Randall E. Rush, Darrell L. Moore, Zia Haq, Timothy E. Pinkston, P. Vimalchand, James D. McClung, and Michael T. Quandt 127

Session 5 -- Advanced Filter Systems

5.1 Status of the Morgantown Energy Technology Center's Particulate Cleanup Program: Enabling Technology for Advanced Coal-Based Power Systems -- Richard A. Dennis 141

5.2 Potential Industry Use of Continuous Fiber Ceramic Composites -- Jill Jonkouski 144

5.3 Ceramic Fiber Ceramic Matrix Filter Development -- Roddie R. Judkins, Melvin A. Leitheiser, David P. Stinton, Robert G. Smith, and Edward M. Fischer 145

5.4 Westinghouse Advanced Particle Filter System -- Thomas E. Lippert, Gerald J. Bruck, Zal N. Sanjana, and Richard A. Newby 152

5.5 IF&P Fibrosic™ Filters -- Paul M. Eggerstedt 166

5.6 Multi-Contaminant Control Granular Bed Filter -- Keith B. Wilson, John C. Haas, and Cheryl Anne Olivo 176

5.7 Westinghouse Standleg Moving Granular Bed Filter Development Program -- Richard A. Newby, Wen-Ching Yang, Eugene E. Smeltzer, and Thomas E. Lippert 186

5.8 MTCI Acoustic Agglomeration Particulate Control -- Ravi R. Chandran, Momtaz N. Mansour, Alan W. Scaroni, Gary H. Koopmann, and John L. Loth 195

Contents
(Continued)

Session 6 -- Desulfurization Systems

6.1 METC Hot Gas Desulfurization Program Overview -- Daniel C. Cicero 219

6.2 Integrated Operation of a Pressurized Gasifier, Hot Gas Desulfurization System and Turbine Simulator -- Steve Bevan, David Najewicz, Eli Gal, Anthony H. Furman, Raul Ayala, and Alan Feitelberg 222

6.3 Enviropower Hot Gas Desulfurization Pilot -- Kari Salo, Reza Ghazanfari, Gabor Feher, Jukka Konttinen, Arto Lehtovaara, and Wahab Mojtahedi 236

6.4 Slipstream Testing of the Direct Sulfur Recovery Process -- Santosh K. Gangwal, Jeffrey W. Portzer, Gary B. Howe, Daniel H. Chen, and Michael H. McMillian 246

6.5 METC Fluid-Bed Hot-Gas Desulfurization PDU -- Larry A. Bissett 256

Session 7 -- Turbine Systems

7.1 Development of Topping Combustor for Advanced Concept Pressurized Fluidized Bed Combustion -- William F. Domeracki, Thomas E. Dowdy, and Dennis Bachovchin 265

7.2 Development and Testing of Low Btu Fuel Gas Turbine Combustors -- Stephen Bevan, Nesim Abuaf, Alan S. Feitelberg, Stephen L. Hung, Martin S. Samuels, and Anil K. Tolpadi 280

7.3 Advanced Turbine Systems Program Overview -- Holmes A. Webb 290

Poster Session

P1 High Temperature Electrochemical Separation of H_2S from Coal Gasification Streams -- E. Faith Gleason and Jack Winnick 295

P2 Characterization and Fixed-Bed Testing of a Nickel-Based Hot Gas Desulfurization Sorbent -- Lee D. Gasper-Galvin, James H. Swisher, and Kurt Hammerbeck 308

Contents

(Continued)

P3 Pilot Gasification and Hot Gas Cleanup Operations -- John M. Rockey, Edwin Galloway, Teresa A. Thomson, Jay Rutten, and Alain Lui 321

P4 Coal Ash Behavior in Reducing Environments -- Steven A. Benson, Thomas A. Erickson, David W. Brekke, Bruce C. Folkedahl, James E. Tibbetts, and Jan W. Nowok 322

P5 Hot Coal Gas Desulfurization with Manganese-Based Sorbents -- Malcolm T. Hepworth and Rachid Ben-Slimane 337

P6 A Calcium Oxide Sorbent Process for Bulk Separation of Carbon Dioxide -- Douglas P. Harrison and C. Han 351

P7 COMPCOAL™: A Profitable Process for Production of a Stable High-Btu Fuel from Powder River Basin Coal -- Verne E. Smith and Norm W. Merriam 361

P8 Development of Biological Coal Gasification (MicGAS Process) -- Daman S. Walia and Kailash C. Srivastava 376

P9 Simultaneous Removal of H_2S and NH_3 in Coal Gasification Processes -- K. Jothimurugesan, Adeyinka A. Adeyiga, and Santosh K. Gangwal 398

P10 Granular Filtration in a Fluidized Bed -- J. S. Mei, P. C. Yue, and J. S. Halow 403

P11 Dust Cake Behavior in Filters With High Surface Area to Volume Ratios -- Douglas Straub, Ta-Kuan Chiang, and Richard A. Dennis 405

P12 Computer Simulations of IGCC/PFBC Components -- Edward J. Boyle, Thomas J. O'Brien, Lawrence J. Shadle, Madhava Syamlal, and Suresh Venkatesan 411

P13 Scaling of Pressurized Fluidized Beds -- Susan Guralnik and Leon R. Glicksman 413

P14 Evaluation of Options for CO_2 Capture/Utilization/Disposal -- David K. Schmalzer, Richard D. Doctor, and C. David Livengood 422

P15 Absorption of Hydrogen Sulfide by Zinc Ferrite in the Temperature Range 315 to 538 °C (600 to 1,000 °F) -- Thomas Grindley and C. Elaine Everitt 431

Contents

(Continued)

P16 High Temperature Hydrogen Sulfide Removal with Stannic Oxide -- Michael E. Karpuk, Robert J. Copeland, D. Feinberg, D. Wickham, B. Windecker, and J. Yu 444

P17 Fossil Fuel Conversion - Measurement and Modeling -- Peter R. Solomon, L. Douglas Smoot, Michael A. Serio, David G. Hamblen, B. Scott Brewster, and Predrag T. Radulovic 458

P18 CeraMem Filters for Removal of Particles from Hot Gas Streams -- Bruce A. Bishop and Robert L. Goldsmith 469

P19 Development of Disposable Sorbents for Chloride Removal from High-Temperature Coal-Derived Gases -- Gopala N. Krishnan, B. J. Wood, A. Canizales, R. Gupta, S. D. Sheluker, and R. Ayala 478

P20 PyGas Design Support -- Lawrence J. Shadle, Abolghasem Shamsi, Guo-Qing Zhang, Edward J. Boyle, Yau-Hsin Wang, Madhava Syamlal, and Kalkunte Seshadri 490

P21 Chloride and Mercury Monitors for Air Toxics Measurements -- William H. Buttermore, Glenn A. Norton, Colin D. Chriswell, Dave E. Eckels, and Rachel E. Peters 492

P22 Cooperative Research and Development Agreements at METC -- J. Christopher Ludlow, Lisa A. Jarr, and William F. Lawson 498

P23 Optimal Design and Synthesis of Advanced Power Systems under Uncertainty -- Urmila M. Diwekar, Edward S. Rubin, and H. Christopher Frey 499

P24 Development of a Radio Frequency Surface Contour Mapping System -- William H. Buttermore, Robert J. Weber, and Warren E. Straszheim 513

Contents
(Continued)

Volume II

Session 8a -- Filter Technical Issues

8a.1 Tidd PFBC Hot Gas Filter Operating Experience: July 1993 - April 1994 -- Michael J. Mudd and John D. Hoffman 519

8a.2 Karhula Hot Gas Cleanup Test Results -- Thomas E. Lippert, Gerald J. Bruck, and Juhani Isaksson 535

8a.3 Durability of Ceramic Filters -- Mary Anne Alvin, Richard E. Tressler, Thomas E. Lippert, Edward S. Diaz, and Eugene E. Smeltzer 545

8a.4 Properties of Ceramic Candle Filters -- Duane H. Pontius and H. Stuart Starrett 572

8a.5 Results of Patch Tests -- Duane H. Pontius 575

8a.6 PFBC Dust Cake Studies -- Thomas E. Lippert, Richard A. Newby, Mary Anne Alvin, Dennis M. Bachovchin, and Eugene E. Smeltzer 580

Session 8b -- Hazardous Air Pollutants

8b.1 Comprehensive Assessment of Toxic Emissions From Coal-Fired Power Plants -- Thomas D. Brown 591

8b.2 Trace Element Emissions -- Steven A. Benson, Thomas A. Erickson, Edward N. Steadman, Christopher J. Zygarlicke, William B. Hauserman, and David J. Hassett 592

8b.3 HAP Sampling at Tidd PFBC -- Michael J. Mudd and Patrick A. Dal Porto 607

8b.4 Trace Species Emissions for IGFC -- A. Ed Pigeaud and J. J. Helble 616

8b.5 Hazardous Air Pollutant Sampling for Advanced Power Systems -- Gwen Eklund, Robert G. Wetherold, Al Williams, David P. Maxwell, Robert M. Mann, and Don B. Burrows 627

8b.6 Instrumentation for Trace Emission Measurements -- William P. Chisholm 632

Contents
(Continued)

Session 9a -- Sorbents and Solid Wastes

9a.1 Development of Sorbents for High-Temperature Desulfurization in Moving-Bed Systems -- Raul E. Ayala, Timothy Chuck, Eli Gal, and Raghubir P. Gupta 637

9a.2 Fluidized-Bed Sorbents -- Santosh K. Gangwal and Raghubir P. Gupta 646

9a.3 Fluidization Studies Using Phillips Z-SORB Sorbent -- Santosh K. Gangwal, Raghubir P. Gupta, Gyanesh P. Khare, Gary A. Delzer, and Don H. Kubicek 654

9a.4 Desulfurization Sorbent Development at the Morgantown Energy Technology Center -- Ranjani V. Siriwardane, Ulrich Grimm, James Poston, and Steven Monaco 662

9a.5 Stabilization of Spent Calcium-Based Sorbent -- Philip J. Shires, Satyan Katta, and Gunnar B. Henningsen 668

9a.6 Market Assessment and Technical Feasibility Study of PFBC Ash Use -- Verne E. Smith, Alan E. Bland, Terry H. Brown, Demetri N. Georgiou, and John Wheeldon 679

9a.7 Co-Firing Waste Materials in an Advanced Pressurized Fluidized-Bed Combustor -- Lynn N. Rubow, Michael R. DeLallo, and Roman Zaharchuk ... 690

Session 9b -- Membranes

9b.1 High Temperature Size Selective Membrances -- Stephen F. Yates, S. James Zhou, David J. Anderson, and Alan E. van Til 703

9b.2 A Catalytic Membrane Reactor for Facilitating the Water-Gas Shift Reaction at High Temperature -- David J. Edlund 709

9b.3 New Developments in Hydrogen Permselective Membranes -- George R. Gavalas 714

9b.4 Preparation and Characterization of Composite Membrane for High Temperature Gas Separation -- Shamsuddin Ilias, Franklin G. King, and Nan Su 721

Contents
(Continued)

9b.5 Development of Hollow Fiber Catalytic Membrane Reactors for High Temperature Gas Cleanup -- Y. H. Ma, W. R. Moser, S. Pien, and A. B. Shelekhin 727

9b.6 Thermal/Chemical Degradation of Inorganic Membrane Materials -- Gopala N. Krishnan, Angel Sanjurjo, Ashok S. Damle, Bernard J. Wood, and Kai-Hung Lau 736

Appendices

Appendix A. Agenda 747

Appendix B. Meeting Participants 758

Appendix C. METC Participants 774

Session 8a

Filter Technical Issues

8a.1 Tidd PFBC Hot Gas Filter Operating Experience: July 1993 - April 1994

CONTRACT INFORMATION

Contract Number DE-FC21-89MC26042

Contractor

Ohio Power Company
c/o American Electric Power Service Corporation
1 Riverside Plaza
Columbus, Ohio 43215
(614)223-1585

Contractor Project Manager Michael J. Mudd

Principal Investigator John D. Hoffman

METC Project Manager Richard A. Dennis

Period of Performance August 2, 1989 to June 30, 1995

Schedule and Milestones

Program Schedule

	FY1990	FY1991	FY1992	FY1993	FY1994	FY1995
	1 2 3 4	1 2 3 4	1 2 3 4	1 2 3 4	1 2 3 4	1 2 3 4
Design Specification/ APF Procurement	———					
Detailed Design	———	———				
Test Plan		———				
Hardware Procurement	———	———	———			
Testing			———	———	———	
Data Analysis			———	———	———	

OBJECTIVES

The objective of this program is to evaluate the design and obtain operating experience for up to two Advanced Particle Filter (APF) systems through long-term testing on a slipstream at Ohio Power Company's Tidd Pressurized Fluidized Bed Combustion (PFBC) Demonstration Plant. Performance and reliability of commercial-scale filter modules will be monitored to aid in an assessment of the readiness and economic viability of this technology for commercial PFBC applications.

BACKGROUND INFORMATION

The 70 MWe Tidd PFBC Demonstration Plant in Brilliant, Ohio was completed in late 1990, and is currently in a four-year test program as part of the Department of Energy's (DOE) Clean Coal Technology Program. Provisions were included as part of the original design to install a slipstream on the PFBC exhaust gases between the fluidized bed and the gas turbine to test an APF system. In November 1988, AEP submitted a proposal to the DOE for the HGCU Program, and in August 1989, a cooperative agreement was signed. In July 1990, AEP awarded a contract to Westinghouse Science and Technology Center to provide a candle-based APF. Installation of the slipstream began in December 1991, and the filter was commissioned in October 1992. Since then, over 3,000 hours of operating time have been logged on the filter.

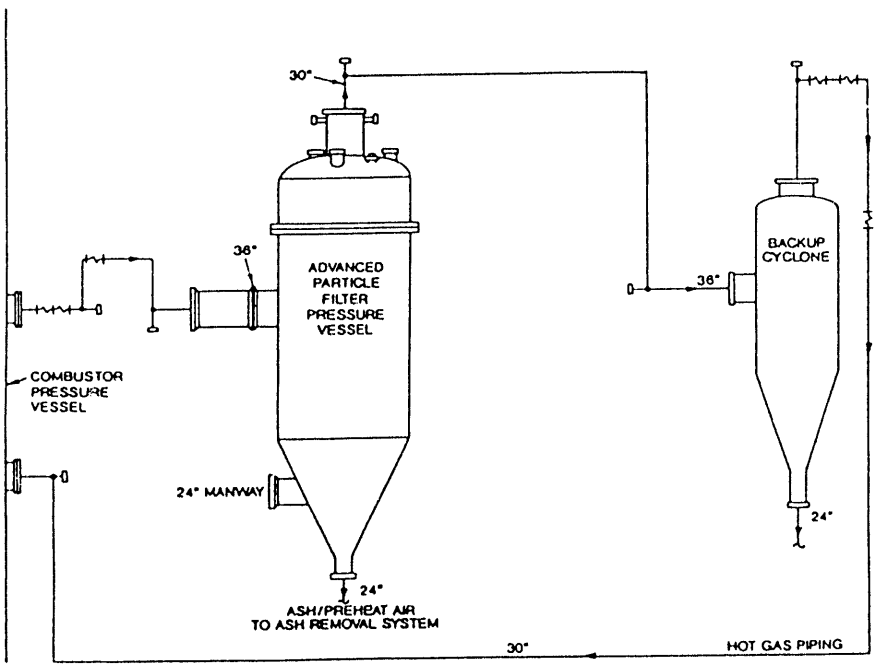


Figure 1. HGCU System Schematic

PROJECT DESCRIPTION

System Design

In the original design, the Tidd PFBC Demonstration Plant utilized seven strings of primary and secondary cyclones to remove 98% of the particulate matter from the gases between the fluidized bed and the gas turbine. The HGCU slipstream replaces one of the seven secondary cyclones by taking the discharge gas of one of the primary cyclones to outside of the combustor vessel and into the APF. After passing through the APF the gas flows through a backup cyclone, and then returns to the combustor vessel, where the slipstream flow rejoins the combustor gas at the discharge of the other six cyclone strings.

Figure 1 provides a simplified schematic of the APF system, and Figure 2 shows an isometric view of the system.

At maximum load conditions, gas at approximately 150 psig, 1550F flows into the filter at 7600 acfm with a dust loading of approximately 600 ppmw. (In January, 1994, the dust loading to the filter was increased from approximately 600 ppmw to 3400 ppmw by detuning the primary cyclone upstream of the APF.) Ash collected in the APF is discharged to a screw cooler and into lockhoppers which feed a vacuum pneumatic ash transport system. A backup cyclone downstream of the filter is installed to clean the gas in case of a filter malfunction, and to balance the pressure drop of the slipstream with the other six cyclone strings.

Table I provides the design basis of the APF system.

Table I
APF Design Basis

Maximum Temperature	1670F
Operating Temperature	1550F
Operating Pressure	164 psia
Gas Flow Rate	100,700 lb/hr
Inlet Dust Loading	500 - 5,000 ppmw
Outlet Dust Loading	<15 ppm
Average Particle Size	1.5 microns
Temperature Drop	5F
Pressure Drop	3 psi
Face Velocity	7.1 ft/min

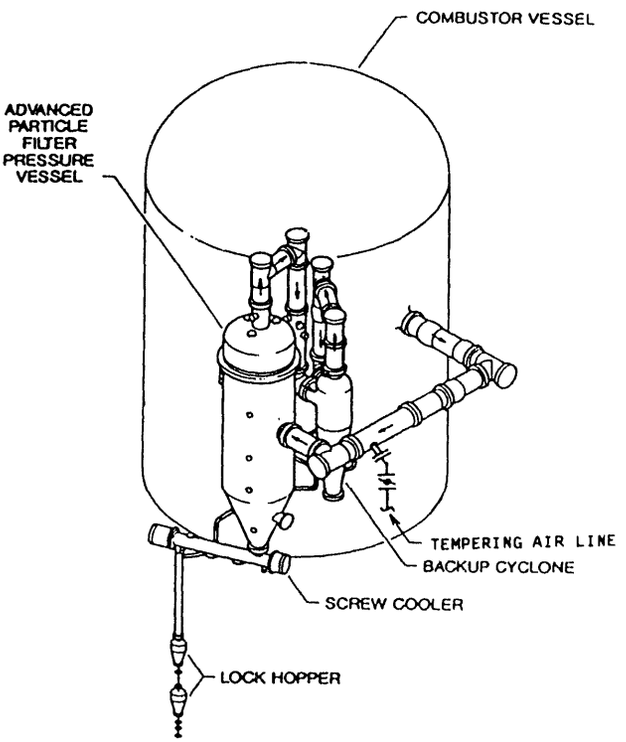


Figure 2. Isometric View of HGCU System

Filter Vessel

The filter vessel is 10 ft. in diameter and 44 ft. long. It is internally insulated with alumina-silica ceramic insulation, with an internal 310 stainless steel liner to protect the insulation from erosion. The hot gas enters the side of the vessel radially, flows through the candle elements, through the tubesheet, and exits from the top of the vessel head. The exterior of the APF vessel is not insulated, and is coated with temperature sensitive paint to indicate hot spots.

Filter Internals

The filter, shown in Figure 3, contains 384 candle filter elements, arranged in three clusters, spaced 120 degrees apart. Each cluster holds three plenums, each arranged vertically, with 38 candles in each of the upper and middle plenums, and 52 candles in each of the lower plenums. The candles are attached to the tubesheets in each plenum by bolted collars and high temperature gaskets.

The candles are Schumacher Dia-Schumalith F40 candles consisting of a clay-bonded sintered silicon carbide support matrix that is coated by an aluminosilicate fibrous membrane. Each candle is 2.36 in. OD and 4.92 ft. long.

The 2-in. thick tubesheet is made of RA-333 alloy, and is supported from an inverted "V" expansion cone.

Backpulse System

The backpulse system receives high pressure backpulse air from a reciprocating compressor rated at 282 scfm and 1500 psig. The air discharges from the compressor to an air dryer, and to a primary air accumulator. The air is then directed to a backpulse skid installed near

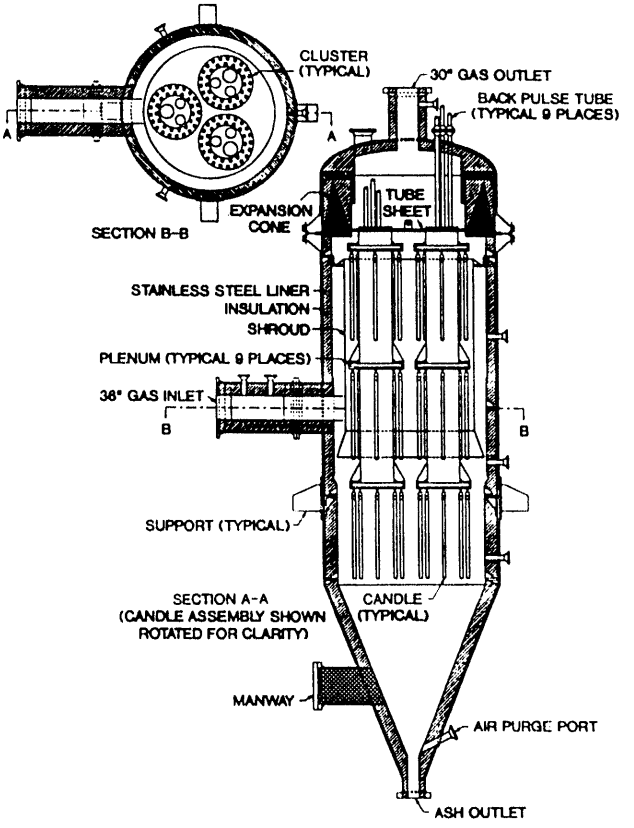


Figure 3. APF Candle Arrangement

the APF, which is comprised of secondary accumulators and the backpulse valves. The backpulse valves are fast acting (200 to 700 msec stroke time) 2-inch pilot-operated Atkomatic solenoid valves. There are three strings of backpulse valves, with redundant valves on each string.

RESULTS

The Tidd Hot Gas Filter was commissioned on coal fire on October 28, 1992. Table II presents operating statistics through April, 1994. There have been three distinct test periods since initial operation, as summarized in Table II. The results of Test Period I have been

documented in Reference 1, and will not be discussed in this paper. The results of Test Periods II and III are discussed below and summarized in Table III.

Table II
Tidd HGCU Test Periods

Test Period	I	II	III
Date	10/92-12/92	6/93-9/93	1/94-4/94
No. of Runs	4	7	7
Test Period Total Hours	464	1295	1279
Longest Run, Hours	286	597	444

Test Period II: 6/93 - 9/93

Test Runs 5 and 6 - 6/30 to 7/5/93

The unit was operated for 60 hours on coal fire during Run 5, and 17 hours during Run 6. While burning Pittsburgh No. 8 coal and Plum Run Greenfield dolomite, the unit achieved a maximum load during Run 5 of 53 MW and 116-inch bed level resulting in an APF gas temperature of approximately 1400F. The APF differential pressures (DPs) remained stable during these runs and reached a maximum of 90 inches at 1400F gas temperature. (NOTE: All DP's are expressed in inches of water.)

Test Run 7 - 7/18 to 8/5/93

The unit was operated for 426 hours on coal fire burning Pittsburgh No. 8 coal and Plum Run Greenfield dolomite. PFBC performance tests were conducted at 95-inch and 80-inch bed levels and at 85%, 90%, and 95% sulfur retention. Due to problems with gas turbine vibration, the maximum unit load obtained was 46 MW at 110-inch bed level resulting in 1350F APF gas temperature.

Most of the operating time during this run was at 80-inch bed level and 1150F gas temperature. During these operating conditions, the APF DPs were stable at approximately 60-inches trigger and 50-inches baseline. The maximum DP obtained during this run was 105 inches during an excursion at 100-inch bed level and 1250F gas temperature.

The unit was shut down on 8/5 due to ash buildup in the APF hopper that was approaching levels up to the candles. Following shutdown, an inspection revealed three to four inches of ash buildup in areas on the hopper walls. Additionally, a large amount of ash fell off the hopper walls during unit shutdown. Prior to this test series, a pneumatic vibrator was installed in the APF vessel manway and linked to the hopper liner in an effort to keep ash from accumulating on the wall of the hopper. The vibrator, however, did not prove to be effective. Therefore, it was replaced with a larger single impactor-type pneumatic vibrator following this run.

Post-test inspection revealed a small amount of ash buildup on the candles; however, there was no splotching. In general, the candles appeared to be in good shape.

Test Runs 8 and 9 - 8/9 to 8/14/93

During most of the run the unit was operated at 115-inch bed level resulting in 1400 and 1450F APF gas temperatures. The APF DPs were unstable at this load. The trigger DP increased from 90 inches on the afternoon of 8/11 to 150 inches on the morning of 8/14. On 8/12, the backpulse pressure was increased

Table III
Summary of HGCU Operation - Test Periods II and III

	Operating Hours	Cumulative Hours	Operating Temp.	Pressure Drop	Inspection Observations
Test Period II					
Run 5 & 6	75	541	<1400°F	Stable	• No filter issues
Run 7	426	967	1150°-1350°F	Stable	• No filter issues
Run 8 & 9	80	1047	1450°F	Increasing Δp, Pulse pressure increased from 800 to 1000 to 1200 psig	• Patchy cleaning • No ash bridging
Run 10	116	1163	1450°F	Slowly increasing Δp, pulse pressure at 1200 psig	• Patchy cleaning • No ash bridging
Run 11	597	1759	1450°F 1200°F	Increasing Δp Δp = 240 in. wg Stable Δp	• Outlet dust first detected (after 300 hours) • Significant ash bridging, failed candles
Test Period III					
Run 12	19	1778	1300°-1400°F	Stable	—
Run 13	333	2111	1300°-1400°F	Stable	• Uniform residual ash cake • No failures • Ash accumlated on dust sheds
Run 14	23	2134	1200°-1300°F	Stable	—
Run 15	151	2285	1250°-1370°F	Stable	--
Run 16	145	2430	1350°-1400°F	Stable	—
Run 17	164	2594	1300°-1425°F	Gas flow rate decreased during run	• Ash cake about 1/4" thick • No failures • Ash accumlation on sheds
Run 18	444	3038	1350°-1450°F	Baseline Δp increased ≈ 20 in. wg	• 28 broken candles • Inner rows of top and middle plenums heavily bridged

from 800 to 1000 psig. On 8/13, the tank pressure was increased to 1200 psig and the backpulsing time interval was increased from 30 minutes to 60 minutes. Prior to the unit trip on 8/14, the APF DP reached 150 inches trigger and 115 inches baseline.

Test Run 10 - 8/19 to 8/24/93

The unit was operated for 116 hours burning Pittsburgh No. 8 coal. The unit was started up using Plum Run Greenfield dolomite, and on 8/24 sorbent feed was switched to Delaware limestone. The unit was shut down 13 hours later due to unstable bed and evaporator conditions experienced while burning limestone. Sulfur retention was maintained at 95% from start-up through the morning of 8/22 and then at 90% for the remainder of the run. The unit was operated at 115-inch bed level and 1450F APF gas temperature for most of the run. The maximum unit load was 52 MW at the conditions stated above.

During operation at 115-inch bed level and 1450F gas temperature, the APF DPs were somewhat unstable; however, not as severe as in Run 9. The trigger DP increased from 95 inches on 8/21 to 115-inches on 8/24, while backpulsing at 1200 psig. When sorbent feed was switched over to Delaware limestone, the baseline DP increased from 90 to 100 inches while the trigger DP remained fairly constant.

Post-test inspection revealed splotchy areas of ash buildup on the candles. The candles were backpulsed during unit shutdown with little success in removing the ash buildup. The APF hopper walls also had areas of ash buildup.

Test Run 11 - 8/29 to 9/23/93

The unit was operated for 597 hours burning Pittsburgh No. 8 coal. The maximum unit load achieved during this run was 55 MW at 125-inch bed level, resulting in an APF gas temperature of 1500F. During start up while increasing load to 115-inch bed level and 1450F gas temperature, sorbent fines (Plum Run Greenfield dolomite, 100% less than 75 microns) were added to the coal water paste while reducing the pneumatic sorbent feed rate by approximately 50%. During this time period the APF DPs started to increase at a rate greater than had been experienced during previous load increases. While at temperatures over 1400F, the APF trigger DP increased from 100 to 168 inches over a period of two days. The baseline DP increased from 84 to 154 inches during this same time period. It is unknown whether this increase in DPs was due to the sorbent fines or whether it was a more aggressive deterioration of APF performance (due to some other phenomenon) than what had been experienced previously at temperatures above 1400F.

On 9/9, the APF trigger DP reached 250 inches, at which time it was decided to reduce unit load to 50-inch bed level, 1000F gas temperature to backpulse the APF. The APF DP was reduced to 145 inches by load reduction and dropped to 36 inches after minimum load backpulsing. However after unit load was brought back to 115-inch bed level, 1450F gas temperature, the APF trigger DP reached a level of 250 inches in less than two days. Load was reduced to 80-inch bed level, 1200F gas temperature to maintain DPs within acceptable limits.

On 9/12 and again on 9/13, indications of candle breaks were noticed by a sudden decrease in APF DP (by approximately 10 inches) and a sudden increase in individual plenum gas flow which occurred simultaneously while backpulsing. Later on 9/13, fragments of broken candles were recovered from the ash removal system. The total fragments recovered could not positively account for more than one

candle. Figure 4 shows a graph of filter pressure drop and temperature for the entire run. The unit was removed from service on 9/23 due to a leak in the sorbent transport pipe caused by erosion.

Post-Test Inspection and Modifications

The APF internals were inspected through instrument nozzles and the manway nozzle on 9/27 and 9/28. During this inspection approximately 24 candles were observed to be broken. The ash hopper was filled with ash and broken candles to a level approximately 6 to 12 inches above the manway nozzle.

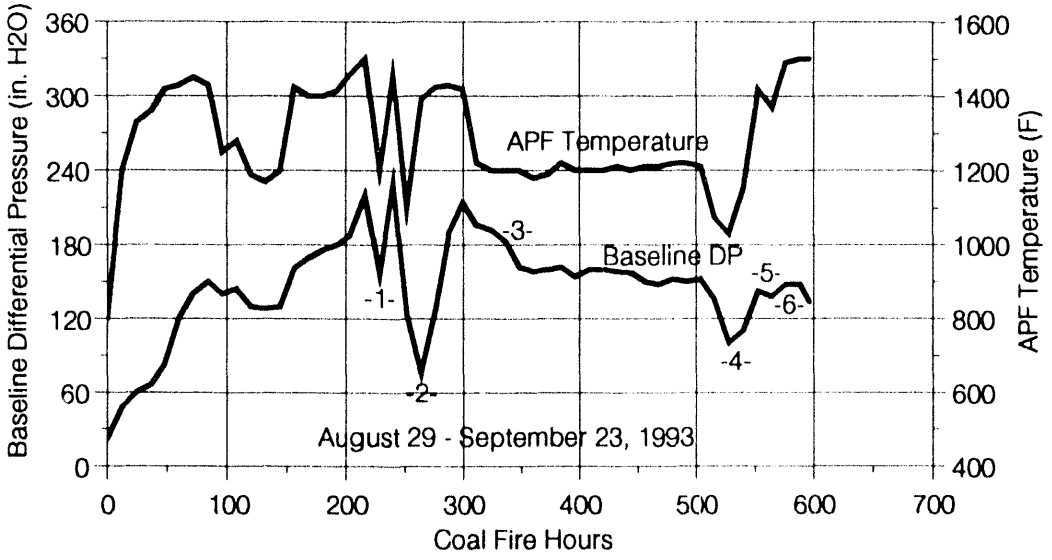
On 9/30, the APF internals were removed from the APF. Upon inspection, 62 candles were found to be broken. Approximately three candles were broken during removal from the APF vessel. The following table shows a summary of the location of the broken candles.

Location of Broken Candles
September 1993

	Plenum A	Plenum B	Plenum C
Top	3	1	2
Middle	6	24	5
Bottom	0	1	20

Very heavy ash bridging was apparent between candles and between candles and support pipes. The deposits were very hard and difficult to break into smaller pieces. Many candles were also found to be bowed. During subsequent cleaning of the ash deposits from the candles, approximately 40 more candles broke.

Two surveillance candles were recovered by Westinghouse and tested for remaining hot strength. One candle from the original set, which had been exposed to operating conditions for 1,759 hours, exhibited a 37 percent loss of



1. Reduced load.
2. Reduced load.
3. Candle breaks.
4. Reduced load.
5. Spoiling air on.
6. Candle breaks.

Figure 4. Filter DP and Temperature - Test Run 11

its original strength. The second candle, which had been installed in December 1992 and had experienced 1,295 hours of operation, had lost 51 percent of its strength.

All filter candles were replaced with new silicon carbide candles between Test Series II and III, except for nine surveillance candles which were reused.

The backpulse solenoid valves exhibited random failures to actuate during these tests. In all cases, the backup valve functioned properly. Following Test Period II, the backpulse solenoid valves were inspected and found to be galled on both the piston and cylinder walls. The valve pistons were Stellite coated and the valve body bores were nickel-boron plated to improve resistance to galling. Following these modifications, the valves successfully underwent accelerated cycle testing to verify the design. Operation of the valves during Test Period III was much improved, and subsequent inspections revealed no galling.

At the end of Test Period II, one backpulse tube was cut up and examined for degradation. Microcracking was evident on the inside surface of the tube, with cracks as deep as 0.020". Based on this observation it was decided to replace the Incoloy 800HT material with Haynes 230 alloy, which has better resistance to thermal fatigue. The new backpulse tubes were fabricated and installed prior to the start of Test Period III.

Between Test Series II and III, nine additional air purge nozzles were installed on the APF hopper to facilitate the removal of ash accumulation in the hopper. The hopper vibrator was moved from inside the APF nozzle to outside the nozzle because it proved to be unreliable inside the nozzle. It was mechanically linked to the hopper liner.

In an effort to improve the filter performance, it was decided to install a system to detune the primary cyclone upstream of the filter. It was believed that the resulting coarser ash would be easier to remove from the filter candles and less likely to accumulate on the hopper walls. An air line was connected to the dip leg of the cyclone and a valve was installed external to the combustor to allow the detuning air to be controlled. Air injected into the dip leg created on upward velocity and thereby detuned the cyclone. All testing during Test Period III was conducted with the cyclone detuned.

It was noted in previous runs that the filter DP sometimes became unstable at gas temperatures over 1400F. To prevent limiting the load on the unit because of the 1400F limit, a tempering air line was installed upstream of the filter which allowed 580F process air at a slightly higher pressure to be mixed with the gas and thereby reduce the gas temperature by as much as 150F.

Test Period III: 1/94 - 4/94

Test Run 12 - 1/10 to 1/11/94

This test run was terminated after 19 hours of coal fire when several primary cyclones became plugged. Due to the brevity of this run and lack of steady state operation near design conditions, it will not be discussed further.

Test Run 13 - 1/15 to 1/29/94

The unit was operated for 333 hours on coal fire burning Pittsburgh No. 8 coal and Plum Run Greenfield dolomite. The primary objective of this run was to assess the performance of the APF while operating with the primary cyclone ahead of the filter detuned to produce a coarser ash and higher ash

loading. The tempering air system was commissioned during this run and functioned without any problems.

During the run ash sampling was performed upstream and downstream of the APF using specially designed sampling probes. The results showed that by detuning the primary cyclone, the ash loading to the filter increased from a design value of 600 ppmw to about 3400 ppmw, and the mean particle size of the ash increased from about 3 to 7 microns. The higher ash concentration resulted in significantly higher ash loading. Despite the higher ash loading, the filter performed very well.

Figure 5 shows a graph of filter pressure drop and temperature for Run 13. The unit load was reduced at about 200 and 250 hours into the run due to bed sintering problems, which accounts for the dips in temperature and DP during these periods. During the remaining periods of this run, the filter pressure drop remained stable and exhibited the usual trend of following gas temperature. During the last 50 to 75 hours of the run, the unit bed height was increased to the maximum (142 inches) and the filter DP increased somewhat due to higher gas flow and dust loading.

Following shutdown of the unit, the filter was inspected via nine 3-in. nozzles on the side of the vessel. In general the candles looked in good condition with very little residual ash accumulation. However, some ash bridging was seen between the bottoms of the inner rows of candles and the dust sheds on the plenum support pipes.

Test Run 14 - 2/17 to 2/18/94

This test run was terminated after 23 hours of coal fire when a 1" nipple on the HGCU piping developed a leak that could not be repaired in service.

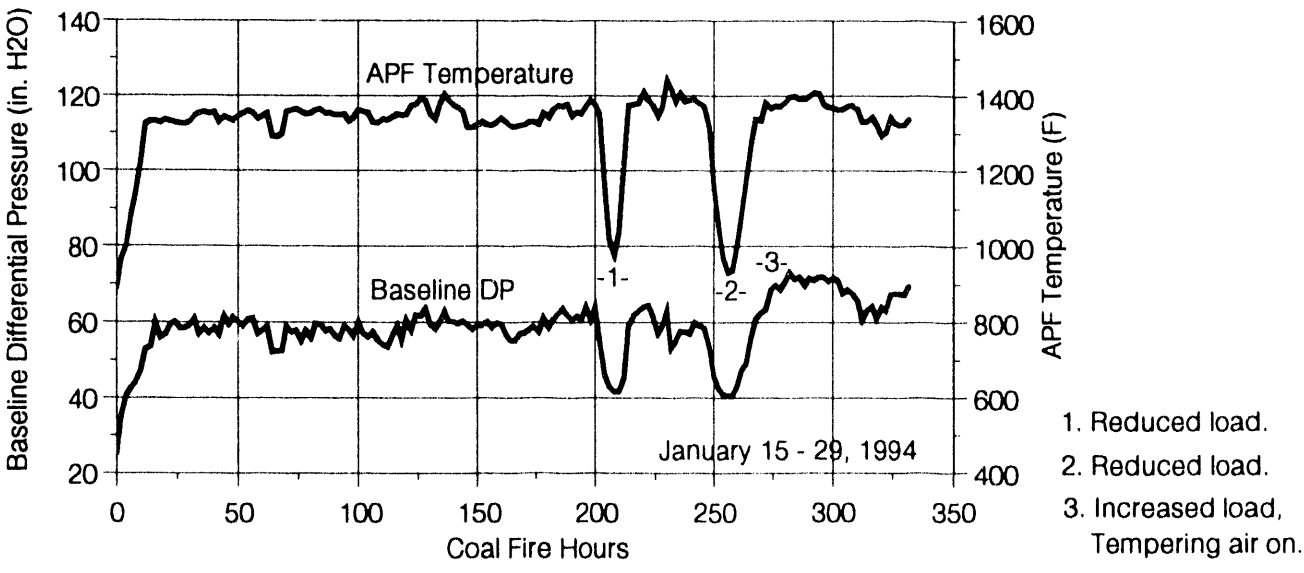


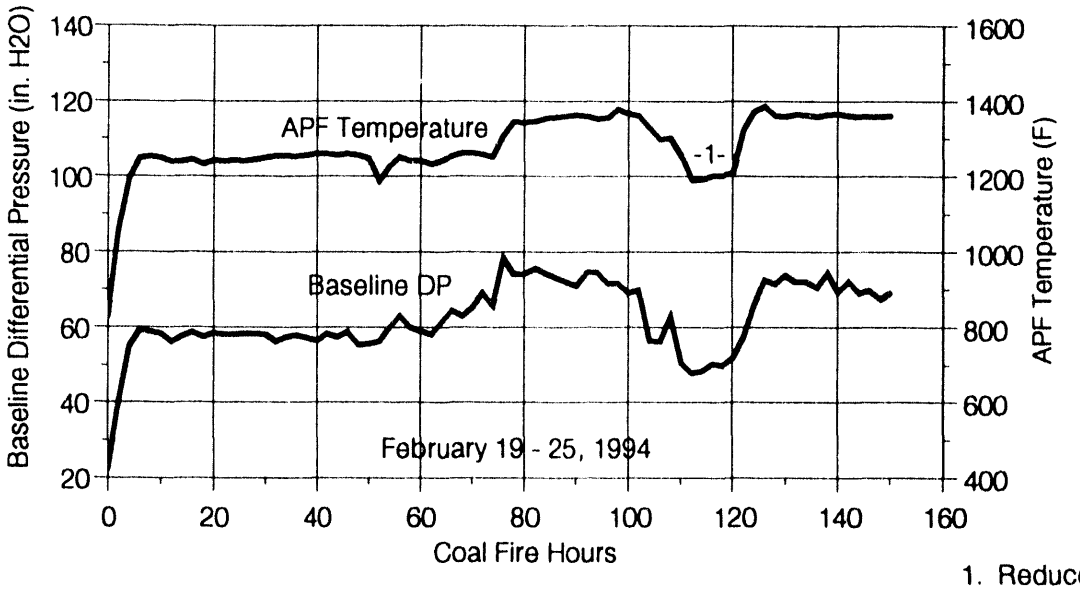
Figure 5. Filter DP and Temperature - Test Run 13

Test Run 15 - 2/19 to 2/25/94

This run was a hot restart of the previous run. The APF performed without any major problems during this run. Some minor problems, however, arose. Shortly after start-up, the APF dome exhibited elevated temperatures (up to 730F) near the gas outlet nozzle. The gas temperature was held to the 1250F range in order to keep the hot areas below 750F. On 2/21 an on-line repair was successfully made which reduced the hot areas to below 300F in some areas and to below 400F in others. The repair involved drilling and tapping three 1/4" holes in the outlet nozzle near the head and pumping in 45 gallons of pumpable insulation. Following this repair, the unit was brought up to full bed height (142 inches). Tempering air was again used to limit the gas temperature in the APF to 1400F. Figure 6 shows a graph of APF DP and temperature versus time for this run. The unit load was reduced about 110 hours into the run when a coal paste pump stopped working. After the bed again stabilized, the unit was returned to full load. The HGCU system functioned without further problems from this point until the unit tripped due to loss of the sorbent booster compressor.

Test Run 16 - 3/3 to 3/9/94

Most of this test run was conducted at 142 and 150-inch bed levels. As in the previous run, tempering air was used to limit the filter gas temperature to 1400F. This run was the smoothest so far the HGCU system. The system operated for over 145 hours without any major problems. Figure 7 shows a plot of APF DP and temperature during Run 16. Figure 8 shows DP and flowrate. The APF DP exhibited a gradual decline throughout this run. The reason for this is unknown. The test conditions throughout Run 16 were the most steady of all the runs. Therefore, data from this run should be considered a good baseline reference for APF operation at 1400F. This run was termin-



1. Reduced load.

Figure 6. Filter DP and Temperature - Test Run 15

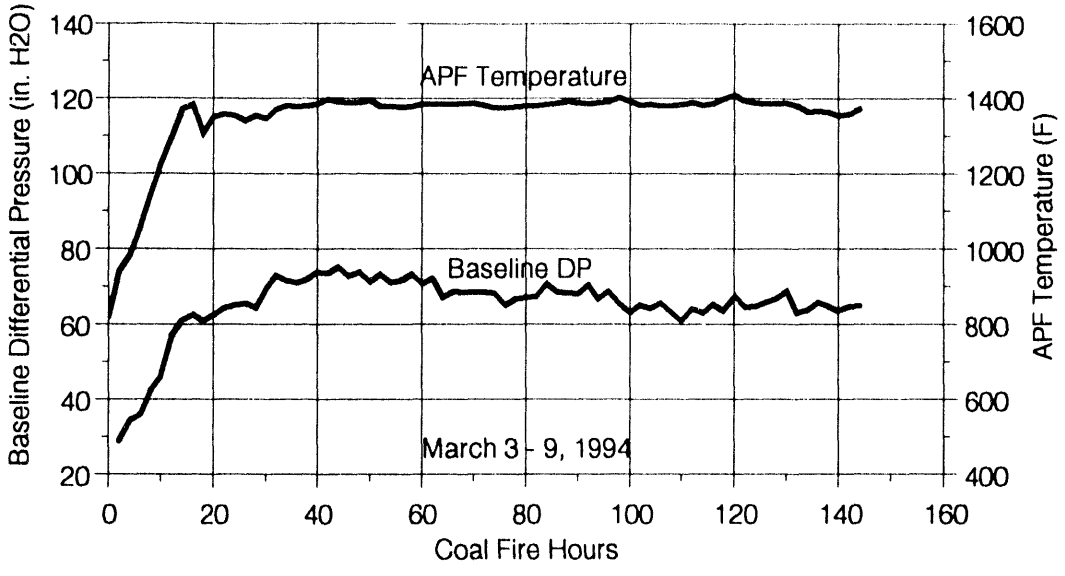


Figure 7. Filter DP and Temperature - Test Run 16

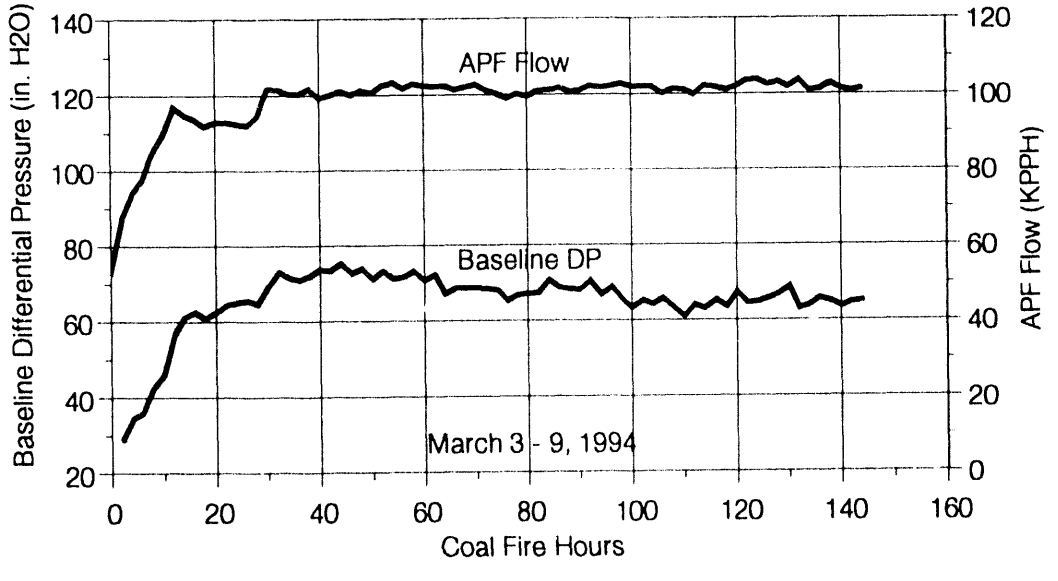


Figure 8. Filter DP and Flow - Test Run 16

ated when the unit tripped due to the loss of two coal paste pumps.

Test Run 17 - 3/16 to 3/23/94

This was another relatively uneventful run on the HGCU system. The unit operated for approximately 164 hours on coal fire. Most of the run was conducted at 128-inch bed level, with portions at 142-inch and 115-inch. Due to bed sintering problems, the bed level could not be maintained at 142 inches. The tempering air was turned off during this run which allowed the APF to operate up to 1450F. The filter pressure differential was relatively stable throughout the run as shown in Figures 9 and 10. However, the gas flowrate through the filter decreased throughout the run. During this run additonal insulation was pumped into the APF head to lower the surface temperature in one area from 550F to 400F. The unit tripped due to a low oil pressure indication on the gas turbine.

The APF internals were inspected through the nine instrument nozzles following Test Run 17. No broken candles were observed. The residual ash layer on the candles was somewhat thicker than seen following Test Run 13 and appeared to be about 1/8" to 1/4" thick. The ash coating was uniform from candle to candle but also very rough looking on all the candles. The ash bridging previously seen between the dust sheds and the inner rows of candles was still evident, but not obviously worse than before. The amount of ash accumulation on the dust sheds varied considerably (1/2" to 4") among the six dust sheds. No candle-to-candle bridging was seen.

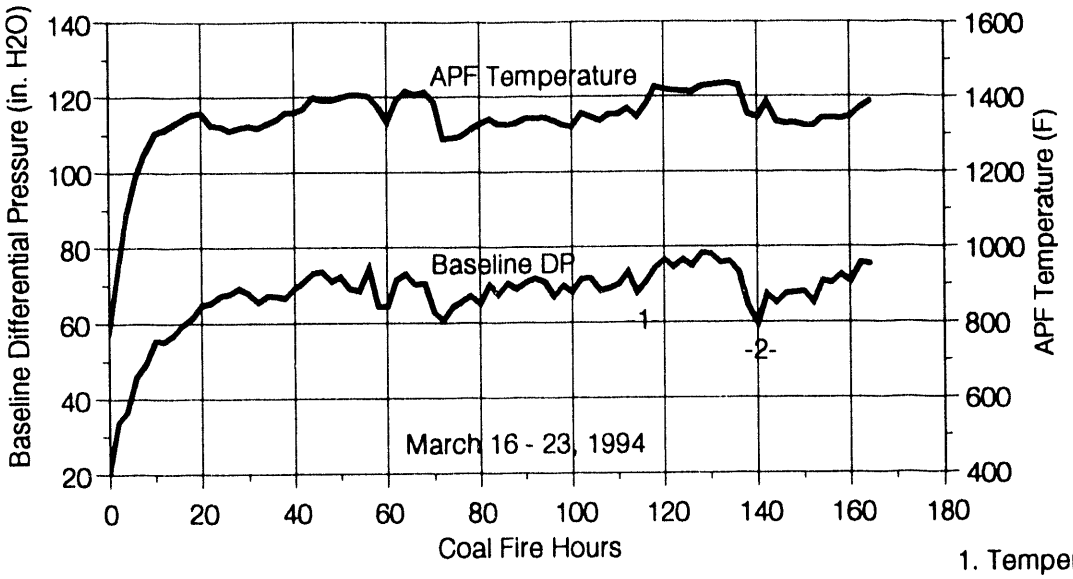
Test Run 18 - 3/31 to 4/18/94

This was the longest run of this test period with almost 444 hours of coal fire. The bed height during most of the run was 115 inches and the APF temperature was generally in the 1350 to 1400F range. The temperature was approximately 1450F for about 30 hours of the run. Due to a corroded instrument tube, flowrate data were not obtained during this run. Hazardous air pollutant sampling was conducted during this run. No major problems arose with the APF during this test. The baseline pressure differential increased during this run from about 70 to 90 inches as shown in Figure 11. This was the first run of this test series in which the DP increased noticeably from the beginning to the end of the run.

As part of Hazardous Air Pollutant testing, SO_2 data were obtained upstream and downstream of the APF. Preliminary results indicated that the SO_2 level in the gas was reduced approximately 45% by the APF. Post-test analysis of ash samples retrieved from the APF and precipitator hoppers confirmed this observation. The percent sulfation (calculated as moles of SO_3/ moles of CaO) of the APF hopper ash was 78.6% as compared to 50.0% for ash that did not pass through to APF sampled from the precipitator hopper. Additional data will be obtained in future tests to confirm these results.

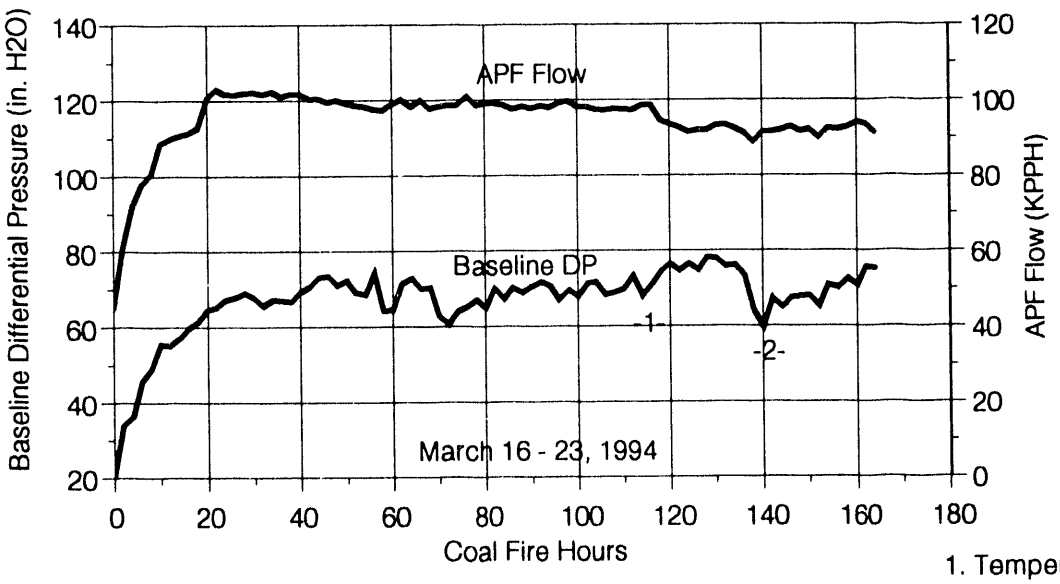
Post-Test Inspection and Modifications

The APF internals were inspected via the instrument ports after this run. The filter candles had a thin layer (about 1/8") of residual ash, however broken candles were observed during this inspection. The filter internals were removed from the APF vessel on 5/5/94 and a more detailed inspection was performed. A total of 28 broken candles were found at the following locations:



1. Tempering air off.
2. Reduced load.

Figure 9. Filter DP and Temperature - Test Run 17



1. Tempering air off.
2. Reduced load.

Figure 10. Filter DP and Flow - Test Run 17

Location of Broken Candles
May 1994

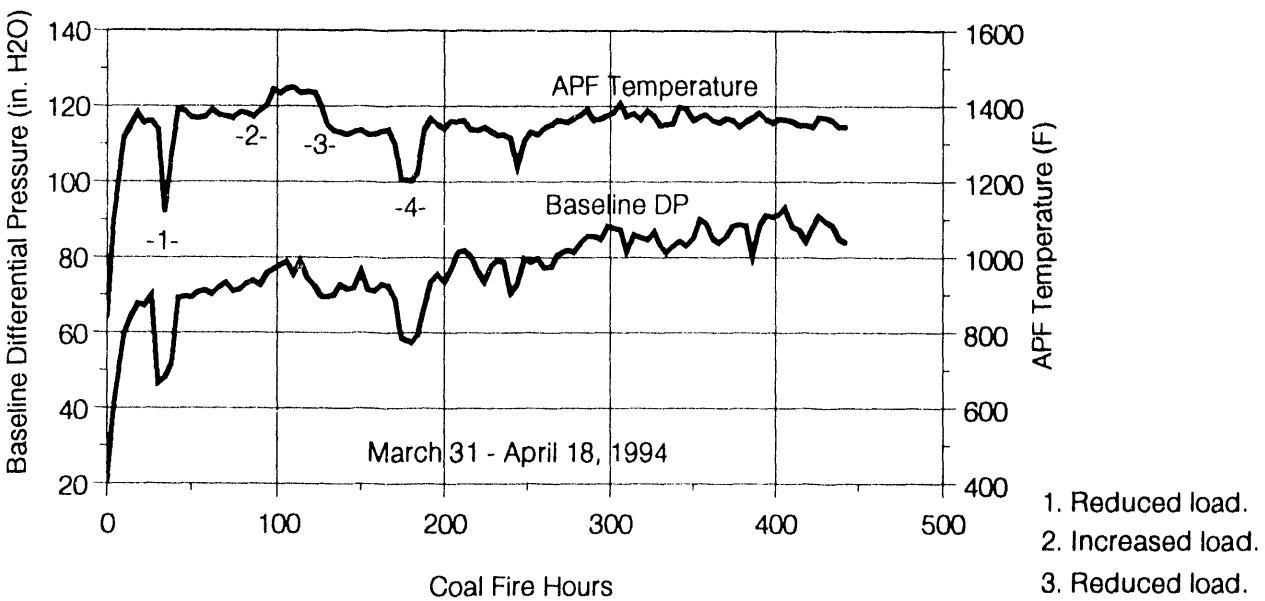
	Plenum A	Plenum B	Plenum C
Top	7	7	2
Middle	0	2	8
Bottom	0	2	0

The two breaks in the bottom plenum are believed to have occurred during removal of the filter internals from the filter housing. Very heavy ash bridging was observed between the inner rows of candles and the support pipe on the top and middle plenums. The ash build-up extended over the entire length of the inner candles. In some cases the ash bridging extended into the outer rows of candles. Many of the inner candles were bowed outward and in some cases almost contacted the candles in the outer row. All of the candle breaks except one appeared to be fresh breaks judging from the clean fracture surfaces. All of the breaks occurred at the top of the candle just below the candle holder. The breaks appeared to result from bending forces from ash bridging from the inner candles to the outer candles. Only one break was in an inner row; the remainder were in outer rows.

The outlet side of the filter internals were very clean with virtually no ash deposits. This is further indication that the failures occurred during or after plant shutdown, and that the filter was not leaking ash to the clean side during operation.

FUTURE WORK

At the end of April the system was out of service and plans were being formulated for modifications and future testing. It is planned to remove the inner rows of candles from the



1. Reduced load.
2. Increased load.
3. Reduced load.
4. Reduced load.

Figure 11. Filter DP and Temperature - Test Run 18

top and middle plenums since the ash bridging phenomenon appeared to begin with ash building up on the dust sheds and bridging across to the bottoms of the inner candles. It is hoped that the removal of the inner rows of candles will eliminate this problem. In addition, plans are being implemented to modify the primary cyclone ahead of the filter so it can be rendered totally inactive. This will increase the ash loading and mean particle size to the filter and thereby improve the flowability of the ash. During this shutdown some alternate filter candle materials will be installed to expose them to the Tidd PFBC service conditions.

Assuming that these modifications are successful in overcoming the ash bridging problem, the sytem will be operated until the fall of 1994 with the current silicon carbide candles and selected alternate candles. The condition of the alternate materials will be assessed when the filter is re-opened in the fall of 1994. At that time, a decision will be made as to what filter materials will be installed for the final phase of testing which will run until February, 1995.

REFERENCES

1. Hoffman, J. D. and M. J. Mudd, 1993. Initial Operation of the Tidd PFBC Hot Gas Clean Up Filter, pp. 483-495, Proceedings of the Coal-Fired Power Systems 93 - Advances In IGCC and PFBC Review Meeting, Morgantown, WV, June 28-30, 1993, DOE/METC-9316131 (DE93000289).

2. Mudd, M. J. and Hoffman, J. D., 1993. Operating Data from the Tidd Hot Gas Clean Up Program, Proceedings of the 12th International Conference on Fluidized Bed Combustion, San Diego, CA, May 1993, (American Society of Mechanical Engineers).

3. Dennis, R. A., Lippert, T. E., Bruck, G. J., Alvin, M.A., and Mudd, M. J., 1993. Initial Test Results from the Department of Energy's Pressurized Bed Combustion Hot Gas Clean Up Program, Presented at the Tenth Particulate Control Symposium and Fifth International Conference on Electrostatic Precipitation, Washington D.C., April 5-8, 1993, Sponsored by EPRI and the International Society for Electrostatic Precipitation.

4. Mudd, M. J. and Hoffman, J. D., 1992. Initial Operation of the Tidd PFBC HGCU Test Facility, 27-35, Proceedings of the Ninth Annual Coal-Fueled Heat Engines, Advanced Pressurized Bed Combustion (PFBC) and Gas Stream Clean Up Systems Contractors Review Meeting, Morgantown, WV, October 27-29, 1992, DOE/METC-93/6129 (NTIS/DE 93000232).

5. Tidd PFBC Demonstration Project Public Design Report, 1992, DOE/MC/24132-3195 (NTIS/DE93000234).

8a.2

Karhula Hot Gas Cleanup Test Results

CONTRACT INFORMATION

Contract Number	DE-FC21-89MC26042
Contractor	Westinghouse Electric Corporation Science & Technology Center 1310 Beulah Road Pittsburgh, PA 15235 (412) 256-2210
Contractor Project Manager	Thomas E. Lippert
Principal Investigators	Gerald J. Bruck Juhani Isaksson (Ahlstrom)
METC Project Manager	Richard A. Dennis
Period of Performance	October 1992 thru September 1994

Schedule and Milestones

Schedule and Milestones FY94

	S	O	N	D	J	F	M	A	M	J	J	A
Filter Supply	Completed											
Test Segment 1	Completed											
Test Segment 2		———										
Test Segment 3					———							
Test Reports					Δ			Δ			Δ	

OBJECTIVES

The objective of this work is to develop a practical hot gas filter design that meets the performance and operational requirements of pressurized fluidized bed combustion - bubbling bed, circulating bed and second generation - applications. The Westinghouse hot gas candle filter system is currently installed in the Ahlstrom Pyropower 10 MW (thermal) pressurized circulating fluidized bed combustor (PCFB) test facility located in Karhula, Finland. The overall objective of the testing is to evaluate the filter design and operating reliability for selection and implementation into the Midwest Power DMEC-1 PCFB 150 MW_e repowering project (Clean Coal III Selection).

BACKGROUND INFORMATION

High temperature particulate filters are a key component in the advanced, coal based gas turbine cycles (IGCC and PFBC) that are

currently under development by DOE/METC for clean coal demonstration and future commercialization. In these applications the hot gas particulate filter protects the downstream heat exchanger and gas turbine components from particle fouling and erosion effects and cleans the gas sufficient to meet environmental particulate emission requirements (Newby et al., 1992). Both PFBC and IGCC plants benefit because of lower cost downstream components, improved energy efficiency, lower maintenance and the elimination of additional and expensive flue gas treatment systems.

Ceramic barrier filter devices such as candles and cross flow filters are under development for hot gas filter application. These devices have been shown to be basically absolute filters on ash material, can be operated at relatively high gas throughput with acceptable pressure drop and cleanable by simple reverse pulse jet methods. Clay bonded silicon carbide (SiC) candle filters are commercially available. The structure of these elements is mainly a coarse-grained SiC bonded by a clay-based glass binder. Each element is provided with a fine grained SiC and aluminosilicate fiber outer skin that serves as the filtration surface. Alternate, oxide based ceramic materials are also being developed for ceramic barrier filter application. Both first generation, full scale cross flow and candle filter elements have been constructed using a homogeneous sintered structure that is an alumina/mullite (A/M) matrix containing a small percentage of amorphous (glass) phase. Laboratory and field evaluation of these and other materials are being conducted to identify, characterize and compare their respective chemical and thermal stability for IGCC and PFBC applications (Alvin et al., 1992).

Westinghouse is developing system designs to effectively package and operate these barrier filter elements and exploit their beneficial operating features (Lippert et al., 1993). An important aspect of the filter system development includes the selection and qualification of the ceramic filter element and the implementation and integrated operation of these filters in pilot plant IGCC and PFBC facilities. Hot gas filters have been implemented and operated in four different test facilities: Subpilot scale entrained gasifier, located at the Texaco Montebello Research facilities in California, Foster Wheeler Advanced Pressurized Fluidized Bed Combustion pilot plant facilities, located in Livingston, New Jersey, Slipstream of the American Electric Power (AEP) 70 MW (electric) Tidd-PFBC, located in Brilliant, Ohio, and in the Ahlstrom 10 MW (thermal) Circulating PFBC facility, located in Karhula, Finland (Lippert et al., 1993). Table 1 identifies and summarizes the key operating characteristics of these facilities and the type and scale of filter unit tested. This paper updates the results of the pilot plant testing currently being conducted at the Ahlstrom Pyropower PCFB facility.

PROJECT DESCRIPTION

Ahlstrom Pyropower has designed and built a pilot-scale 34 mm Btu/hr Pressurized Circulating Fluidized Bed (PCFB) Combustor - Ceramic Barrier Filter Testing Facility in Karhula, Finland. This facility is a key tool for verifying the design and scaleup parameters of the first commercial scale PCFB, a repowering demonstration planned by Midwest Power Co. of Des Moines, awarded under Round 3 of the Department of Energy Clean Coal Technologies Program. A key aspect of the PCFB testing is the evaluation of the ceramic barrier filter technology.

In 1989, Electric Power Research Institute (EPRI) and Pyropower Corporation (PPC) signed an agreement (RP3161-1) for EPRI's support in the testing of Asahi Ceramic Tube Filter (ACTF) on the Ahlstrom's 10 MW_{th} PCFB pilot plant. The testing of ACTF was completed in June 1992.

Table 1. Characteristics of Coal Based Test Facilities Used in Hot Gas Filter Testing

	Entrained Gasifier (Texaco)	Advanced PFBC (Foster Wheeler) Carbonizer	Advanced PFBC (Foster Wheeler) Combustor	PFBC (AEP-Tidd)	PCFB (Ahlstrom)
Facility Size	<2 MW_t	2 MW_t	1.2 MW_t	10 MW_e	10 MW_t
Coal Type	Pgh #8	Varied	Varied	Pgh #8	Varied
Coal Feed Method	Slurry	Dry	Dry	Paste	Paste
Oxidant	Air/O_2	Air	Air	Air	Air
Process Gas	Reducing	Reducing	Oxidizing	Oxidizing	Oxidizing
Method of Sulfur Control	External	In Bed	In Bed	In Bed	In Bed
Precleaning	None	None	None	Cyclone	None
Filter Unit(s)	Cross Flow Candle	Cross Flow Candle	Candle (Cross Flow)	Candle	Candle
Filter Arrangement	Full Flow With Bypass	Full Flow No Bypass	Full Flow No Bypass	Full Flow No Bypass	Full Flow No Bypass
Status	Completed	Ongoing	Ongoing	Ongoing	Ongoing

( ) - Planned

PPC, in cooperation with American Electric Power Service Corporation (AEP), the U.S. Department of Energy (DOE), Electric Power Research Institute (EPRI), and Westinghouse Electric Corporation (WEC), have developed a program for testing of the Westinghouse Candle Filter (WCF). The Westinghouse Candle Filter is being tested in tandem with the PCFB combustor. Testing was initiated in the Fall of 1992. The agreement between EPRI and PPC was modified in the summer of 1992 to include continued support of EPRI for the WCF testing. EPRI's participation has included supply of coal and technical consultation. The design and supply of the Westinghouse candle filter unit was conducted in support of the cooperative agreement (DE-FC21-89MC26042) between the American Electric Power Service Corporation and U.S. Department of Energy. Westinghouse is cost sharing operation of the test facility.

The prime objectives of the WCF test program are:

I. To demonstrate a commercial scale HTHP filter to operate at the downstream of a PCFB.

II. To study the performance characteristics of the filter with specific reference to:

- pressure drop across the candle elements as a function of gas velocity, dust loading, pressure, temperature, and time of operation
- pulse cleaning frequency, air pressure and quantity required.

III. To establish the reliability of the system by monitoring:

- the effect of cleaning under different operating conditions

- the collection efficiencies
- the mechanical capability to withstand normal and abnormal operation transients such as startup, part load, load change, loss of load reflected by sudden drop in pressure or emergency shutdown, and normal shutdown
- the aging of the filter material and metal specimens
- the degradation in physical and chemical properties, if any, due to chemical effects and mechanical disturbances
- the limits of the material to withstand chemical and mechanical extremes
- the downstream dust loading.

The PCFB facility, schematically shown in Figure 1, consists of five major components: compressor, circulating bed combustor, barrier filter, flue gas cooler and pressure reduction station. High pressure air is used to burn coal in the circulating bed combustor unit. The high temperature, high pressure product gases, containing significant particulate (ash/sorbent), pass through the high temperature barrier filter, are then cooled prior to pressure reduction and discharged through the plant stack. The barrier filter removes substantially all of the particulates entrained in the hot flue gas stream.

The primary design parameters for the test facility are given in Table 2. The PCFB test facility is started by first burning natural gas. Air is provided by an electrically driven, radial four-stage compressor. As the plant pressure is increased, the gas burner is switched off and heavy fuel oil is fed into the combustor. When adequate bed temperature and plant load are achieved, coal is fed into the furnace as a paste. The paste is a mixture of crushed coal, sorbent and water. Bed material (either sieved natural sand or limestone) is injected through a separate pneumatic line into the combustor. Solids recycle is achieved with a cyclone unit housed within the combustor pressure vessel.

Table 2. PCFB Test Facility Design Parameters

Thermal Rating	34 mm Btu/hr	10 MW_{th}
Fuel Feed (Max)	15870 lb/hr	3 kg/s
Air Flow (Max)	43650 lb/hr	5.5 kg/s
Operating Temperature	1615°F	880°C
Operating Pressure (Max)	232 psia	16 bar

The Westinghouse candle filter unit, schematically shown in Figure 2, installed in the Ahlstrom facility, was backfitted to the pressure vessel previously housing the Asahi ceramic tube filter unit. The Westinghouse unit consists of a single filter cluster containing 128 candle elements that are arrayed on three plenums. The top and middle plenums each contain 38 candles. The bottom plenum contains 52 candle elements. The total filter surface area is approximately 384 ft^2 (35.7 m^2). The three plenum sections connect to a common support pipe and hot seal plate arrangement that hangs from a water cooled tubesheet. The water cooled tubesheet is integral with the pressure vessel. The tubesheet and seal plate arrangement form the separation between the dirty and clean gas chambers inside the pressure vessel. The filters are cleaned on-line by high-pressure air pulses that are controlled by fast acting valves and directed through pulse pipes that are connected through the pressure vessel and terminate at the outlet side of the filter seal plate. Three pulse pipes are provided, corresponding to the three plenum sections. Air for the pulse cleaning is provided by a booster compressor (from the main plant air source) that discharges to a high pressure reservoir.

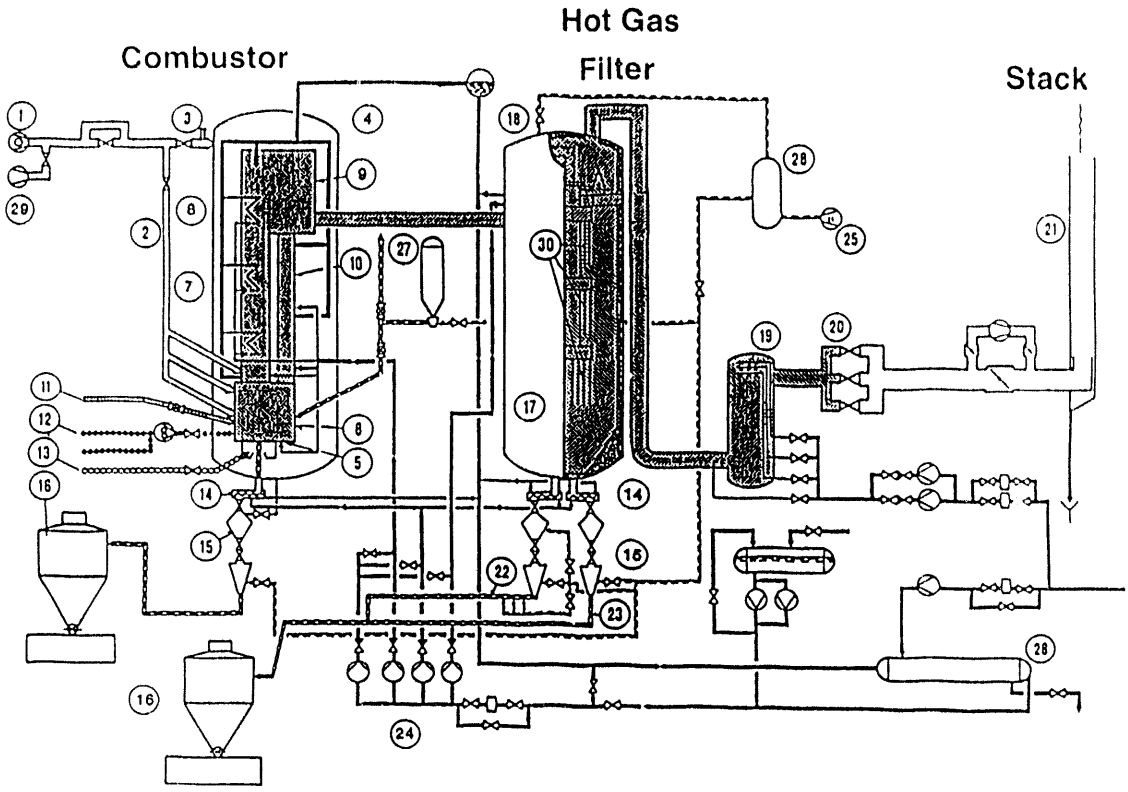


Figure 1. Ahlstrom/Karhula PCFB - HGF Test Facility

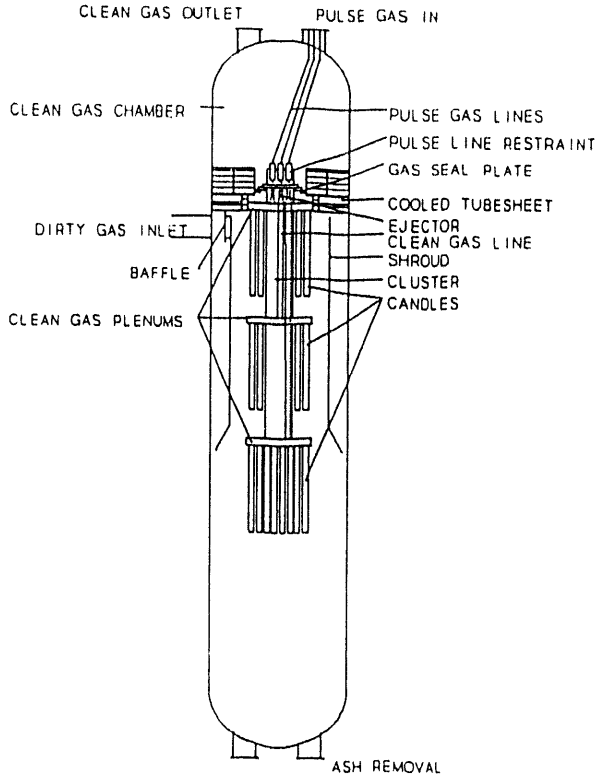


Figure 2. Schematic of PCFB Hot Gas Candle Filter

The test facility and filter unit are instrumented to monitor the key process and filter performance parameters. Measurements include gas flow, system pressure, filter pressure drop, gas temperatures, metal temperatures, and reservoir pressure.

The Westinghouse filter was installed in September 1992 and operated in accordance with schedule given in Figure 3. The testing is divided into three segments with the goal of achieving between 500 to 1000 hours operation in each segment. To date a total of 1741 hours of coal operation has been achieved, Table 3. Test segments 1 and 2 have been completed while testing in segment 3 is ongoing. Results from the first test segment have been reported (Lippert, et al., 1993).

Following Test Segment 1 operation several facility and filter modifications were implemented to address expected root cause events that had resulted in candle element damage during this testing. These modifications addressed the occurrence of process upsets and thermal transient events and include:

- improved main air compressor surge control
- increased the range of control to the fuel feed pump
- improved pulse valve operation
- improved distribution of the gas flow entering the filter unit by modifying the inlet baffle and shroud.

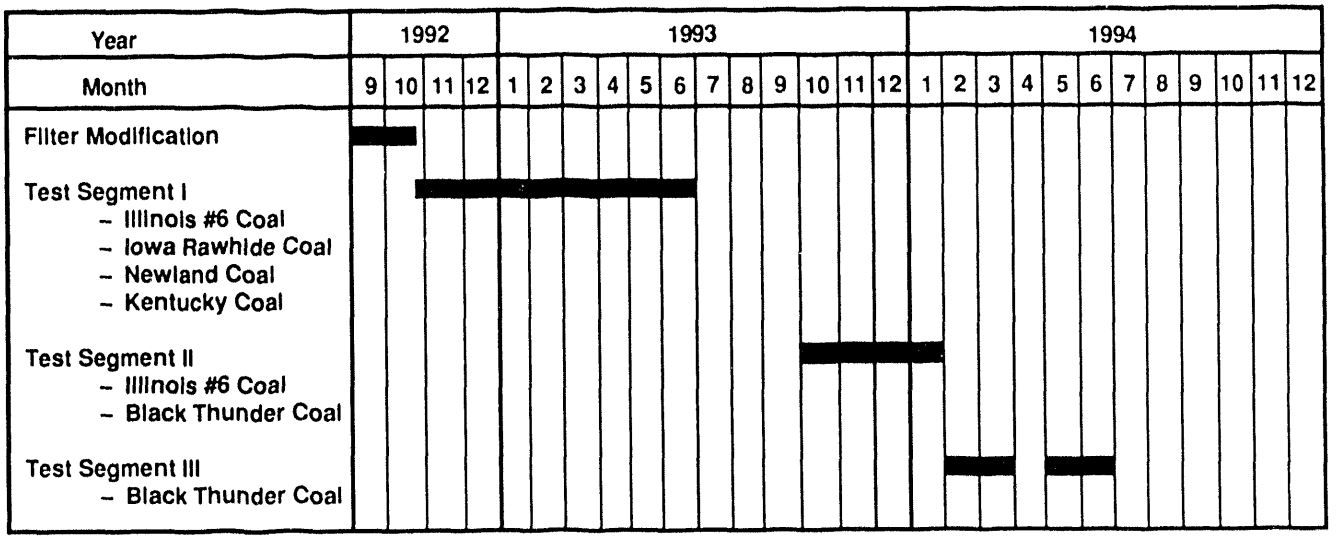


Figure 3. Westinghouse Filter Testing - Karhula PCFB Schedule

Table 3. Summary of Westinghouse Hot Gas Filter Operation at the Ahlstrom PCFB Facility - Karhula

Coal	Segment 1 (Hours)	Segment 2 (Hours)	Segment 3 (Hours)	Total
Illinois No. 6	85	221	-	306
Iowa Rawhide	61	-	-	61
Newland	300	-	-	300
Kentucky	270	-	-	270
Black Thunder	-	291	513	804
Total Coal	716	512	513	1741

RESULTS

This section summarizes Test Segment 2 results and current status of Test Segment 3. During 1026 hours of operation represented by Test Segment 2 and current testing in Test Segment 3, the filter unit and test facility has performed very well and operated without major equipment failures. The filter has demonstrated stable pressure drop and has operated without candle failure. Tables 4 and 5 summarize the filter operating parameters during the Test Segments 2 and 3, respectively. In Test Segments 2 and 3, commercially available clay bonded silicon carbide candle filters (Vitropore^{R}) have been utilized, and filter operating conditions maintained below approximately 1560° F (850° C) to better accommodate these candles.

Test Segment 2

Test Segment 2 test runs, Table 4, were initiated on November 6, 1993 and continued until December 17, 1993. Operation was initiated utilizing high sulfur Illinois No. 6 coal and an Iowa industrial No. 1 limestone sorbent. Operation on the Illinois coal consisted of a relatively short run (1 to 2 days) due primarily with coal feeding problems associated with frozen coal. Nine separate test runs were made on the Illinois coal with plant load ranging from about 65 to 75%, and operating pressures between 138 to 152 psi (9.5 to 10.5 bar). Stable filter operation was observed through each test segment as determined by the filter baseline pressure drop measurements. In this testing with high sulfur Illinois coal, changes of the coal paste Ca/S (calcium to sulfur) molar ratio and load changes resulted in corresponding changes in the filter inlet dust loading ranging from 7200 to 12,300 ppm. Under these widely varying conditions, the filter operated without issue.

The longest continuous test run on the Illinois coal was approximately 53 hours. Thus, during this period of 221 coal operating hours, the filter was cycled through nine startups and, in addition, experienced over 170 hours of additional operation on oil firing.

Table 4. Summary of Representative Filter Operation During Karhula Test Segment 2

Filter Parameter	Test Segment 2 (511 Hrs) 11/6/93 through 12/17/93		
Coal Sorbent	Illinois #6 Iowa	Black Thunder Iowa	Black Thunder None
Coal Operation, hrs	221	116	174
Fuel Input, MW	6.9 - 8.2	4.9 - 8.2	7.6 - 8.6
Operating Temperature, °F (°C)	1470 - 1522 (800 -828)	1333 - 1488 (723 - 809)	1471 - 1509 (800 - 821)
Filter Face Velocity, ft/min (cm/s)	5.5 - 6.5 (2.8 - 3.3)	3.4 - 6.5 (1.7 - 3.3)	6.2 - 6.4 (3.1 - 3.2)
Baseline Pressure Drop, in wg (mbar)	18 - 30 (46 - 75)	7 - 26 (18 - 66)	26 - 29 (65 - 72)
Cleaning Cycle, min	45 - 55	30	20
Dust Loading, ppmw	7200 - 12300	2000 - 6900	6400

Table 5. Sumary of Representative Filter Oepration During Karhula Test Segment 3

Filter Parameter	Test Segment 3* (513 Hrs) 2/7/94 through 3/20/94	
Coal Sorbent	Black Thunder None	Black Thunder Iowa Ind #1
Coal Operation, hrs	258	256
Fuel Input, MW	7.8 - 10	4.6 - 5.1
Operating Temperature, °F (°C)	1490 - 1560 (810 - 850)	1273 - 1327 (690 - 720)
Filter Face Velocity, ft/min (cm/s)	5.9 - 7.9 (3.0 - 4.0)	3.0 - 4.2 (1.5 - 2.1)
Baseline Pressure Drop, in wg (mbar)	26 - 48 (65 - 120)	10 - 14.1 (25 - 35)
Cleaning Cycle, min	40 - 55	40 - 55
Dust Loading, ppmw	4000 - 7000	3000 - 6000

* Additional Testing Planned - May/June 1994

Operation with the low sulfur Black Thunder coal included testing both with and without sorbent addition and under plant load conditions between 50 to 75 percent and system pressure ranging from 152 to 167 psi (10.5 to 11.5 bar). The Black Thunder coal testing occurred in two operating segments of 53 and 238 hours. Stable filter operation was again achieved with the Black Thunder coal. The filter was operated without issue over a range of inlet loadings that depended on plant load and use of sorbent.

Following the 238 hour continuous operation on the Black Thunder coal, the filter testing was terminated by a scheduled shutdown and the unit inspected. Visual inspection showed all the candles to be intact with no ash bridging evident between candles. Ten of the bottom plenum candles were removed (and replaced) for subsequent destructive testing. Ash samples were also collected for analysis. Routine facility maintenance was performed prior to restarting of the unit, initiating Test Segment 3.

Test Segment 3

Test Segment 3 testing, Table 5, was initiated early February 1994, with continuing operation utilizing Black Thunder coal, and operating both with and without sorbent addition. The initial operation in this test segment was at full load conditions, but cold weather again resulted in frozen coal and subsequent coal feeding problems causing frequent interruptions resulting in shutdown or hot standby on oil firing. After approximately 258 hours of coal operation under this mode, plant operation was reduced and maintained to about 50% load conditions. This circumvented the issues caused by the cold weather condition and provided opportunity to obtain important filter performance and operating data at the low load conditions. With this data, the ability to extrapolate filter operating characteristics and performance over a range of conditions is improved. Later testing in this test segment will focus on full load operation.

During this testing, filter operation was stable with no pressure drop issues. Testing was terminated late March 1994 for scheduled facility maintenance. Preliminary inspection of the filter again showed the filter to be in good operating condition. No dust was present on the clean side of the filter confirming filter performance. Following the initial inspection several candle filters were removed from the bottom plenum and inspected. This inspection showed several of the candle elements to be slightly elongated and some with hairline cracks near the flange neck. Subsequent follow-up showed the manufacturing (firing conditions) of these candles had been modified relative to standard processing. The filter elements from these manufacturing lots (approximately 45 candles) have been identified and removed and replaced with candles manufactured using standard processing. Test Segment 3 candle testing has now been resumed.

Summary. Over 1741 hours of operation have now been achieved with the Westinghouse candle filter unit operating in the Ahlstrom PCFB facility. Extended, trouble-free, operating periods have been achieved in which the candle filter unit has demonstrated excellent particle collection efficiency and stable filter pressure drop while operating over a wide range of coal/sorbent types and gas temperature to 1650°F (900°C).

FUTURE WORK

Operation of the Westinghouse candle filter unit will be continued through June 1994. Following this testing the unit will again be inspected and decisions for continued testing made.

REFERENCES

Alvin, M. A. et al., 1992. Hot Gas Cleanup and Gas Turbine Aspects of an Advanced PFBC Power Plant. In *Proceedings of the Ninth Annual Coal-Fueled Heat Engines, Advanced Pressurized Fluidized-Bed Combustion (PFBC) and Gas Stream Cleanup Systems Contractors Review Meeting*, p. 168, DOE/METC-93/6129.

Lippert, T. E. et al., 1993. Specific Filter Designs for PFBC. Companion paper - In *Proceedings of Coal Fired Power Systems 93 - Advances in IGCC and PFBC Contractors Review Meeting*, DOE/METC June 28-30, 1993.

Lippert, T. E. et al., 1993. Westinghouse Filter Update. In *Proceedings of Coal Fired Power Systems 93 - Advances in IGCC and PFBC Review Meeting*, DOE/METC-93,6131, p. 497.

Newby, R. A. et al., 1992. Hot Gas Cleanup and Gas Turbine Aspects of an Advanced PFBC Power Plant. In *Proceedings of the Ninth Annual Coal-Fueled Heat Engines, Advanced Pressurized Fluidized-Bed Combustion (PFBC) and Gas Stream Cleanup Systems Contractors Review Meeting*, p. 55, DOE/METC-93/6129.

8a.3

Durability of Ceramic Filters

CONTRACT INFORMATION

Contract Number	DE-AC21-89MC25034 (DE-FC21-89MC26042) (DE-AC21-86MC23252)
Contractor	Westinghouse Electric Corporation Science & Technology Center 1310 Beulah Road Pittsburgh, PA 15235-5098 (412) 256-2066
Contractor Project Manager	Mary Anne Alvin
Principal Investigators	Mary Anne Alvin Richard E. Tressler (Pennsylvania State University) Thomas E. Lippert Edward S. Diaz Eugene E. Smeltzer
METC Project Manager	Theodore J. McMahon
Period of Performance	September 30, 1988 - February 28, 1995

Schedule and Milestones

Schedule and Milestones FY94

	S	O	N	D	J	F	M	A	M	J	J	A
Experimental Testing	———											
Field Analysis	———											
Model Development	———											

OBJECTIVES

The objectives of this program are to identify the potential long-term thermal/chemical effects that advanced coal-based power generating systems have on the stability of porous ceramic filter materials, as well as to assess the influence of these effects on filter operating performance and life.

BACKGROUND INFORMATION

Westinghouse Advanced Particulate Filtration (W-APF) systems have typically operated between temperatures of 540° C and 900° C in both oxidizing and reducing advanced coal-fired process applications (Table 1). First generation Coors alumina/mullite and clay bonded silicon carbide Pall Vitropore 442T and

Table 1. Westinghouse Advanced Particulate Filtration Systems

Process	Temp., °C	Conditions	Operating Hours	Candle Filter Type	Facility
AEP PFBC	540-810	Oxidizing	3038	SiC	Demonstration
Karhula CFBC	850-900 690-850	Oxidizing Oxidizing	716 1341	Alumina/Mullite SiC	Pilot Plant Pilot Plant
FW PFBC	700-870 700-870	Oxidizing Oxidizing	58 210	Alumina/Mullite SiC	Pilot Plant Pilot Plant
FW Carbonizer	<760	Reducing	63	Alumina/Mullite	Pilot Plant
Texaco Gasifier	700	Reducing	400	SiC and Alumina/Mullite	Pilot Plant

Schumacher Dia Schumalith F40 candle filters have been utilized in these installations, and to date have operated for test periods as long as 3,038 hours.

The porous alumina/mullite filter matrix consists principally of mullite which co-exists with an amorphous phase that contains anorthite and corundum. In contrast both the Vitropore 442T and Dia Schumalith F40 candle filters consist of silicon carbide grains that are bonded together via a silica-rich binder phase. Both clay bonded silicon carbide candle filters have outer membrane coatings (i.e., a finer grain silicon carbide layer along the Vitropore 442T candles; an aluminosilicate fibrous mat along the Dia Schumalith F40 candles), while the alumina/ mullite candle filter is currently manufactured without an external membrane or coating.

When the alumina/mullite, Vitropore 442T or Dia Schumalith F40 filter materials are subjected to 870° C process temperatures in a static air environment, the bulk material strength of these porous ceramic filter matrices is generally retained during the first 3,000 hours of exposure (Table 2). The as-fabricated morphology of the oxide and nonoxide-based materials is also retained, with negligible observable changes occurring in the ceramic microstructure (i.e., crystallization, etc.) during the extended static air exposure period. These results are expected in view of the substantially higher manufacturing temperatures that are used to produce the various candle filter elements.

Recent field experience in the W-APF systems has indicated that porous ceramic candle filter elements are subjected to damage and degradation resulting from ash bridging within the various candle filter cluster arrays, thermal process transient events, and pulse gas cleaning cycles which are required for dust cake removal. An assessment of the alumina/mullite and clay bonded silicon carbide candles which experienced 712 and 1,341 hours of operation, respectively, in

Table 2. High Temperature Static Air Exposure of As-Fabricated Porous Ceramic Candle Filters

Candle ID	Temp., °C	Time, Hrs	Room Temperature Strength		Hot Strength	
			C-Ring Compression, psi	C-Ring Tension, psi	C-Ring Compression, psi	C-Ring Tension, psi
Alumina/Mullite						
AC-0	—	—	3287 ± 213	4001 ± 477	2841 ± 300 (a)	2996 ± 304 (a)
AC-0	870	1824	NA	NA	2474 ± 265 (b)	2441 ± 172 (b)
AC-0	870	3000	NA	NA	2635 ± 262 (b)	2926 ± 245 (b)
Dia Schumalith F40						
S/482-315C	—	—	1790 ± 112	2308 ± 275	1569 ± 90 (a)	3158 ± 271 (a)
S/482-315C	870	1824	NA	NA	1468 ± 58 (b)	1836 ± 144 (b)
S/482-315C	870	3000	NA	NA	1327 ± 203 (b)	1745 ± 108 (b)
Vitropore 442T						
R4-143	—	—	2585 ± 202	2235 ± 174	2406 ± 247 (b)	2536 ± 360 (b)
R4-148	—	—	2510 ± 158	2654 ± 256	2497 ± 227 (b)	2730 ± 238 (b)
R10-151	870	8	2576 ± 314	3027 ± 114	2646 ± 137 (b)	2683 ± 178 (b)
R3-148	870	1815	2593 ± 156	2734 ± 407	2489 ± 116 (b)	2765 ± 326 (b)
R3-148	870	3000	2335 ± 225	2464 ± 206	2403 ± 87 (b)	2705 ± 165 (b)

(a) Hot Strength Tested at 900°C
(b) Hot Strength Tested at 870°C
NA: Not Available

in the circulating fluidized-bed combustion (CFBC) test facility in Karhula, Finland, and 3,038 hours of operation of the clay bonded silicon carbide candles in the pressurized fluidized-bed combustion (PFBC) test facility at the American Electric Power (AEP) demonstration plant in Brilliant, Ohio, indicated that the porous ceramic filter materials typically lose bulk strength during hot gas filtration. In addition both the oxide and nonoxide-based filter materials undergo various phase changes within the bulk matrix and/or binder phases which reflect operating temperature and process flue gas chemistry. Microcrack formations have been observed within the field-tested alumina/mullite filter matrix, and are also expected to occur within the binder phase, and possibly through the silicon carbide grains in the clay bonded filter materials.

Thermal fatigue has been identified, particularly along the ID wall of the alumina/ mullite candle filters as a result of contact with cold pulse cleaning gas. Similarly a decrease in the fracture toughness of the alumina/mullite matrix resulted during high temperature, pressurized process operation. Alternately creep crack growth has been observed in the Vitropore 442T clay bonded silicon carbide candle filters after 500 hours of service at process operating temperatures of 800-850° C. Bowing and tilting of the clay bonded silicon carbide candles have frequently been encountered when ash bridges form within the candle arrays, as well as during creep crack growth. Debonding of the outer candle filter membrane, and binder coating that encapsulates the silicon carbide grains resulted when the porous ceramic filters were contacted with a mixed sodium-potassium sulfate phase in the Foster Wheeler PFBC test facility. The resulting phase and microstructural changes, microcrack formations, and thermal conditioning effects that occur during hot gas filtration will be discussed in depth throughout the remainder of

this paper for both the alumina/mullite and clay bonded silicon carbide filter materials.

PROJECT DESCRIPTION

Westinghouse has undertaken a two phase program to determine the possible long-term, high temperature influence that advanced coal-based power systems have on the stability of porous ceramic filter elements. Accomplishments during the past year have included:

- Developing an understanding of the fundamental changes or "conditioning" mechanisms that have occurred in the alumina/mullite and clay bonded silicon carbide candle filters during test operation in the AEP PFBC and Ahlstrom CFBC test facilities, and identifying how these changes impact bulk filter material strength, and possibly filter operating life.

- Conducting high temperature, thermal fatigue tests in which as-manufactured alumina/mullite, Vitropore 442T clay bonded silicon carbide, and Dia Schumalith F40 clay bonded silicon carbide filters, as well as alumina/mullite candle filters which had been exposed to CFBC operations for periods of up to 716 hours, were subjected to 10,000 pulse cleaning cycles under simulated PFBC process operating conditions. All candles retained their physical integrity after experiencing the extended accelerated thermal fatigue tests.

- Establishing the threshold stress intensity for slow crack growth in the alumina/ mullite and clay bonded silicon carbide filter materials at temperature of 800 and 900 ° C via interrupted static and dynamic fatigue testing.

A discussion of the results in each of these areas follows.

RESULTS

Field Testing

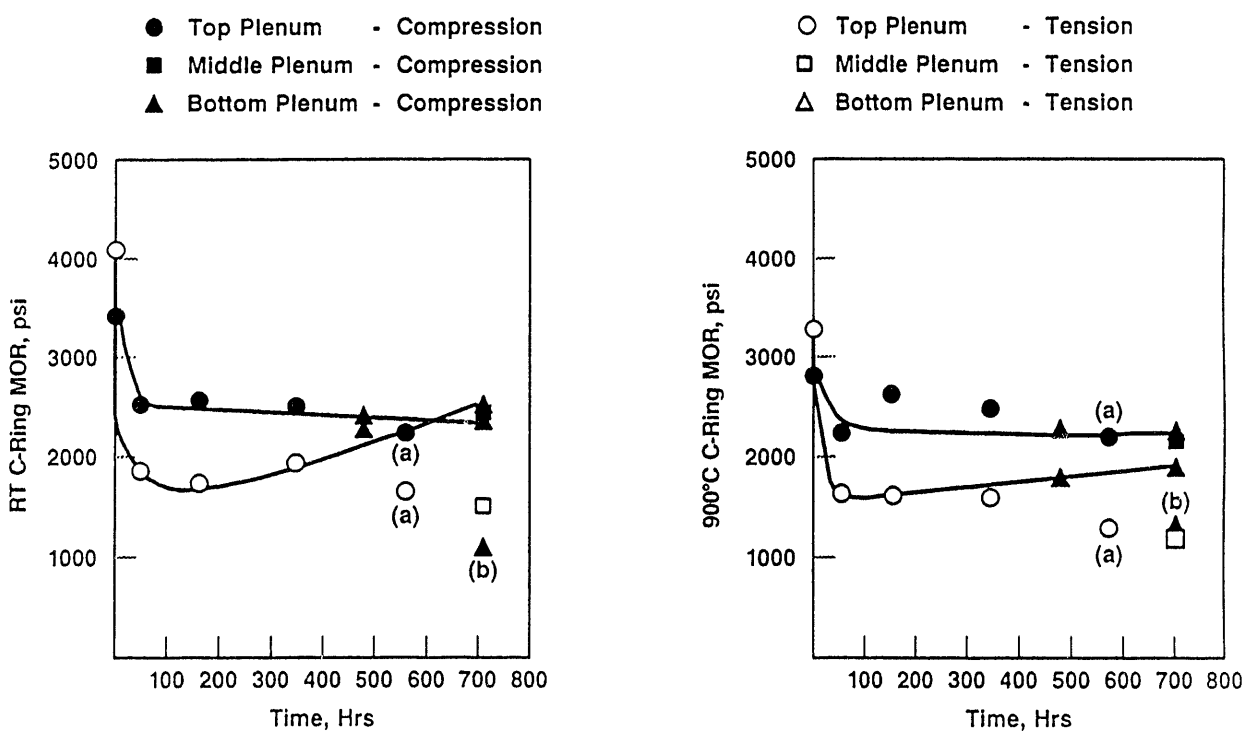
Characterization of the Alumina/Mullite Candle Filters after Exposure in the W-APF System at the Ahlstrom CFBC Test Facility in Karhula, Finland (Test Segment 1). One hundred twenty-eight (128), 1.5 m full length alumina/mullite candle filters were installed in the W-APF system in the Ahlstrom circulating fluidized-bed combustion (CFBC) pilot plant in Karhula, Finland prior to October 1992. As shown in Table 3, the W-APF operated for a period of 716 hours at nominal temperatures of 900 ° C. Post-test characterization of the CFBC-exposed alumina/mullite candle filters typically included room temperature and process temperature (i.e., 900 ° C) C-ring compressive and tensile strength testing, burst strength and fracture toughness analyses, x-ray diffraction (XRD) analyses, and scanning electron microscopy/ energy dispersive x-ray analyses (SEM/EDAX).

Figure 1 illustrates the residual bulk strength of the CFBC-exposed alumina/mullite filter matrix as a function of process operating time. An initial loss of the bulk strength of the alumina/ mullite filter matrix is experienced within the first 50 to 100 hours of operation in the CFBC process gas environment. The bulk strength of the matrix then appears to stabilize, remaining relatively constant throughout the remainder of the 616 to 666 hours of test operation.

Typically a greater loss of bulk material strength is experienced along the ID surface of the CFBC-exposed alumina/mullite filter matrix (i.e., tensile testing: 46-49% residual ID wall strength vs compressive testing: 71-83% residual OD wall strength; Table 4). Strength reduction is

Table 3. W-APF Testing at Karhula Using Alumina/Mullite Candle Filters

Test Segment 1 Run No.	Coal Fire Date	Coal Fire Time, Hrs	Comment	Coal/Sorbent
1	Oct/Nov 92	98	2 Broken Candles	Illinois #6/Iowa #6
2	Nov/Dec 92	45	Fuel Gas Ignition	Rawhide
3	Jan/Feb 93	202	1 Broken Candle In Middle Plenum	Illinois #6/Iowa #6 Newland/Fujiwara
4	March 93	144	Ash Bridging 23 Broken Candles	Newland/Fujiwara Kentucky
5	May/June 93	227	Shroud Shift 10 Broken Candles	Kentucky/Wilbur Newland/Tsukumi



(a) Candle Installed During Last Three Test Segments (No Fuel Event)
(b) Fractured Filter Element

Figure 1. Residual Bulk Material Strength of the Alumina/Mullite Filter Matrix After Exposure to CFBC Process Gases in the W-APF System

Table 4. Percent Strength Retention in CFBC-Exposed P-100A-1 Alumina/Mullite Candle Filters

Candle ID	Temp., °C	Time, Hrs	Room Temperature C-Ring		Hot Strength, 900°C C-Ring	
			Compression	Tension	Compression	Tension
AC-106RA (T14)	900	45	76	45	80	49
AC-170 (T35)	900	143	76	41	93	51
AC-129RA (T5)	900	345	73	47	88	50
AC-160 (B1)	900	488	69	55	84	55
AC-128RA (T3)	900	572 (a)	65	37	76	40
AC-274 (B22)	900	716	70	61	81	59
AC-204 (M2)	900	716	71	36	78	37

(a) AC-128RA Was Installed and Operated During the Last Three Test Segments and Did Not Experience the Initial Fuel Ignition/Thermal Shock Event

principally attributed to thermal fatigue of the alumina/mullite filter matrix as a result of the ID surface being contacted with the cold pulse cleaning gas.

During the 716 hours of CFBC test operation in Karhula, Finland, the W-APF vessel experienced a fuel ignition event, isolated ash bridging, and a shift in the vessel shroud position -- all of which were considered to contribute to failure of thirty-six (36) candle filter elements throughout the entire test period. As shown in Figure 1 and Table 5, the fractured candles and/or ash hopper candle sections exhibited a lower residual bulk strength, as well as reduced fracture toughness and/or elastic modulus in comparison to candles that remained intact throughout the course CFBC testing.

Optical microscopy analyses were conducted on several of the CFBC field-tested alumina/ mullite candle filters in order to determine whether microcracks were present in the porous ceramic matrix. "Tight" microcrack formations were infrequently identified to extend into the 10 mm alumina/mullite candle filter wall from the ID surface. The position and number of microcracks randomly varied along the length of the candle filter. Microcracks infrequently extended completely across the candle wall thickness. Characterization of as-manufactured alumina/mullite candle filters which had not undergone field testing also indicated the presence of microcracks within the porous ceramic filter body.

Characterization of the alumina/mullite filter matrix utilizing SEM/EDAX analytical techniques indicated that during the initial several hundred hours of test operation, surface crystallization of the amorphous phase occurs in the CFBC-exposed filter matrix. Mullitization (i.e., rod-like grain growth) is evident along the ID pore cavity walls. Nucleation or grain growth within the amorphous phase of the matrix leading

Table 5. Fracture Toughness and Elastic Modulus of Alumina/Mullite Candle Filters Tested at Karhula

Candle	Location	CFBC Process Test Runs	Time Hrs	Density, g/cc	Strength, MPa	Fracture Toughness, MPA√m	Elastic Modulus, GPa
1992 Production Lot							
C-35	---	---	---	1.69±0.05	---	0.62±0.03	21.6±1.4
AC-0	---	---	---	1.72±0.01	23.9±1.2	0.71±0.003	25.5±1.8
AC-Section	(a)	1-2	<143	1.67±0.02	---	0.43±0.01	12.9±2.2
AC-79	T19	1-2	143	1.73±0.06	18.8±1.3	0.51±0.20	17.7±2.4
AC-121RB	T22			1.69±0.04	15.2±0.9	0.50±0.01	15.3±2.7
AC-150RA	B38	1-4	488	1.69±0.02	13.6±1.8	0.41±0.01	---
AC-128RA	T3	3-5 (b)	573	1.70±0.01	16.4±2.3	0.61±0.01	22.3±7.1
AC-204	M2	1-5	716	1.73±0.11	13.0±3.3	0.61±0.01	19.2±4.5
AC-274	B22	1-5	716	1.71±0.02	19.8±0.9	0.60±0.01	26.8±3.9
AC-80 (c)	B19	1-5	716	1.69±0.01	18.4±1.6	0.70±0.01	27.5±6.5
1993 Production Lot							
BC-337	---	---	---	1.69±0.02	21.7±1.0	0.70±0.004	24.5±0.9

(a) Fractured Section Of Candle Removed From The Ash Hopper.
(b) AC-128RA Was Installed And Operated During The Last Three Test Run Segments.
Note This Candle Did Not Experience The Initial Fuel Event As All Of The Other Candle Filters.
(c) Fractured Candle.

to the formation of mullite, appears to be enhanced as a result of repetitive exposure to cold pulse gas cycling conditions.

After 716 hours of CFBC-exposure, the alumina/mullite filter matrix appears to be nearly fully crystallized. Grain growth is evident throughout the entire ligament structure of the filter body. Extensive mullitization is also evident, particularly along the pulse cycled surface (i.e., 2-4 μm from the ID wall).

As shown in Table 6, the as-fabricated amorphous phase in the alumina/mullite matrix is converted initially into alumina and cristobalite. Further reactions include depletion of the anorthite phase, as the concentrations of mullite (i.e., the principal phase), and cristobalite (i.e., a secondary phase) increase. Note that after 488 hours of CFBC-exposure, the glass phase in the alumina/mullite matrix appears to have been completely converted into a crystalline phase.

After 716 hours of CFBC-exposure, tridymite which is a mineralized form of cristobalite, is not detected within the alumina/mullite filter matrix. This implies that virtually little or no gas phase sodium was sorbed via the alumina/mullite filter matrix during the 900° C CFBC-test operation. Cristobalite or tridymite are expected to crystallize from the silica glass phase that is rejected during production of the anorthite in the alumina/mullite matrix. The formation of cristobalite can lead to displacive phase transformations and large volume changes in the 150-200° C temperature range. Microcrack formations can be expected to result during cooling through this temperature range, unless the grain size and volume fractions are very small.

During the last 227 hours of test operation with the alumina/mullite candle filters, fourteen (14) Vitropore 442T and seven (7) Dia Schumalith F40 candle filters were placed in various positions throughout the top, middle, and

Table 6. Phase Composition of Alumina/Mullite Candle Filters Tested at Karhula

Candle ID	Time, Hr (Karhula)	Phase, Wt% Mullite	Anorthite	Alumina	Glass	Cristobalite	Tridymite	Cordierite
P-100A-1 As-Manufactured	—	67.8	29.5	2.7	5*	—	—	vm
Fracture Section Retrieved From Hopper	45	60.9	31.0	2.1	5*	t	—	—
AC-170	143	M	s	m**	5*	~5+	—	—
AC-129RA	345	M	s	m**	<5*	~10	—	—
AC-160	488	M	s	m**	5*	~5	—	—
AC-128RA	572 (a)	M	m	t	—	m	—	—
AC-204	716	M	m	t	—	m	—	—

* May Be As High As 10%
** >2.1%
M: Major
s: Significant
m: Minor
t: Trace
(a) AC-128RA Was Installed and Operated During the Last Three Test Runs at Karhula. This Candle Did Not Experience the Initial Full Event as All of the Other Candle Filters

Table 7. W-APF Testing at Karhula Using Alumina/Mullite and Clay Bonded Silicon Carbide Candle Filters

Candle Filters	Alumina/Mullite* Test Segment 1	Vitropore Test Segment 2			Vitropore Test Segment 3	
Coal Operating Hours	716	221	116	174	258	256
Operating Temperature, °C	850-900	800-828	723-809	800-821	810-850	690-720
Coal	Illinois #6 Rawhide Newland Kentucky	Illinois #6	Black Thunder	Black Thunder	Black Thunder	Black Thunder
Sorbent	Iowa #6 Fujiwara Wilbur Tsukumi	Iowa	Iowa	None	None	Iowa

* Last 227 Hours of Operation Included 14 Vitropore 442T and 7 Dia Schumalith F40 Candle Filters

bottom plenums in the W-APF vessel. As shown in Table 7, the operating temperature of the W-APF vessel was nominally 900 ° C during this phase of testing.

Post-test inspection of several Vitropore 442T filters matrix which had been operated for 227 hours in the 900 ° C CFBC process gas environment indicated that bowing and/or tilting of the filter elements had occurred. Westinghouse as-manufactured candle filter dimensional tolerance specifications permit a 3 mm maximum candle bow, and a perpendicularity tolerance of 0.5 ° over the 1,500 mm candle length (i.e., 12.7 mm from the center line at the bottom of the candle filter end cap). After 227 hours of operation in the 900 ° C CFBC gas environment, one candle was shown to have a bow of 5.3 mm, and was 50.8 mm out-from-perpendicular. Bowing and/or tilting of the Dia Schumalith F40 candles was not observed.

Characterization of the residual strength of the 227 hour, 900 ° C, CFBC exposed Vitropore 442T candle filter material indicated a loss of bulk material strength, primarily along the ID surface of the candle (Table 8). As shown in Figure 2, both Vitropore 442T and Dia Schumalith F40 clay bonded silicon carbide filters tend to lose bulk material strength within the first 227 hours of 900 ° C CFBC test operation.

For the Vitropore 442T matrix crystallization results along the outer surface of the binder phase that coats the silicon carbide grains, as well as along the binder ligaments that bond adjacent silicon carbide grains together. Frequently void formations are evident below the binder coating surface (i.e., adjacent to the silicon carbide grain). Crystallization of the binder phase surface results in the formation of ~1 μm silica-enriched grains (i.e., cristobalite) which follow the contour of the binder coated grains and/or ligament bond posts.

As identified by XRD analysis, the Vitropore 442T matrix initially consists of hexagonal α-SiC, mullite, and a trace of tridymite. When the Vitropore 442T matrix is ground in order to extract the binder phase for analysis, a glass phase and trace concentrations of cristobalite are observed in the powder patterns of the binder phase. After 227 hours of CFBC exposure at 900 ° C, the Vitropore 442T matrix consists of α-SiC, mullite, cristobalite, and trace concentrations of tridymite. Extraction and analysis of the binder phase composition indicates the presence of mullite, cristobalite, and tridymite. Note that cristobalite is detected at a higher concentration in the Vitropore 442T matrix after 227 hours of exposure in the 900 ° C CFBC gas phase environment. A simultaneous increase in the mullite concentration in the binder phase is also observed. The formation of cristobalite and mullite are expected to result from crystallization of the binder phase as opposed to oxidation of the SiC grain surface.

Similar crystallization of the binder phase occurs within the Dia Schumalith F40 matrix that experienced 227 hours of operation in the 900 ° C CFBC gas environment. Silica-enriched phase formations (i.e., cristobalite) are evident along the binder coated silicon carbide grains. Coalescence of the binder phase is also evident, leading to what appears to be the formation of a mullite or rod-like structure. As crystallization of the cristobalite and/or mullite phases occurs, voids or areas of limited binder phase exist along the surface of the silicon carbide grains. Frequently bubble-like, raised pockets of the binder coating are evident along the silicon carbide grains. Out-gassing of the bubble formations is clearly evident by the jagged crack-like features that result from perhaps diffusion of the process gas through the binder to the surface of the silicon carbide grain where reactions lead to the formation of silica and release of carbon dioxide.

Table 8. Percent Strength Retention in CFBC-Exposed Clay Bonded Silicon Carbide Candle Filters

Candle ID	Temp., °C	Time, Hrs	Room Temp. Strength		Hot Strength, 830°C		Hot Strength, 900°C	
			C-Ring Compression	C-Ring Tension	C-Ring Compression	C-Ring Tension	C-Ring Compression	C-Ring Tension
S2855/374C (T12)	900	227 (a)	46	55	—	—	63	76
R3-0061 (M19)	900	227 (a)	71	63	—	—	80	69
R4-135 (B22) *	830	512 (b)	59	57	61	64	—	—
R1-147 (B4) **	830	512 (b)	53	58	58	64	—	—
R5-140 (B8) ***	830	1026 (b,c)	67	66	79	75	—	—
R2-151 (B19) ***	830	1026 (b,c)	55	67	68	69	—	—
R6-142 (B20) ***	830	1026 (b,c)	60	71	73	73	—	—
R2-118 (B37)	830	1026 (b,c)	53	63	71	67	—	—
R7-134 (B6)	830	514 (c)	65	61	72	72	—	—
R2-110 (B17)	830	514 (c)	71	78	80	90	—	—

* Intact Candle But Bowed
** Candle Broke During Shipment; Cracks on OD Near Flange; Bow Evident
*** Cracks on OD Near Flange; Tilt or Bow Evident; 12-17 mm Elongation of Body
(a) Test Segment 1
(b) Test Segment 2
(c) Test Segment 3

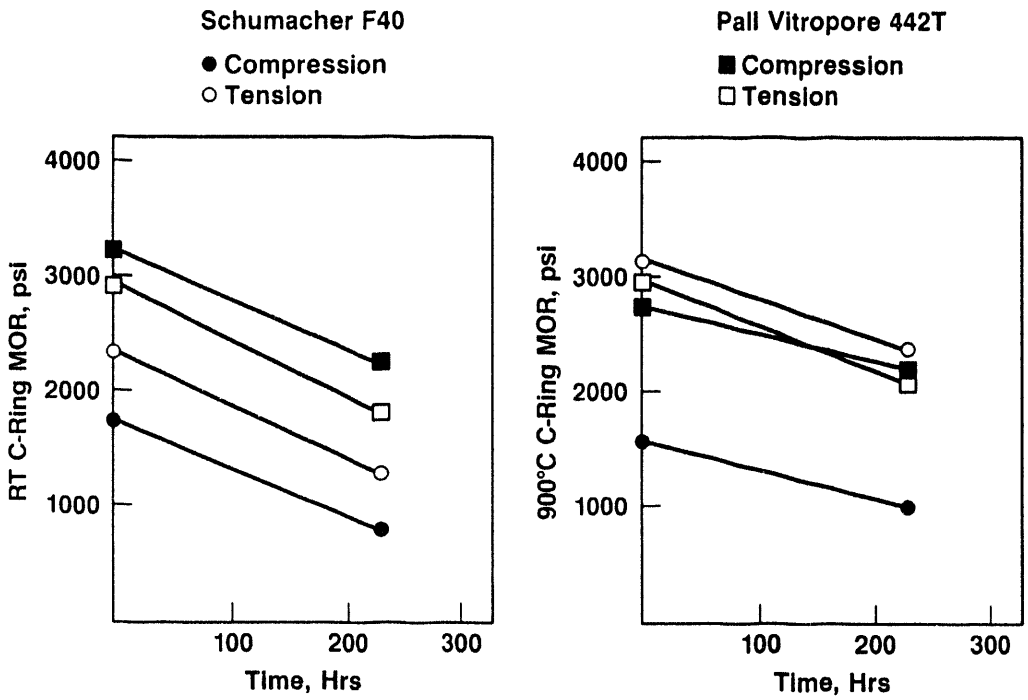


Figure 2. Residual Bulk Strength of the Vitropore 442T and Dia Schumalith F40 Candle Filters After Exposure in the CFBC Karhula Gas Environment in Test Segment 1

Characterization of the Vitropore 442T Clay Bonded Silicon Carbide Candle Filters after Exposure in the W-APF System at the Ahlstrom CFBC Test Facility in Karhula, Finland (Test Segments 2 and 3). The W-APF vessel was entirely re-candled in the fall of 1993 with new Vitropore 442T candle filters for use in testing in Test Segment 2. Testing was initiated on November 6, 1993, and continued for 512 hours at nominal temperatures of 830° C (Table 7). Post-test inspection of ten (10) Vitropore 442T candle filters from the bottom plenum indicated that candle R1-147 which had been located in position B-4 showed evidence of creep crack growth in the area of the body directly below the hemispherical flange. All ten candles subsequently underwent strength and microstructural characterization at Westinghouse, Ahlstrom, SRI, and Pall. Ten new Vitropore 442T candle filters were installed in the W-APF prior to reinitiation of testing in Test Segment 2.

Testing was reinitiated in February 1994, and continued until March 1994, accumulating an additional 514 hours of operation at nominal temperatures of 830° C. Post-test inspection of the Vitropore 442T candles included the removal of fourteen (14) candles from the bottom plenum, six (6) of which showed evidence of creep crack growth (i.e., crack formation and elongation of the candle filter body). Since these candles were identified to have been manufactured via a known production method, and similarly processed candles remained within the bottom array, all bottom plenum candles were removed, and the unit was re-candled once again with new Vitropore 442T candle filters. Post-test inspection of the removed candles indicated that eighteen (18) of the fifty-two (52) bottom plenum candles had developed cracks below their flanges. Based on the manner in which the Vitropore 442T candles had been manufactured, elongation of the candle body ranged between 0-2 mm (i.e., manufacturing process No. 1 and No. 2), and 11-12 mm (i.e., manufacturing process No. 3) for candles which had been operated in the later 514 hours of CFBC operation. Similar elongation measurements were made for candles that had experienced the entire 1026 hours of 830° C CFBC operation. These measurements indicated that candles which were produced via manufacturing process No. 1 elongated by 1-12 mm, while candles produced via manufacturing process No. 2 elongated by 9-14 mm, and candles produced via manufacturing process No. 3 elongated by 13-26 mm.

Figure 3 illustrates the residual bulk strength of the Vitropore 442T candle filters as a function of filter manufacturing process, and operating time in the CFBC process gas environment. Irrespective of how the Vitropore 442T candle filters were manufactured, all candles appear to lose bulk material strength as a function of time at 830° C. Although we did not have the opportunity to characterize the Vitropore 442T filter matrix after 50-100 hours of test operation, as had been done for the alumina/mullite filter matrix, a general trend of matrix conditioning is evident after 500-1,000 hours of operation in the 830° C CFBC gas environment. As shown in Table 8, a nearly equivalent loss of bulk material strength is indicated along both ID and OD surfaces of the Vitropore 442T matrix. This is in contrast with the residual bulk material strength of the Vitropore 442T matrix after 227 hours of exposure in the 900° C CFBC gas phase environment.

SEM/EDAX analyses illustrate the progression of the changes that occurs within the microstructure of the Vitropore 442T candle filter matrix as a function of process operating time. After 512 hours of exposure in the 830° C CFBC gas phase environment, holes and voids are evident in the binder ligaments that bond adjacent silicon carbide grains together. Crystallization of the binder phase that coats the fine silicon carbide grains in the Vitropore 442T OD membrane

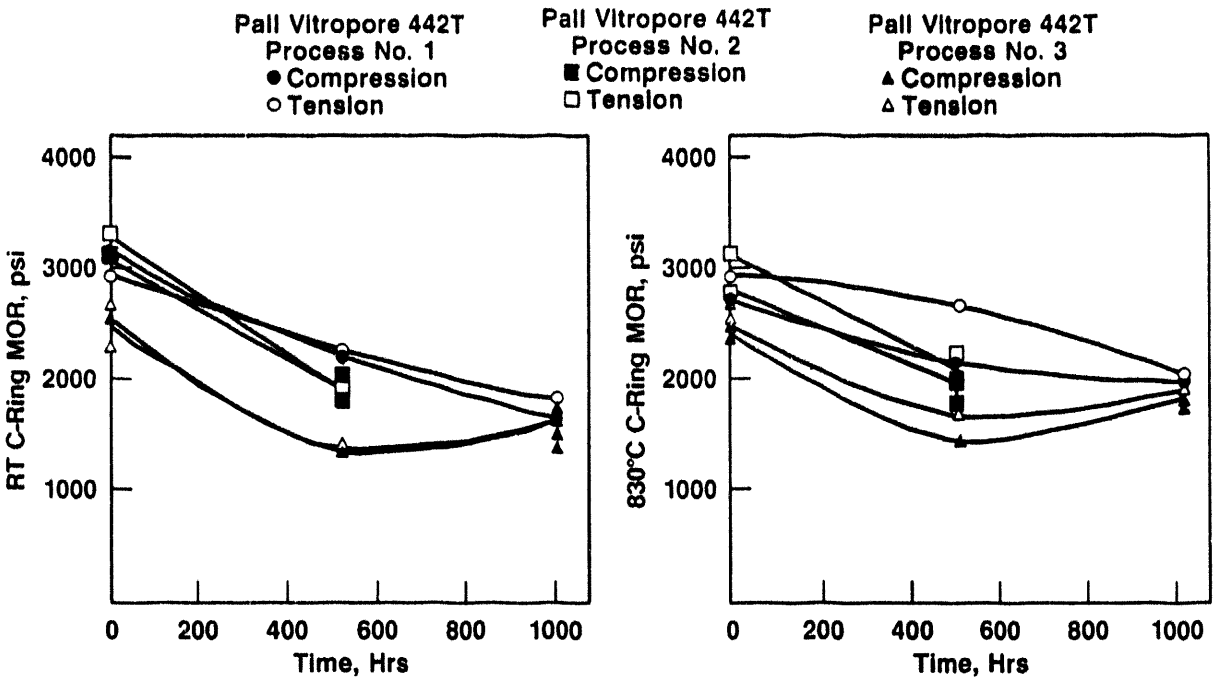


Figure 3. Residual Bulk Strength of the Vitropore 442T Clay Bonded Silicon Carbide Candle Filters After Exposure in the CFBC Karhula Gas Environment in Test Segments 2 and 3

occurs, leading to the formation of silica-enriched (i.e., cristobalite) areas. Similarly crystallization of the binder phase occurs along the coarse support silicon carbide grains. Along either the fine or coarse support silicon carbide grains, areas that are adjacent to the crystalline formations appear to either have a thinner binder coating layer, or an exposed grain surface. Typically along the coarse support grains where silica-enriched crystalline phases form are associated depressions which often mark the initiation site for microcrack formation(s) along the binder coating surface.

Bubble formations in the binder phase are evident at the silicon carbide grain-binder ligament post areas. Frequently cracks occur along the surface of the bubbles, indicating that out-gassing has occurred from what was expected to be the release of carbon dioxide from reaction of diffused oxygen and/or steam through the binder coating with the surface of the silicon carbide grain.

Infrequently "patchy" rod-like crystalline phases (i.e., mullite) are evident within the binder phase that coats the coarse support silicon carbide grains of the Vitropore 442T filter matrix that was exposed for 512 hours to the 830° C CFBC gas environment. The presence of the rare earth additives used in the manufacture of the Vitropore 442T filter matrix is also evident in the rod-like mullite features.

Moving toward the ID surface of the 512 hour, 830° C CFBC-exposed matrix are areas of the binder phase that have undergone extensive crystallization. In these areas the crystallized binder appears to be lifted and is somewhat detached from the underlying binder phase and/or surface of the silicon carbide grain. XRD analysis of the Vitropore 442T matrix after 512 hours of

exposure to the CFBC gas environment identifies the presence of α-SiC as a major phase, traces of cristobalite (<5%), mullite (~5%), and very little glass.

After 1,026 hours of exposure to the 830° C CFBC gas environment, extensive surface crystallization of the Vitropore 442T binder phase is evident. Crystallization continues to result in the formation of a silica-enriched phase (i.e., cristobalite). Void formations are readily evident along the surface, as well as throughout the binder ligament posts. Surface and internal ligament holes are expected in part to reduce the bulk strength of the CFBC-exposed Vitropore 442T matrix.

Due to existence of creep crack growth and elongation of the Vitropore 442T filters in the bottom plenum after 512 and 1,026 hours of exposure in the 830° C CFBC gas environment, all candles were removed and replaced with new Vitropore 442T candles. The W-APF system was then operated for an additional 315 hours at nominal temperatures of 830° C. Candle filters located in the top and middle plenums accumulated 1,341 hours of test operation. Post-test inspection of the W-APF Vitropore 442T candle arrays indicated that one candle from the top plenum, and another candle from the middle plenum had failed as a result of creep crack growth (i.e., crack formation(s) below the hemispherical flange; absence of ash bridging), while an additional ten (10) candles from the top and middle plenums showed evidence of creep growth cracks below the flange of each filter body. Elongation of the candles (i.e., 2-35 mm) resulted within the top and middle plenum filters. Characterization of the residual filter bulk material strength, changes within the microstructure, and creep crack propagation will be initiated when the 315 and 1,341 hour CFBC-exposed Vitropore 442T candles become available.

Characterization of the Dia Schumalith F40 Clay Bonded Silicon Carbide Candle Filters after Exposure in the W-APF System at the AEP PFBC Test Facility in Brilliant, Ohio (Test Segments 1, 2, and 3). Hot gas filter operation of the W-APF system at the AEP PFBC Demonstration plant was conducted in three test campaigns in which Schumacher Dia Schumalith F40 clay bonded silicon carbide candle filters were exposed to PFBC process gases at temperatures of 732° C for periods of 464, 1,296, and 1,278 hours (i.e., 3,038 hours of total test operation). Irrespective of the manner in which the Dia Schumalith F40 matrix was manufactured (i.e., higher initial bulk material strength as a result of high firing procedures, etc.), the clay bonded silicon carbide matrix tends to initially lose bulk material strength, and stabilize to a conditioned strength after extended operating time (Figure 4). Preliminary bulk material strength characterization as determined by room temperature and process temperature C-ring compressive and tensile testing indicates comparable strengths of the matrix after 3,038 hours of hot gas filtration as after 1,760 hours of hot gas filtration in the 732° C PFBC gas environment (Table 9). Typically a greater loss of bulk material strength appears to occur along the ID surface of the 15 mm Dia Schumalith F40 filter wall (Table 10), implying that the matrix has undergone thermal fatigue as a result of contact with the cold pulse cleaning gas.

During the course of 3,038 hour PFBC exposure, the fibrous aluminosilicate OD membrane remained intact, preventing fines penetration into the candle filter wall. SEM/EDAX characterization of the matrix indicates that with prolonged filtration at temperatures of 732° C, the clay bonded silicon carbide matrix undergoes extensive crystallization of the binder phase that coats the silicon carbide grains. A silica-enriched phase (i.e., cristobalite) forms as a continuous layer or "crust" (i.e., ~5 μm) along the binder coating that

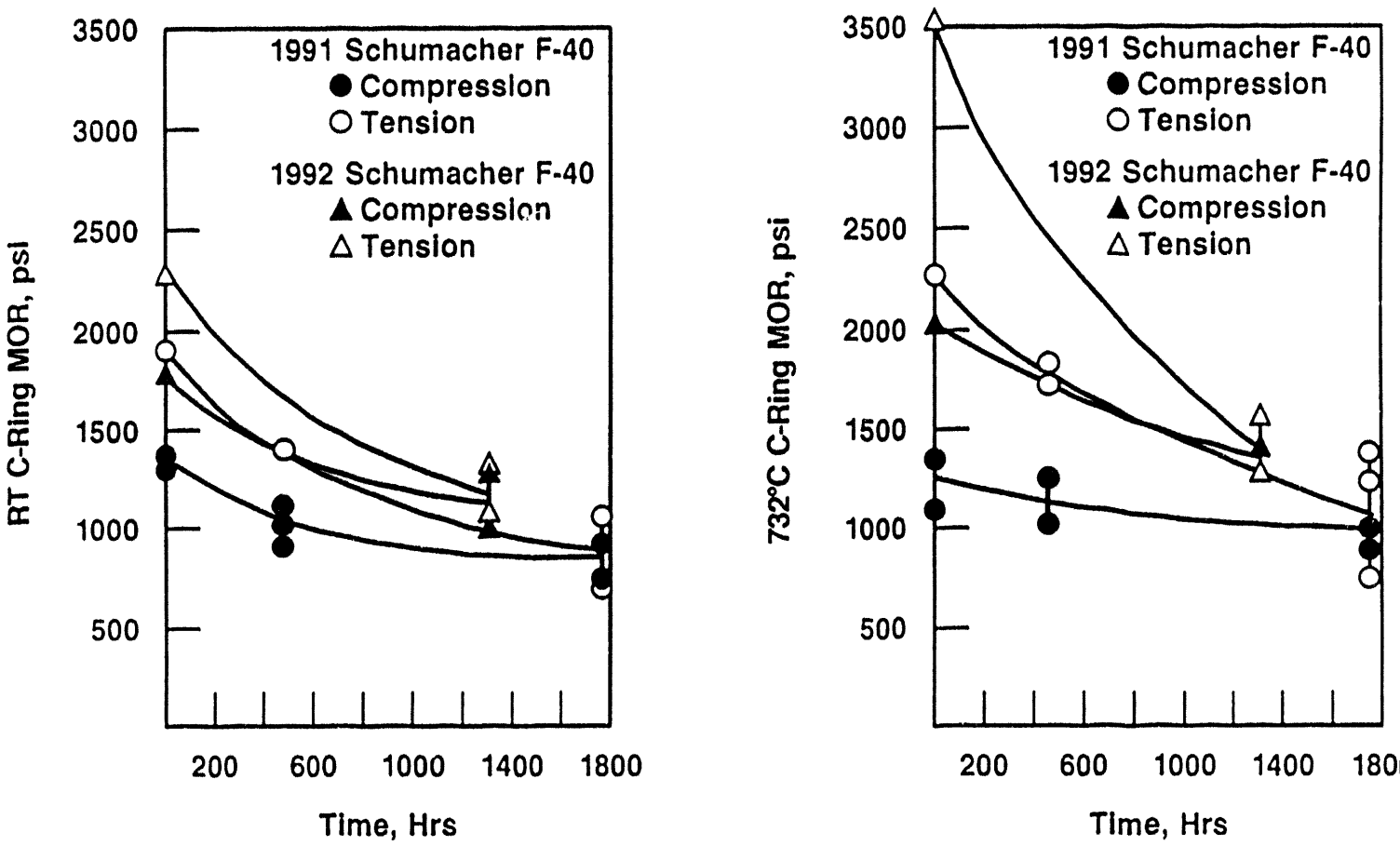


Figure 4. Residual Bulk Strength of the Dia Schumalith F40 Clay Bonded Silicon Carbide Matrix After Exposure in the AEP PFBC Gas Environment

Table 9. Residual Bulk Strength of the Dia Schumalith F40 Matrix as a Function of Exposure Time in the AEP PFBC Gas Environment

Production Lot	PFBC Temp., °C	PFBC Time, Hrs	Room Temperature Strength, psi C-Ring Compression	Room Temperature Strength, psi C-Ring Tension	Hot Strength (730°C), psi C-Ring Compression	Hot Strength (730°C), psi C-Ring Tension
1991	732	464	1083±148	1438±108	1137±101	1778±246
			1140±120	1424±162	1132±112	1873±174
1991	732	1760	908± 72	1117± 91	1064±72	1418±122
			794± 50	709± 71	1028±94	973±121
			793± 58	711± 89	989±77	885± 54
			793± 39	1016±134	968±96	1252±241
1991	732	3038	720± 57	944±172	890±65	1284±199

Table 10. Percent Strength Retention in PFBC-Exposed Dia Schumalith F40 Clay Bonded Silicon Carbide Candle Filters

Production Lot	Temp., °C	Time, Hrs	Test Segment	Room Temperature C-Ring Compression	Room Temperature C-Ring Tension	Hot Strength, 732°C C-Ring Compression	Hot Strength, 732°C C-Ring Tension
F40 1991	732	464	1	85	75	83	78
F40 1991	732	1,760	1,2	64	47	72	49
F40 1991	732	3,038	1,2,3	56	50	63	55
F40 1992	732	1,294	2	64	54	69	43
F40 1992	732	2,574	2,3	63	51	75	49

originally encapsulated the silicon carbide grains. Below the silica-enriched phase are what appears to be mullite-like rod formations. Mullite is considered to result from the crystallization of alumina and silica that was originally present in the binder. Further effort will be required to determine if oxidation of the silicon carbide grain has occurred, as well as any variations in the microstructure that may have resulted throughout the 15 mm Dia Schumalith F40 candle filter wall.

The complete or nearly complete crystallization of the binder phase, leading to what appears to be a stable binder phase, is considered to be responsible for the bulk material strength conditioning that results after extended exposure of the Dia Schumalith F40 matrix in the 732 ° C PFBC gas environment.

Summary. Each of the first generation porous ceramic candle filters have performed as complete barrier filters, preventing fines penetration into the clean gas passages of the W-APF systems. As complex ceramic matrices, the alumina/mullite and clay bonded silicon carbide filters undergo numerous phase changes (i.e., crystallization) that result from contact with the high temperature process gas environment. The progressive phase changes and/or crystallization that occurs is considered in part to lead to the early conditioning or stabilization of the bulk material strength. For both the alumina/ mullite and Vitropore 442T matrices at 900 ° C, thermal fatigue appears to initially reduce the bulk material strength along the candle filter ID surface. The effects of thermal fatigue appears to be mitigated in the Vitropore 442T matrix at CFBC operating temperatures of 830 ° C, while our most recent information indicates that thermal fatigue occurs along the ID surface of the Dia Schumalith F40 matrix at PFBC temperatures of 732 ° C. Evidence of microcrack formations through the structural matrix of the alumina/ mullite filter material can be readily seen, while difficulty is encountered in attempting to establish the existence of extensive microcrack formation within the clay bonded silicon carbide filter materials.

The manner in which each of the candle filter elements has failed during process operation is relatively unique.[1,2] For the alumina/mullite candle filters, thermal shock events resulting from process system transient (i.e., fuel ignition events, etc.), led to thermal-mechanical fracture of the brittle ceramic matrix through the formation of longitudinal cracks which traversed large lengths of the candle filter body. For the Vitropore 442T matrix, creep crack growth and elongation of the filter body at temperatures of 830 ° C led to failure of the candle body directly below the hemispherical flange. Frequently bowing or bending of the Vitropore 442T matrix was observed in the absence of ash accumulation or bridging. For the Dia Schumalith F40 matrix, extensive bowing of the matrix can be observed at temperatures of 732 ° C when extensive ash bridges form between adjacent candle filters. The accumulation of ash frequently causes failure of the filter elements during cool-down of the W-APF units, resulting in fresh fracture of the filter elements immediately below the hemispherical flange of the candles.

As technology moves forward to mitigate ash bridging within the filtration systems, and process operations are maintained to reduce the impact of thermal transients, operation of the filtration systems can be expected to surpass the number of hot gas filtration hours already accumulated via the existing alumina/mullite and clay bonded silicon carbide filters. It will then be possible to demonstrate the actual filter operating life of these materials, in view of the phase changes that occur during the initial hours of hot gas filtration. Long-term effects of gas phase alkali if released into the filtration system, gaseous sulfur dioxide, trioxide, carbonyl, and hydrogen sulfide, and volatile chlorides, as well as ash or char particulates, can then be

investigated in order to demonstrate the ultimate stability and operating life of the porous ceramic filter materials.

Surveillance Coupons. Two separate filter sample surveillance baskets were fabricated for installation at the AEP PFBC site, each of which contained samples of the following porous ceramic filter materials: Coors P-100A and P-100A-1 alumina/mullite; Refractron 505; Schumacher Dia Schumalith F40; Coors mullite; GTE cordierite and cordierite-silicon carbide; and AirResearch sintered silicon nitride. Each material was positioned along an 0.5 in SS316 rod, and was separated via either a Fiberfrax layer or a Nextel 312/MM mat gasket. Inconel 600 metal end plates and a surrounding wire mesh cage were used to fabricate the surveillance baskets which contained the filter material coupons.

One of the surveillance baskets was positioned above the freeboard area in the AEP combustor, while the second surveillance basket was positioned above the tubesheet in the W-APF vessel at AEP. All material samples appeared to remain intact, retaining their physical integrity after ~6,000 hours of exposure in the 815-843 ° C (1500-1550 ° F) freeboard area, as well as after ~3,038 hours of exposure in the ~732 ° C (1350 ° F) W-APF tubesheet area. Characterization of these materials will be initiated after the surveillance baskets have been removed from the freeboard and tubesheet areas during the scheduled September-October 1994 maintenance period.

A similar surveillance coupon array was fabricated and placed above the W-APF tubesheet during the first week of June 1994. This array contained samples of the second generation porous ceramic filter materials which included: DuPont filament wound PRD-66; DuPont SiC-SiC continuous fiber ceramic composite (CFCC); 3M CVI-SiC; Pall Vitropore 442T and clay bonded mullite; Brunswick calcium aluminosilicate; Ultramet CVI-SiC reticulated foam; Third Millennium sintered silicon carbide; and swatches of the 3M Nextel 312 and 550 cloth which are utilized in the manufacture of ceramic filter bags or which serve as the structural support fiber or woven braid in the 3M CVI-SiC ceramic composite candle.

Accelerated Thermal Fatigue Testing

Accelerated pulse testing of as-manufactured Coors alumina/mullite, Schumacher Dia Schumalith F40 clay bonded silicon carbide, and Pall Vitropore 442T clay bonded silicon carbide 1.5 m candle filters was completed under high temperature, high pressure (HTHP), simulated pressurized fluidized-bed combustion (PFBC) gas conditions at Westinghouse. In addition two alumina/mullite candle filters which had been exposed for 227 and 716 hours in the circulating fluidized-bed combustion (CFBC) gas environment in the W-APF system in Karhula, Finland, were also tested with the as-manufactured candle filters. Each filter was subjected to temperatures of 843 ° C (1,550 ° F), system pressures of 100 psig, and either 771 or 10,000 simulated pulse cleaning cycles. Air was utilized as the pulse gas media. During HTHP testing, the pulse duration was 0.4 sec, with 1.5 minute intervals between each delivered pulse. The thermal duty of the pulse gas was 25-50 Btu/pulse-ft^2, typical of the pulse gas thermal load used in the W-APF system at AEP. All of the first generation monolithic candle filters remained intact during the entire 10,000 pulse cycle test. Cracks were not visibly evident along any of the filters after testing had been completed.

As shown in Figure 5, a greater loss of bulk material strength in the alumina/mullite, Vitropore 442T and Dia Schumalith F40 materials generally resulted along the ID surface of the candle filters, implying thermal fatigue of the matrices had occurred primarily as a result of

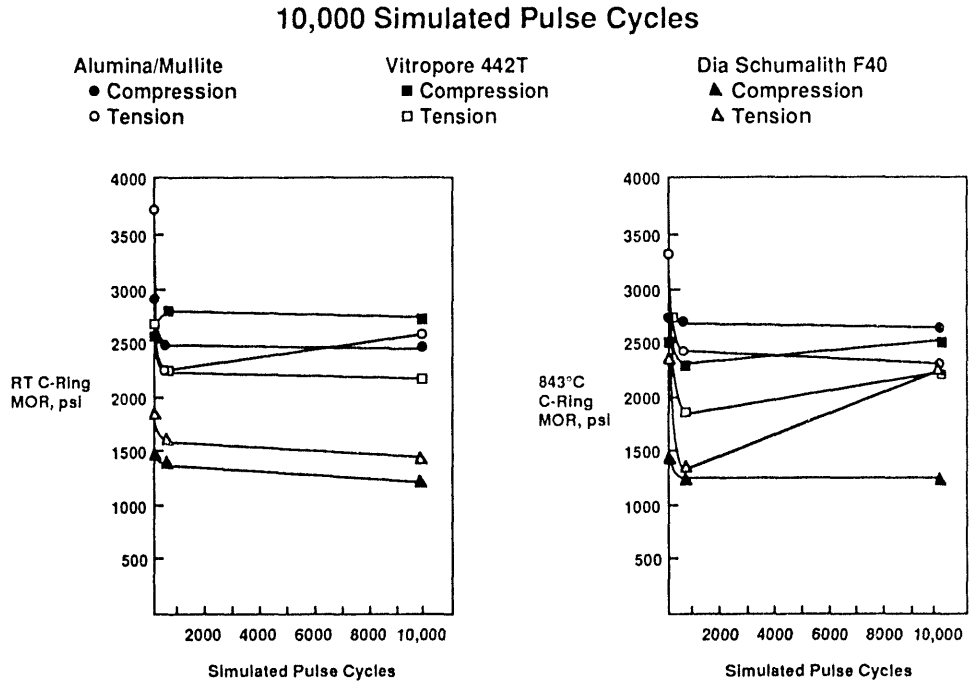


Figure 5. Accelerated Thermal Fatigue Testing

contact with the cold pulse gas. Conditioning of the matrices appears to rapidly occur during the accelerated thermal cycling life of the filters (i.e., <771 pulse cycles). Similar conditioning of the filter matrices was evident in the field-tested filter materials.

Candle filters which were subjected to the entire 716 hours of test operation in the CFBC gas environment, including the initial fuel ignition event, in Karhula, Finland, were similarly exposed to 10,000 additional pulse cycles in the W-HTHP test facility. As shown in Table 11, the room temperature OD surface strength of the CFBC-exposed, 10,000 pulse cycled candle appears to be comparable with that of the 716 hour CFBC-exposed candle filter. The data indicate that the additional 10,000 pulse cycles further reduces the room temperature ID wall strength by 30%. At process temperatures of 843 ° C, the CFBC-exposed, 10,000 pulse cycled candle appears to strengthen along its OD surface, while a 15-25% reduction in bulk material strength is observed along the alumina/mullite ID wall.

Cross-sectioning of the 716 hour CFBC-exposed, 10,000 accelerated pulse cycled alumina/mullite candle filter revealed the existence of a circumferential crack that was located at ~1 mm from the candle's ID surface. The crack morphology typically resembled spalling of the surface of a ceramic component which is initially at high temperature and is then rapidly cooled by contact with water or room temperature air. The location of the resulting circumferential crack confirms the Westinghouse thermal stress model calculations which identifies the location of maximum stress within the porous ceramic filter matrix during pulse cleaning as 1-2 mm from the ID surface.[2]

Candles that were installed in the later segment of the hot gas filtration test at Karhula did not experience the fuel ignition event. The

Table 11. Accelerated Thermal Fatigue Testing

CFBC-Exposed Alumina/Mullite
10,000 Simulated Pulse Cycles

Candle ID	CFBC Process		Simulated Pulse Cycling		Room Temperature Strength		Hot Strength	
	Temp., °C	Time, Hrs	Cycles	Temp., °C	C-Ring Compression, psi	C-Ring Tension, psi	C-Ring Compression, psi	C-Ring Tension, psi
AC-128 RA (T3)	900	572*	—	—	2195 ± 147	1512 ± 181	2118 ± 129(a)	1283 ± 139(a)
AC-122RB (M27)	900	227*	10,000	843	2380 ± 117	2445 ± 299	2652 ± 196(b)	1916 ± 239(b)
AC-135RB (M26)	900	227*	10,000	843(c)	2137 ± 97	2005 ± 133	2354 ± 246(b)	1808 ± 269(b)
AC-274 (B19)	900	716**	—	—	2369 ± 147	2469 ± 503	2254 ± 208(a)	1900 ± 170(a)
AC-162 (M32/M31)	900	716**	10,000	843	2389 ± 106	1766 ± 188	2617 ± 152(b)	1601 ± 250(b)
AC-206 (M28/M32)	900	716**	10,000	843(c)	2474 ± 120	1701 ± 118	2565 ± 150(b)	1407 ± 111(b)

* Later Portion of CFBC Test Segment, Excluding Fuel Ignition Event
** Complete CFBC Test Segment, Including Fuel Ignition Event
(a) Hot Strength Testing at 900°C
(b) Hot Strength Testing at 843°C
(c) Failsafe/Regenerator Device Included

post-fuel ignition event candle that was used as our background material strength had 572 hours of CFBC operation, while our post-fuel ignition event CFBC-exposed candles which underwent an additional 10,000 pulse cycles had only experienced 227 hours of CFBC operation. The difference in CFBC operation of 227 versus 572 hours is expected to provide some variation in the strength of the ceramic matrix, making any comparison of the CFBC-exposed and CFBC-exposed, 10,000 pulse cycled candle strength results somewhat difficult. Clearly the 572 hour CFBC-exposed candle had initially lower room temperature and hot strengths along both ID and OD surfaces in comparison to the 227 hour CFBC-exposed, 10,000 pulse cycled candle.

Interrupted Static and Dynamic Fatigue Testing

The propensity for flaws to grow in ceramics at applied stress intensities (K_{app}) well below the critical stress intensity (K_{Ic}) has been established. For dense silicon carbides and nitrides, as well as ceramic fibers, a threshold stress intensity (K_{Th}) above which cracks grow and below they do not grow can be established. These values have been estimated using a combination of two experimental techniques – the stressing rate dependence of strength (dynamic fatigue) and interrupted static fatigue testing. The first technique provides an estimate of the stress level required for crack growth and, using this value, the effects of sustained static stress in the range of this estimate on the strength distribution of sample materials subjected to static stress and then rapidly fractured provides a realistic estimate of the threshold stress and, thus K_{Th}, if K_{Ic} is known. For opaque, complex materials, the crack growth cannot be measured directly, so indirect techniques such as these must be used.

Approach. Dynamic fatigue testing was conducted at 800° C and 900° C to assess the stressing rate dependence of strength for the

alumina/mullite and Vitropore 442T clay bonded silicon carbide filter matrices. If materials exhibit slow crack growth, then strength increases will be observed with increasing stressing rates. At faster stressing rates, there is less time for slow crack growth (SCG) to occur and thus higher strengths are observed.

The crack growth velocity (v) has been shown to be described empirically by the following exponential relationship:

$$v = A K_I^N \tag{1}$$

where K_I is the stress intensity is raised to the power of N (the susceptibility for SCG), and A is the pre-exponential constant. In the absence of a threshold stress intensity for SCG, the dependence of the strength (σ_f) of the material on stressing rate ($\dot{\sigma}$) is given by the following expression:

$$\sigma_f = \left(B\,(N+1)\,\dot{\sigma}\,S_i^{(N-2)}\right)^{1/(N+1)} \tag{2}$$

where S_i is the inert strength (strength in the absence of any SCG), and B is a constant that is related to the crack geometry (Y), the critical stress intensity or fracture toughness (K_{Ic}), and the two SCG parameters (A and N, given in equation 1) via the expression:

$$B = \frac{2}{A\,Y^2\,(N-2)\,K_{Ic}^{(N-2)}} \tag{3}$$

By measuring the strength of a material using a range of stressing rates, typically several orders of magnitude, and plotting the natural log of the average strength as a function of the natural log of the stressing rate, the SCG susceptibility parameter N can be determined from the slope of the regression line which is equal to 1/(N+1). B and subsequently A are then evaluated based on the intercept of the regression.

If a material exhibits a threshold stress intensity for SCG, then the dependence of stress on stressing rate is expressed as follows:

$$\sigma_f = \frac{K_{Th}}{Y\sqrt{c_i}}\left[1 + \frac{2\,Y\,(N+1)\,\dot{\sigma}\,c_i^{3/2}}{A\,(N-2)\,K_{Th}^{(N+1)}}\right]^{1/(N+1)} \tag{4}$$

where c_i is the initial crack size prior to slow crack growth. The initial crack size, when possible, should be measured directly from the fracture surface of sample. However, this can prove to be a very formidable, if not impossible, task for highly porous materials such as the candle filter materials.

While the dynamic fatigue tests are used to estimate the SCG parameters, the interrupted static fatigue tests are needed to identify the existence of a threshold stress intensity for SCG. The interrupted static fatigue technique involves loading samples to and holding the stress level constant such that the average nominal stress intensity is below the critical stress intensity, but near the threshold stress for SCG, for a certain length of time (typically 1 to several hundred hours).

The choice of static stress levels can be approximated from the results of dynamic fatigue testing. For example, if the dynamic fatigue tests yield decreasing strengths with decreasing stressing rates followed by an apparent strength independence or strength increase at the slowest stressing rates, then a threshold for SCG and/or other mechanisms (i.e., crack blunting) may be operative. If the dynamic fatigue results exhibit

such a behavior, then stress levels in the range of the lowest stresses that exhibited a dependence of stressing rate should be used for the static fatigue tests.

The objective of the interrupted static fatigue tests is to identify stress levels at which some of the material samples survive for the entire hold period and are subsequently loaded to failure, and some of the material samples fail during the static hold period. Stress levels where mixed behavior (i.e., survival and failure) is observed indicate the possible existence of a threshold stress intensity for SCG. Several stress levels and possibly several hold times are needed to accurately determined the threshold stress intensity for SCG. In parallel with this effort, models are being developed to assure that the true thresholds are being determined.

Finally, the critical stress intensity was measured using a single edge-notched C-ring technique at both 800 ° C and 900 ° C. A notch was machined into the outer surface of the C-ring at the location of the maximum tensile stress. The notch depth was approximately 20% of the thickness of the C-ring. The sample was then heated to the test temperature, held for fifteen minutes to thermally equilibrate the porous ceramic filter matrix, and was subsequently loaded to failure. The failure load, notch depth and sample dimensions were then used to determined the critical stress intensity or fracture toughness for each material. The ratio of the threshold stress intensity to the critical stress intensity is directly related to the ratio of the threshold stress to critical fracture stress. These ratios can be used as the basis for filter design criteria.

Results

Dynamic Fatigue. Strengths as a function of stressing rates were measured for both materials at 800 ° C and 900 ° C in air. Table 12

Table 12. Average Strength and Weibull Parameters for Alumina/Mullite and Vitropore Candle Filter Materials at 800 ° C and 900 ° C

	800°C			900°C			SLOW CRACK GROWTH PARAMETERS			
STRESS RATE (psi/sec)	AVERAGE STRENGTH (ksi) (MPa)	m*	σ_0† (ksi) (MPa)	AVERAGE STRENGTH (ksi) (MPa)	m*	σ_0† (ksi) (MPa)	N	B (MPa^2/min)	A	K_{Ic}‡ (MPa√m)
ALUMINA/MULLITE								800°C		
10^{+3}	3.1±0.4 21.2±3.0	11.6	3.4 23.1	2.4±0.2 16.6±1.4	23.9	2.5 17.1	48	3.43	25.08	0.84
10^{+2}	2.9±0.2 20.0±1.6	19.1	3.1 21.1	2.8±0.3 19.5±2.2	12.9	3.0 20.9		900°C		
10^{+1}	2.8±0.1 19.3±0.9	32.0	2.9 20.1	2.6±0.3 17.7±2.4	10.2	2.7 18.8	15	8.47	0.01	1.00
1	2.9±0.3 19.7±2.0	10.1	3.0 20.8	2.1±0.1 14.6±1.1	15.9	2.2 15.5				
VITROPORE										
17,000	3.3±0.1	22.8	3.4					800°C		
	22.7±1.0		23.2				18	0.79	1.67	0.82
1,700	3.4±0.1 23.6±1.0	27.9	3.5 24.0	2.7±0.2 18.6±1.4	17.5	2.8 19.2				
850				2.6±0.2 17.8±1.2	17.7	2.7 18.3		900°C		
170	3.1±0.1 21.1±0.8	34.6	4.0 27.5	2.7±0.3 18.8±1.9	10.9	2.8 19.2	13	0.98	2.86	0.75
17	2.7±0.3 18.5±2.3	8.7	2.8 19.6							

* Weibull modulus based on maximum likelihood regression method
† Characteristic strength based on maximum likelihood regression method
‡ Single Edge Notched C-ring Technique

lists both the average stresses and Weibull parameters obtained for each stressing rate. In addition, Table 12 also identifies the slow crack growth parameters based on Equations 2 and 3. Figures 6 and 7 show the strength dependence as a function of stressing rate for the alumina/mullite and Vitropore 442T clay bonded silicon carbide C-rings, respectively. At 800 ° C the alumina/mullite matrix exhibited decreasing strength with decreasing stressing rate for the three fastest stressing rates, followed by a strength increase for the slowest stressing rate. This strength increase may be indicative of crack blunting suggesting the possible existence of a threshold stress intensity. Based on these results, interrupted static fatigue studies were conducted using stress levels ranging between 2,500 and 3,000 psi.

At 900 ° C, decreasing strengths with decreasing stressing rates were observed for the alumina/mullite filter matrix for the three slowest stressing rates. Unlike the 800 ° C results, no strength increase was observed at the slowest stressing rate. However, an apparent strength decrease was observed for the highest stressing rate. The exact cause of this behavior is not known. It is likely that the decrease in strength may in part be due to the electronic limitations of the Instron testing machine. The Instron may not be able to capture the true peak load at failure for C-rings tested using the fastest stressing rate. However, this does not explain why similar behavior was not observed for the alumina/mullite C-rings tested at 800 ° C using the fastest stressing rate. Due to the uncertainty of the failure loads at the highest stressing rate, only the data for the slowest three stressing rates at 900 ° C were used to estimate the SCG parameters. At 800 ° C, the data for the slowest stressing rate was not used to estimate the SCG parameters, since a crack blunting mechanism may be operative and dominant over any SCG mechanisms.

Based on these results (Figure 6) and Equations 2 and 3 (assuming no threshold stress intensity), N values of 48 and 15, were estimated at 800 ° C and 900 ° C, respectively. The higher the N value the less susceptible a material is to SCG. Thus, increasing the temperature by 100 ° C significantly increases the susceptibility for SCG for the alumina/mullite material.

Dynamic fatigue tests conducted at 800 ° C and 900 ° C for the Vitropore 442T material (Figure 7) were complicated by the onset of creep, which was observed using the slowest stressing rate at 800 ° C and the two slowest stressing rates at 900 ° C. Due to the electronic limitations of the Instron, higher stressing rates did not yield accurate stress measurements (i.e., strengths decrease for fastest stressing rate at 800 ° C). Thus, one-half order of magnitude increments in stressing rates were used to test the Vitropore 442T clay bonded silicon carbide C-rings at 900 ° C.

The estimated SCG parameters listed in Table 12, were obtained using the middle three stressing rates (slowest rate not shown because material crept), and the fastest two rates at 900 ° C. Unlike the alumina/mullite material, the Vitropore 442T material did not exhibit a large reduction of N with an increase in temperature from 800 ° C to 900 ° C. However, the creep behavior at the slower stressing rates limited the estimate of the N value to strengths obtained at two stressing rates. The SCG parameters are being used to model the static fatigue behavior of the clay bonded silicon carbide Vitropore 442T candle filter matrix.

Static Fatigue. The preliminary indications of a threshold for sub-critical crack growth for the alumina/mullite material at 800 ° C are shown in Figure 8. Superimposed on this figure are the results of the static fatigue tests from the previous Weibull strength distribution plot for the dynamic fatigue data (open squares) obtained using the

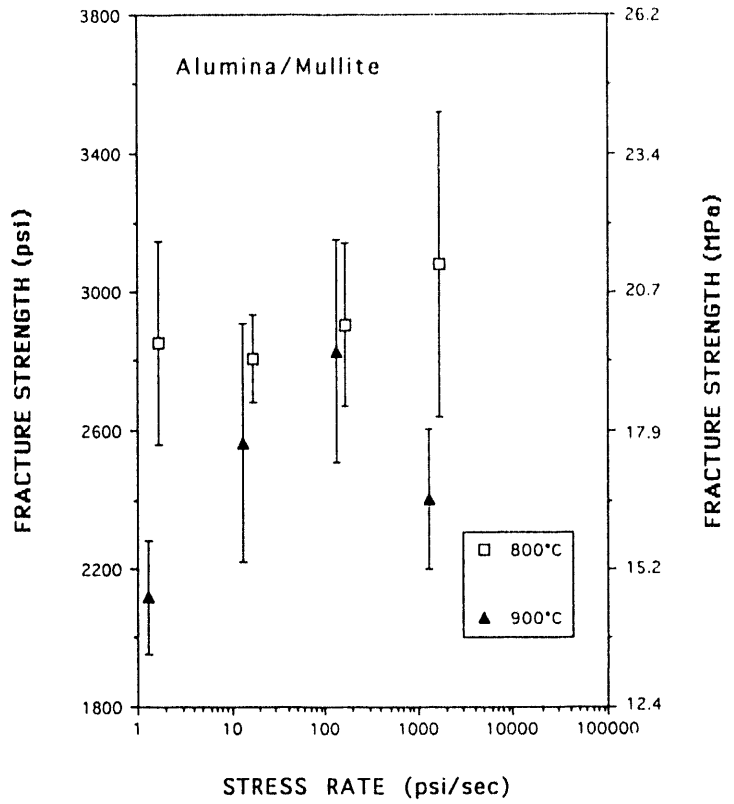


Figure 6. **Dynamic Fatigue Strength Data as a Function of Temperature for Alumina/Mullite. Errors Bars Represent One Standard Deviation Based on 10 Samples/Stress Rate**

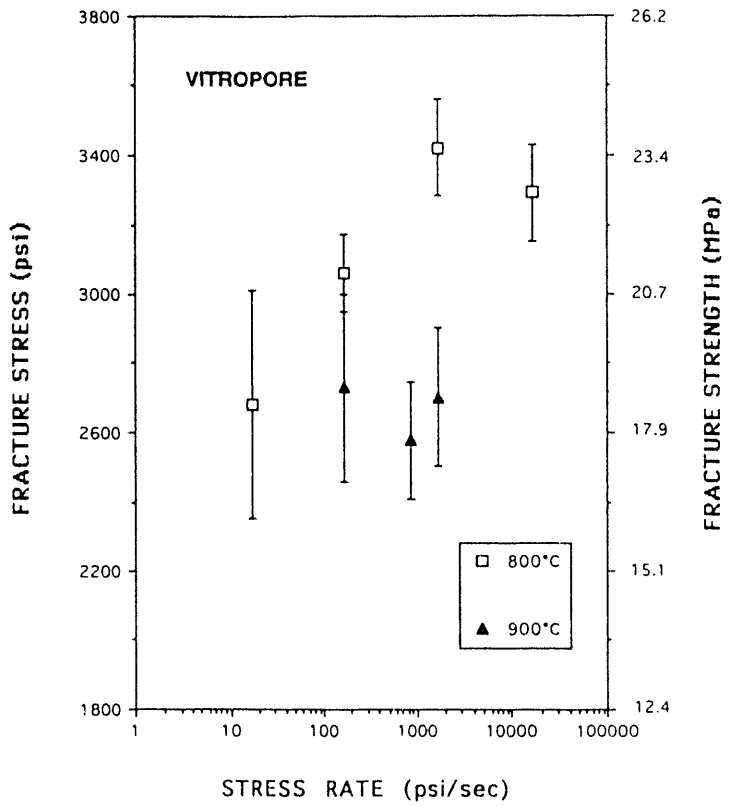


Figure 7. **Dynamic Fatigue Strength Data at 800 ° C and 900 ° C for Vitropore 442T C-Rings Loaded in Compression. Error Bars Represent One Standard Deviation Based on 10 Samples/Stress Rate**

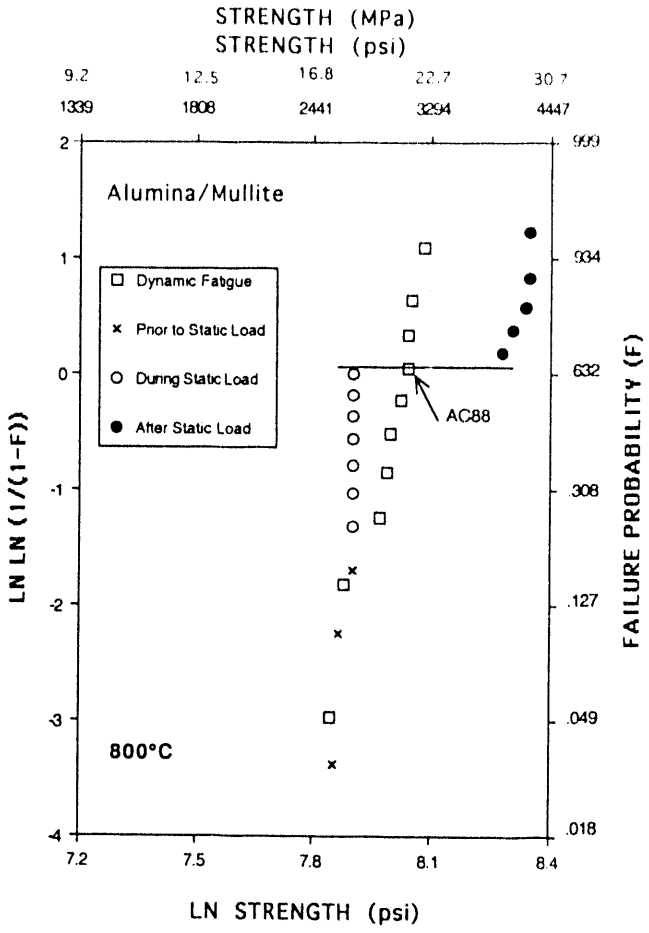


Figure 8. Weibull Strength Distribution of Both the Dynamic Fatigue C-Rings Tested Using a Loading Rate of 0.05 in/min, and the Results of Interrupted Static Fatigue Tests for the Alumina/Mullite Matrix at 800° C Using a Stress of 18.6 MPa (2700 psi)

same loading rate (0.05 in/min). Samples that failed while loading to the static stress (represented by the symbol x) exhibited a strength distribution equivalent to the dynamic fatigue data. In contrast, material samples that survived (solid circles) exhibited significant apparent strengthening (~40%) as compared to the strength distribution from the dynamic fatigue tests. The material samples that failed during the 10 hour static hold (open circles) represent the transition between those samples that exhibited fast fracture (stress intensities greater than the threshold for SCG), and those material samples that survived (stress intensities less than the threshold for SCG). These results indicate that a stress of 2,700 psi (18.6 MPa) yields stress intensities that straddle K_{Th} for the size C-rings used in this study at 800° C. Future modeling efforts will attempt to confirm these conclusions.

The cross-over point for this transition in strength behavior of the alumina/mullite filter matrix, illustrated by the horizontal line in Figure 8, is represented by the alumina/mullite filter matrix obtained from candle filter AC88. Based on the measured fracture toughness (K_{Ic}) of 0.84 MPa$\sqrt{m}$ and the fracture stress (σ_f) of 20.8 MPa (3,013 psi) for the alumina/mullite filter matrix, a flaw size (C) of ~1,060 μm was determined via the following expression:

$$K_{Ic} = 1.24\ \sigma_f \sqrt{C} \qquad (5)$$

where 1.24 is a constant for the crack geometry (Y) based on the elliptical integral of the second kind for a semi-elliptical surface flaw. Flaws greater than 1,060 μm presumably grew and caused catastrophic failed, while flaws smaller than 1,060 μm were blunted. Thus, the initial estimate of the K_{Th} is 0.75 MPa$\sqrt{m}$ based on the flaw size of 1,060 μm and the static stress of 18.6 MPa (2,700 psi). The value is a very high fraction of the critical stress intensity (fracture toughness, K_{IC}) indicating that slow crack

growth will apparently only occur at stresses that are a high fraction of the short term fracture stress ($\sigma_{Th}/\sigma_{Ic} = K_{Th}/K_{Ic}$).

To date, static fatigue tests on ten alumina/mullite C-rings at 900° C using a static stress to 1,800 psi (12.4 MPa) exhibited mixed behavior: five material samples survived, and five failed during the 10 hour static hold with time-to-failure ranging from 45 to 356 minutes. For those material samples that survived and were subsequently loaded to failure, the average strength was 3,450 ± 133 psi (23.7 ± 0.9 MPa), which represent an apparent strength increase of ~22%.

The indications of a threshold for sub-critical crack growth in the alumina/mullite material at 900° C are shown in Figure 9. Superimposed on this figure are the results of the static fatigue tests from the previous Weibull strength distribution plot for the dynamic fatigue data (open squares) obtained using the same loading rate (0.05 in/min). Material samples that survived (solid circles) exhibited significant strengthening (~22%) as compared to the strength distribution from the dynamic fatigue tests. Material samples that failed during the 10 hour static hold (open circles) represent the transition between those samples that exhibited fast fracture (stress intensities greater than the threshold for SCG), and those samples that survived (stress intensities less than the threshold for SCG). These results indicate that a stress of 1,800 psi (12.4 MPa) yields stress intensities that straddle K_{Th} for the size C-rings used in this effort at 900° C. Future modeling will attempt to confirm these results.

The cross-over point for this transition in the strength behavior of the alumina/mullite filter matrix, illustrated by the horizontal line in Figure 9, is represented by the alumina/mullite filter matrix obtained from candle filter AC38. Based on the measured fracture toughness (K_{Ic}) of 1.0 MPa$\sqrt{m}$, and the fracture stress (σ_f) of

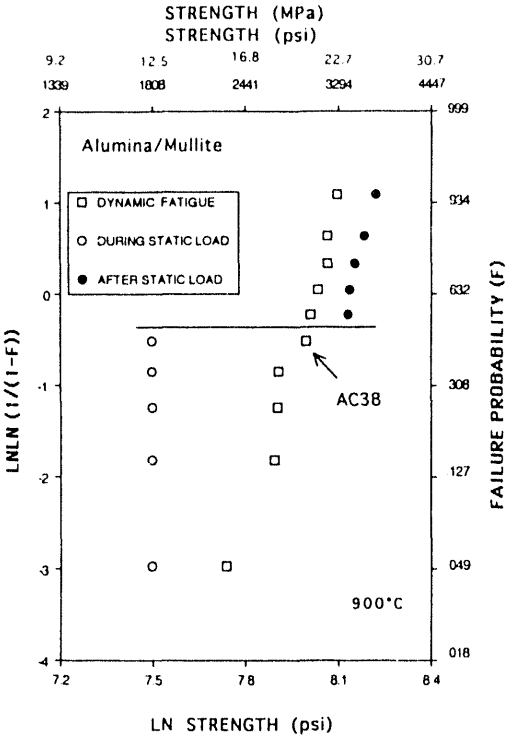


Figure 9. Weibull Strength Distribution of Both the Dynamic Fatigue C-Rings Tested Using a Loading Rate of 0.05 in/min, and the Results of Interrupted Static Fatigue Tests for the Alumina/Mullite Matrix at 900° C Using a Stress of 12.4 MPa (1800 psi)

19.5 MPa (2,827 psi) for the alumina/mullite filter matrix, a flaw size (C) of ~1,710 μm was determined via Equation 5. Flaws greater than 1,710 μm presumably grew and caused catastrophic failure, while flaws smaller than 1,710 μm were blunted. Thus, the initial estimate of the K_{Th} is ~0.51 MPa$\sqrt{m}$ based on the flaw size of 1,710 μm and the static stress of 12.4 MPa (1,800 psi). The value, which is ~50% of the critical stress intensity (fracture toughness, K_{IC}) indicates that slow crack growth will apparently only occur at stresses that are about half of the short-term fracture stress.

As for the Vitropore 442T clay bonded silicon carbide matrix, creep behavior is observed under static load condition for temperatures ranging from 800° C to 900° C. Testing was aborted after ~2 hours because the C-ring completely collapsed the notch (initial notch width of ~0.5 in). Examination of the sample revealed no visible evidence of creep crack formation on the outer surface.

Even at 800° C, significant creep occurs so as to render the elastic stress solutions invalid. This was evident after re-examining the extend of crosshead travel during the 800° C testing. In contrast to the alumina/mullite material, which exhibited essentially no travel (0-0.001 in) during the static hold, the Vitropore 442T material tested at 800° C exhibited two orders of magnitude greater crosshead travel than the alumina/mullite material. Although a constant load was maintained at 800° C for the Vitropore 442T material, the extent of crosshead travel indicates that creep was operative. The stress redistribution associated with creep, yields a non-constant stress, despite a constant applied load.

In addition to the problem associated with creep, further complications are involved due to apparent material variations among the rings machined from the various candle filters which demonstrated different resistances to crack growth.

Fracture Toughness. Fracture toughness measurements were made using the single edge notched C-ring technique for both materials at 800° C and 900° C (Table 12). While the Vitropore 442T material exhibited a slight decrease in toughness with increasing temperature, the alumina/mullite showed a slight strength increase.

Conclusions. The results of the dynamic fatigue tests indicate that both materials exhibit slow crack growth. The alumina/mullite material shows a large change in susceptibility to SCG (N) from 800° C to 900° C, while the clay bonded silicon carbide material (Vitropore 442T), which is more susceptible to SCG, shows only a small change in susceptibility from 800° C to 900° C.

The interrupted static fatigue tests for the alumina/mullite material have yielded encouraging results which suggest the existence of a threshold stress intensity. Modelling efforts to more accurately determine the threshold stress intensity at both 800° C and 900° C are continuing.

Due to complications of both creep behavior under static load conditions and apparent candle-to-candle variations for the Vitropore 442T material, accurate assessment of a threshold for crack growth will involve considerably more effort. The most appropriate direction to proceed in this area is currently being addressed.

FUTURE WORK

Similar to the accelerated thermal fatigue testing which was conducted in this program, the

as-manufactured alumina/mullite and clay bonded silicon carbide Vitropore 442T and Dia Schumalith F40 candle filters will be subjected to a series of thermal shock exposures in which the number and/or the severity of the thermal shock (i.e., temperature change) delivered to the filter array will be increased. Field-tested alumina/ mullite candle filters which have experienced up to 716 hours of CFBC exposure at temperature at processs operating temperatures of 900° C will also be included in this effort.

First generation candle filter surveillance coupons which have been exposed above the freeboard area of the AEP combustor, as well as above the W-APF tubesheet will be characterized in order to demonstrate the possible impact of long-term exposure to PFBC process temperatures, transients, ash and gas compositions on filter material stability. Similarly the Dia Schumalith F40 and Vitropore 442T candles which have been operated in W-APF systems at AEP and at Ahlstrom will continue to be characterized as materials become available. The information generated during both the coupon and candle filter characterization efforts will provide the underlying basis for filter life model development.

ACKNOWLEDGEMENTS

We wish to acknowledge Ted McMahon and Richard Dennis at DOE/METC for their continued support.

We also wish to acknowledge the efforts of Bob Walko for performing the destructive strength testing on the various candle filter elements. In addition we wish to extend our sincere thanks to Richard Kunkle, George Schneider, Art Fellers, Bill Kuba, Bud Kittle, John Meyer, and Joe Condle for performing the extensive bench-scale and HTHP filtration testing subtasks in this program. We also wish to acknowledge the efforts of Bob Palmquist and Tom Mullen who have performed the analytical microscopy work throughout all of our material characterization programs. A special acknowledgement is extended to J. P. Singh at the Argonne National Laboratory for his efforts in providing the CFBC-exposed alumina/mullite fracture toughness measurements. And finally we express our thanks to David L. Shelleman at Penn State for performing the static and dynamic fatigue testing.

REFERENCES

1. John D. Hoffman et al., "Tidd PFBC Hot Gas Filter Operating Experience: July 1993 - April 1994," Coal-Fired Power Systems 94 -- Advances in IGCC and PFBC Review Meeting, June 21-23, 1994, Morgantown, WV.

2. Thomas E. Lippert et al., "Karhula Hot Gas Cleanup Test Results," Coal-Fired Power Systems 94 -- Advances in IGCC and PFBC Review Meeting, June 21-23, 1994, Morgantown, WV.

8a.4 Properties of Ceramic Candle Filters

CONTRACTOR INFORMATION

Contract Number	DE-AC-21-89MC26239
Contractor	Southern Research Institute 2000 Ninth Avenue South Post Office Box 55305 Birmingham, AL 35255-5305
Contractor Project Manager	Duane H. Pontius
Principal Investigators	Duane H. Pontius H. Stuart Starrett
METC Project Manager	Thomas P. Dorchak
Period of Performance	September 9, 1993 to August 22, 1994

Schedule and Milestone

FY94 Program Schedule

	S	O	N	D	J	F	M	A	M	J	J	A
Material Characterization												
Topical Report												

BACKGROUND

The mechanical integrity of the ceramic filter elements is a key issue for hot gas cleanup systems. To meet the demands of the advanced power systems the filter components must sustain the thermal stresses of normal operations (pulse cleaning), of start-up and shut-down conditions and of unanticipated process upsets, such as excessive ash accumulation, without catastrophic failure; they also must survive the various mechanical loads associated with handling and assembly, normal operations, and process upsets. For near-term filter systems, these elements should survive at operating temperatures of 1550°F for three years.

Ceramic filter materials have proven to be less inert and durable than originally supposed. The monolithic ceramic materials are susceptible to thermal stresses and possibly slow crack growth. The clay-bonded silicon carbide particle

filters have shown substantial creep and chemical degradation of the binder material. In-service failures have occurred for both monolithic alumina mullite and clay-bonded silicon carbide materials.

OBJECTIVE

The objectives of this program have been: (1) the post-test evaluation of candle filters, (2) to measure the material properties of current filter materials, destructively and non-destructively, and to relate these properties and behaviors to in-service performance, (3) to develop an understanding of the material requirements for hot gas filter elements, (4) to develop material property goals for filter materials, and (5) to establish test matrices and a protocol to evaluate candidate filter materials. This last objective is particularly critical to the government and to potential material suppliers. An effective protocol for evaluating candidate materials would increase the likelihood of success when a commitment was made by the government for large scale testing in one of the process development units such as Tidd or Karhula. It would also decrease the financial burden for material manufacturers because they would not scale-up fabrication and/or manufacturing on materials until they had reasonable chance for success in large scale evaluations. The program objectives were defined based on a materials characterization philosophy to (1) measure intrinsic material properties, (2) use test methods, test conditions, and test matrices that are sensitive to applications and the particular material being evaluated, (3) support system designers by providing predictive properties and properties for performance assessment, and (4) support materials manufacturers.

PROJECT DESCRIPTION

The objectives of this program have been pursued by measuring the basic material properties of current materials. The fundamental properties are tensile stress-strain responses at ambient and elevated temperature, thermal expansion, compressive stress strain responses at room and elevated temperature, thermal conductivity versus temperature and tensile creep. Macro and microstructural evaluations have been performed and various nondestructive inspection techniques have been used to look at bulk response of material, for quality control, for property changes, and for flaws or defects. All of the measurements have been made on new and exposed materials.

The information developed from these tests has been combined with post-exposure failure analyses and calculations of stress states using engineering models to give an overall understanding of the material requirements of a hot gas filtration system. Macrostructurally based material models have been developed to understand fundamental limitations of current materials and to generate information that can be used to develop better materials and assess them with minimum expenditure of time and money.

RESULTS

For the three current HGCU materials - Refractron and Schumacher clay-bonded materials and the Coors alumina-mullite material - limited data packages have been developed. While both the clay-bonded materials most likely experience local microcracking because of thermal stresses during pulse cleaning, the materials are somewhat "damage tolerant." Individual binder bridges are probably cracked, but extensive crack propagation is difficult particularly for the Schumacher material. Results from a single METC/SRI patch test specimen showed that slow crack propagation may be possible in the Refractron materials, but more data are needed.

For both of the clay-bonded materials the high temperature creep of the binder and the degradation of the binder with temperature, time

and environment for operating times up to ~20,000 hours are the critical issues. The two materials appear to be somewhat different with respect to their binder properties and macrostructure. These differences do affect performance somewhat but it is more a matter of degree rather than fundamental differences. The Refractron material (442T) may have a slightly higher temperature capability, 50-100°F, but shows more variability than the Schumacher material. Both materials have limited life above ~1400°F. Life is affected by both creep rates and binder degradation. Hot tears have been observed in the Refractron material after ~1000 hours in Karhula. With some realistic engineering models it may be possible to set creep rate limits for lifetimes up to 5000 hours, but more data are needed on both materials; creep and effects of environmental exposure are interactive. To achieve lifetimes of up to 20,000 hours basic changes in the binder materials are required.

The Coors alumina-mullite material definitely has microcracking during pulse cleaning. The tensile strain-to-failure and thermal expansion data show that temperature difference in the filter on the order of 180°F will cause microcracking. Microcracking from thermal stresses have been verified in a single METC/SRI patch test specimen and by microstructural observations on the ID of rings removed from used filters. The basic material issue at present is slow crack growth from the microcracks. In high temperature creep tests, creep has not been observed but specimens have failed at relatively low stresses after short times. One specimen at 1700°F and 1000 psi failed after <1 hour. A second specimen at 1550°F and 200 psi had not failed after ~ 500 hours.

The previous brief discussions have been concerned with normal operating conditions. Process upsets such as unexpected thermal transients and ash bridging compound the problems creating higher loads and stresses. Candles bowed by as much as 0.60 in. have been observed. These candles would eventually fail from creep if the lateral load from ash-bridging was not removed.

FUTURE WORK

Evaluation will continue on the clay-bonded and alumina-mullite materials. Generating data and understanding requirements for life prediction will be the focus of the efforts. In addition preliminary assessments are underway on:

I F and P Fibrosic Filters
3M Filter Material
Dupont Lanxide PRD 66 Filters
Dupont Lanxide, SiC Ceramic Composite

Data being generated on these materials include tensile stress-strain curves at room and elevated temperatures and thermal expansion. Southern is working with METC and Westinghouse to develop some nominal property goals for future material manufacturers.

REFERENCES

Spain, J. D., Starrett, H.S.,"Physical, Mechanical, and Thermal Properties of Schumacher SiC Filter Material," Technical Report to DOE/METC under DE-AC21-89MC26233, SRI-MME-94-253, March 1994.

Spain, J. D., Starrett, H.S.,"Physical, Mechanical, and Thermal Properties of Refractron SiC Filter Material," Technical Report to DOE/METC under DE-AC21-89MC26233, SRI-MME-94-301, April 1994.

Spain, J. D., Starrett, H.S.,"Physical, Mechanical, and Thermal Properties of Coors Alumina Mullite Filter Material," Technical Report to DOE/METC under DE-AC21-89MC26233, SRI-MME-94-513, July 1994.

8a.5

Results of Patch Tests

CONTRACT INFORMATION

Contract Number	DE-AC21-89MC26239
Contractor	Southern Research Institute P. O. Box 55305 Birmingham, Alabama 35255-5305 (205) 581-2268
Contractor Project Manager	Duane H. Pontius
Principal Investigator	Duane H. Pontius
METC Project Manager	Thomas P. Dorchak
Period of Performance	August 23, 1989 to August 22,1994

Schedule and Milestone

FY94 Program Schedule

	S	O	N	D	J	F	M	A	M	J	J	A
Material Characterization	———	———	———	———	———	———	———	———	———	———		
Patch Testing	———	———	———	———	———		———	———	———	———		
Topical Report										———		

OBJECTIVES

The objectives of this work were to construct, install, and operate a patch testing unit on a hot gas stream at a coal-fired fluidized-bed boiler. A 2000-hour "patch test" was conducted on ceramic disks of materials used in the fabrication of ceramic candles and ceramic cross-flow filters. The primary issues addressed in these tests were the long-term physical, thermal, and chemical stability of the ceramic materials; long-term pressure drop and filtration characteristics of the ceramic filters; potential for irreversible blinding of filter elements; and long-term performance and reliability of auxiliary hardware, such as the tube sheet and pulse-cleaning systems.

BACKGROUND INFORMATION

Ceramic filters are among the primary candidates for particulate removal from gas streams at high temperature and high pressure. There are, however, some concerns about the durability of such filters and their resistance to penetration of fine particles into the pores of the material. Because there are many possible sources of particulate matter, operating over a

range of conditions and a variety of filter configurations, tests of full-scale or pilot-scale filter systems are not economically favorable for screening materials for optimal filter characteristics. However, small-scale tests can be very effective, if care is taken to ensure that realistic gas and particulate characteristics are provided. Tests with resuspended dust are questionable because clusters and agglomerates of submicron particles cannot be effectively separated and dispersed, so the particles that would be the most challenging in practical applications are absent in such a test.

All of the above considerations favor the use of a sidestream from an active source of primary particles with appropriate gas chemistry and temperature.

PROJECT DESCRIPTION

The apparatus (patch tester) developed for this program was designed to test three ceramic filter samples simultaneously and independently on a gas stream extracted from a full-scale system. Figure 1 is a schematic diagram of the device.

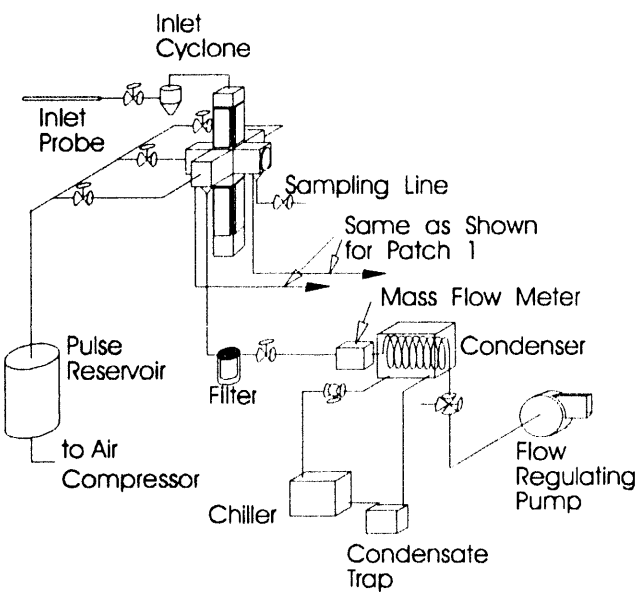


Figure 1. Schematic diagram of Patch Tester

The samples, or patches, were ceramic disks, approximately 10 cm in diameter, mounted on three sides of a rectangular stack. The fourth branch was used for making measurements of the inlet particle loading and size distribution.

The inlet side of the system was kept at the required temperature by a set of ceramic heaters. Because of the small filtration area, the total gas flow rate required to operate all three filters at a face velocity of 5.6 cm/s was only about 74 l_{actual}/min. Independent flow controllers, flow meters, and positive displacement pumps were provided on all four branches of the patch tester. A heat exchanger and back-up filter were provided on each line to protect the moving parts from hot or dirty gases. The system was designed to operate automatically and unattended, and a dedicated computer system was included in the setup for continuous data acquisition. Remote access to the data was available by modem connection to a dedicated telephone line.

Patch Material Characterization

Before the patch tests were carried out the patches were examined by various techniques, and their mechanical properties were measured. Nondestructive methods were used to determine bulk density, open porosity, and sonic velocity. Advanced methods of spectral acoustics were also applied, including Fast Fourier Transform techniques and measurements of attenuation as a function of frequency. X-rays were made of all disks to determine whether any large voids, cracks or other inhomogeneous features could be found.

The patches were made especially for this test program by the manufacturers of filter candles. Specifications, in terms of granularity, pore size, and membrane thickness corresponded to those of functioning candles, but it cannot be assumed that the manufacturing technique was

an exact analog of that used for candle production. Methods of forming the granules into the desired shape and consolidating the mass before sintering might very well be dependent upon the specific geometry of the product. Of course the manufacturers were aware of the purpose of this program, so we can assume that they made every effort to provide patches that would exemplify the properties and characteristics of their commercial products.

A few of the disks were sacrificed to make samples for measuring tensile strength, compressive properties, and coefficient of thermal expansion. These data provided benchmarks for comparison with measurements on used disks after the test, and they also verified that the disks used were reasonable representative of the corresponding candle filters.

The Test Program

The patch tester was set up at the Unit 2 atmospheric fluidized-bed combustor on the campus of Iowa State University during the second half of 1992. The sidestream was extracted by methods similar to those used for stack sampling. A probe inserted into the gas stream was used to draw an aliquot of gas. The patches were characterized before the test, as mentioned above, to provide base line data on mechanical strength and permeability. The materials selected for the first test included two different types of clay-bonded SiC, provided by Refractron and Schumacher, and one patch made of an alumina mullite by Coors.

In September 1993 the patch tester was brought up to approximately 840 °C, and gas flow from the duct was initiated. After we completed preliminary measurements of operating parameters and took samples of the inlet particulate matter, we put the device into a timed pulse-cleaning mode, with an interval of 4 hr between cleaning pulses. The gas flow rate was controlled to maintain a constant filtering face velocity of 5.6 cm/s. for each of the three filters independently. The back pulse reservoir was maintained at 410 kPa (60 lb/in^2) throughout the test. Nearly steady-state operation continued for more than 2300 hr. The system was monitored by computer link from SRI's offices in Birmingham.

RESULTS

Figure 2 is a plot of pressure drop vs. time for two of the filter patches during a period of about 18 hours in mid-November, which was roughly in the middle of the test program. (The trace for the other SiC patch is not included in this figure because it is nearly identical with the one shown, and is therefore difficult to distinguish in this black and white representation.)

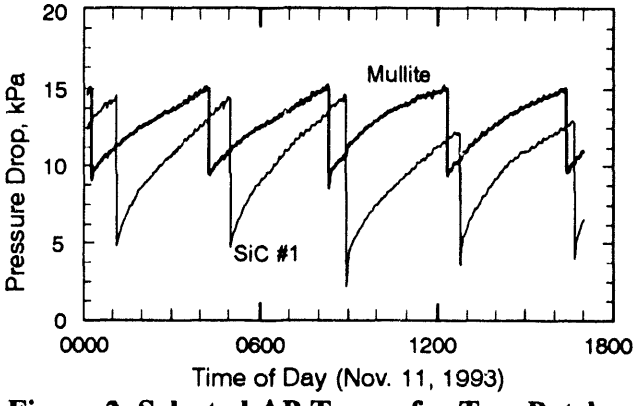


Figure 2. Selected ΔP Traces for Two Patches

The mullite disk (as received) had a lower value of permeability than either of the SiC disks. This difference explains the lower values of ΔP that can be seen in figure 2 for the SiC filter immediately after cleaning.

The slopes of the curves shown in figure 2 also seem to be slightly different, which is not expected to occur if the filtering face velocities

were the same. The slope is the rate of change in ΔP, which should depend only upon the face velocity and the characteristics of the particulate matter (assuming the mass loading in the inlet gas remains constant). Because a planar filtering geometry is used, the ΔP traces should be linear, but in every case, there is a perceptible decrease in the slope of the curve with increasing time.

The curvature of these data can be explained in part by the usual tendency for dust cake to come off the filter in patches, rather than as a monolithic whole. The pressure drop rises most rapidly immediately after cleaning, because there are isolated areas of low permeability that fill up quickly, resulting in a rapid rise in ΔP. When the dust cake begins to smooth out over the filter surface, the rate of increase in ΔP slows. If the gas flow rate is held constant the slope of ΔP *vs.* time should always approach the same asymptotic value.

A downward curvature of the ΔP trace could also result from leaks in the system downstream of the filter and ahead of the mass flow meter. As the pressure drop across the filter is increased to maintain a constant total gas flow rate through the flow meter, the rate of gas flow through such a leak would increase. The result would be a decreasing flow rate through the filter, with a concomitant reduction in the rate of dust cake accumulation. Both of these effects would contribute to an external appearance of decreasing dust cake permeability.

Since the asymptotic behavior of the ΔP traces for the three filters is similar, we have concluded that the effects of inleakage were relatively small.

Particulate Collection Efficiency

We measured total particulate loading in the gas at the inlet and outlet of each of the filters. The inlet mass loading was approximately 1000 ppm (1.37 g/m^3_{normal}). Outlet mass loadings and collection efficiencies are given in Table 1.

A sampling time of 5 hours was used for the two SiC discs, and the time was extended to 15 hours for the Coors filter.

Table 1. Outlet Mass Loading

Filter	Outlet Mass mg/m^3_{norm}	ppm	Collection Efficiency
Refractron	19	14	98.6%
Schumacher	*	*	>99.99
Coors	0.015	0.012	>99.999

*Less than measurement sensitivity.

The relatively low collection efficiency of the Refractron filter was attributed to cracks in the filter which were found when the system was opened and the filters were examined. Reviewing the data, we found a gradual increase in the pressure drop across the backup filter downstream of the Refractron disk. This trend appears to have begun approximately in mid-December. There were no associated process upsets or changes in operating parameters at that time.

The very high values of collection efficiency found for the Schumacher and Coors filters indicates that the gaskets and mountings remained secure throughout the test.

Pulse Cleaning Effectiveness

During the last few days of the test period, we performed a limited evaluation of pulse cleaning pressure requirements. We gradually

reduced the pressure in the reservoir and observed the pressure drop across the filter disks after cleaning. With a pulse pressure of about 215 kPa (30 lb/in^2) the clean value of ΔP could be recovered consistently. When the pulse pressure was reduced to 110 kPa, the filtering pressure drop could no longer be controlled.

Although these results are specific to the configuration of the patch tester, they indicate that ceramic filters can be cleaned effectively by reverse pulses of gas at relatively low pressure.

Effects of Tests on Filter Materials

Some problems with the ceramic filters were evident when they were examined before removing them from the system. One of the clay-bonded SiC disks (Refractron) was broken, although it remained held in place by the mounting. Subsequent detailed examination of the surfaces of the cracks indicates that the damage began near the center of the disk and propagated outward. It does not appear that excessive stresses arose from the supporting ridges around the periphery of the disc. No corresponding cracks or flaws had been indicated in advance by nondestructive testing.

The other SiC disk (Schumacher) was obviously bowed, the distortion being toward the direction of filtering gas flow. The axial displacement at the center was approximately 2.0 mm. The pressure over the face of the disk during filtration averaged approximately 10 kPa. Of course the pressure during reverse pulsing was considerably greater, but the duration of pulsing was infinitesimal in comparison with the duration of forward gas flow. The bowing indicates that this material is susceptible to creep under relatively small stress when operated at temperatures of about 840 °C or higher.

The creep rate calculated from this measurement confirms that the thermal and mechanical behavior of this material is dominated by the vitreous binder, which will ultimately limit the range of applicability of this kind of ceramic.

FUTURE WORK

A second test program has been developed for testing three diverse kinds of filter materials. This test, also be carried out at Iowa State University, is scheduled to be carried out this summer.

8a.6

PFBC Dust Cake Studies

CONTRACT INFORMATION

Contract Number	DE-AC21-87MC24257
Contractor	Westinghouse Electric Corporation Science & Technology Center 1310 Beulah Road Pittsburgh, PA 15235 (412) 256-2240
Contractor Project Manager	Thomas E. Lippert
Principal Investigators	Richard A. Newby Mary Anne Alvin Dennis M. Bachovchin Eugene E. Smeltzer
METC Project Manager	Heather M. McDaniel
Period of Performance	Sept. 30, 1987 to Sept. 30, 1994

Schedule and Milestones

FY94 Program Schedule

	S	O	N	D	J	F	M	A	M	J	J	A	S
Phase III													
Testing													
Evaluation													
Report													

OBJECTIVES

The Westinghouse Electric Corporation, Science & Technology Center is developing an Integrated Low Emissions Cleanup (ILEC) concept for high-temperature gas cleaning to meet environmental standards, as well as to provide economical gas turbine life. The ILEC concept simultaneously controls particulate, sulfur, alkali, and other contaminants in high-pressure fuel gases, or combustion gases, at temperatures up to about 1700° F in advanced, coal-fired, power generation systems. The overall objective of this program is to demonstrate, at a bench scale, the conceptual, technical feasibility of the ILEC concept for multi-contaminant control, and to provide test data applicable to the design of subsequent field tests. The current program objective is to conduct ceramic barrier filter testing under simulated PFBC conditions to deal with filter cake permeability and pulse cleaning issues that have been identified in recent PFBC filter field testing.

BACKGROUND INFORMATION

Westinghouse filter field testing is currently being conducted at three PFBC installations at temperatures up to 1700° F. The characteristics of these hot gas ceramic barrier filter facilities are summarized in Table 1. These facilities provide critical data supporting the design of five new PFBC filter facilities:

- Foster Wheeler (FWDC), Phase 3, Advanced-PFBC facility (Livingston, NJ),
- Southern Company Services, PCD test facility (Wilsonville, Alabama),
- Foster Wheeler, Wilsonville Advanced-PFBC plant,
- Midwest Power, Pyropower Circulating-PFBC, DMEC-1, Clean Coal Technology Program,
- Air Products/Foster Wheeler Advanced-PFBC, FREMP, Clean Coal Technology Program.

Test observations made at the three PFBC filter facilities are summarized in Table 2, and indicate that issues with filter cake permeability, pulse cleaning, fly ash bridging, and fly ash bulk flow can arise in PFBC, depending on the nature of the fly ash and the filter operating conditions.

PROJECT DESCRIPTION

The ILEC development program has a three phase structure:

- Phase 1 - Laboratory-Scale Testing
- Phase 2 - Bench-Scale Equipment Design and Fabrication
- Phase 3 - Bench-Scale Testing

Phases 1 and 2 have been completed (Newby, et al., 1990). ILEC feasibility testing is now being conducted in Phase 3. The current test program is focussing on PFBC filter cake issues. Six test sets have been defined, and are being carried out in the following sequence:

1) Cake Permeability Tests (impact of temperature)

2) Cake Pulse Removal Tests (impact of temperature)

3) Additive Tests

4) Pulse Intensity Tests

5) Continuous Operation Tests

6) Sulfur/Alkali Removal Tests

The first set of tests have nearly been completed, and are highly controlled tests examining changes in filter cake permeability primarily as a function of temperature. The results of these tests are discussed in this report. The second set of tests are directed toward measuring the impact of temperature on pulse cleaning effectiveness. Test set three is again directed toward difficult filter cake conditions, examining the performance of various filter cake additives and the additive application procedures. The impact of the pulse cleaning intensity is measured in test set four. Test set five will confirm observations for selected test conditions during several longer duration tests. Finally, test set six will measure sulfur removal and alkali removal performance in the filter vessel. This final test set will also note the influence of the injected sorbents on the filter cake behavior.

Table 1. Westinghouse PFBC Filter System Characteristics

	AEP Tidd Brilliant, OH	Foster Wheeler Livingston, NJ	Ahlstrom Pilot Karhula, Finland
Facility Size (MW_t):	30	1.2	10
Number Candles:	384	14-22	128
Gas Flow (acfm):	7500	300	3070
Face Velocity (ft/min):	7	2-8	7-8
Pressure (psig):	135	100-200	160
Temperature (°F):	1300-1550	1450-1700	1450-1650
Fuels/Sorbents:	Pgh #8/Plum Run dolomite	Several	Wide Range
Hours of Test Operation			
- Longest Continuous:	550	72	280
- Cumulative:	3000	800	2000

Table 2. General PFBC Filter Cake Observations

	AEP Tidd Brilliant, OH	Foster Wheeler Livingston, NJ	Ahlstrom Pilot Karhula, Finland
Fly Ash Size: (μm)	1-3	5 - 25	12-22
Dust Loading: (1000 ppmw)	0.5-1	2 - 30	4 - 18
Permeability:	Low Decreases T>1400F	Medium to High Decreases T>1500F	Medium to High
Pulse Frequency: (1/hr)	1-2	0.5-3	1-2
Pulse Intensity Required	Large	Medium to Low	Low
Occurrence of Bridging and Hard Residue	At T>1400F	At T>1600F	None
Cake Composition	Highly Sulfated and Carbonated High $CaMg_3(SO_4)_4$	Highly Sulfated and Carbonated Alkali Eutectic Sublayer	Little Information
Vessel Drainage Performance:	Periodic Difficulties	Periodic Difficulties	Good

RESULTS

Bench-Scale Facility Description

A natural gas-fired, bench-scale, high-pressure, high-temperature, ceramic barrier filter test facility is being used to study ILEC performance under simulated PFBC conditions. The objective of the bench-scale simulation is to produce a gas having pressure, temperature, gas composition (SO_2, alkali content, and particulate content), and fly ash particulate characteristics similar to actual coal-fired PFBC. An assembly drawing of the facility is shown in Figure 1. A horizontal, natural gas combustor is attached to the vertical, filter pressure vessel. The combustor is a carbon steel pressure vessel, refractory-lined, with an internal, high-alloy steel liner. It is designed to operate entirely on natural gas, or with coal and natural gas combinations. Sulfur sorbents, alkali sorbents, or deposit additives are also injected into the secondary zone of the combustor.

The uncooled tubesheet, with a 31-inch plate diameter, has been designed with commercial candle holder features that included fail-safe/ regenerator devices. The tubesheet, capable of holding up to 19 candles, supports four ceramic candle filter elements in this program, each 1.5 meter in length. The inlet gas enters the vessel horizontally, near the level of the base of the candles, with no baffle to deflect the inlet jet. The four candles are located so that direct impaction by the inlet gas stream is avoided. The candles are pulse cleaned simultaneously. The outlet piping section incorporates gas sampling for particulate content, alkali content, sulfur content, and other gas species of interest, such as CO_2, as well as instrumentation to measure total gas flow and temperature.

The cake permeability tests have been conducted under the following nominal conditions:

- Face velocity: 7 ft/min (fixed gas volumetric flow at all conditions)
- Pressure: 100 psig

Key measurements made during the tests are:

- Gas and fly ash mass flow rates,
- Filter gas inlet and outlet temperature,
- Tubesheet ΔP,
- Gas CO_2 content.

The tests are conducted by heating the unit to 1300° F, at the test pressure (100 psig) and face velocity (7 ft/min). A filter cake, having specified pressure drop, is deposited on the ceramic candles, and fly ash feeding is halted. The system temperature is them increased in a series of steps to about 1650° F, holding at each step for about 1/2 to 1 hour. The system temperature is then reduced in steps down to 1300° F. Figure 2 is a plot of test data from a typical run, showing the temperature record, the face velocity, the filter cake weight deposited per unit area of the filter elements, and the tubesheet pressure drop record.

Filter cake permeabilities are extracted from the pressure drop data recorded during the tests. The total system pressure drop is contributed by several separate components:

$$\Delta P = \Delta P_f + \Delta P_r + \Delta P_c + \Delta P_p \qquad (1)$$

where ΔP is the total system pressure dro· , and the component subscripts represent the filter elements (f), the filter cake permanent residue (r), the active filter cake (c), and the other system losses (p). The filter cake mass permeability (k_m) is defined by the equation

$$\Delta P_c = \mu \, U \, M / k_m \qquad (2)$$

where μ = gas viscosity, U = face velocity, and M = mass per unit area.

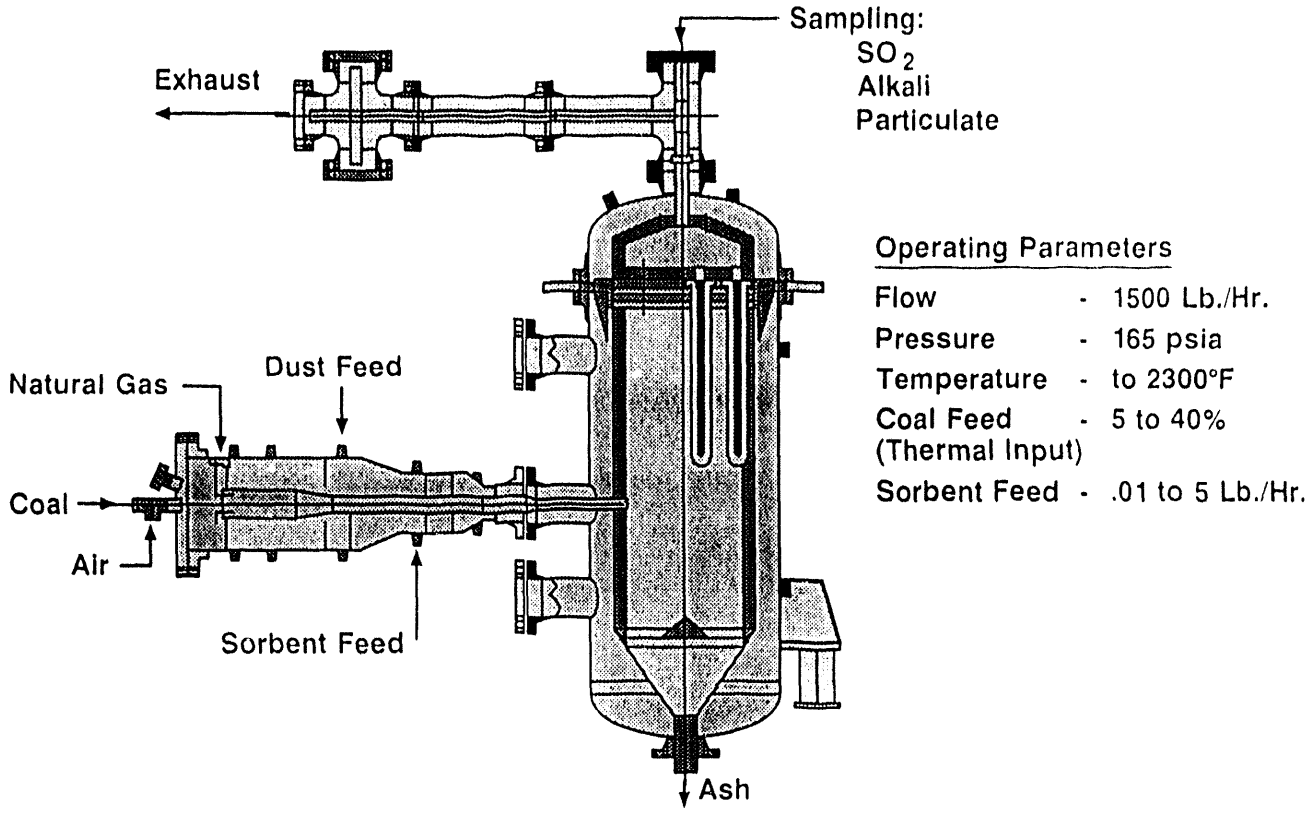


Figure 1. Test Facility Assembly Drawing

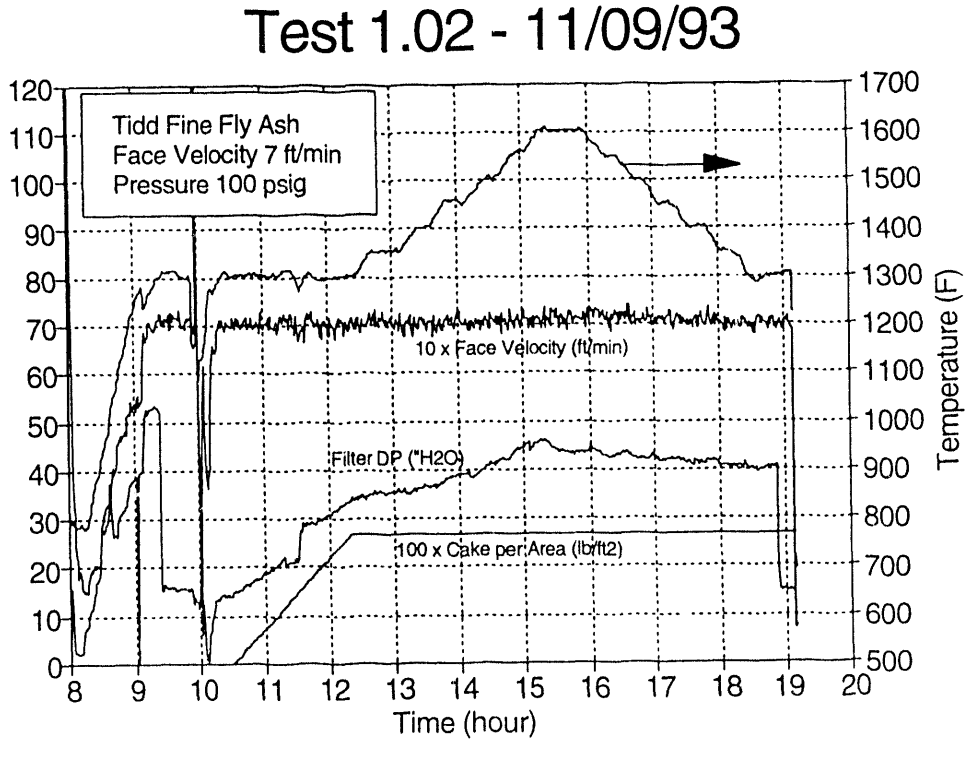


Figure 2. Typical Filter Cake Permeability Test Record

In each test, it has been observed that the filter cake permeability falls as the temperature is initially increased above 1300° F, and it reaches a minimum value at the temperature where the calcium in the filter cake calcines from $CaCO_3$ to CaO. As the temperature is again reduced, the filter cake permeability increases slightly, but does not return to its original value because irreversible structure changes in the filter cake have occurred. This behavior is illustrated for a typical run in Figure 3, showing the mass permeability and temperature as a function of time.

Thirteen tests have been completed using the following PFBC fly ashes:

- Tidd bubbling-PFBC fine fly ash,
- Tidd bubbling-PFBC primary cyclone,
- Grimethorpe Red fly ash (Grimethorpe Run 129),
- Karhula circulating-PFBC fly ash.

All have shown this same behavior. This behavior is explained with respect to calcium-based sorbent material sintering phenomena. It is known from prior evidence (eg., studies of calcium sorbent surface area on injection into hot gas streams, and calcium-based deposits on boiler heat transfer surfaces) that sintering is a fast process at these temperatures. The rate and extent of calcium sintering increases with:

- increased temperature
- reduced particle size
- increased CO_2 and H_2O in gas
- increased content of Na and K in the cake
- increased content of $CaCO_3$ and $CaSO_4$ vs CaO and MgO
- occurrence of sulfation and carbonation reactions

Table 3 lists some of the test results obtained, showing variations with pressure, face velocity, and fly ash source. The results are consistent with field test trends, and direct comparison of the laboratory test and field test permeabilities are shown in Table 4. The laboratory permeabilities are generally greater than the field test permeabilities, and this may be because the CO_2 and SO_2 partial pressures are lower in the laboratory tests than in the field tests. Figure 4 plots the CO_2 partial pressure and filter operating temperature for Tidd PFBC filter tests, for Karhula CPFB filter tests, for FWDC filter tests, and for the laboratory filter cake permeability tests.

Conclusions reached in the program are:

- Laboratory filter cake trends are consistent with field unit data trends;
- PFBC filter cake permeability is largely controlled by sintering of limestone constituents in the fly ash;
- Filter cake sintering is induced by CO_2 and SO_2 in the gas;
- Increased filter cake sintering results from:
  - higher CO_2 and SO_2 pressures,
  - higher temperatures,
  - finer fly ash particles,
  - calcitic limestone vs dolomitic limestone;

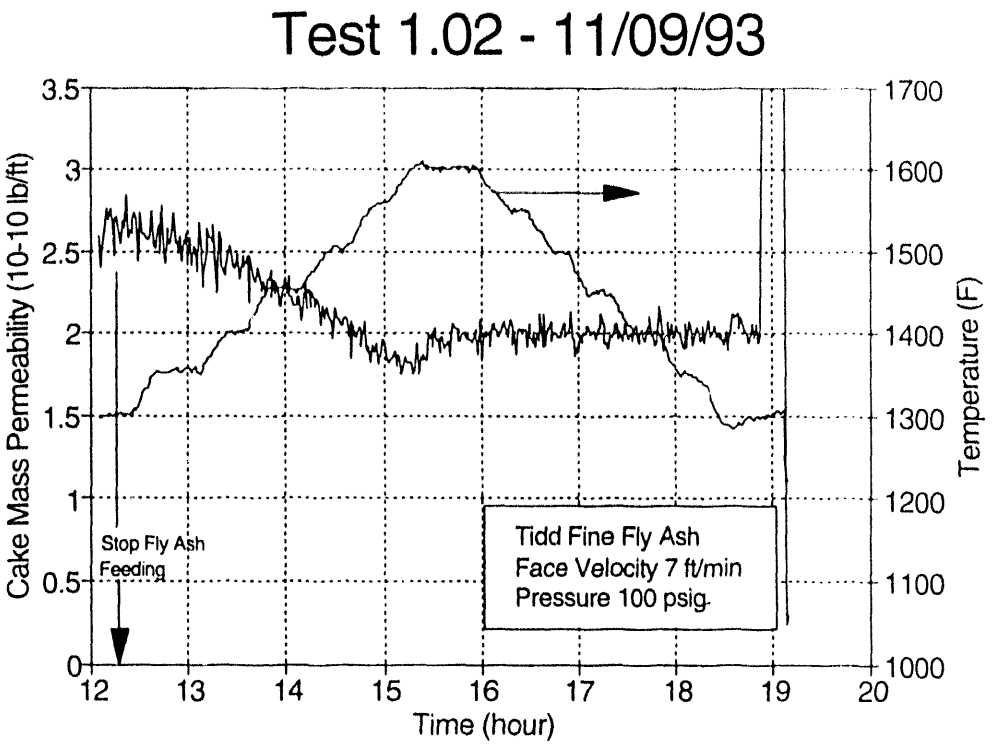


Figure 3. Typical Filter Cake Mass Permeability Result

Table 3. Filter Cake Permeability Test Results

Fly Ash Source	Pressure (psig)	Face Velocity (ft/min)	Cake Permeability at 1300°F (10^{-10} lb/ft)	Minimum Permeability (10^{-10} lb/ft)	Temperature at Minimum (°F)
Tidd Fine	100	7	3.0	1.8	1550
Tidd Fine	150	7	3.2	1.6	1550
Tidd Fine	50	7	3.0	2.0	1500
Tidd Fine	100	12	2.4	1.6	1550
Tidd Cyclone + Fly Ash	100	7	4.3	3.8	1535
Grimethorpe Red	100	7	1.4	1.0	1550
Karhula	100	7	9.3	8.1	1600

Table 4. Comparison of Laboratory and Field Permeabilities

Fly Ash Source:	Tidd	Karhula	Grimethorpe	FWDC
Laboratory Permeability (10^{-10} lb/ft):	1.6-1.3	8	1.1	ND
Field Permeability (10^{-10} lb/ft):	0.2-0.6	2-6	ND	2-5

ND: Not Determined

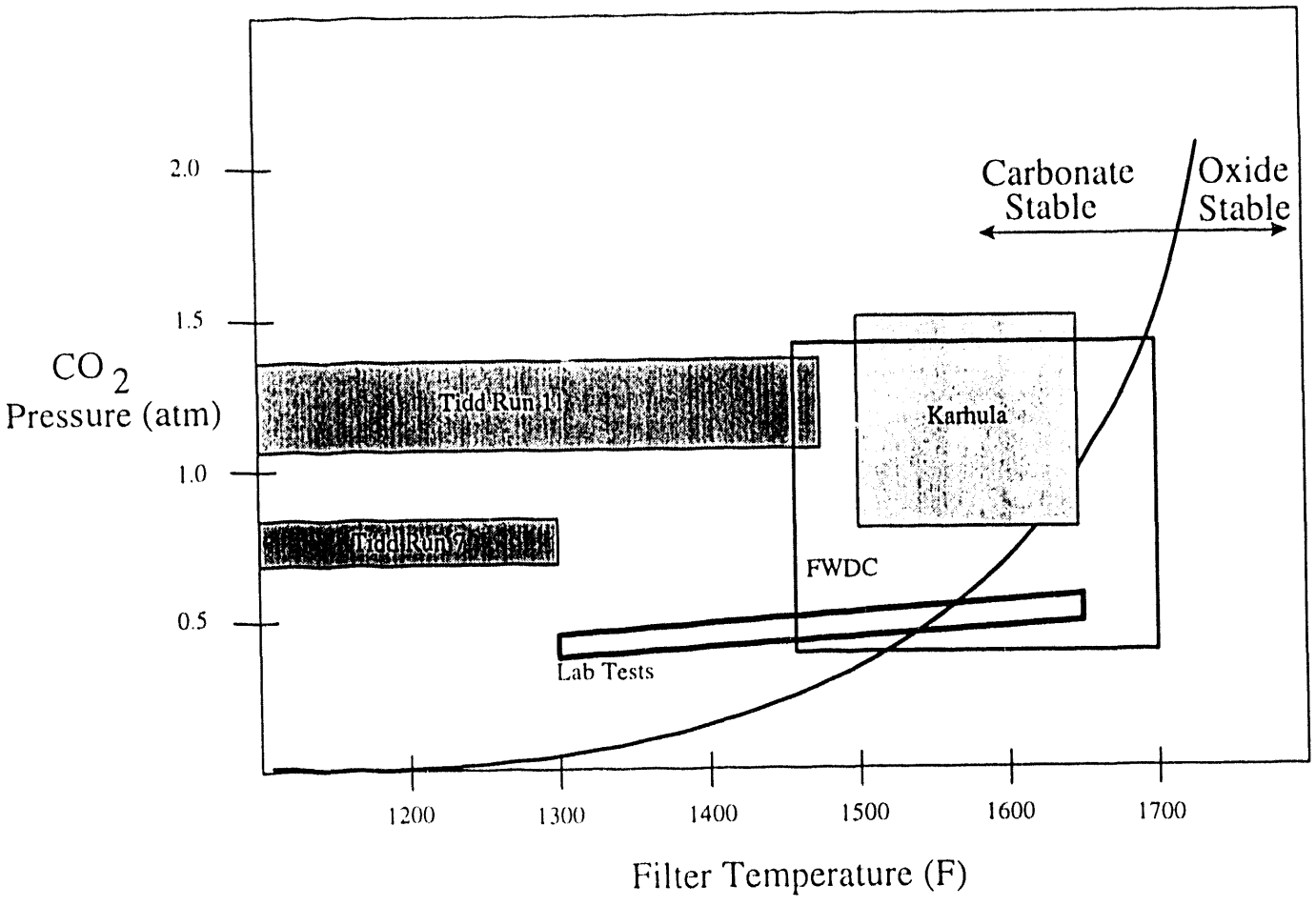


Figure 4. Comparison of Field Filter and Laboratory Filter Test Conditions

- Control of PFBC cake permeability and bridging might be realized by:
  - limiting PFBC temperature,
  - limiting primary cyclone performance,
  - making proper PFBC sorbent selection.

REFERENCES

R. A. Newby, et al., Integrated Low Emissions Cleanup System for Direct Coal Fueled Turbines, Phase I Final Report to DOE under Contract No. DE-AC21-87MC24257, May 1990 (DOE/MC/24257--2927).

Session 8b

Hazardous Air Pollutants

8b.1 Comprehensive Assessment of Toxic Emissions From Coal-Fired Power Plants

CONTRACT INFORMATION

Location

U.S. Department of Energy
Pittsburgh Energy Technology Center
Office of Project Management
Environmental Control Division
Air Toxics and Fine Particulates Control Program

Program Manager Thomas D. Brown

ABSTRACT

The Department of Energy through the Air Toxics Control Program at the Pittsburgh Energy Technology Center (PETC) has been conducting comprehensive assessments of toxic emissions from coal-fired power plants since 1990. The power plants assessed represent an excellent cross section of the combustion and pollution control technologies in current use, with power plants demonstrating advanced control technologies being funded under PETC's Office of Clean Coal Technology. Data from the assessments will be used in the mandated risk assessment being performed by the Environmental Protection Agency. A presentation on the Air Toxics Control Program and results from the assessments will be made at the upcoming Advances in IGCC and PFBC Review Meeting.

A paper will not be available at the time of the meeting. A summary report on the results of the toxic assessments of seven power plants and five Clean Coal technologies will be available in August 1994. If you want a copy of the report, please give me your business card at the conference or write/call at:

Thomas D. Brown
U.S. Department of Energy
Pittsburgh Energy Technology Center
P.O. Box 10940
Pittsburgh. PA 15236-0940

Phone 412 892-4691
FAX 412 892-4604

8b.2 Trace Element Emissions

CONTRACT INFORMATION

Contract Number DE-AC21-92MC28016

Contractor

Energy & Environmental Research Center
University of North Dakota
PO Box 9018
Grand Forks, ND 58202-9018
(701) 777-5000

Contractor Project Manager Steven A. Benson

Principal Investigators

Thomas A. Erickson
Edward N. Steadman
Christopher J. Zygarlicke
William B. Hauserman
David J. Hassett

METC Project Manager Dr. Norman T. Holcombe

Period of Performance August 1, 1992, to September 30, 1994

Schedule and Milestones

FY94 Program Schedule

	S	O	N	D	J	F	M	A	M	J	J	A
Partitioning	———	———	———	———	———	———	———	———	———	———		
Modeling	———	———	———	———	———	———	———	———	———	———	———	———
Verification								———	———	———	———	———
Reporting				*					*			

* Project Review Meetings

OBJECTIVES

The Energy & Environmental Research Center (EERC) is carrying out an investigation that will provide methods to predict the fate of selected trace elements in integrated gasification combined cycle (IGCC) and integrated gasification fuel cell (IGFC) systems to aid in the development of methods to control the emission of trace elements determined to be air toxics. The goal of this project is to identify the effects of critical chemical and physical transformations associated with trace element behavior in IGCC and IGFC systems. The trace elements included in this project are arsenic, chromium, cadmium, mercury, nickel, selenium, and lead. The research seeks to identify and fill, experimentally and/or theoretically, data gaps that currently exist on the fate and composition of trace elements. The specific objectives are to 1) review the existing literature to identify the type and quantity of trace elements from coal gasification systems, 2) perform laboratory-scale experimentation and computer modeling to enable prediction of trace element emissions, and 3) identify methods to control trace element emissions.

BACKGROUND INFORMATION

Trace element emissions pose a potential problem to two emerging coal gasification electric power-generating systems: IGCC and IGFC. The potential problems associated with trace elements are the release of substances that are considered air toxics and the degradation of fuel cell efficiency due to contamination with minor elements. In order to develop effective technologies to control trace element emissions within anticipated regulatory requirements and to ensure the efficient operation of fuel cells, the type and quantity of trace elements emitted from coal gasification-based systems must be determined as a function of system, system conditions, and coal composition.

The fate of trace elements in coals used in IGCC and IGFC systems is closely tied to how the trace elements are associated in the coal and the gasification conditions. Trace elements in coals are associated in several forms, including organic associations, such as salts of carboxylic acid groups and organic coordination complexes, and mineral associations, such as sulfides, sulfates, silicates, phosphates, and carbonates. During gasification, these inorganic elements are partitioned into gases, liquids, and solids. The transformation of these trace elements into the various states and phases depends upon the fundamental characteristics of the elements and their association with minerals and coal particles. Minerals that are not directly associated with coal particles experience a different process environment than minerals that are intimately associated with coal particles during gasification.

In order to predict the form of the inorganic species during gasification, it is essential that detailed information on the distribution of major mineral phases and organically associated inorganic elements be determined. This information is critical since the transformations and interactions during utilization impact the partitioning of trace elements. The primary transformations that occur to major and minor trace species during coal conversion are illustrated in Figure 1. Modeling the transformations using thermochemical equilibrium calculations combined with various chemical and physical constraints to reach equilibrium can be effectively used to estimate the distribution of

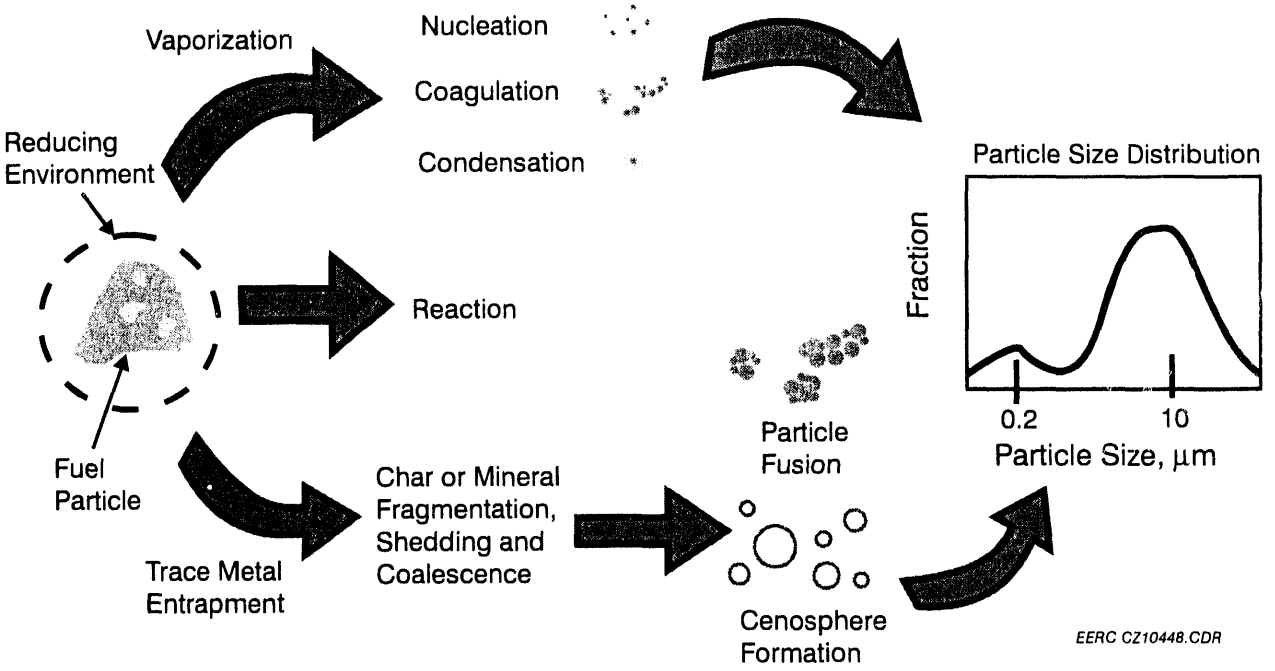


Figure 1. Trace Metal Transformations and Partitioning

gas, liquid, and solid components as a function of gasification conditions.

PROJECT DESCRIPTION

The approach of this project is to identify and model important physical and chemical transformation mechanisms of the trace elements during gasification as a function of coal compositions (trace element abundance and association) and gasification conditions. Identification of the reactions and transformations, coupled with accurate modeling of trace element behavior, is providing essential information for the identification of the form of the inorganic species. Gasification conditions—such as reducing and oxidizing atmospheres, gas-phase composition, pressure, and temperature—influence the partitioning of the air toxics between various gases, liquids, and solid inorganic components as a function of location in the gasifier. This information will be used to identify the most effective control technology by predicting the form of the trace element as a function of operational conditions. The model will be used to predict the initial partitioning of the metals in the gasifier and their form downstream of the gasifier in the gas cleanup systems.

This project has four work categories: partitioning experiments and analysis, modeling, identification of control technologies, and model testing and verification. The partitioning experiments and analysis have concentrated on the operation of closely controlled experimental equipment to produce the appropriate samples and the analysis/characterization of those samples by state-of-the-art analytical techniques.

A pressurized drop-tube furnace (PDTF) and integrated bench-scale gasifier (IBG) are utilized for the experiments at temperatures from 750° to 1500°C and pressures from 50 to 200 psi. Testing has been conducted for three coals under the following conditions: 1000°–1500°C, 50–200 psi, and 0.5–2.0 O/C ratio. The samples produced in the PDTF and IBG systems have been analyzed using inductively coupled plasma spectroscopy, atomic absorption, x-ray fluorescence (XRF), scanning electron microscopy (SEM), and various other techniques.

The modeling work has concentrated on the modification of two existing codes at the EERC: ash transformations (ATRAN) and thermochemical equilibrium analysis of coals and ashes (TEACH). Both codes are being modified to include specific algorithms associated with trace element behavior. The resultant model is a consolidation of the aforementioned codes into a single program capable of predicting the size, composition, and phase of the inorganic species at a given temperature and pressure. An operational shell is being developed to incorporate the two codes.

The identification of control technologies will be incorporated into the project after most of the testing and modeling is complete, at which time multiple scenarios can be addressed using the data and models. The model testing and verification will consist of testing the model and assumptions on the transport reactor scaleup facility located at the EERC.

RESULTS

Coal Selection and Characterization

A survey of the trace metals in several coals was performed. The distribution of the seven elements is listed in Table 1. Three coals have been selected for testing: Illinois No. 6, Sufco (Utah), and Pittsburgh No. 8.

Many of the recently developed computer models to predict the particle-size and composition distribution of major and minor elements during coal combustion and gasification were made possible through the use of highly quantitative analytical data on coal mineral composition and size, computer-controlled scanning electron microscopy or (CCSEM) (Steadman and others 1990). CCSEM provides particle-size and composition distribution for the mineral grains in coal. These raw CCSEM data are the primary input to the newest computer models of ash formation.

To determine associations of trace elements with minerals, the standard CCSEM procedure using automated image analysis and energy-dispersive x-ray analysis is performed on the coal. At the completion of each frame of analysis, the operator can locate the specific minerals and reanalyze them with the more sensitive wavelength-dispersive x-ray spectrometer (WDS) to determine trace metal abundance. The WDS data analysis can then be manually compared to the standard CCSEM data to correlate the presence of trace

Table 1. Abundance of Trace Metals in Coals Tested (μg/g dry coal basis)

	Illinois No. 6	Sufco Utah	Pittsburgh No. 8
Arsenic	1.5	0.66	7.80
Cadmium	0.33	0.048	0.10
Chromium	26.0	26.9	18.8
Lead	2.84	0.86	3.87
Mercury	0.067	0.033	0.082
Nickel	15.1	8.35	14.9
Selenium	3.03	1.05	1.41

elements with specific mineral species. A generalized trace element profile can then be created for a number of coals (to be used for data correlations in the model until the more rigorous technique is completed). In addition, the chemical fractionation technique (Benson and Holm, 1985) is being used to support the CCSEM WDS by providing data on the general association of the seven trace metals.

The association of arsenic, cadmium, chromium, mercury, nickel, lead, and selenium were determined for Illinois No. 6, Sufco (Utah), and Pittsburgh No. 8. The associations were determine through a combination of chemical fractionation (Benson and Holm, 1984) CCSEM combined with WDS (CCSEM/WDS) (Galbreath and Brekke, 1994). The summary of the associations are listed in Table 2. This information is combined with the CCSEM data listed in Table 3 and used as input to the TraceTran model to predict the partitioning of trace as well as major and minor inorganic components. Table 3 only reports the abundance of the minerals; size information is also available. Table 4 summarizes the levels of trace metals found in individual minerals.

Partitioning of Trace Metals

The fate and distribution of trace elements as a function of temperature, pressure, and gas composition in IGCC systems are important to the emerging IGCC and IGFC technologies. Laboratory experiments performed in the EERC PDTF and the IBG have been used to determine the partitioning of important trace elements and to enable the prediction of the fate of trace elements in IGCC and IGFC systems.

Testing of all three coals in the PDTF is nearly complete. A parametric study has been conducted on two of the coals to produce solid, liquid, and gaseous products under a range of conditions to determine the partitioning of the trace elements as a function of the association of the trace elements in the coals and of gasification conditions. Based on the literature survey, a standard condition of temperature, pressure, and gas composition was chosen for one test. The other tests were performed with temperature, pressure, and gas composition at values above and below the standard.

Table 2. Trace Element Associations in Coals Examined

Element	Associations
As	Pyrite, arsenates
Cd	Sulfides, clays
Cr	Clays, organic compounds
Hg	Pyrite
Ni	Pyrite, clays, organic compounds(?)
Pb	Pyrite, other sulfides, clays
Se	Pyrite, other sulfides, organic compounds, sulfate

Table 3. Mineral Composition of Coals Used in Trace Element Emissions Program (determined by CCSEM)

	Illinois No. 6	Sufco (Utah)	Pittsburgh No. 8
Quartz	23.3	32.0	14.8
Calcite	0.8	25.0	5.0
Dolomite	0.1	2.9	1.1
Kaolinite	13.8	10.4	21.0
Montmorillonite	3.8	1.3	5.5
K Aluminosilicate	12.2	0.1	20.0
Na Aluminosilicate	0.4	5.6	0.0
Pyrite	26.7	6.6	13.4
Gypsum	5.8	4.3	1.4
Other	13.1	11.8	8.8

The resulting inorganic phases were aerodynamically classified, using a two-stage cyclone system, with a set of impingers/mercury trap for vapor-phase collection. In some cases, the cyclones are replaced with an impactor. The multicyclone is an Environmental Protection Agency Southern Research Institute five-stage cyclone with the first, third, and fourth stages removed. The impactor that is used is a University of Washington Mark 5 source test cascade impactor. The cyclone, impactor, and filter were heated to maintain the temperature of the product gas above 100°C to reduce the risk of water condensation during collection. Three size distributions were analyzed to quantify the forms and concentrations of important trace elements. Detailed analysis of the size-fractionated ash allowed for the

Table 4. Trace Element Levels Determined for Individual Mineral Grains in Selected Coals Using CCSEM/WDS (μg/g in mineral grains)

Element	Pyrite	Clays
Ni	100–350	--
As	300–400	--
Se	800–2900	--
Cd	n.d.[1]	--
Hg	80–2700	--
PB	n.d.	--
Cr	n.d.	300–950

[1] Not detected.

determination of size and composition partitioning between the gas and solid phases, since the vaporized components will be concentrated in the smallest-size fractions. The coal and gas flow through the system will be controlled and monitored to allow determination of trace element concentration and mass balance.

A detailed description of the PDTF furnace assembly can be found elsewhere (Benson and others, 1993). Briefly, the PDTF consists of a 2.875-inch-ID alumina tube (55 inches long) with a slightly reduced end, used to support a flow accelerator in a fixed position, nested on top of a tube of the same dimensions (25 inches long). These tubes are concentrically surrounded by a tube of slightly larger dimensions. The tubes are heated externally by high-temperature tube furnaces equipped with Kanthal Super 33 elements. The entire reactor and the heating elements are housed in a water-jacketed pressure vessel. Coal is introduced into the reactor with a carrier gas through a traversing, water-cooled injector located in the center of the tube. Optional secondary air enters the reactor at the top of the tube and flows through the tube, around the injector assembly. The coal residue and process gases travel down the tube in a laminar flow regime and pass through the accelerator where they are collected by a water-cooled, nitrogen-quenching ash collection probe. Various collection devices can be attached to the collection probe to collect the solids. Size segregation of the ash is obtained by using a multicyclone or impactor in conjunction with a final filter. A bulk filter is used to collect ash for bulk chemistry. A water-cooled deposition probe can also be inserted, in place of the ash collection probe, to simulate the deposition conditions in a utility boiler. The product gases are monitored on-line by O_2, CO, and CO_2 gas analyzers or are intermittently sampled for a gas chromatograph (GC).

The PDTF can operate at temperatures as high as 1500°C and pressures up to 250 psi. Efforts are currently underway to attach an atomic absorption unit to the exiting gas line to acquire on-line mercury analysis from the furnace. Burnouts in excess of 95% with high carbon monoxide/carbon dioxide ratios have been produced under gasification conditions.

In the experimental effort, three coals were run under multiple temperatures, pressures, gas compositions, and residence times. The resultant samples will be collected in a three-stage multicyclone and characterized by using SEM, wavelength-dispersive x-ray fluorescence (WDXRF), inductively coupled plasma (ICP) spectrometry, and atomic absorption (AA).

Tests to determine the partitioning of trace metals into gases, liquids, and solids were conducted in the PDTF. The partitioning was ascertained by determining the fraction in which the material was collected. Metals that are not vaporized during gasification remain in the residual ash and are collected in the size fraction greater than one micrometer. Metals that are vaporized but condense in the system are collected in the submicron fraction. Metals such as Se and Hg may not condense in the system and be emitted in a vapor state. These vapors are collected in the impinger train. The results summarized in this report are for Illinois No. 6 and are focused on the vapor-phase components. Testing was conducted to determine the effect of temperature, O/C ratio, and pressure on the abundance of vapor-phase species. Figure 2 illustrates the effect of O/C ratio on the abundance of As, Cd, Se, and Hg in the vapor phase at 1500°C initial gasification temperature. The results indicate a slight increase in vapor-phase Hg and As. Se showed an even distribution with a slight increase in Se in the vapor phase at higher oxygen levels. The cadmium shows some variation in the abundance with changing oxygen levels. At a 1000°C initial gasification temperature shown in Figure 3, a clear trend in increasing vapor-phase As, Cd, and Hg with decreasing O/C ratios is demonstrated. Se showed the opposite trend, with increasing abundance in the gas phase with increasing O/C ratio. This trend is likely due to the lower volatility of reduced Se relative to the oxide form as discussed by Dismukes (1994). The effect of initial gasification temperature on the abundance of trace metals in the gas phase is depicted in Figure 4. Figure 4 shows that with increasing temperature, the abundance of trace metals in the gas phase increases.

Predicting Trace Metals Behavior

Predicting inorganic transformations (major and minor components) during coal combustion has long been the focus of many research programs (Zygarlicke and others, 1992; Wilemski and others, 1992; Baxter, 1992). In the program, the techniques that have been applied to combustion have been modified to predict inorganic transformations under gasification conditions. The approach used in this program is to combine inorganic transformation algorithms and the thermochemical equilibrium calculations (Ramanathan and others, 1989, 1991). These techniques have been developed to predict the particle-size and composition distribution of the resulting coal ash particulate, along with the state of the vapor species at selected conditions for major, minor, and trace constituents.

A computer model to predict the evolution of major, minor, and trace elements during the gasification of coal is being created, based on the algorithm shown in Figure 5. The shaded boxes in Figure 5 represent the inputs required, while the boxes with a drop shadow are the outputs generated from the model. The first task of the model is to determine the associations of the major, minor, and trace elements in the coal prior to utilization. The association of the elements prior to utilization will affect their phase, size,

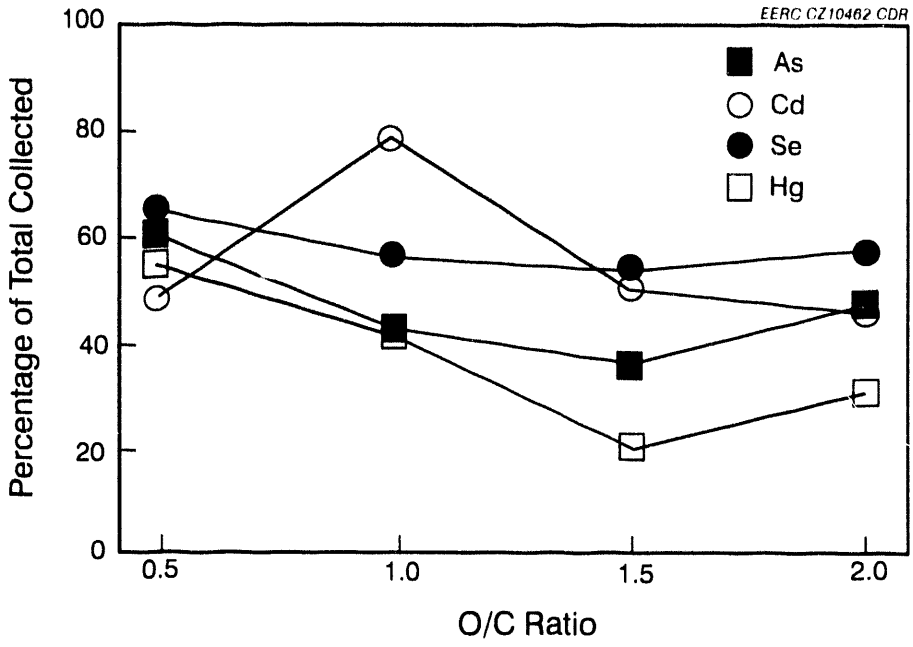


Figure 2. Trace Metal Distribution vs. O/C Ratio for Illinois No. 6

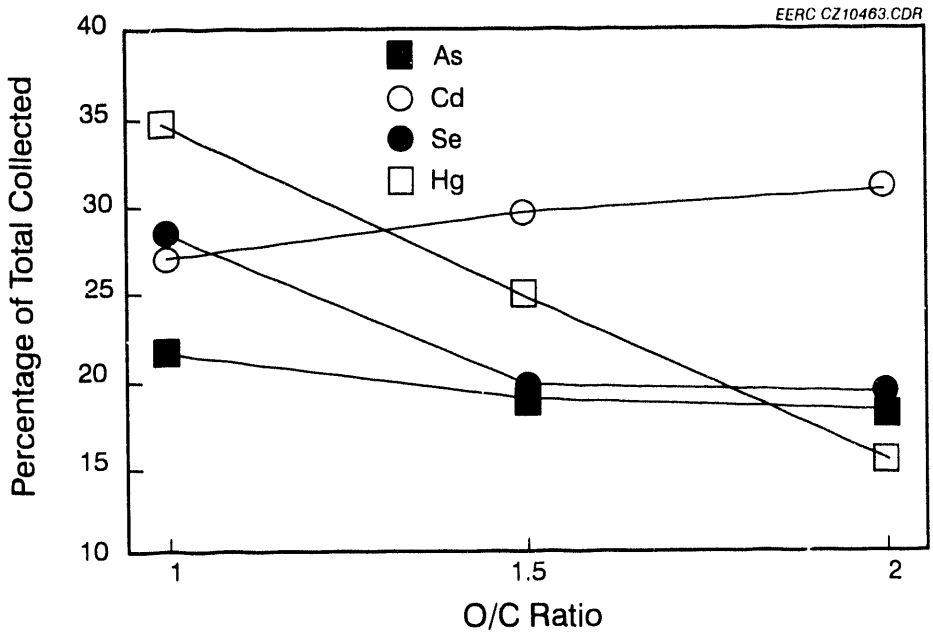


Figure 3. Trace Metal Distribution vs. O/C Ratio for Illinois No. 6

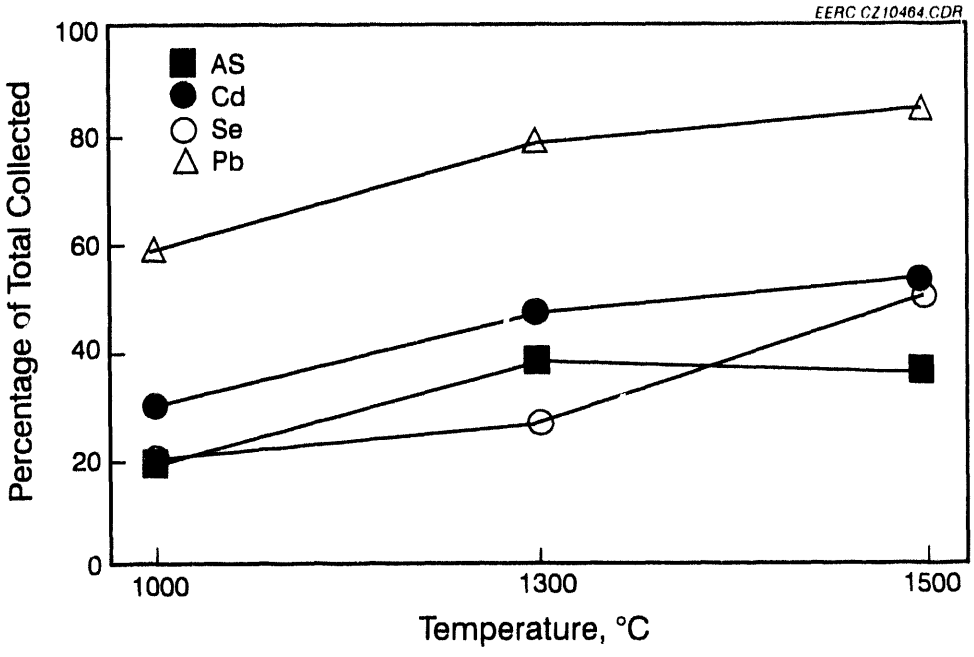


Figure 4. Trace Metal Distribution vs. Gas Temperature for Illinois No. 6

and composition distribution in the residual ash and gas streams. Bulk chemistry, CCSEM/WDS, and chemical fractionation are used as input data.

Once a mass balance is performed around the coal input data, it is necessary to determine which of the inorganic components will be vaporized during the initial gasification process. These calculations will be performed with the use of a thermochemical equilibrium program, TEACH (Ramanathan and others, 1989, 1991), created at the EERC. This code is currently being upgraded to include the appropriate trace element phases. With the exclusion of the vaporized species, the remaining constituents will be processed through algorithms for mineral fragmentation, coalescence of both minerals and organically associated species, and the shedding of resulting particles. Examples of data obtained from the calculations are illustrated in Figure 6 for major ash components and Figure 7 for trace metals.

The state of the volatile species under given conditions will then be determined, again using the TEACH code. The distribution of Hg species is illustrated in Figure 8.

FUTURE WORK

The future work will involve the following:

- Completing the interpretation of the results obtained from testing Sufco and Pittsburgh No. 8 using the PDTF system.
- Completing the integration of the TraceTran computer code.

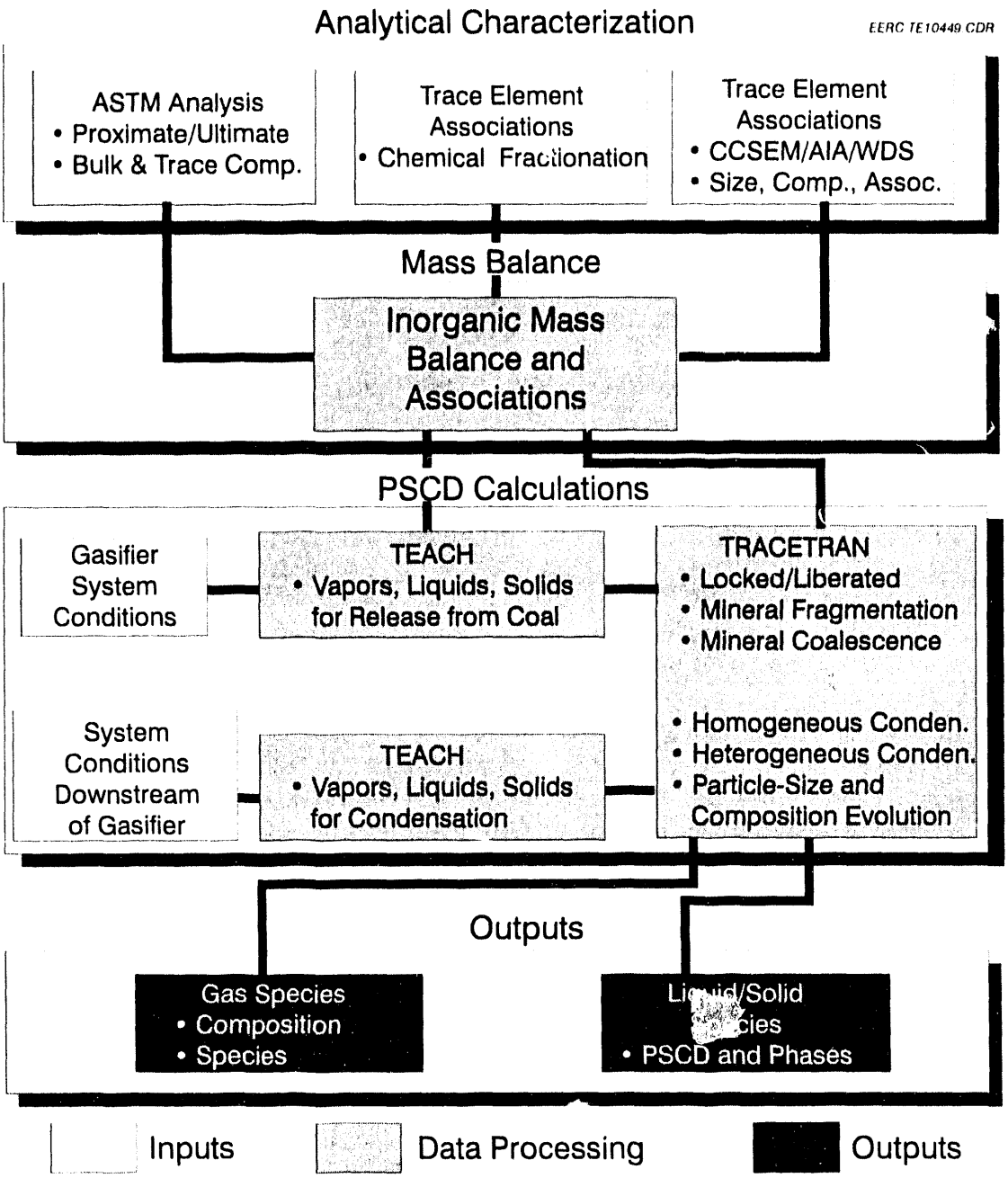


Figure 5. Trace Element Emissions Model Algorithm

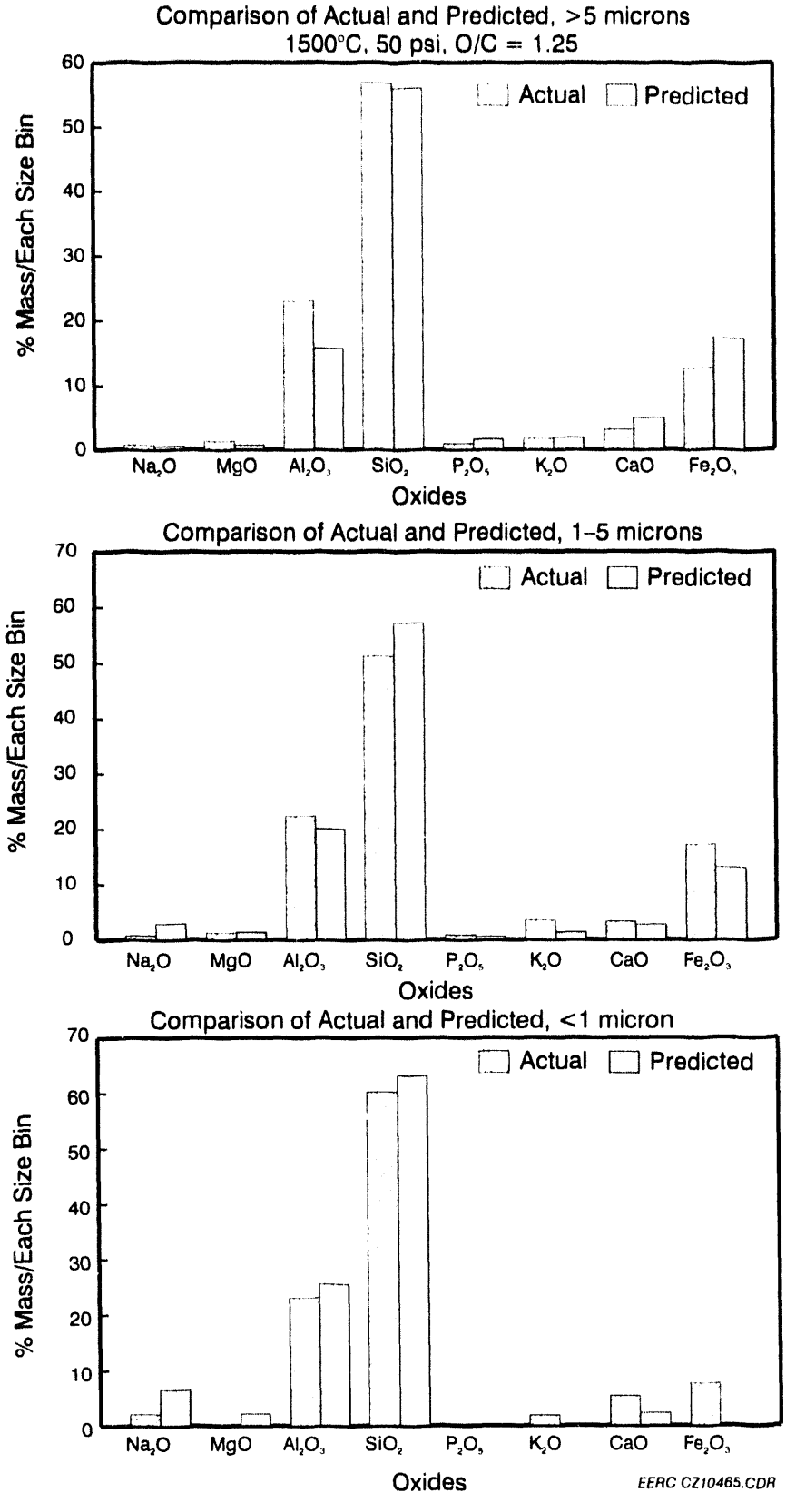


Figure 6. Comparison of Predicted and Actual Particle-Size and Composition Distribution for Major Elements

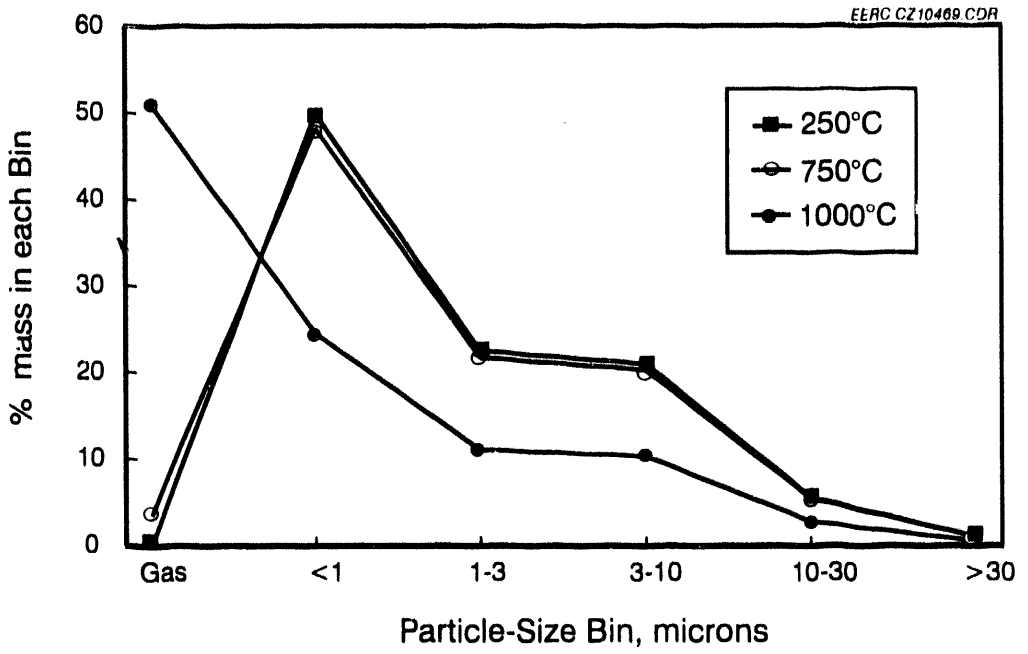


Figure 7. TraceTran Predictions for Partitioning of Pb During Gasification of Illinois No. 6 (O/C = 1.0, pressure = 20 atm)

- Verifying the predictive capability of TraceTran using data obtained from larger-scale systems.

REFERENCES

Baxter, L.L. 1992. Char Fragmentation and Fly Ash Formation During Pulverized-Coal Combustion, *Combustion and Flame*, *90*, 174-184.

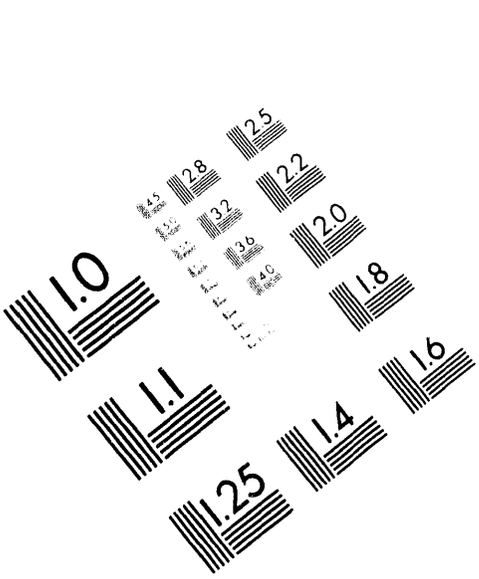
Benson, S.A.; Erickson, T.A.; Steadman, E.N.; Zygarlicke, C.J.; Hauserman, W.B.; and Hassett, D.J. 1994. Presented at Coal-Fired Power Systems 93—Advances in IGCC and PFBC Contractors' Review Meeting, DE-AC21-92MC28016.

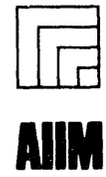
Benson, S.A.; Holm, P.L. 1985. Comparison of the Inorganic Constituents in Three Low-Rank Coals, *Ind. Eng. Chem. Prod. Res. Dev.*, *24*, 145.

Clarke, L.B.; Sloss, L.L. 1992. Trace Elements - Emissions from Coal Combustion and Gasification. International Energy Association Coal Research, London, Report IEACR/49, July 1992, 111 p.

Currie, L.A. 1968. Limits of Qualitative Detection and Quantitative Determination, Application to Radiochemistry, *Analytical Chemistry*, *40*, 586-593.

Dismukes, E.B. 1994. Trace Element Control in Electrostatic Precipitators and Fabric Filter, In Trace Element Transformations in

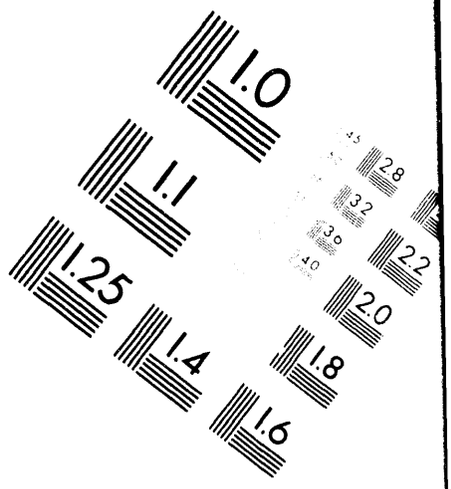


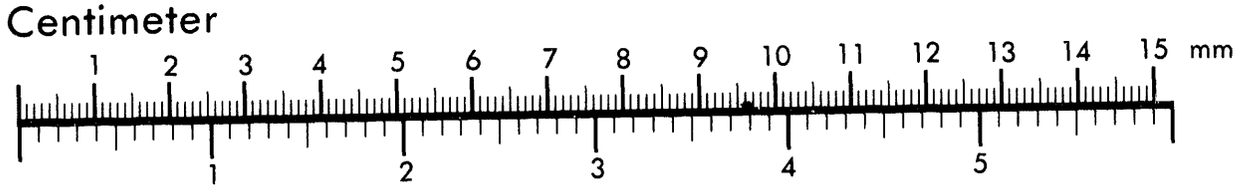


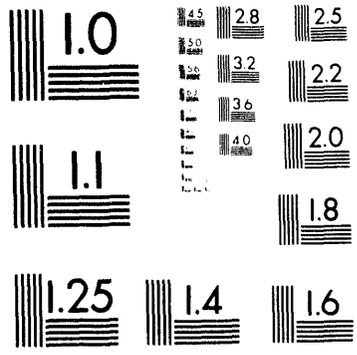
Association for Information and Image Management

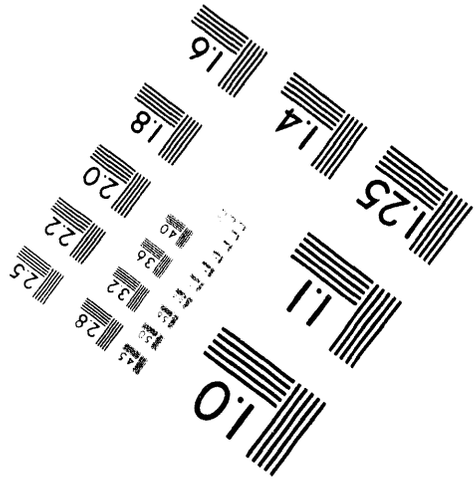
1100 Wayne Avenue, Suite 1100
Silver Spring, Maryland 20910

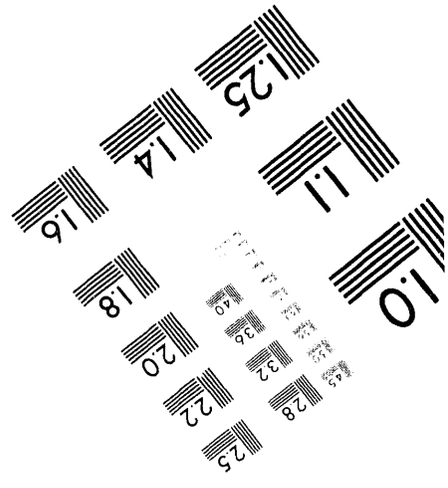
301/587-8202











MANUFACTURED TO AIIM STANDARDS
BY APPLIED IMAGE, INC.

2 of 3

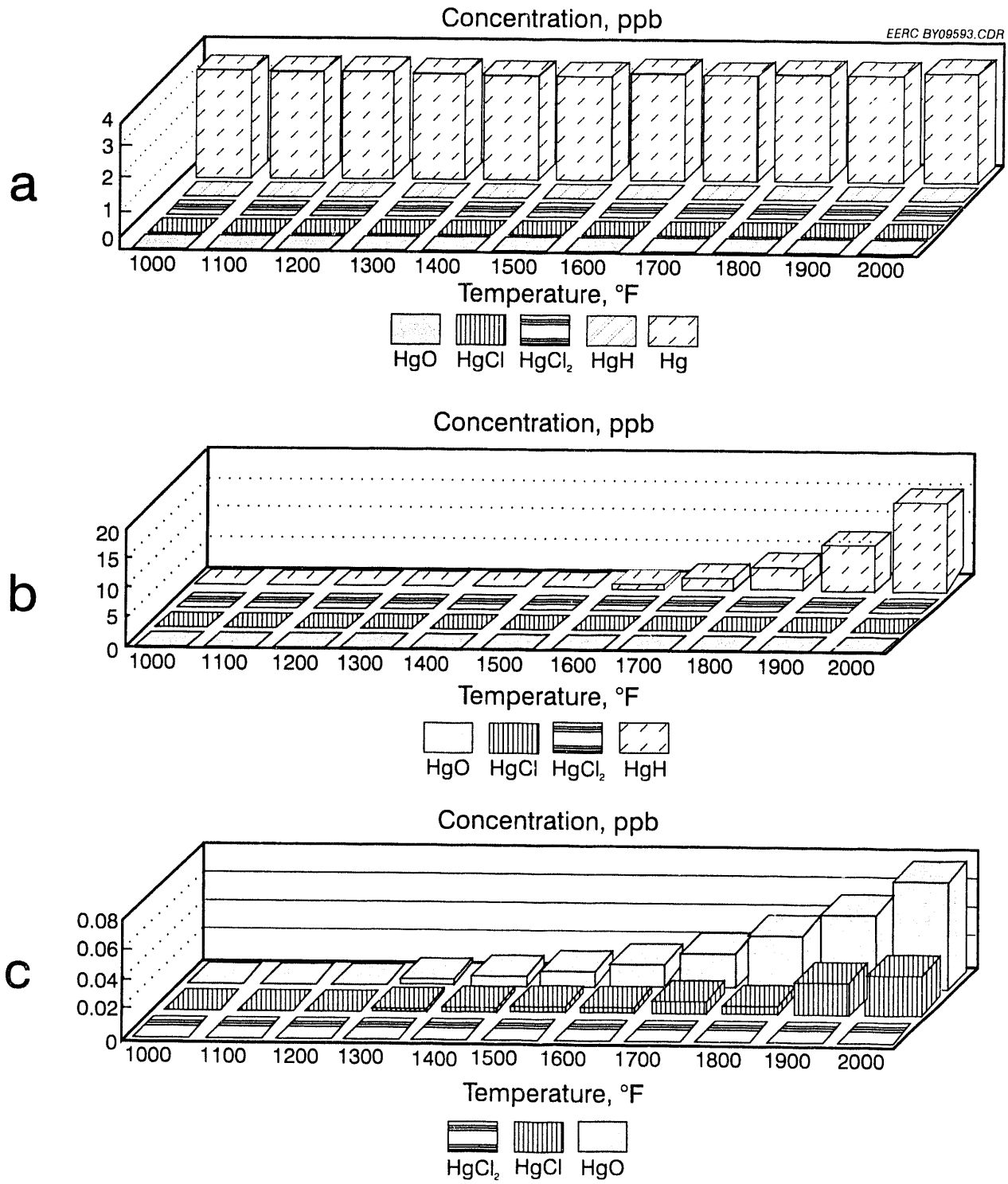


Figure 8. Distribution of Hg Species as a Function of Temperature for Sufco Coal Using Thermochemical Equilibrium Calculations

Coal-Fired Power Systems,"Special Issue of *Fuel Processing Technology*; Benson,S.A.; Steadman, E.N.; Mehta, A.K.; and Schmidt, C.E.; Eds.; Vol. 39, in press.

Galbreath, K.C.; Brekke, D.W. 1994. Feasibility of Combined Wavelength/Energy-Dispersive Computer-Controlled Scanning Electron Microscopy for Determining Trace Metal Distribution, In Trace Element Transformations in Coal-Fired Power Systems, Special Issue of *Fuel Processing Technology*; Benson, S.A.; Steadman, E.N.; Mehta, A.K.; and Schmidt, C.E.; Eds.; Vol. 39, in press.

Ramanathan, M.; Ness, S.R.; Kalmanovitch, D.P. 1989. New Techniques for Thermochemical Phase Equilibrium Predictions in Coal Ash Systems - I, 197th Annual Meeting of the American Chemical Society, April 9-14, 1989, Dallas, TX, p 7.

Ramanathan, M.; Kalmanovitch, D.P.; Ness, S.R. 1991. New Techniques for Thermo-chemical Phase Equilibrium Predictions in Coal Ash Systems - II, Sixth International Conference on High Temperatures - Chemistry of Inorganic Materials, April 3-7, 1991, Gaithersburg, MD, p 17.

Steadman, E.N.; Zygarlicke, C.J.; Benson, S.A.; Jones, M.L. 1990. A Microanalytical Approach to the Characterization of Coal, Ash, and Deposits, ASME Seminar on Fireside Fouling Problems, Brigham Young University, Provo, UT, April 1990.

Swaine, D.J. 1990. Trace Elements in Coal. Butterworth & Co., Publishers Ltd, 278 p.

Wilemski, G.; Srinivaschar, S.; Sarofim, A.F. 1992. Modeling of Mineral Matter Redistribution and Ash Formation in Pulverized Coal Combustion, In *Inorganic Transformations and Ash Deposition During Combustion*; Benson, S.A., Ed.; American Society of Mechanical Engineers: New York, pp 545-564.

Ziebold, T.O. 1967. Precision and Sensitivity in Electron Microprobe Analysis, *Analytical Chemistry*, *39*, 858-861.

Zygarlicke, C.J.; Ramanathan, M.; Erickson, T.A. 1992. Fly Ash Particle-Size Distribution and Composition: Experimental and Phenomenological Approach, In *Inorganic Transformations and Ash Deposition During Combustion*; Benson, S.A., Ed.; American Society of Mechanical Engineers: New York, pp 525-544.

8b.3 HAP Sampling at Tidd PFBC

CONTRACT INFORMATION

Contract Number	DE-FC21-89MC26042
Contractor	Ohio Power Company c/o American Electric Power Service Corporation 1 Riverside Plaza Columbus, Ohio 43215 (614)223-1585
Contractor Project Manager	Michael J. Mudd
Principal Investigator	Patrick A. Dal Porto
METC Project Manager	Richard A. Dennis
Period of Performance	August 2, 1989 to June 30, 1995

Schedule and Milestones

Program Schedule

	FY1990	FY1991	FY1992	FY1993	FY1994	FY1995
	1 2 3 4	1 2 3 4	1 2 3 4	1 2 3 4	1 2 3 4	1 2 3 4
Design Specification/ APF Procurement	———					
Detailed Design	———	———				
Test Plan		———				
Hardware Procurement	———	———	———			
Testing			———	———	———	
Data Analysis			———	———	———	

OBJECTIVE

The objective of this project was to sample process streams of the Tidd PFBC plant and to characterize the HAPs associated with those various process streams. The data are comparable to HAP data collected by DOE and EPRI studies at conventional coal-fired utility plants.

BACKGROUND INFORMATION

Passage of the 1990 Clean Air Act Amendments (CAAA) has dramatically increased the interest in hazardous air pollutants (HAPs) from all sources. Title III of the amendments specifically commissioned a study of the hazards to public health reasonably anticipated to occur as a result of emissions of pollutants listed in Title III by electric utility steam generating units. A study of mercury must also be conducted by U.S. Environmental Protection Agency (U.S. EPA) and transmitted to Congress. U.S. EPA, the Utility Air Regulatory Group (UARG), the Electric Power Research Institute (EPRI), and the U.S. Department of Energy (DOE) are studying emissions of HAPs at numerous fossil-fuel fired utility plants with various configurations and emissions control systems. U.S. EPA will use these data and health risk assessment models to evaluate the hazards to public health associated with the Title III HAPs. Findings from these studies will be used to determine if regulation of electric utility HAPs is appropriate and necessary.

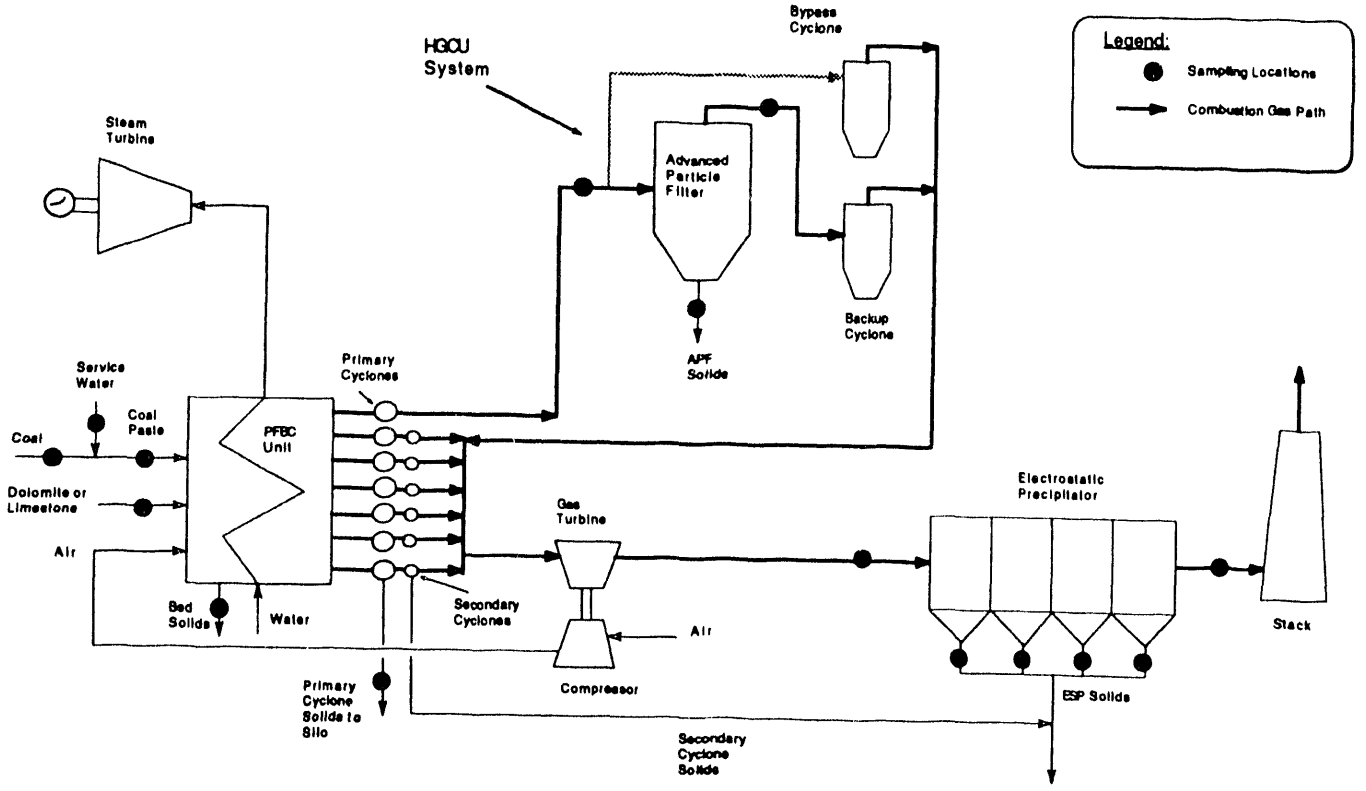


Figure 1. Plant Tidd Process Flow Diagram

The pressurized fluidized bed combustor at Tidd Plant provides a unique opportunity to collect comparable data with the DOE and EPRI studies. A demonstration-scale hot gas clean-up (HGCU) system presents an exceptional occasion not only to evaluate collection of HAPs by the HGCU, but to compare the performance of the HGCU to an electrostatic precipitator (ESP).

PROJECT DESCRIPTION

Twelve sampling locations throughout Tidd PFBC plant were selected to characterize the HAPs in the plant cycle. Sampling was conducted at the input and output of the combustor, before and after the HGCU and before and after the ESP. (See Figure 1).

Seven solid process streams were sampled including coal and sorbent to the PFBC unit and ash from the PFBC bed and ash collection devices. Service water which is mixed with the coal to make coal paste was the only liquid process stream sampled. The four gas stream samples collected were the inlets and outlets of the HGCU and ESP (See Table 1).

Gas Streams Sampling

Each of the gas streams were sampled and will be analyzed for metals, anions, ammonia, cyanide, formaldehyde, volatile organics, semivolatile organics, dioxins/furans, and particulate loading (See Tables 2-1 thru 2-3 and Tables 3-1 thru 3-3). Particulate size

Table 1

Samples To Be Collected at Plant Tidd

Process Stream	Sample Type	Sampling Location
Coal[a]	Solid	Automatic sampler on feed belt to crusher.
Coal Paste	Solid	Paddle belt feeder to storage tank.
Sorbent (Limestone or Dolomite)	Solid	Automatic sampler on east sorbent injector.
Bed Ash	Solid	Entrance to ash storage silo.
ESP Ash	Solid	ESP hopper No. 11 (Nos. 12, 13 and 14 if available).
Primary Cyclone Ash	Solid	Automatic samplers on ash storage silo.
APF Ash	Solid	Sampled upon loading into disposal trucks.
Service Water	Liquid	Tap on service water header.
APF Inlet	Gas	Single 4-inch-diameter port on APF inlet duct.
APF Outlet	Gas	Single 4-inch-diameter port on APF outlet duct.
ESP Inlet	Gas	Five 4-inch-diameter ports on ESP inlet duct.
ESP Outlet	Gas	Two 4-inch-diameter ports on ESP outlet duct.

[a] Raw coal samples held for possible analysis pending data quality assessment of coal paste results.

distribution was conducted at the ESP inlet and outlet. All solid and liquid stream samples were collected at the appropriate times to account for residence times within the system so the solid and liquid samples will be representative of gas sampling periods.

One of the most challenging aspects of this program was the gas stream sampling around the advanced particle filter (APF) of the HGCU system. The system operates at approximately 1550°F and 185 psig. The high temperature and pressure at the HGCU system require that a fixed sampling probe be used for gas sampling in the APF inlet and outlet. A schematic of the fixed probe sampling system designed and employed at the APF is shown in Figure 2. An Incoloy 800 tube (1/2" O.D.) serves as the sampling probe and nozzle. This sample probe is contained in a 315 stainless steel (SS) 4" diameter tube. Cooling air is supplied to the large tube to accomplish cooling of the gas sample from 1500°F to a temperature range of 800-600°F. A flow orifice and sample control valve downstream of the filter are used to control isokinetic sample rates.

RESULTS

Throughout the sampling period, the PFBC unit was very stable and provided steady-state conditions while sampling was conducted. All samples enunciated in Radian Corporation's sampling plan were collected and only minor problems were encountered. Isokinetic sampling was achieved for the samples taken around the ESP and HGCU systems and the samples were also reproducible. Sampling periods for the ESP and APF were 6 to 8 hours to assure sufficient sample was collected for

Table 2-1

Field Sampling Requirements for Gas Streams

Analysis	ESP Inlet	ESP Outlet	APF Inlet	APF Outlet	Field Blanks[a]	Media Blanks[b]	PE Audit Samples
Particulate Loading	3	3	3	3	2	1	1
Metals[c]	3	3	3	3	2	1	1
Anions[c]	3	3	3	3	2	1	1
Ammonia/Cyanide[d]	3	3	3	3	2	1	1
Formaldehyde[d]	3	3	3	3	2	1	—
Volatile Organics[d]	6[e]	6[e]	6[e]	6[e]	12[f]	1	—
Semivolatile Organics[c]	3	3	3	3	2	1	—
Dioxins/Furans[c]	3	3	3	3	2	1	—
Particle Size Distribution	3	3	—	—	—	1	—
Hexavalent Chromium[g]	—	3	—	—	1	1	1

[a] One field blank each is collected at the ESP inlet and APF inlet to assess impact of sample handling at these two locations.
[b] Media blanks refer to prepared reagents for impinger solutions, blank VOST tubes, XAD resin catridges, and blank filters.
[c] Both particulate and vapor phases analyzed, separately.
[d] Vapor phase analysis only.
[e] Two 20 L samples collected per run.
[f] One field blank collected per locatino per run.
[g] Particulate and vapor phases combined for single analysis.

Table 2-2

Field Sampling Requirements for Coal, Sorbent, and Service Water

Analysis	Raw Coal	Coal Paste			Sorbent (Dolomite)			Service Water		
	Field Samples	Field Samples	Field Duplicates	PE Audit Samples	Field Samples	Field Duplicates	PE Audit Samples	Field Samples	Field Duplicates	PE Audit Samples
Ulitimate/ Proximate/ HHV	1 [a]	3	1	1	—	—	—	—	—	—
Metals	1 [a]	3	1	1	3	1	1	3	1	1
Anions	1 [a]	3	1	1	3	1	1	3	1	1
Radionuclides	1 [a]	3	1	—	—	—	—	—	—	—
% Moisture	1 [a]	3	1	—	3	1	—	—	—	—

[a] Raw coal samples held for possible analysis pending data quality assessment of coal past results.

Table 2-3

Field Sampling Requirements for Ash Samples

Analysis	Bed Ash		Primary Cyclone Ash		ESP Ash (4 Hoppers)		APF Ash		QC Audit Samples
	Field Samples	Field Duplicates	Field Samples	Field Duplicates	Field Samples	Field Duplicates	Field Samples	Field Duplicates	
Metals	3	1	3	1	3 [a]	1	3	1	1
Anions	3	1	3	1	3 [a]	1	3	1	1
Radionuclides	3	1	3	1	3 [a]	1	3	1	—
Carbon	3	1	3	1	3 [a]	1	3	1	—
Semivolatile Organics	3	1	3	1	3 [a]	1	3	1	—
Dioxins/ Furans	—	—	3	1	3 [a]	1	3	1	—
Particle Size Distribution	—	—	—	—	12 [b]	4	—	—	—

Table 3-1
Analyte List for Inorganic Parameters

Trace Elements	Major Elements
Antimony [a]	Aluminum
Arsenic [a]	Calcium
Barium [a]	Iron
Beryllium [a]	Magnesium
Boron	Potassium
Cadmium [a]	Sodium
Hexavalent Chromium [b]	Titanium
Chromium, total [a]	**Ultimate/ Proximate Parameters**
Cobalt [a]	Carbon
Copper [a]	Hydrogen
Lead [a]	Nitrogen
Manganese [a]	Sulfur
Mercury	Ash
Molybdenum [a]	Volatile Matter
Nickel [a]	Fixed Carbon
Selenium [a]	
Silver	
Vanadium [a]	
IONIC SPECIES	
Chloride (Cl)	
Fluoride (F)	
Phosphates (as Total P)	
Sulfates (SO_4^{-2})	
Ammonia	
Cyanide	

Table 3-2

Analyte List for Organic Parameters

Volatile Organics [a] (Method 8240)	Semivolatile Organics (Method 8270/CARB 429 [b])	
Benzene	Acenaphthene [b]	2,4-Dimethylphenol
Bromoform	Acenaphthylene [b]	Dimethylphthalate
Carbon Disulfide	Acetophenone	4,6-Dinitro-2-methylphenol
Carbon Tetrachloride	4-Aminobiphenyl	2,4-Dinitrophenol
Chlorobenzene	Aniline	2,4-Dinitrotoluene
Chloroform	Anthracene [b]	2,6-Dinitrotoluene
1,4-Dichlorobenzene	Benzidine	bis(2-Ethylhexyl)phthalate
cis-1,3-Dichloropropene	Benzo(a)anthracene [b]	Fluoranthene [b]
trans-1,3-Dichloropropene	Benzo(a)pyrene [b]	Fluorene [b]
Ethyl Benzene	Benzo(b)fluoranthene [b]	Hexachlorobenzene
Ethyl Chloride (Chloroethane)	Benzo(g,h,i)perylene [b]	Hexachlorobutadiene
Ethylene Dichloride (1,2-Dichloroethane)	Benzo(k)fluoranthene [b]	Hexachlorocyclopentadiene
Ethylidene Dichloride (1,1-Dichloroethane)	Benzoic Acid	Hexachloroethane
Methyl Bromide (Bromomethane)	Benzyl Alcohol	Indeno(1,2,3-cd)pyrene [b]
Methyl Chloride (Chloromethane)	4-Bromophenyl Phenyl Ether	Isophorone
Methyl Chloroform (1,1,1-Trichloroethane)	Butylbenzylphthalate	2-Methylnaphthalene
Methyl Ethyl Ketone (2-Butanone)	4-Chloro-3-Methylphenol	2-Methylphenol (o-cresol)
Methylene Chloride (Dichloromethane)	p-Chloroaniline	4-Methylphenol (p-cresol)
Propylene Dichloride (1,2-Dichloropropane)	bis(2-Chloroethoxy)methane	N-Nitrosodimethylamine
Styrene	bis(2-Chloroethyl)ether	N-Nitrosodiphenylamine
1,1,2,2-Tetrachloroethane	bis(2-Chloroisopropyl)ether	N-Nitrosopropylamine
Tetrachloroethene	2-Chloronaphthalene	Naphthalene [b]
Toluene	2-Chlorophenol	2-Nitroaniline
1,1,2-Trichloroethane	4-Chlorophenyl Phenyl Ether	3-Nitroaniline
Trichloroethene	Chrysene [b]	4-Nitroaniline
Vinyl Acetate	Di-n-octylphthalate	Nitrobenzene
Vinyl Chloride	Dibenz(a,h)anthracene [b]	2-Nitrophenol
Vinylidene Chloride (1,1-Dichloroethene)	Dibenzofuran	4-Nitrophenol
m,p-Xylene	Dibutylphthalate	Pentachloronitrobenzene
o-Xylene	1,2-Dichlorobenzene	Pentachlorophenol
	1,3-Dichlorobenzene	Phenanthrene [b]
	1,4-Dichlorobenzene	Phenol
	3,3'-Dichlorobenzidine	Pyrene [b]
	2,4-Dichlorophenol	1,2,4-Trichlorobenzene
	Diethylphthalate	2,4,5-Trichlorophenol
	p-Dimethylaminoazobenzene	2,4,6-Trichlorophenol

[a] These are the volatile organic compounds detected by VOST (Method 8240) that are listed in the Clean Air Act list of hazardous air pollutants.

[b] These semivolatile organic compounds will be analyzed in the gas samples by CARB Method 429 using high resolution GC/MS.

Table 3-3

List of Radionuclides

Gamma Emitters
Actinium-228 @ 338 KeV
Actinium-228 @ 911 KeV
Actinium-228 @ 968 KeV
Bismuth-212 @ 727 KeV
Bismuth-214 @ 609.4 KeV
Bismuth-214 @ 1120.4 KeV
Bismuth-214 @ 1764.7 KeV
Lead-210 @ 46 KeV
Lead-212 @ 238 KeV
Lead-214 @ 295.2 KeV
Lead-214 @ 352.0 KeV
Potassium-40 @ 1460 KeV
Radium-226 @ 186.0 KeV
Thallium-208 @ 583 KeV
Thallium-208 @ 860 KeV
Thorium-234 @ 63.3 KeV
Thorium-234 @ 92.6 KeV
Uranium-235 @ 143 KeV

analysis. Preliminary indications are that particulate collection efficiency of the APF is over 99.9%. An interesting observation of the APF sampling shows some removal of SO_2 across the APF. Inlet sampling at the APF required some adjustment to the sampling train. Higher than expected particulate loading required an additional alundum filter and a fiber filter to be added to the sampling train to assure full collection of the particulate and prevent contamination of other non-particulate parameters.

Analysis of the samples collected during this project is proceeding throughout the summer. The first draft report is expected by September 1.

FUTURE WORK

No additional HAP sampling of this nature is planned at PFBC.

REFERENCES

1. Sampling and Analysis Plan for Hazardous Air Pollutants at Tidd PFBC Demonstration Plant, 1994, Radian Corporation, Austin, Tx, DCN 93-633-021-01, RCN 633-021-01-01.

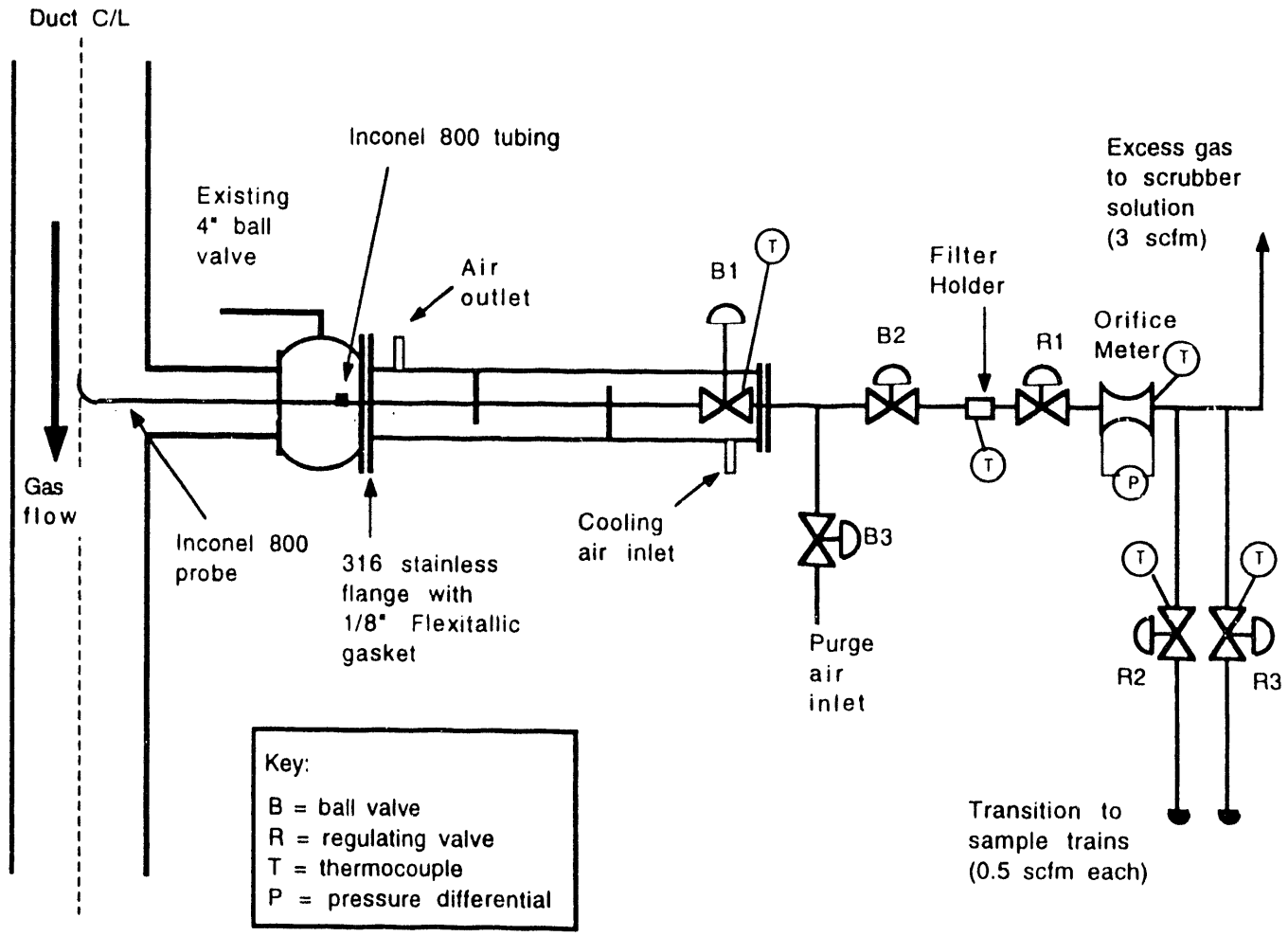


Figure 2. APF High Pressure Sampling System

8b.4 Trace Species Emissions for IGFC

CONTRACT INFORMATION

Contract Number DE-AC21-92MC29261

Contractor **ENERGY RESEARCH CORPORATION**
3 Great Pasture Road
Danbury, CT 06813
(203) 792-1460

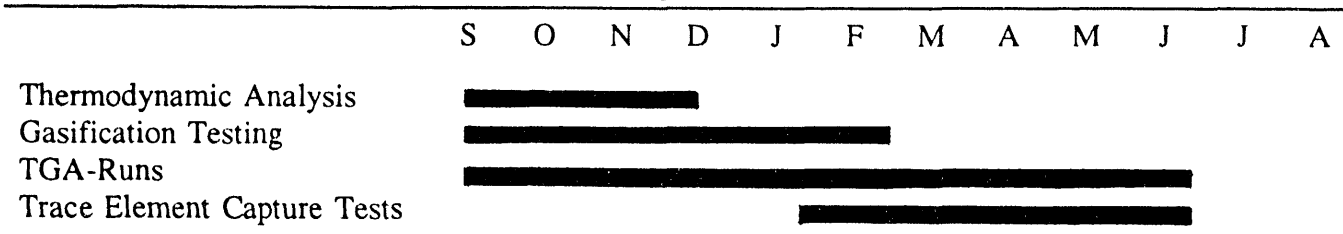
Contractor Project Manager A. Ed Pigeaud

Principal Investigators A. Pigeaud
J. J. Helble, PSIT

METC Project Manager Norman T. Holcombe

Period of Performance 9/30/1992 to 7/31/1994

Schedule of Milestones FY 1994 Program Schedule



OBJECTIVES

The objectives of this investigation are to study both the fate and distribution of at least five significant, coal-derived "trace" elements commonly present in coal-gas, in terms of their vaporization during gasification, their condensation and sorption during hot-gas cleanup, as well as their effects on fuel cells, gas turbines, and ultimately the environment. The definition here of "trace" does not include the major contaminants of sulfur and chlorine, etc., although the simultaneous presence of such major species is always considered in our thermochemical calculations. Of course, many other elements can vaporize in trace quantities from raw coal as either volatile, molecular compounds or as metallic vapors which, besides their deleterious action on the energy conversion systems, can also be detrimental to plant and animal life when emitted into the atmosphere. Hence, an understanding is sought of how the type and quantity of significant trace species in coal-gas changes from the coal pile through cleanup subsystems and the electric generators to the exhaust stack of an integrated system.

INTRODUCTION AND BACKGROUND

Behavior of coal contaminants toward potentially "very clean," highly efficient, integrated power generating systems, is becoming increasingly important from both a system's performance and endurance, as well as an environmental point of view. The overall project under this contract is entitled "TRACE ELEMENT EMISSIONS," and the goal is to investigate the fate and downstream effects of "trace" contaminant species during and after coal gasification.

The work has been performed in connection with the effects of trace elements on two advanced, coal gasifier with hot-cleanup, electric power generating technologies: viz., on Integrated Gasification Combined Cycle (IGCC) and on Integrated Gasifier Fuel Cell (IGFC) systems. A reasonably good understanding exists of the fate of major coal contaminants (i.e., sulfur, chlorine, alkali and nitrogen compounds) after coal combustion in steam-type power generating plants with back-end cleanup. But only a limited amount of information exists concerning minor or trace contaminants and toxic species deriving from coal-gas, which may affect fuel cell and/or turbine systems. Attention is also paid to possible differences in 'toxic' emissions into the environment from these trace elements; especially in connection with integrated, substoichiometric, or mild gasification as compared to direct, high temperature, complete combustion of coal.

Thus the present study is a follow-on to several contaminant investigations at ERC (each time in cooperation with PSI-Technology Company) regarding the "Effects of Coal-derived Trace Species on Performance of Molten Carbonate Fuel Cells".[1] To implement the current study, ERC and PSIT again formed a team to respond to this research challenge with a side by side comparison of the two power conversion systems (i.e., a dual energy plant) consisting of one gasifier feeding two types of electric power generators. As shown in Figure 1, a variety of

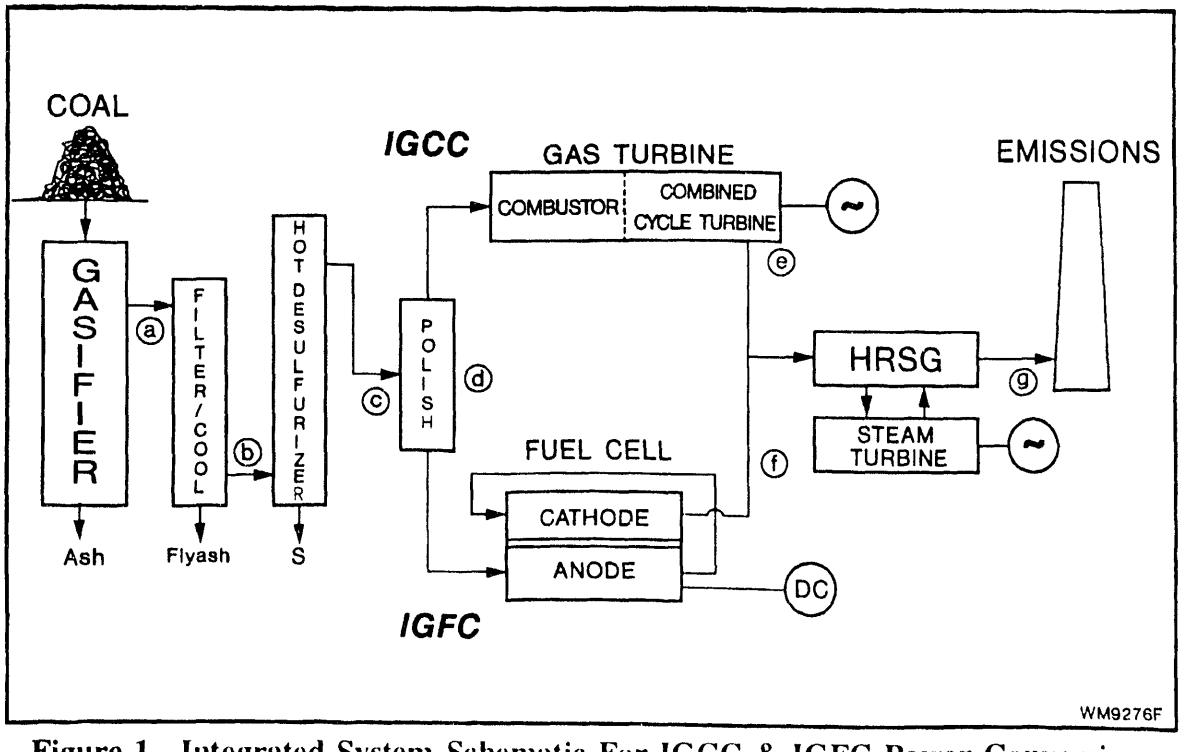


Figure 1. Integrated System Schematic For IGCC & IGFC Power Conversion
Configuration for Comparision of the 2 Emerging Technologies as to Trace Element Effects.

node points between the gasifier and hot-cleanup subsystems and power convertors, were targeted as to the contaminant levels remaining at these locations. An understanding of what was required to achieve successful completion of this effort, such as technical expertise and past experience with the subject systems, as well as available equipment for simulating the relevant processes, was well represented by the two companies and the background[2] they possess in this area.

Selection of 5 Most Significant Trace Elements

Before the five trace elements that were to be studied in depth were selected, it was decided that a scoping experiment should determine the most significant elements being actually evaporated in typical coal gasification. Table 1 presents the information initially available in the form of an overview ranking contaminant elements by weighting factors (+) according to the

Table 1. Ranking of Coal Contaminants in Terms of Abundance, Volatility, and Toxicity
As, Se, Sb, Zn, and Pb, Were Selected as Most Significant Elements to be Studied.

ERC's Original Contaminant Ranking List showing gaseous concentrations (ppmv) in coal-gas if all species are vaporized as acid gases, halides, and metal vapors between 600° and 1000°C		UND-EERC[3] In Illinois #6 Solid Coal (wppm)		UND-EERC Highest Potential Vaporization of Elements into Coal-gas estimated from the solid coal data (ppmv)	Preliminary Ranking			
					ABUNDANCE	VOLATILITY	TOXICITY LISTS	
		1st sample	2nd sample				EPA 17	DOE 11
Majors								
S	15,000	29,000	55,000	15,600	++++	+++		
Cℓ	500		470	120	++	+++	+	
Na	300		820	320	++	+++		
Trace-metalloids								
As	3.0	1.7		0.2	+	+++		+
Se	1.0	1.5		0.17	+	+++		+
Sb	0.1		< 1.0	0.07		++	+	+
Trace-metals								
Zn	100		65	9.0	++	+++		
Pb	3.0	3.2	6	0.26	+	++	+	+
Cd	0.2	0.14		0.011		+	+	+
Hg	0.01	0.032		0.0015		+	+	+
Cr	4	19	34	6.0	+		+	+
Ni	3	8.8	24	3.0	+		+	+
Mn	19				++			+
Be	2.3				+	?		+
Additional								
K			2200	512	++	+		
Co	1.5				+			+
Fe			23,000		+++			
Generally Also Present					Ti Al Si P Ca Mg Cu Ga Ge Mo Br			

WM9893

criteria of abundance in coal, volatility during gasification, and toxicity with respect to the environment. These early data have generally correlated quite well with subsequent gasification screening experiments, with Illinois #6 coal, that were done to definitively select arsenic (As), selenium (Se), antimony (Sb), zinc (Zn), and lead (Pb) as the five most significant elements to be studied in terms of coal-gas contaminant effects.

PROJECT DESCRIPTION

Thermochemical Calculations

The project was begun by conducting a literature search and developing the chemical properties data base for the different contaminant species that would be needed to compute site-specific thermodynamic equilibria of trace species interactions and possible condensed phase formation. Using this data base and the input from later gasification experiments which provided the types and concentrations of elements under initial gasifier exit conditions, theoretical trace species concentrations were calculated at various node points along the gas flow path from gasifier to power generating system. In this project, equilibrium modeling was conducted using a PC-based version of the SOLGASMIX computer code which minimizes the system free energy at certain locations (nodes) to predict the equilibrium phases - vapors, solids, liquids and condensed phase mixtures - as a function of local variables for complex multicomponent closed systems. In previous studies, the so-called SGM-CIS software was used to provide for calculation of 'Combined Ionic Solution' behavior as part of the SOLGASMIX program to especially account for sorption of trace species in the fuel cell's molten carbonate electrolyte.

Gasification Experiments

Experimental studies of the parameters of contaminant partitioning and distribution in coal-gas streams were begun with gasification studies performed at PSIT with Illinois #6 coal in a laminar flow, drop tube reactor, as shown in Figure 2, which was specially configured for ash classification and analysis. The unit was operated mostly by simulating conditions that occur in an oxygen-blown, Texaco gasifier, but were modified for ambient pressure application. Ash and flyash particles produced in these gasification runs were classified as to particle size distribution immediately after the reactor, and fractions separately analyzed for their elemental content by Neutron Activation Analysis (NAA) and Proton Induced X-ray Emission (PIXE).

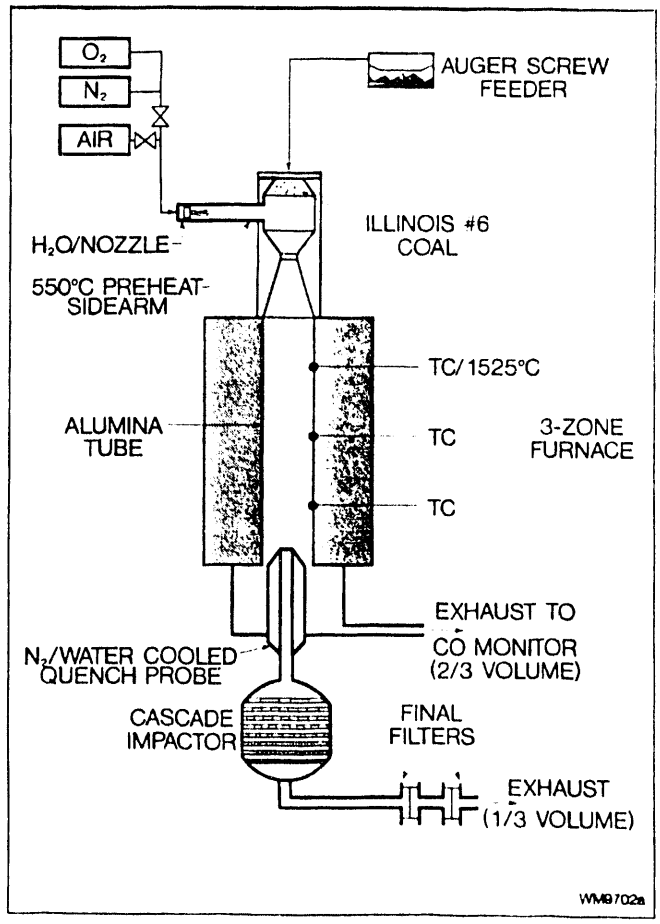


Figure 2. Laminar Flow, Drop Tube Reactor Configured for Ash Generation & Classification

Hence, volatile trace species sorption on both the ash particles produced in the reactor and trapped on the exit filters could be accurately studied for trace elemental content. Three types of gasification experiments were conducted. The first was an initial screening test to establish the five most significant volatile elements that were to be monitored in this work, and the second and third set of experiments were operated to further establish the effects of temperature, different oxygen levels, and hot ash filtration conditions on trace element partitioning.

Thermogravimetric Experiments

Numerous experiments to investigate desulfurization sorbents for their additional ability to also remove the 5 selected trace contaminants have been performed at ERC both in the past with early types of Zn-based sorbents (ZnO and $ZnFe_2O_4$) and now with the latest most promising zinc titanate sorbent (ZT-4). In all these experiments there has been a concern that generically all zinc compounds, even though they may be made mechanically strong and regenerable, may at too high a temperature be thermodynamically unstable in reducing environment and eventually lose their active zinc constituent. These studies are now being further pursued in a Cahn, TG-131, thermogravimetric apparatus as shown in Figure 3. Studies of equilibrium sorption of the five most significant elements and their interaction species on ZT-4 are currently being performed at 500°C.

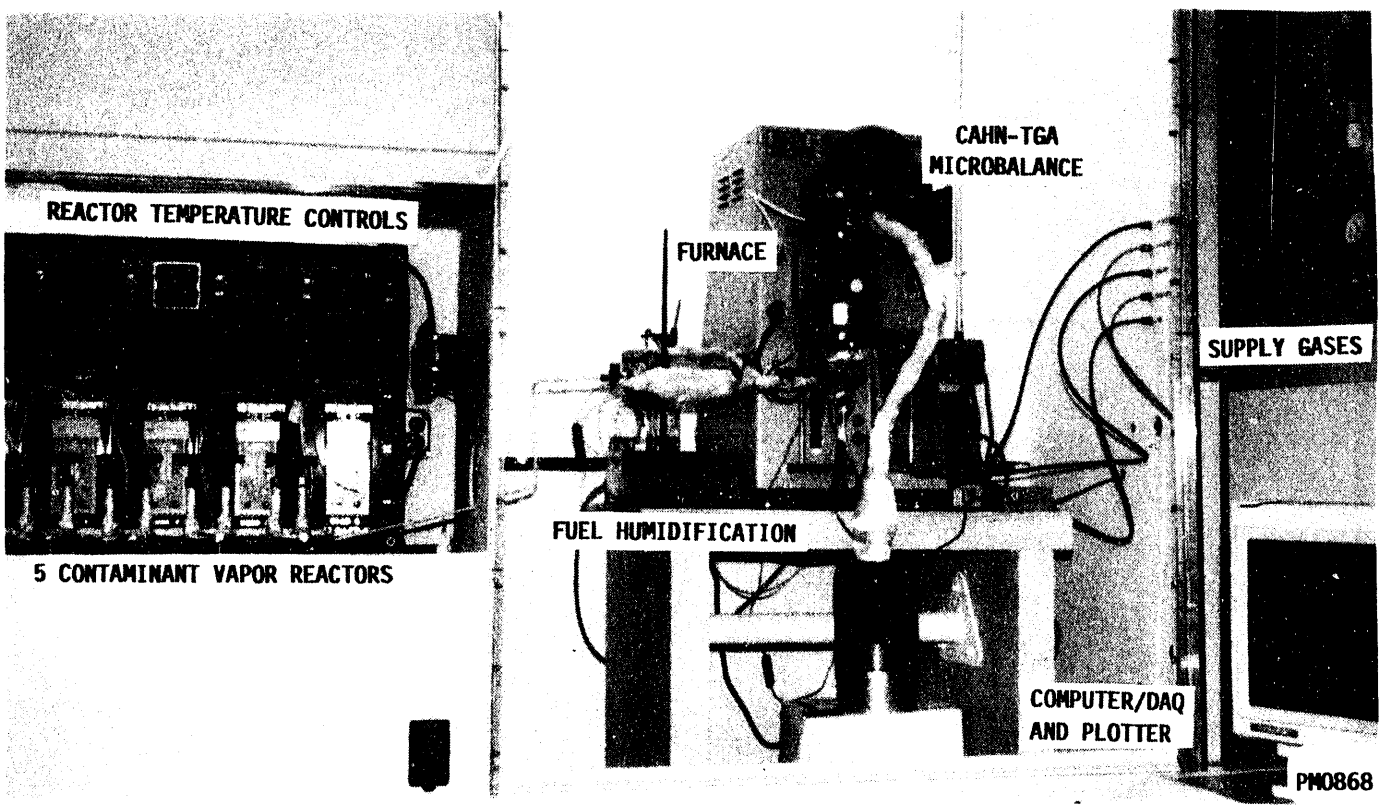


Figure 3. Thermogravimetric (TGA) Sorption Analysis Facility
Combinations of 5 Trace Elements Simultaneously, Plus H_2S and HCl, can be Handled.

Trace Element Capture Experiments

Prior work at PSIT has shown that aluminosilicates (perhaps as alkaline earth compounds) can react with several of the selected trace metals and metalloids at very high temperature (i.e., post-combustion) and in the presence of HCℓ and/or SO_2. The effectiveness of these sorbents is now being evaluated under conditions relevant to gasifier fuel conditions (i.e., in a strongly reducing environment) to be able to recommend useful, pre-combustion, control strategies. Trace species capture experiments with the five contaminants to be investigated are currently being performed by studying a number of different materials in PSI's Trace Capture Reactor as shown in Figure 4. Low concentrations of trace contaminants are generated in this equipment in simulated coal-gas flow and immediately afterwards tested for absorption on various sorbents.

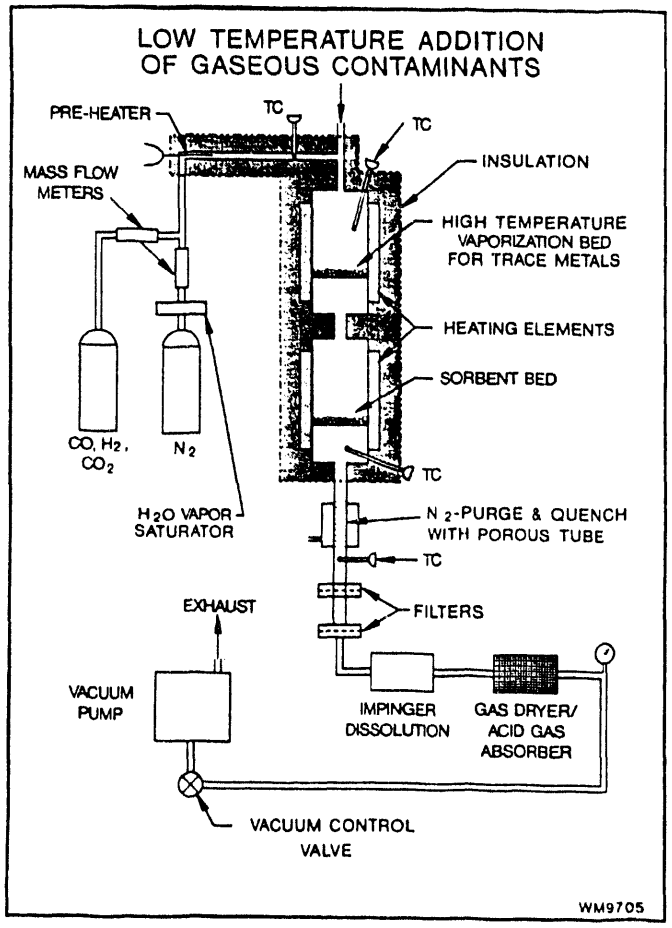


Figure 4. In-Line Element Capture Reactor
Tests of Absorption of Generated Trace Species Can Be Rapidly Performed.

RESULTS & DATA

Thermodynamic Analysis

Because of the large variations in temperature, pressure, and gas composition throughout the IGCC and IGFC systems, the actual experimental determination of different amounts of each trace element, either neat or as binary interaction compounds, in gaseous or condensed form at the different node points, would have been prohibitively expensive. Therefore, as was also done in previous fuel cell studies, we have again resorted to thermochemical computation methods before performing the selective experiments representing an actual situation. Effects of the different variables on the partitioning of trace species among the different phases, including sorbent materials and other equipment components, can be quickly determined if the basic free energy data for all the species are available. For example, at 550°C and at 3 different pressures, computations were done for the high temperature incoming gaseous trace contaminant concentrations after node:b to become the lower temperature contaminant levels after node:c when the gas has been scrubbed in the presence of excess Zn_2TiO_4, as shown in Table 2. This clearly illustrates that merely by calculation very important conclusions can be quite rapidly drawn, such as the large amount of zinc that may be removed in the presence of HCℓ at the lower desulfurizer temperatures.

Table 2. Effects of Temperature, Pressure and Presence of Zn_2TiO_4 Sorbent on Gas Equilibria
Thermodynamic Calculation Provides Important Insights into 'Fate' of Trace Element Species.

Species	@ 827° before Sorbent Addition, Node:b			@ 550° C after Sorbent Addition, Node:c		
	1 atm	3 atm	10 atm	1 atm	3 atm	10 atm
As_2	46.5	41.6	30.8	41.2	31.5	20.8
AsH_3	5.6	15.6	40.1	12.3	18.8	24.8
As_4	-	-	-	6.9	12.2	17.7
Sb	6.1	3.7	2.1	-	-	-
Sb_2	11.7	13.0	14.1	7.0	4.6	2.8
Sb_4	-	-	-	5.7	7.5	8.9
H_2Se	98.5	98.9	101.8	122.5	130.7	137.2
ZnSe	-	-	-	-	-	-
Zn	984.1	985.9	1005.7	247.2	46.3	7.5
$ZnCl_2$	1.0	3.1	12.1	1077.8	993.1	951.7
ZnS	-	-	-	-	-	-
Pb	9.9	9.5	8.7	10.8	4.0	0.9
PbCl	1.0	1.7	2.9	38.4	31.0	18.1
$PbCl_2$	-	-	-	24.0	43.0	60.9
PbS	48.1	48.2	49.3	0.3	0.2	0.1
% increase (decrease) in gas phase zinc before/after desulfurization due to presence of bulk Zn_2TiO_4				8%	(20%)	(30%)

WM9957

Gasification Testing

Knowing that inorganic contaminant elements and compound species present as vapors or as submicron-condensed particles, are extremely difficult to remove for analysis (from hot product gas) when using just cyclones, electrostatic precipitators, or even ceramic filter matrices, the approach taken was to combine several methods to provide gradual condensation, absorption, and (cold) submicron filtration to trap most of the trace element species vaporized from coal. During gasification, inorganic trace species will partition as both vapors and as condensed phase species that become part of, or adsorbed on, the ash and flyash particles (e.g., mostly alumino-silicates) that are produced at the same time in a wide range of particle sizes. Thus, by simultaneously cooling and allowing the condensing trace species to adsorb on ash particles while also segregating the ash particles by size in a cascade impactor, it was possible to use this flyash as an analytical aid in identifying the time/temperature histories (and therefore volatility) of many of the trace element species that are of interest both qualitatively and quantitatively.

As shown in Table 3, once species were segregated on the 7 cascade impactor stages (representing d_{50} particle ranges of 10μm down to <0.3μm) and then on 2 submicron filters, it was clearly evident which elements were not present as volatile species (e.g., Fe, Ni, Mn, Cr, etc) and which had remained volatile toward the end until being adsorbed at the lowest temperature finest filtration stages (e.g., As, Se, Sb, Zn and Pb).

Table 3. Composite NAA and PIXE (wppm) Data of Filter and Impactor Stage Ash Analysis
Combined Data from 8 Experimental Runs Have Elucidated Relative Trace Element Volatilities.

ELEMENTS	Cascade Impactor Stages, wppm				Polycarbonate Filter wppm	Final Filter Activated Carbon
	1	3	5	7		
Majors						
S	1900	-	-	1900	37,000	-
Br	120	2	11	~16	1240	0
Na	2700	4700	-	0	~400	0
K	7500	-	1500	66	1600	-
Minors						
As	2	5	-	11	28	0
Se	3	6	-	9	~51	0
Sb	-	1	-	4	12	0
Trace Metals						
Zn	~130	450	1300	~785	~5600	17,000
Pb	-	-	250	300	2500	-
Cd	1	2	-	1	2	-
Hg	-	1	-	1	1	2000
Metals						
Ni	590	-	140	95	140	-
Fe	~71,000	~61,000	19,000	~570	~1200	0
Mn	350	-	100	4.4	-	-
Cr	~765	430	280	~24	52	0

WM9958

TGA - Runs

The concern in our TGA-sorption experiments with regard to baseline stability of sorbent material before introducing the various trace element species, has led to several initial runs with H_2, 20% humidified H_2, and with simulated coal-gas of a nominal composition (i.e., 26% H_2, 38% CO, 25% H_2O, 9% CO_2). Alternating temperature ramping (50°C steps starting at 400°C) and isothermal equilibration periods of ~12 hours, were used to investigate the baseline stability of zinc titanate, as shown in Figure 5. A susceptor with titanate sorbent evenly distributed in 5 levels or pans (average of ~1.2 gram per pan), was used to follow the weight changes of the sorbent material for total run periods of up to 72 hours. It is seen that at the max. 500°C temperature, the material remains sufficiently stable to follow low level weight increases that we expect to observe in connection with trace species absorption of a number of trace elements on this sorbent. These runs are currently in progress.

Trace Element Capture Testing

Tests are in progress but insufficient data are available at this time.

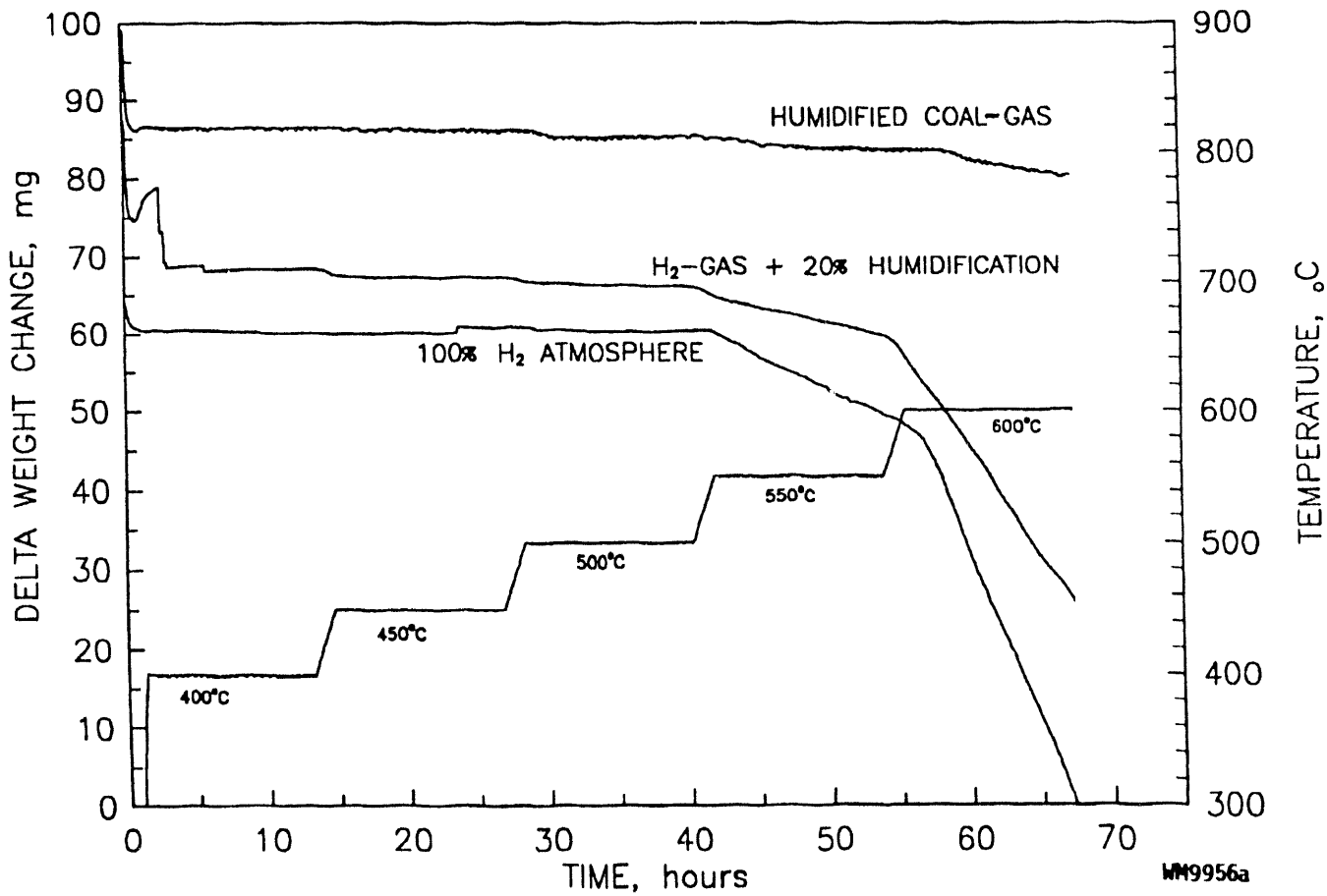


Figure 5. TGA Experimental Runs with (~6 gram) Samples of Sorbent
Examination of Effects of Temperature and Humidity on Stability of Zn_2TiO_4 in Reducing Atmosphere for Trace Element Sorption Studies.

FUTURE WORK

To sum up this present investigation of the 'fate' of contaminants at various sites that are of concern to evolving integrated power systems, it is seen that the five most significant trace elements generated by coal gasification, have been identified. And also, that a pattern for their control and removal at high temperature is evolving. However, since only limited theoretical calculations were done within the scope of the current program and experimental con-firmations are also needed, there are still a number of areas where future work in a follow-on program is recommended. For example:

Thermochemical Calculations

The power of our computer research technique has become well established and together with additional modeling would further advance the general ability to quickly predict trace element behavior and effects on IGCC and IGFC systems.

Three specific areas requiring calculational effort are at: 1) *The Gasifier.* Formation of complex aluminosilicates with the 5 trace elements, and correlation with experimental partitioning data as a function of existing gasification conditions. Clearly, the ability to develop a model that better defines aluminosilicate formation from different coals, and which is gasification conditions specific, would be of great use to tailor the type of gasifier and operating conditions needed for optimum integration into power conversion systems; 2) *Hot-Gas Cleanup.* Interaction of trace elements with other than zinc titanate desulfurization sorbents should be considered. Modeling of contaminant interactions with zinc titanate sorbents using equilibrium thermochemistry has been successful. Similar calculations should now be done for other sorbents to determine the utility of a variety of likely desulfurization materials that could also be beneficial for trace contaminant or metal vapor removal; 3) *NiO-cathode on O_2-rich side of Matrix.* Interactions of trace elements in this part of the carbonate fuel cell, after anode exit-gas is recycled (and oxidized for CO_2 recovery) and trace species become reexposed to the molten carbonate electrolyte, are still a concern that has not yet been addressed.

Gasification Experiments

In our current program, the concentration of trace elements as a function of ash particle size sorption was measured primarily for volatility determination. Only limited experiments were conducted to start assessing the effects of gasification conditions and temperature on changes in trace element volatilization. Results indicate that trace element vaporization is dependent on gasifier stoichiometric conditions, where the amount of an element vaporizing decreases with increasing partial pressure of oxygen in the system; this also increases the ash particle temperature. To explore this interaction in more detail and to determine whether gasification conditions can be optimized to improve trace element capture, a detailed study examining trace element partitioning as a function of gasification stoichiometry, pressure, and other parameters, should be considered.

Thermogravimetric Experiments

Initial equilibrium experiments of weight loss or gain should usually be considered as a preliminary test in determining a sorbent's stability and its affinity for removing low level gaseous trace species, which can than serve to confirm whatever the thermochemical calculations may have indicated. These TGA-runs can be very simply and rapidly performed, and can also be used to establish the regenerability of materials in different gas atmospheres. Such runs are currently being performed at ERC in connection with a new material and a method for trace element polishing.

Trace Element Capture Experiments

In-line experiments which can closely simulate high temperature contaminant absorption conditions, can elucidate the kinetics of immediate (post-gasification) trace element capture using a variety of materials. Studies of activated sorbents for early removal of the five significant elements are now employing this methodology. In this respect, it is also recommended to expand the test matrix to study early capture of additional elements such as chlorine, cadmium, and mercury species. Another area would be to combine activated sorbents with zinc-based, hot-gas desulfurization (in a single or dual bed reactor) and evaluate the combined effect of also removing trace elements together with sulfur.

REFERENCES

1. Pigeaud, A. and Wilemski, G.; "Effects of Coal-drived Trace Species on Performance of the Molten Carbonate Fuel Cell". In ERC's 1991 Topical Report and 1992 Final Report to DOE/METC under Contract DE-AC21-88MC25009. NTIS/DE9300-0203.

2. Helble, J.J., Srinivasachar, S., Wilemski, G., et al.; "Transformation of Inorganic Coal Constituents in Combustion Systems". In PSI's 1992 Final Report (3 volumes) to DOE/PETC under Contract DE-AC21-86PC90751. NTIS/9301-3076, -7, -8.

3. Benson, S.A. and Erickson, T.A.; Illinois #6 Coal Sample supplied by the ENERGY & ENVIRONMENTAL RESEARCH CENTER at Univ. of North Dakota - Private Communications, 7/93 and 11/93.

8b.5 Hazardous Air Pollutant Sampling for Advanced Power Systems

CONTRACT INFORMATION

Contract Number

Contractor

Radian Corporation
P.O. Box 201088
Austin, TX 78720-1088

Contractor Project Manager

Gwen Eklund

Principal Investigators

Robert G. Wetherold
Al Williams
David P. Maxwell
Robert M. Mann
Don B. Burrows

Project Manager

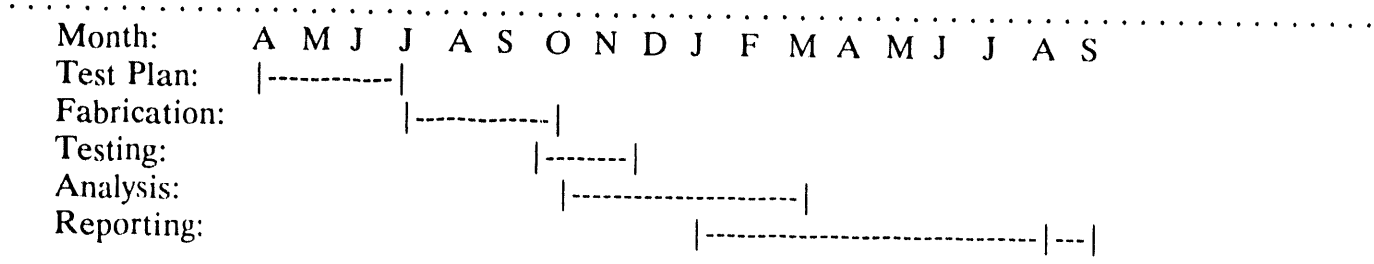
Lori Gould

Period of Performance

June 1, 1994, to September 30, 1995

Schedule Milestones

FY 1994 & 1995 Schedule



OBJECTIVES

This program will characterize an advanced power system to fulfill the following objectives:

- To quantify HAP emissions;
- To determine HAP distribution;
- To define internal control device effectiveness; and
- To characterize the hot, raw syngas.

Two additional project objectives are (1) to compile data in a relational database system to enhance its review and analysis and (2) to determine emission factors for the turbine and incinerator exhaust streams. The project will use innovative sampling techniques, very sensitive analytical techniques, and an enhanced quality assurance/quality control

program.

BACKGROUND INFORMATION

The 1990 Clean Air Act Amendments have resulted in the review of the fate of hazardous air pollutants (HAPs) within and from advanced power systems. HAP assessment has not been conducted at most of the advanced power system demonstration facilities, but efforts have been undertaken recently to conduct HAP data collection.

Both the U.S. Department of Energy (DOE) and the Electric Power Research Institute (EPRI) have programs to address HAP data collection for conventional power systems. Radian Corporation has performed HAP measurements to support both the DOE and EPRI programs. Radian has also performed HAP measurements at the General Electric gasification pilot plant and turbine simulator located at the GE Research and Development Center in Schenectady, New York, and at the American Electric Power Tidd Plant, a 70-MW PFBC facility in Brilliant, Ohio.

Many of the sampling and analytical methods used by DOE and EPRI for conventional coal-fired power systems may not be applicable for advanced power systems because of the reducing gas conditions produced by gasification facilities (IGCC or IGFC). The purposes of this paper are (1) to review current programs under which Radian has provided advanced power system HAP assessment in association with DOE and (2) to review methods which will be useful in both conventional and special systems with reduced/fuel environments.

Emphasis will be placed on the work proposed for the IGCC system which Destec Energy Systems operates as the Louisiana Gasification Technology Inc. (LGTI) at Dow's Louisiana Division in Plaquemine, Louisiana.

PROJECT DESCRIPTION

Radian will conduct a HAP monitoring program at Destec's LGTI facility. A schematic of the system, showing sample collection points, is presented in Figure 1.

The program will include preparation of a detailed test plan for HAP determination, determination of the fate of HAPs through the process units at the facility, determination of the effectiveness of control systems at the facility, and collection of HAP data for the hot raw gas exiting the reactor to provide input data to hot gas cleanup research. The program will consist of an 18-month effort from planning through reporting.

The Destec LGTI gasifier is a slagging design, high-pressure, entrained flow system which has been operational since 1987. The unit produces 30,000 MMBtu/day of equivalent syngas while operating on 2,200 tons per day of western subbituminous coal from the Rochelle mine in Wyoming. The unit produces 169 MW equivalent net power. A second demonstration of the technology will be conducted at the Wabash River Coal Gasification Repower Project in West Terre Haute, Indiana. That system, with 262 MW net power, will be the largest single-train coal gasification combined-cycle facility in the United States.

Samples will be collected around the

following process units in the LGTI system:

- Gasifier;
- Particulate removal;
- Gas cooling;
- Acid gas removal;
- Gas turbine;
- Sulfur recovery;
- Sour water stripper;
- Incinerator; and
- Coal preparation.

Consistent with the DOE and EPRI HAP program design, three sample sets will be collected during the test program. The components of interest will include:

- **Hydrocarbons:** C_1-C_6, benzene, toluene, xylenes, aldehydes, and polynuclear aromatic hydrocarbons;

- **Sulfur species:** hydrogen sulfide, carbonyl sulfide, carbon disulfide, dimethyl sulfide, dimethyl disulfide, mercaptans, and sulfur dioxide;

- **Nitrogen species:** ammonia, cyanides, thiocyanates, and nitrogen oxides;

- **Halogen species:** hydrogen chloride and hydrogen fluoride; and

- **Trace elements:** 11 HAPs and 13 other substances.

Table 1 shows the primary differences expected between emitted streams (oxidized environments) and gasification streams (reduced environments). For example, metal oxides, primarily particles, are expected in oxidizing environments, but carbonyls, hydrides, or sulfides might be found in reducing environments. The forms of the various metal species are not known; organometallic compounds may be present.

Radian will use U.S. EPA reference methods for most emissions streams; however, internal streams will require method modifications, in addition to alternative methods and techniques, to provide accurate data. Specific sampling and analytical issues are discussed below.

Organic Compounds

While a volatile organic sampling train (VOST) can be used for the collection of volatile organic compounds in oxidized environments, reduced sulfur species in internal streams can interfere with instrumental analyses. For the reduced environments, on-site analysis by gas chromatography (flame ionization detection) is used to conduct volatile organic compound analysis. Grab samples can be collected in Tedlar® bags or in glass or stainless steel bombs.

Sulfur Species

On-site GC analysis is also required for sulfur species; in this case, flame photometric detection is used. For some species, direct iodimetric titration is used.

Nitrogen Species

The principal modification to be made when collecting and analyzing nitrogen species from reducing environments is sulfide removal, which is critical. For example, sulfides *must* be removed immediately after collecting samples for cyanide. An acidic solution of lead nitrate or lead acetate is commonly used.

Halogens

The determination of the halogenated species HCl and HF requires no modification in approach. As in oxidized environments, the species are determined as chloride and fluoride, respectively.

Trace Elements

The collection of trace elements requires the use of charcoal (carbon) adsorption and on-line AAS in addition to Method 29, which is used for oxidized environments.

Charcoal Adsorption. Radian has found that charcoal adsorption is efficient for the collection of iron and nickel (as their carbonyls) as well as for arsenic, antimony, lead, mercury, and zinc. Specially cleaned and prepared charcoal tubes are used in series to assess capture and breakthrough; parallel trains are used to compare results by different analytical techniques.

On-Line AAS. In on-line atomic absorption spectrophotometry, a slipstream of the syngas is used as fuel in the flame of an atomic absorption spectrophotometer. Radian has applied this single-element technique for measuring arsenic, nickel, chromium, selenium, cadmium, mercury, lead, and zinc.

Hot Gas Sampling Probe

A unique feature of this program is the requirement to separate and collect particulate matter and vapor at the following conditions:

- 850–1250° F;
- 300–500 psig; and
- High particulate loading.

The sample components must be preserved for quantitative determination.

The design of the hot gas sampling probe is based on probes used by Radian for similar sampling in other projects. The sample gas passes through the probe as the gas pressure is reduced. Particulate matter is either collected or prevented from entering the probe by an in-stack filter or thimble. After passing into the probe, the collected gas is quenched with nitrogen before being directed to the sample collection/analytical device.

CURRENT STATUS

Radian has prepared a detailed test plan for the LGTI HAP monitoring study. The plan has been reviewed by Destec, DOE/PETC, DOE/METC, and EPRI. The detailed plan presents:

- Facility description;
- Approach to HAP testing;
- Methods used to collect, prepare and analyze samples;
- Quality assurance for program data;
- Process data requirements; and
- Data reduction procedures.

In addition, an important aspect of the testing is the collection of hot, raw pressurized gas (gas representative of this gasifier technology), which would be fed to a hot gas cleanup system. Characterization of this stream provides vital stream information for METC's hot gas cleanup program. Radian has prepared a design document for a hot gas probe to be used at the LGTI facility. The probe will allow collection of vaporous and particulate

samples at stream temperature and pressure.

FUTURE WORK

Testing will take place in October and November of 1994. October testing will consist of checkout and verification of the hot gas sampling system. November testing will address HAP monitoring and sample collection of the system streams. Samples will be transported to laboratories for detailed characterization. Following data assessment and results validation, a report will be prepared for the testing. Although most of the internal streams are considered proprietary data sources by Destec, data review procedures have been defined by Destec, DOE, and EPRI to permit data transfer to those important HAP control programs of DOE and EPRI.

Table 1. Primary Differences Between Oxidized and Reduced Streams

Class	Combustion (Oxidized)	Gasification (Reduced)
Organic Compounds	Very Low	Low - High
Sulfur Species	SO_2	H_2S, COS, CS_2, DMS, DMDS, mercaptans
Nitrogen Species	NO_x	NH_3, HCN
Metals	Metal Oxide (Particle)	Carbonyls? Hydrides? Sulfides?

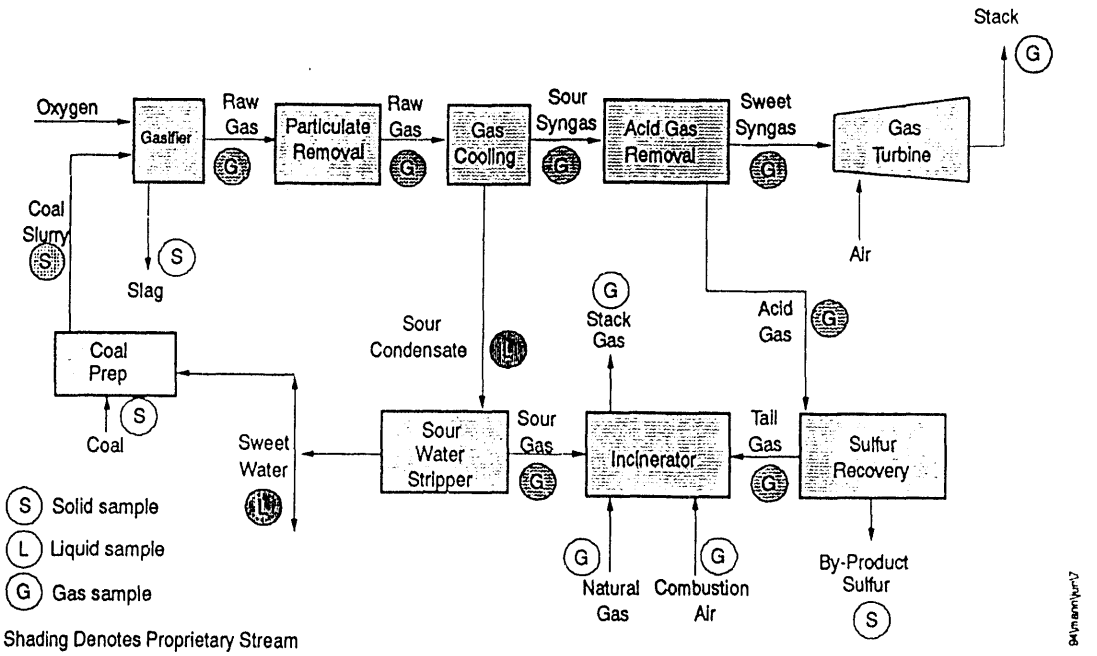


Figure 1. LGTI Gasification System with Sampling Points Shown

8b.6 Instrumentation for Trace Emission Measurements

William P. Chisholm
Morgantown Energy Technology Center

Rising concerns about the potential release of harmful elements into the environment from coal utilization have driven the development of new analytical capabilities. And recent environmental regulations, such as the Clean Air Act and Amendments, demand superior performance from new coal-based technologies as regards their pollution emission potential. In particular, a number of toxic or hazardous trace elements found in coal must be measured and controlled.

Currently available instrumentation for fossil fuel process and combustion monitoring requires sample extraction and remote analysis in a laboratory. This type of monitoring is not adequate for commercialization of many of the advanced technologies under development at METC. In particular, on-line or real-time data, though difficult to obtain, may be necessary for advanced process characterization or control. Especially challenging is the task of sampling and characterizing systems at high temperature and pressure. The inductively coupled plasma (ICP) spectrometer has the potential to perform elemental composition analysis for the purpose of continuous emissions monitoring.

The shortcomings of conventional ICP systems plumbed directly to high-temperature and high-pressure process systems have been previously discussed [1]. In brief, these systems cannot sustain a plasma in a gas stream containing a large proportion of molecular gases, they cannot be connected to hot, pressurized sample lines, and the plasma emission spectrum contains strong interfering molecular bands. The ICP system we are developing addresses all these difficulties.

To enable sampling hot, pressurized sample streams, we have developed a new torch, which is sectioned into several pieces with o-ring seals protected by a cooling fluid. The new torch may be made of an insulating ceramic capable of direct connection to a hot sample line. Our plasma support gas is a mixture of argon and helium. The addition of helium allows the torch to operate at relatively high powers, up to 10 kilowatts. With this power level, molecular band emission is inhibited and the plasma operates stably with sample gas flow rates as high as 90 cubic centimeters per second.

The simultaneous multielement detection system has previously been described in detail [1]. It comprises a battery of small monochromators equipped with 4800-groove per millimeter gratings, and a silica fiber optic bundle optical train.

In order to make the ICP system suitable for field deployment, it was made modular and mobile. The ICP torchbox, the detectors and optics, and the calibration system will be located near the point of sample extraction. The data acquisition system, controlling computer, gas cylinders, and the radio frequency power generator can be located up to 30 meters away. Therefore, the operator and the more sensitive electronics can be in a safe, protected enclosure, while the actual sampling is preformed at a restricted or exposed location.

Given the limitations of typical methods of ICP data analysis, a better way to determine elemental concentration was needed, a method that could account for the interferences and

complications sometimes present in spectra. It was decided that a back-propagation Artificial Neural Network (ANN) might be a tool useful in analyzing this data.

ANNs are computer programs inspired by, and functioning similarly to, biological neural networks. The ANN is trained on a set of ICP data generated with the calibration system, but also including the effects of flow rates, power, easily ionized elements, and spectral interferences. It can incorporate all of these to relate measured spectral intensities to elemental concentrations. Initial experiments have proved promising.

Future work with METC's on-line ICP system will include actual data acquisition from a bench-scale gasifier and further refinement of the current data acquisition and processing software. Also, a two-dimensional array detector coupled to an echelle spectrograph is being developed.

REFERENCES

1. Romanosky, R.R., A.S. Viscomi, S.S. Miller, and W.P. Chisholm. Proceedings of March 1993 American Chemical Society Conference. Denver, Colorado, March 28 - April 2, 1993.

WCHISH\1:940852

Session 9a

Sorbents and Solid Wastes

9a.1 Development of Sorbents for High-Temperature Desulfurization in Moving-Bed Systems

CONTRACT INFORMATION

Contract Number	DE-AC21-88MC25003
Contractor	GE Corporate Research and Development P.O. Box 8 Schenectady, NY 12301 (518) 387-5850
Contractor Project Manager	Raul E. Ayala
Principal Investigators	Raul E. Ayala, Timothy Chuck, GE Corporate R&D Eli Gal, GE Environmental Services, Inc. Raghubir P. Gupta, Research Triangle Institute
METC Project Manager	Daniel C. Cicero
Period of Performance	September 21, 1988 to January 31, 1995

Schedule and Milestones

FY94 Program Schedule

	S	O	N	D	J	F	M	A	M	J	J	A	S
Sorbent Preparation	———												
Bench-Scale Mods. and Testing	———												
Bench-Scale Analysis			———									———	
Topical Report*													

* Task Scheduled for FY95

OBJECTIVES

The objective of the option 3 program within this contract is to develop chemically reactive and mechanically durable mixed-metal oxide sorbent formulations that are suitable for moving-bed, high-temperature, desulfurization of coal gas. One optimum formulation will be evaluated in a pressurized 50-cycle bench-scale test.Work on zinc ferrite formulations was performed under the base program (Ayala, 1991). Work on zinc titanate formulations was initiated under the option 2 program (Ayala, 1993) and is continued under the present option 3 program along with testing of other mixed-metal oxides.

BACKGROUND INFORMATION

GE is developing a moving-bed, high-temperature desulfurization system for integrated gasification combined-cycle (IGCC) power systems in which zinc-based regenerable sorbents are currently being used as desulfurization

sorbents (Furman et al., 1992). In addition to zinc ferrite, zinc titanate and other novel mixed-metal oxides are being considered as sorbents, particularly for highly reducing coal gases where iron-containing sorbents can potentially undergo excessive sorbent physical degradation. A key to sucess in the development of high-temperature desulfurization systems is the development of a sorbent for the selected process operating conditions.

Mixed-metal oxide sorbents have been studied quite extensively in the past, including various types of zinc titanates (e.g., Zn_2TiO_4 and $Zn_2Ti_3O_8$) (Gangwal and Gupta, 1993) or as combinations of other metal oxides such as vanadium, copper, manganese, cobalt, tin, and others; see for instance (Lynch and Hepworth, 1993). During absorption from coal gases, H_2S reacts with zinc titanate according to the reaction

$$Zn_2TiO_4 + 2H_2S \Rightarrow 2ZnS + TiO_2 + 2H_2O \quad (1)$$

Similarly, during regeneration, zinc sulfide reacts with oxygen in the regenerant gas to revert back to the original oxide.

$$2ZnS + TiO_2 + 3O_2 \Rightarrow Zn_2TiO_4 + 2SO_2 \quad (2)$$

However, the regeneration zinc may lead to undesired side reactions, depending on process conditions, such as the formation of zinc sulfate according to

$$ZnO + SO_2 + \tfrac{1}{2}O_2 \Rightarrow ZnSO_4 \quad (3)$$

Zinc sulfate formation is undesired because (a) it results in significant density differences between the starting and ending solid phases that induces mechanical stresses within the pellet, and (b) the sulfate so formed during regeneration reacts with the H_2 and CO in the coal gas in subsequent desulfurization cycles, that results in the release of SO_2 according to

$$2ZnSO_4 + 5H_2 \Rightarrow ZnO + ZnS + SO_2 + 5H_2O \quad (4)$$

Although the feasibility of removing H_2S to very low levels (e.g., < 50 ppmv) from coal gases has been shown to be viable in most studies of mixed-metal oxides, one of the major limitations for large-scale use of mixed-metal oxides is the observed weakening and physical deterioration of the pellet and spalling during repetitive use in cycles of absorption and regeneration (Ayala el al., 1993). A need exists to determine best operating conditions that minimize sulfate formation and prevent mechanical degradation.

PROJECT DESCRIPTION

Program participants are: GE Corporate Research and Development (GE-CRD, prime contractor), GE Environmental Systems, Inc., (GEESI, subcontractor), and Research Triangle Institute (RTI, subcontractor). United Catalysts, Inc. (UCI) and Phillips Petroleum Company (PPC), acting as vendors, provided the sorbent samples for testing.

Sorbents developed for moving-bed systems must comply with a minimum of chemical and mechanical durability performance characteristics in order to be considered acceptable for long-term operation. Among the desired properties, a sorbent must have:

- High chemical reactivity, as measured by the rate of sulfur absorption and the total sulfur loading on the sorbent.
- High mechanical strength, as measured by the pellet crush strength and the attrition resistance.

- Suitable pellet morphology, as given by pellet size and shape to promote good bulk flowability and reasonable porosity to increase reactivity.

RESULTS

During the current year, several zinc-based sorbent formulations were tested in the laboratory, including UCI's zinc titanate sorbents and PPC's Z-Sorb sorbent, a family of proprietary sorbent formulations. Preparation methods for UCI's zinc titanate sorbents have been described previously (Ayala, 1993). Preparation methods for Z-Sorb formulations are considered proprietary to PPC, and only analyses that describe performance in hot gas desulfurization are presented here.

Table 1 shows the physical properties of the sorbents tested in the program. Both L-4103 B2 and T-2535M are zinc titanate formulations (Zn_2TiO_4) fabricated by UCI and contain 2.0-2.5% MoO_3 as pore modifier and 3% bentonite binder. L-4103 B2 was prepared as a laboratory formulation while T-2535M2 was produced as a larger batch (6,000 lb) for use in the GE moving-bed pilot plant in Schenectady, New York.

Formulations labeled Z-Sorb A and Z-Sorb B are standard formulations sold under the trade name Z-Sorb III. The other Z-Sorb formulations were developed for GE with a larger pellet size by PPC for GE's moving-bed system. Formulation Z-Sorb C was supplied as a one-gallon batch for laboratory evaluation, while Z-Sorb E was supplied as a 12,000 lb batch for use in the GE moving-bed pilot plant. One major difference between zinc titanate and Z-Sorb sorbents is their bulk density (Table 1), with Z-Sorb being a less dense material.

Testing of the sorbent formulations and assessment of their suitability for use in moving-bed desulfurization systems was carried out by measuring single-pellet chemical reactivity of fresh and cycled sorbents in a thermogravimetric analyzer (TGA), desulfurization performance in bench-scale reactor tests, and mechanical durability and sulfate formation in the cycled pellets. Details of experimental procedures have been published previously (Ayala, 1993; Ayala et al., 1993)

Table 1. Physical Properties of Sorbent Formulations

	L-4103 B2	T-2535M2*	Z-SORB: A, B	Z-SORB C	Z-SORB E*
Pellet Length, mm	5.0	6.1	3.6-3.9	6.5, 7.3	6.4
Pellet Diam., mm	4.0	4.9	2.6-2.9	6.4	4.3
Pellet Mass, mg	200	214	27-32	280	114
Crush Strength, lb/pellet	23.2	17.1	7.6-7.1	14.9	10.2
Attrition Resistance, %	95-96.6	96-98.5	99.6-99.1	98.3	98.4
Bulk Density, lb/ft^3	107	~100	~60	~60	~60

* Tested at the GE-CRD Pilot Plant also.

Table 2. Conditions for Bench-Scale Testing of Zinc Titanate and Z-Sorb

Cycle Number:	Gas Composition	Temperature
A1-A8 (6 hr)	39% CO, 10% CO_2, 30% H_2, 20% H_2O, 1% H2S	1000 °F
R1-R5	0.5-21% O_2, bal. N_2	1000-1300 °F
R6-R8	0.5-20% O_2, 5% SO_2, bal. N_2	1000-1300 °F
R8+1400 °F(2 hours)	20% O_2, 5% SO_2, bal. N_2	1400 °F

A- Absorption; R-Regeneration

Fresh Sorbent Chemical Reactivity

Figure 1 shows the comparison of single-pellet chemical reactivity measured by thermogravimetric analysis (TGA) for various zinc titanate and Z-Sorb formulations. Standard conditions for TGA are 1000 °F, 3% H_2S (Ayala, 1993). The weight gained by a single pellet as a function of time is directly proportional to the amount of H_2S absorbed by the pellet according to equation (1). A strong correlation is seen between the pellet size and the relative reactivity of the pellets: the smaller the pellet size (i.e., a higher ratio of pellet surface area to volume) the higher the weight gained as a function of time, as typical of pore-diffusion controlled reactions.

A desirable rate of H_2S absorption in moving-bed desulfurization systems is a TGA chemical reactivity of 50% of theoretical sulfur loading in less than 1 hr for fresh material, an a minimum of 50% in 2 hours for extended cyclic testing. Overall, pellets with an average diameter greater than 6 mm may not be sufficiently reactive for development of large-scale systems.

Bench-Scale Testing

In order to compare side by side the relative desulfurization performance of zinc titanate and Z-Sorb, an accelerated 8-cycle test in the bench-scale reactor system was performed. L-4103 B2 zinc titanate and Z-Sorb B were loaded in two reactors of the bench unit. The specific objective of the bench test was to determine the limits of operability for the two sorbents under identical conditions, particularly with respect to pellet spalling and mechanical deterioration due to zinc sulfate formation. Conditions for absorption and regeneration reactions are shown in Table 2. Pressure was held constant at 1 atm for both absorption and regeneration. The gas composition for absorption (cycles A1-A8) was chosen to simulate an oxygen-blown gasifier coal gas similar to that proposed for the Tampa Electric hot gas cleanup system program, except for the slightly higher H_2S and H_2O. The H_2S concentration was kept artificially high at 1% to accelerate the testing. Absorption time was held constant at 6 hours for each of the sorbents regardless of the level of H_2S leaving the reactors.

For regeneration, the test conditions were varied to examine their effect on zinc sulfate formation, reactivity and durability of the sorbents. Regenerations R1 to R5 in Table 2 were conducted without added SO_2 (while maintaining the regeneration maximum temperature below 1300 °F). Regenerations R6 through R8 were conducted adding 5% SO_2 to the regenerant gas to simulate the effect of recycled SO_2. In addition,

Table 3. Desulfurization Performance by Sorbents

	L-4103 B2 Zinc Titanate	Z-Sorb B
Max. Sulfur Capacity (lb S/100 lb fresh)	25	20
Pre-breakthrough outlet H_2S	<20 ppm H_2S	<10 ppm H_2S
% Total S (Abs. 5)	6.03 - 8.87	10.62 - 16.17
% of Max Sulfur Capacity	27 - 40	58-88
lb Sulfur/ft^3 of bed	7.3-10.7	7.0-10.7
% Carbon	0.14-0.18	0.14-0.20

after the R8 regeneration the bed temperature was raised to 1400 °F under 20% O_2 and 5% SO_2 to test the response of the sorbents to extremely harsh conditions of accelerated regeneration at high temperatures.

Desulfurization Performance

Table 3 shows the results of desulfurization by zinc titanate and Z-Sorb after the fifth absorption in the bench-scale reactor system. Both sorbents were exposed for six hours to simulated coal gas. Zinc titanate has a theoretical maximum sulfur capacity of 25 lb/100

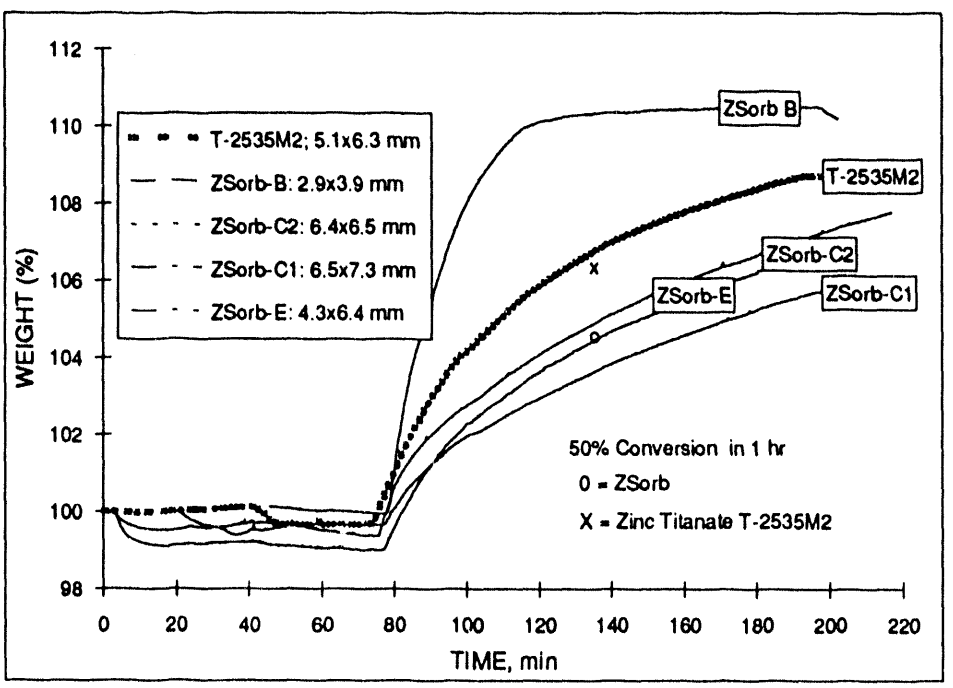


Figure 1. Comparison of fresh pellet TGA chemical reactivity

Table 4. Physical Appearance of Cycled Sorbents

	5th Reg.	8th Reg.	8th Reg. +1400F *
Zn Titanate:			
Pellet Color	white	gray	light gray /yellow
%Cracking	none	none	> 40%
Z-Sorb B:			
Pellet Color	off-white	off-white /yellow	off-white /green
%Cracking	none	none	almost none

* Held for 2 hrs

lb of fresh sorbent while Z-Sorb B has a capacity of 20 lb/100 lb of fresh sorbent. Both sorbents did an excellent job at desulfurization, with H_2S levels leaving the reactor prior to breakthrough of less than 10 ppmv for Z-Sorb B and less than 20 ppmv for zinc titanate. These levels correspond to more than 99% desulfurization (based on 1% H_2S in the inlet gas). Comparison of the total sulfur in the sorbents at the gas inlet and gas outlet locations shows that Z-Sorb B is a more reactive sorbent on a mass basis (comparing 10.6 to 16.2% sulfur in Z-Sorb versus 6 to 8.9% sulfur in zinc titanate). However, after adjusting for bulk densities of the sorbents, both sorbents had a comparable sulfur loading per unit volume of bed between 7 and 10.7 lb sulfur per ft^3 of bed. This result is very important for future reactor design because it suggests that a reactor vessel designed for zinc titanate can operate with Z-Sorb under similar process conditions.

Finally, Table 3 also compares the amount of carbon deposits found in both sorbents after the 6-hr absorption with the simulated coal gas containing 20% H_2O. There is no significant difference in the amount of carbon collected on the sorbents and it appears that cycled Z-Sorb does not catalyze the formation of carbon deposits from the Boudouard reaction ($2CO \leftrightarrow C + CO_2$).

Mechanical Durability of Sorbent Pellets

The level of pellet mechanical deterioration during cycling was assessed, first, semi-quantitatively by measuring the fraction of pellets showing signs of hairline cracking or spalling, and then by measuring crush strength and attrition resistance of the cycled sorbents. Table 4 presents the physical appearance of the sorbents at various stages of testing and shows that zinc titanate suffered severe degree of surface cracking after the 2-hr treatment to 1400 °F (i.e., 8th. Reg + 1400 °F). Z-Sorb B, on the other hand, did not suffer any significant degree of cracking, or very minimal at worst.

The mechanical durability of the pellets was assessed quantitatively by measuring the crush strength (Figure 2) and attrition resistance (based on ASTM D 4058-81 test) (Figure 3). Again, experimental procedures have been described previously (Ayala, 1993). The qualitative observation that zinc titanate deteriorated during the heat treatment to 1400 °F was corroborated by the measurement of crush strength and attrition resistance. Crush strength decreased in L-4103 B2 zinc titanate by almost a factor of two, from 23 to 13 lb/pellet and attrition resistance decreased from 96.6% to 88.0% in the same period. Note that crush strength of the 5-mm diameter zinc titanate is not directly comparable to the strength of the 3-mm Z-Sorb B because of the difference in pellet size and the fact that the pellets, being ellipsoids in shape (i.e., cylinders or spheres with rounded edges), do not have an easily measurable contact

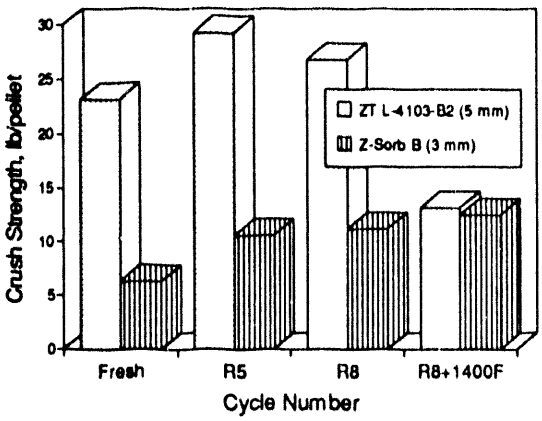


Figure 2. Comparison of Crush Strength During Bench-Scale Testing

line to scale the force per pellet to force per unit length.

Figure 4 shows the corresponding concentration of sulfate sulfur in the sorbents as a function of regeneration cycle for the two sorbents. Zinc titanate underwent mechanical deterioration when the sulfate sulfur level increased from approximately 2% after regeneration R8 to approximately 4% under the 1400 °F treatment. The sulfate sulfur level found in the sorbents correlated very well with the crush strength, attrition resistance, and physical appearance of the zinc titanate through the various

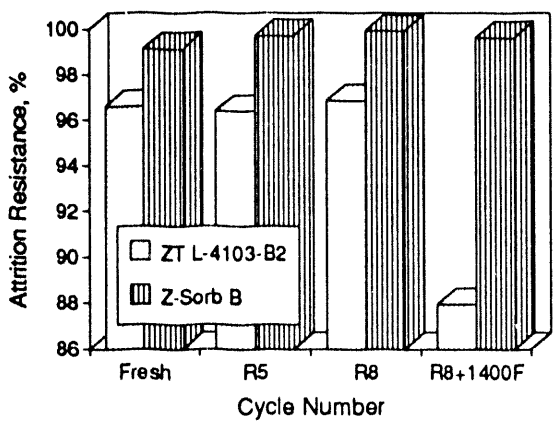


Figure 3. Comparison of Attrition Resistance During Bench-Scale Testing

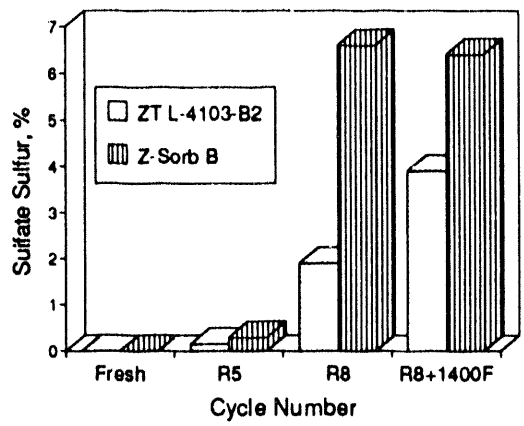


Figure 4. Comparison of Sulfate Formation During Bench-Scale Testing

cycles. On the other hand, Z-Sorb showed that despite forming larger amounts of sulfate sulfur, as high as 6%, did not develop a significant amount of measurable cracks and the sorbent did not lose mechanical strength. The superior mechanical durability of Z-Sorb B compared to L-4103 B2 zinc titanate was clear after the parallel accelerated bench testing of the two sorbents.

The following conclusions can be drawn from the atmospheric testing of L-4103 B2 zinc titanate and Z-Sorb B:

- Reactivity of Z-Sorb B towards H_2S removal from simulated coal gases is comparable to that of zinc titanate when pellets of similar size and shape are considered. The reactivity of the Z-Sorb pellets is a strong function of pellet size.
- Sulfur loading of Z-Sorb B after 6 hours of absorption is higher than that of zinc titanate on a mass basis, but very similar when presented on a bed volume basis. The difference being a result of the lower bulk density of Z-Sorb compared to zinc titanate

- Carbon formation due to the CO dissociation (Bouduard reaction) in cycled Z-Sorb was no different from that of zinc titanate.

- The mechanical durability of zinc titanate deteriorates dramatically under regeneration conditions of high SO_2/air at 1400 °F because of high rate of sulfate formation that produces internal stresses in the pellets resulting in the formation of hairline cracks and spalling.

- Both zinc titanate and Z-Sorb are suitable for operation in a moving-bed system under regeneration conditions below 1400 °F. The higher mechanical durability of Z-Sorb at 1400 °F gives a wider range of operability of the sorbent during pilot plant operation where optimum process conditions are being explored in support of the moving-bed desulfurization system for the TECO Clean Coal Technology Program.

FUTURE WORK

Having determined the conditions for proper regeneration of zinc-based materials, a long-term 50-cycle test of the best Z-Sorb formulation will be initiated in the modified bench-scale reactor system. The test will include:

- Pressurized sulfidation at 10 atm

- Pressurized regeneration up to 7 atm using recirculated gases for closer simulation of the pilot-plant regeneration recycle loop

The objective of the pressurized long-duration test would be to quantify sorbent performance over many cycles (long-term durability) at one set of selected conditions for absorption and regeneration.

REFERENCES

Ayala, R.E. 1993. Enhanced Durability of High-Temperature Desulfurization Sorbents for Moving-Bed Applications. Option 2 Program: Development and Testing of Zinc Titanate Sorbents. Contract DE-AC21-88MC25003. Topical Report submitted to DOE/Morgantown Energy Technology Center. April 1993.

Ayala, R.E. 1991. Enhanced Durability of High Temperature Desulfurization Sorbents for Moving-Bed Applications. Base Program: Development and Testing of Zinc Ferrite Sorbents. Topical Report. DOE/MC/25003-3045. NTIS/DE92001121. Springfield, Va.: National technical Information Service.

Ayala, R.E., E. Gal, and R.P. Gupta. 1993. Testing of Zinc Titanate Sorbents for Moving-Bed Applications. In *Proceedings of the Coal-Fired Power Systems 93 – Advances in IGCC and PFBC Review Meeting*, p. 136-145. DOE/METC-93/6131. NTIS/DE93000289. Springfield, Va.: National Technical Information Service.

Ayala, R.E., E. Gal, and R.P. Gupta. 1992. Enhanced Durability of High-Temperature Desulfurization Sorbents for Moving-Bed Applications. In *Proceedings of the Twelfth Annual Gasification and Gas Stream Cleanup Systems Contractor's Review Meeting*, Vol. 1. p. 230. DOE/METC-92/6128. NTIS/DE93000228. Springfield, Va.: National Technical Information Service.

Furman, A.H., C.S. Cook, E. Gal, and R. Ayala. 1992. Integrated Operation of a Pressurized

Fixed Bed Gasifier and Hot Gas Desulfurization System. In *Proceedings of the Twelfth Annual Gasification and Gas Stream Cleanup Systems Contractor's Review Meeting*, Vol. I. p. 84. DOE/METC-92/6128, Vol. 1. NTIS/DE93000228. Springfield, Va.: National Technical Information Service.

Gangwal, S.K., and R.P. Gupta, 1993. Enhanced Durability of Desulfurization Sorbents for Fluidized-Bed Applications. In *Proceedings of the Coal-Fired Power Systems 93 – Advances in IGCC and PFBC Review Meeting*, p. 146-157. DOE/METC-93/6131. NTIS/DE93000289. Springfield, Va.: National Technical Information Service.

Lynch, D and M.T. Hepworth. 1993. Hot Gas Desulfurization with Manganese-Based Sorbents. In *Proceedings of the Coal-Fired Power Systems 93 – Advances in IGCC and PFBC Review Meeting*, p. 432-444. DOE/METC-93/6131. NTIS/DE93000289. Springfield, Va.: National Technical Information Service. See also Karpuk, M.E., R.J. Copeland, D.Feinberg, D. Wickham, B. Windecker, and J.Yu. High Temperature Hydrogen Sulfide Removal. p. 411.

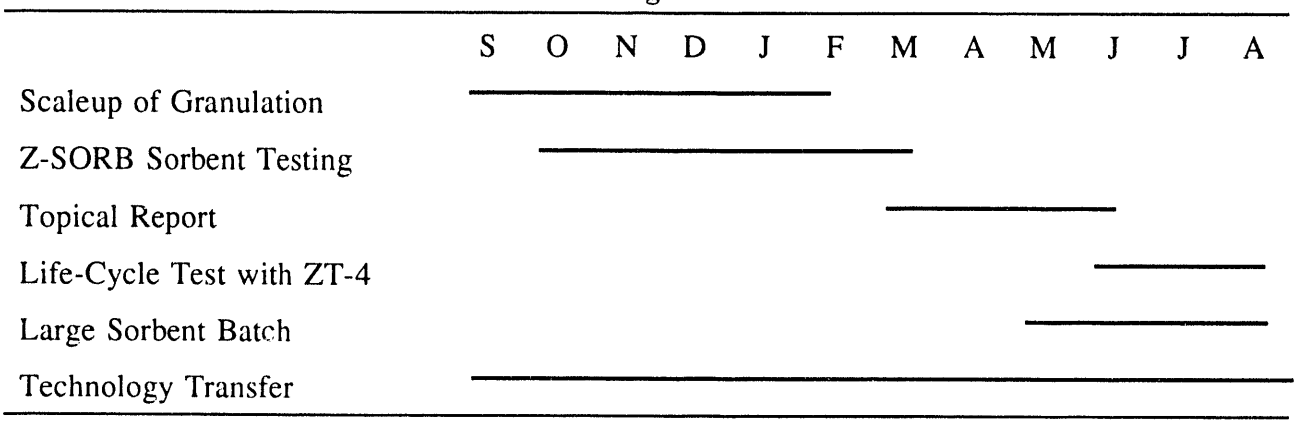
9a.2 Fluidized-Bed Sorbents

CONTRACT INFORMATION

Contract Number	DE-AC21-88MC25006
Contractor	Research Triangle Institute P. O. Box 12194 Research Triangle Park, NC 27709-2194 (919) 541-8023
Contractor Project Manager	Santosh K. Gangwal
Principal Investigator	Raghubir P. Gupta
METC Project Managers	Suresh C. Jain Daniel C. Cicero
Period of Performance	September 21, 1988 to November 20, 1994

Schedule and Milestones

FY94 Program Schedule



OBJECTIVES

The objectives of this project are to identify and demonstrate methods for enhancing long-term chemical reactivity and attrition resistance of zinc oxide-based mixed metal-oxide sorbents for desulfurization of hot coal-derived gases in a high-temperature, high-pressure (HTHP) fluidized-bed reactor. Specific objectives of this study are the following:

- Investigating various manufacturing methods to produce zinc ferrite and zinc titanate sorbents in a particle size range of 50 to 400 μm;

- Characterizating and screening the formulations for chemical reactivity, attrition resistance, and structural properties;
- Testing selected formulations in an HTHP bench-scale fluidized-bed reactor to obtain an unbiased ranking of the promising sorbents;
- Investigating the effect of various process variables, such as temperature, nature of coal gas, gas velocity, and chemical composition of the sorbent, on the performance of the sorbent;
- Life-cycle testing of the superior zinc ferrite and zinc titanate formulations under HTHP conditions to determine their long-term chemical reactivity and mechanical strength;
- Addressing various reactor design issues;
- Generating a database on sorbent properties and performance (e.g., rates of reaction, attrition rate) to be used in the design and scaleup of future commercial hot-gas desulfurization systems.
- Transferring sorbent manufacturing technology to the private sector; and
- Producing a large batch (in tonnage quantities) of the sorbent to demonstrate commercial feasibility of the preparation method.

BACKGROUND INFORMATION

Research Triangle Institute (RTI) is assisting the U.S. Department of Energy/Morgantown Energy Technology Center (DOE/METC) in the development of a fluidized-bed hot-gas desulfurization system employing ZnO-based mixed metal-oxide sorbents for removal of sulfurous compounds (e.g., H_2S, COS, CS_2) at high-temperature (500 to 750 °C [932 to 1,382 °F]), high-pressure (15 to 20 atm) conditions. Desulfurization of hot coal gas in a fluidized-bed reactor offers a number of potential advantages over fixed beds. Although fixed-bed reactors are operationally simple and provide high sorbent sulfur capacity and zinc utilization and low sulfur breakthrough, they suffer from some serious problems including the need to use hot valves and poor ability to control the temperature during highly exothermic regeneration. Recently, severe spalling and decrepitation of zinc titanate sorbent pellets in fixed beds surfaced as a serious problem owing to the formation of zinc sulfate and subsequent expansion in molar volume during regeneration (Mei et al., 1993). In contrast, fluidizable zinc titanate particles became stronger with cycling and do not suffer from sulfate formation problems (Gupta and Gangwal, 1993). Additionally, fluidized-bed reactors have a number of advantages including easier control of temperature during regeneration, use of small particles leading to faster overall kinetics, and nearly continuous steady-state operation. However, a highly reactive and attrition-resistant sorbent is required, and scaleup and turndown limitations exist for fluidized-bed systems.

PROJECT DESCRIPTION

In this program, regenerable ZnO-based mixed metal-oxide sorbents are being developed and tested. These include zinc ferrite, zinc titanate and Z-SORB sorbents. The Z-SORB sorbent is a proprietary sorbent developed by Phillips Petroleum Company (PPCo).

Design and Construction of an HTHP Bench-Scale Sorbent Test Facility

During the first phase (1989) of this program, a 3-in. ID bench-scale HTHP semi-batch fluidized-bed reactor system was designed and constructed. This reactor operates in a semi-batch mode because the flow of gas phase is continuous while sorbent particles remain in the reactor. This system is capable of operation at up to 871 °C

(1,600 °F) at 20 atm. Any simulated coal gas can be generated in this system using a battery of eight mass flow controllers and three positive displacement pumps (for pumping liquid water to generate steam). This system is equipped with a state-of-the-art computer controlled data acquisition system. A series of gas chromatographs (GCs) and continuous on-line analyzer measure the concentrations of various species in the reactor exit gas such as H_2S, COS, SO_2, CO_2, H_2, CH_4, N_2, CO, O_2. A complete description of this test facility is given elsewhere (Gupta and Gangwal, 1992; 1993).

Development and Testing of Zinc Ferrite Sorbents

Earlier work in this program was focused on preparing fluidizable zinc ferrite particles in 50- to 300-μm particle diameter range. A number of sorbent preparation techniques were investigated including spray drying, impregnation, crushing the durable extrudates and screening, and granulation.

Of these techniques investigated, granulation proved to be the most successful and a number of zinc ferrite sorbent formulations were prepared using this technique. Testing of these sorbents in the HTHP bench reactor demonstrated that these sorbents possess sulfur capacity and attrition resistance as good as or better than sorbents prepared by crushing and screening. Results of bench-scale testing of selected sorbent formulations are described elsewhere (Gupta and Gangwal, 1991).

With zinc ferrite sorbents, excessive sorbent loss was observed at a sulfidation temperature of 625 °C (1,157 °F). It is thought that attrition of the sorbent in the reactor is primarily due to chemical transformations rather than mechanical forces. Possible chemical transformations responsible for attrition are excessive reduction of $ZnFe_2O_4$ and iron carbide formation (Gupta and Gangwal, 1991; Gupta et al., 1992).

The applicability of zinc ferrite as a hot-gas desulfurization sorbent, therefore, is conservatively limited to below 550 °C (1,022 °F) and to moderately reducing coal gases, such as low-Btu gas from an air-blown gasifier containing at least 15 percent water vapor. Higher temperatures, as shown in the study, led to excessive sorbent weakening.

Development and Testing of Zinc Titanate Sorbents

To extend the operating temperature and desulfurize highly reducing coal gases, zinc titanate sorbent was developed for fluidized-bed reactors. Following the success of the granulation technique with zinc ferrite sorbents, it was used to prepare a series of zinc titanate formulations in the 50- to 400-μm particle diameter range. A number of sorbent formulations prepared using the granulation technique exhibited excellent durability, attrition resistance, and sulfur capacity during multicycle testing as described in an RTI topical report to METC (Gupta and Gangwal, 1992).

Based on screening tests, a series of promising sorbent formulations were identified. Further testing of these formulations indicated that ZT-4 sorbent had the best overall performance tested in terms of attrition resistance, chemical reactivity, regenerability, sulfur capacity, and other physical and structural properties. RTI was granted a U.S. Patent on manufacture of fluidizable zinc titanate sorbent (Gupta et al., 1993).

Ten HTHP runs were carried out, each involving 10 sulfidation-regeneration cycles in the bench unit. Bench-scale testing variables included sorbent type, temperature (550 to 750 °C [1,022 to 1,382 °F]), gas type (KRW or Texaco gasifier gas), steam content of coal gas, and fluidizing gas velocity (6 to 15 cm/sec). In all 10 multicycle tests, unlike zinc ferrite sorbents, the sulfur capacity utilization for zinc titanate sorbents at breakthrough was consistently between 40 and 60

percent with very little decline with cycling. The attrition resistance of 10-cycle regenerated sorbent was significantly better than the fresh sorbent in all the runs. The detailed test results are described in an RTI topical report to METC (Gupta and Gangwal, 1992).

Reactor Design Issues

During bench-scale testing, it was demonstrated that sulfided sorbent can be completely regenerated with 1 to 5 percent O_2 in N_2. Sulfate formation was not found to occur at 760 °C (1,400 °F) and 15 atm (220 psia). The inlet temperature could be controlled to reach the required 760 °C (1,400 °F) with any of the oxygen contents tested. Also, regeneration of the zinc titanate sorbent demonstrated stoichiometric formation of an essentially O_2-free, SO_2-containing off-gas according to $ZnS + (3/2)\ O_2 \rightarrow ZnO + SO_2$. A quasi-steady-state generation of SO_2-containing off-gas was demonstrated indicating that a nearly constant steady-state SO_2 content in the regeneration off-gas of a commercial fluidized-bed system can be obtained. The constancy of SO_2 concentration in the regeneration tail-gas is believed to be essential for economical downstream processing to elemental sulfur or sulfuric acid.

The sulfidation reaction was found to be controlled by intrinsic chemical reaction rather than external or pore diffusion. The apparent activation energy for the sulfidation reaction ranged from 15 to 20 kcal/mol depending on the sorbent composition, indicating that significant reduction in size of the desulfurization reactor can be achieved by increasing the operating temperature. A simple single-parameter mathematical model that assumed well-mixed solid phase and plug flow of gas made a reasonable prediction of the breakthrough behavior in the semi-batch HTHP reactor. Effects of addition of HCl and NH_3 were also investigated on the sorbent performance (Gupta and Gangwal, 1992).

100-Cycle Test with ZT-4

Following the successful multicycle parametric testing of various zinc titanate formulations in the bench-scale fluidized-bed reactor, a life-cycle test consisting of 100 sulfidation-regeneration cycles was carried out to determine the long-term reactivity and mechanical strength of ZT-4 sorbent. This life-cycle test was carried out at 750 °C (1,382 °F) sulfidation temperature, 15 atm (220 psia) pressure with a medium Btu Texaco O_2-blown gasifier gas containing 11,400 ppmv of H_2S. These highly severe sulfidation conditions were purposely selected to provide possible worst-case results of long-term sorbent durability. Regeneration of the sulfided sorbent was performed using 2 to 2.5 percent O_2 in N_2 in a temperature range of 720 to 760 °C (1,328 to 1,400 °F). The amount of sorbent in the reactor was 500 g and a relatively high superficial gas velocity of 15 cm/s was used to ensure good fluidization and to more closely simulate commercial operation. This resulted in a superficial gas residence time of only about 1.24 seconds.

This life cycle test conducted under extremely severe operating conditions, and highly reducing nature of coal gas, demonstrated superior performance of the ZT-4 sorbent. The following were the pertinent findings of this life-cycle test:

- The ZT-4 sorbent consistently reduced the H_2S content of coal gas from 11,400 ppmv to <20 ppmv in a semi-batch bench-scale fluidized-bed at 750 °C (1,382 °F) and 15 atm.

- The sorbent was found to be fully regenerable, with negligible residual sulfate remaining. An oxygen concentration of 2 to 3 percent with N_2 diluent was found to result in adequate regeneration rates with no temperature control problems due to the exothermicity of the regeneration reaction.

- The sulfur capacity of the sorbent at breakthrough of 500 ppmv H_2S ranged from 12.6 wt% in Cycle 1 to 5.8 wt% in Cycle 100 with an average of about 9 percent. Most of the decline in the sulfur capacity occurred during the first 50 cycles.

- The decline in sulfur capture capacity was found to correlate with a decrease in the BET surface area, pore volume, and internal porosity. The best correlation, as expected with small particles, was with the BET surface area.

- X-ray diffraction (XRD) analysis indicated the presence of zinc silicate in the sorbent, which is believed to result from the reaction of ZnO with free SiO_2 released from the distributor material. Zinc silicate is believed to be a potential cause of some of the reactivity loss.

- Attrition resistance measurements carried out in our 3-hole airjet attrition tester indicated that the attrition resistance of the sorbent after 100 cycles of testing was significantly higher (<3% 5-h loss) over that of the fresh sorbent (about 40% 5-h loss).

- No significant sorbent loss (<2%) from the reactor was detected over 100 cycles. The total zinc loss determined by chemical analysis was negligible.

Complete details of the test conditions and experimental results are reported in RTI's recent topical report to METC (Gupta and Gangwal, 1993).

Z-SORB Sorbent Testing

PPCo developed a fluidizable version of its Z-SORB sorbent for testing in RTI's HTHP fluidized-bed bench-scale test facility as discussed previously. A life-cycle test consisting of 50 cycles of sulfidation and regeneration was carried out with PPCo's involvement and guidance throughout the test to demonstrate long-term durability and mechanical strength. The details of this test and experimental findings are described in a separate paper entitled "Fluidization Studies Using Phillips Z-SORB Sorbent," included in this proceedings volume. A topical report jointly prepared by RTI and PPCo is currently being reviewed and will be submitted to METC by June 30, 1994.

Scaleup of the Granulation Technique

As discussed previously, the fluidizable zinc titanate sorbents (e.g., ZT-4) prepared by granulation technique exhibited superior performance during long-term testing. These sorbents were prepared in a laboratory-scale granulator of 2-L capacity. In order to prepare large sorbent batches for clean coal demonstration plants, the lab-scale granulator was replaced by a 35-L machine. A number of zinc titanate batches were prepared in this machine with the recipe used in preparation of ZT-4.

The physical and chemical properties of the sorbent designated as ZT-4L ('L' refers to the large machine) were compared with those of the original ZT-4. Table 1 shows a comparison of these properties. Figure 1 shows a comparison of the thermogravimetric analyzer (TGA) reactivities of ZT-4 and ZT-4L measured using the standard 1.5-cycle TGA test described in Gupta and Gangwal (1992). It is noteworthy in Figure 1 that at saturation the weight gain is identical for both the sorbents as would be expected owing to their exact chemical composition. The slope of the sulfidation curve in Figure 1, which represents the rate of H_2S absorption, is somewhat greater for ZT-4L compared to ZT-4, indicating a degree of superior chemical reactivity. Examination of physical property data listed in Table 1 for both the sorbents clearly indicates superior attrition resistance of ZT-4L over ZT-4. The difference in the surface areas and the pore size distribution is insignificant.

Table 1. Physical Properties of ZT-4 and ZT-4L

	ZT-4	ZT-4L
ZnO-to-TiO_2 molar ratio	1.5	1.5
Binder content	5 wt%	5 wt%
Particle size range	100 to 300 μm	100 to 300 μm
Mean particle size[a]	174.6 μm	179.9 μm
Surface area	3.53 m^2/g	3.4 m^2/g
Mercury pore volume	0.2229 cc/g	0.1968 cc/g
Median pore diameter	2,175 Å	1,734 Å
Attrition resistance		
5-h loss	39.7%	17.0%
20-h loss	89.0%	71.0%

[a]Harmonic mean.

Other structural properties such as XRD phases and chemical analyses for Zn and Ti were almost identical for both formulations. These data clearly show that the scaleup of the manufacturing process by a factor of 17.5 was highly successful. The sorbent prepared using the 35-L machine possessed better chemical reactivity and attrition resistance. A large sorbent batch (3,000 kg) employing the 35-L machine is currently being produced.

Technology Transfer

RTI and DOE were granted a U.S. Patent (No. 5,254,516) on October 19, 1993 on the manufacture of the fluidizable zinc titanate sorbents by the granulation technique. Discussions were held with a number of U.S. catalyst manufacturers to commercialize the technology. These discussions culminated in identification of a catalyst manufacturer, Contract Materials Processing, Inc. (CMP), in Baltimore, MD. A contract was executed between RTI and CMP. CMP has extensive experience and facilities for manufacturing large quantities of custom (toll) catalysts and adsorbents for a variety of applications.

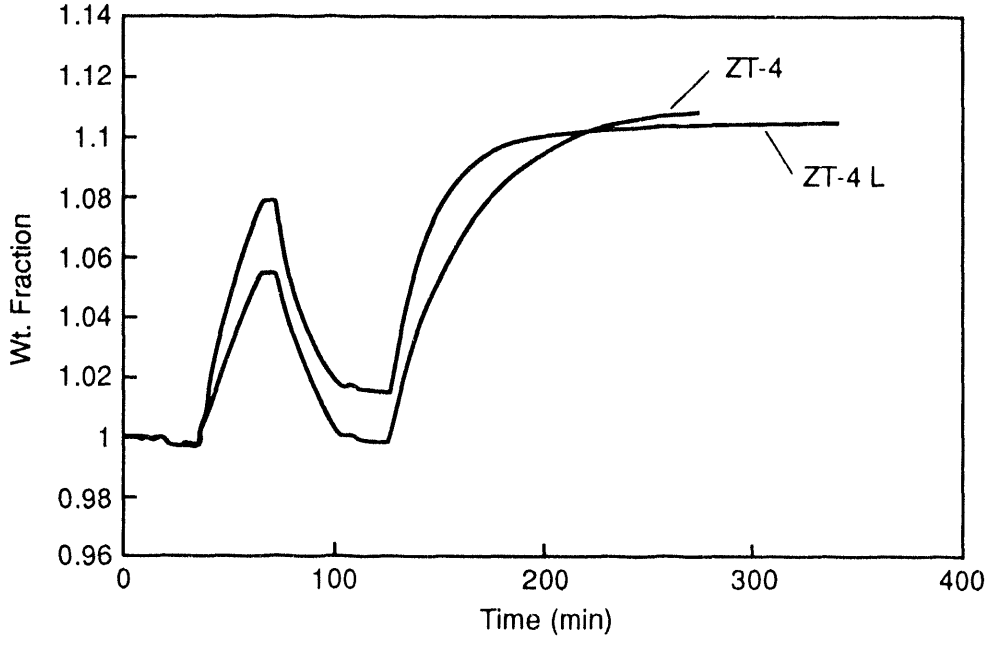


Figure 1. A Comparison of TGA Chemical Reactivities of ZT-4 and ZT-4L

Table 2 shows the cost projections for manufacture of ZT-4 sorbent by granulation independently provided by CMP. Anticipated demand figures were provided by DOE. As can be seen, the current price is $7.91 based on a relatively small demand and, as demand increases, the price will be reduced to about $3.20/lb. This price is close to that contemplated by DOE/METC in their projections for future IGCC plants (Schmidt, 1993).

It may be mentioned here that the ZT-4 sorbent was independently tested by the Institute of Gas Technology (IGT) under a contract with Enviropower to confirm the data obtained at RTI. IGT confirmed the RTI performance data on the sorbent.

Plans are under way to test the ZT-4 sorbent with real coal gas at DOE/METC in the fall of 1994 (Portzer and Gangwal, 1994). This test with real coal gas will demonstrate the applicability of the sorbent with other gas contaminants such as NH_3, HCl, heavy metals, and fine particles.

RTI is working closely or having discussions with a number of private companies in the United States and abroad to promote commercialization of the zinc titanate technology. These include PPCo, Tampella Power/Enviropower, M.W. Kellogg, Texaco and a number of companies in Europe and the Far East.

Table 2. Cost Projections for Manufacture of ZT-4 by Granulation[a]

Year	Quantity (tonnes)[b]	Cost ($/lb) (1994$)
1994	3	7.91
1995	3	7.91
1996	10	7.91
1997	60	5.80
1998	60	5.80
1999	60	5.80
2000	60	3.20
2001 to 2005	60 to 180	<3.20

[a] Independently provided by CMP.
[b] Tonnes = 1,000 kg.

Production of Large Sorbent Batches

RTI arranged a shipment of 2,000 kg of T-2551 zinc titanate sorbent from United Catalysts, Inc. (UCI) of Louisville, KY, to Enviropower in Finland for testing in the pilot plant. UCI produced this sorbent batch on a "best-efforts basis." Table 3 compares the properties of T-2551 with ZT-4L. Clearly, both the TGA reactivity and the attrition resistance of the ZT-4L sorbent is better than the T-2551 formulation. UCI did not disclose the details of the manufacturing method.

Following successful scaleup of the granulation technique and execution of a business agreement between CMP and RTI as discussed previously, commercialization of this technology depends on the success of upcoming pilot-scale demonstration tests and subsequent large-scale demonstration under the DOE Clean Coal Technology Projects. Under a Cooperative Research and Development Agreement (CRADA) between DOE/METC and Enviropower, CMP is currently manufacturing a

Table 3. Comparison of T-2551 and ZT-4L

	T-2551	ZT-4L
Chemical composition ZnO/TiO_2 (molar)	1.5	1.5
% S-capacity at saturation[a]	14	22
Attrition resistance (%)		
5-h loss	39.4	17.0
20-h loss	67.8	71.0
Median pore diameter (Å)	8,887	1,734
Mercury pore volume (cc/g)	0.21	0.20
BET surface area (m^2/g)	0.93	3.4

[a] Measured in the TGA.

3,000-kg batch of ZT-4L using the 35-L machine. Out of the 3,000 kg, 2,000 kg of the sorbent will be shipped to Enviropower in Finland for pilot-plant testing and the remaining 1,000 kg will be delivered to DOE/METC for testing in their process developmental Unit (PDU). The expected date of delivery of the sorbent is about August 15, 1994.

FUTURE WORK

Preliminary investigation of preparing zinc titanate particles by spray drying indicates that highly reactive and attrition-resistant (better than a fluid catalytic cracking [FCC] catalyst used in petroleum refineries) particles can be prepared at a price of about $3/lb. Further development of this technique is continuing.

Currently, the 3,000-kg batch of the ZT-4 sorbent is being produced by CMP. A life-cycle test consisting of 50 cycles of sulfidation and regeneration will be performed with this sorbent to provide long-term reactivity and attrition data to Enviropower prior to their pilot-scale tests.

REFERENCES

Gupta, R., and S.K. Gangwal. 1991. "Enhanced Durability of Desulfurization Sorbents for Fluidized Bed Applications." Topical Report to DOE/METC. Report No. DOE/MC/25006-3011. U.S. Department of Energy/Morgantown Energy Technology Center. Morgantown, WV. NTIS/DE91002090. June.

Gupta, R., S.K. Gangwal, and S.C. Jain. 1992. "Development of Zinc Ferrite Sorbents for Desulfurization of Hot Coal Gas in a Fluid-Bed Reactor." *Energy and Fuels* 6:21-27.

Gupta, R., and S.K. Gangwal. 1992. "Enhanced Durability of Desulfurization Sorbents for Fluidized-Bed Applications—Development and Testing of Zinc Titanate Sorbents." Topical Report to DOE/METC. Report No. DOE/MC/25006-3271. U.S. Department of Energy/Morgantown Energy Technology Center. Morgantown, WV. November.

Gupta, R., and S.K. Gangwal. 1993. "High-Temperature, High-Pressure Testing of Zinc Titanate in a Bench-Scale Fluidized-Bed Reactor for 100 Cycles." Topical Report to DOE/METC. Contract No. DE-AC21-88MC 25006. June.

Gupta, R. et al. 1993. "Fluidizable Zinc Titanate Materials With High Chemical Reactivity and Attrition Resistance." U.S. Patent No. 5,254,516. October 19.

Portzer, J.W., and S.K. Gangwal. 1994. "Slip-stream Testing of the Direct Sulfur Recovery Process." Presented at the Coal-Fired Power Systems 94—Advances in IGCC & PFBC Contractor Review Meeting. DOE/METC No. DE-AC21-93MC 30010. Morgantown, WV. June.

Schmidt, D.K. 1993. "Status and Direction of R&D for High-Temperature Sulfur Removal Sorbents." Workshop held at DOE/METC, January 28.

9a.3 Fluidization Studies Using Phillips Z-SORB Sorbent

CONTRACT INFORMATION

Contract Number	DE-AC21-88MC25006
Contractor	Research Triangle Institute P. O. Box 12194 Research Triangle Park, NC 27709-2194 (919) 541-8023
Contractor Project Manager	Santosh K. Gangwal
Investigators	Raghubir P. Gupta Gyanesh P. Khare, Phillips Petroleum Company Gary A. Delzer, Phillips Petroleum Company Don H. Kubicek, Phillips Petroleum Company
METC Project Managers	Suresh C. Jain Daniel C. Cicero
Period of Performance	October 1, 1993 to June 30, 1994

Schedule and Milestones

FY94 Program Schedule

	S	O	N	D	J	F	M	A	M	J	J	A
Z-SORB Sorbent Testing		———	———	———	———	———						
Data Analysis			———	———	———	———	———	———				
Topical Report								———	———			

OBJECTIVES

The objectives of this project are to determine the long-term chemical reactivity and mechanical durability of a fluidized version of Phillips Petroleum Company's (PPCo's) proprietary Z-SORB sorbent for the desulfurization of coal-derived gases in a high-pressure (20 atm) fluidized-bed reactor under simulated U-Gas conditions and at a moderate operating temperature of 538 °C (1,000 °F).

BACKGROUND INFORMATION

Z-SORB sorbent is a regenerable sorbent for hydrogen sulfide. It is based on zinc oxide supported in a porous matrix and contains a nickel

oxide promoter. Originally, it was developed for tail-gas cleanup (Brinkmeyer and Delzer, 1990), but recently it has been tested for removal of hydrogen sulfide from hot simulated fuel gas that is representative of a coal gasification process. For the latter technology, previous fixed-bed sorbents have shown poor mechanical stability due to spalling when absorbing hydrogen sulfide in reducing gas atmospheres or when being regenerated over many cycles (Mei et al., 1993). Recent tests have shown that Z-SORB sorbent had excellent chemical reactivity and mechanical stability for application in fixed-bed reactors (Campbell et al., 1993).

In an ongoing sorbent research and development program, PPCo has developed a fluidized version of the Z-SORB III sorbent that is the subject of investigation in this paper.

PROJECT DESCRIPTION

Project participants in this study were PPCo and Research Triangle Institute (RTI). This work was part of the project entitled "Enhanced Durability of Desulfurization Sorbents for Fluidized Bed Applications." Sorbents developed for fluidized-bed operation must demonstrate high chemical reactivity, as measured by the rate of sulfur absorption and the sulfur loading capacity, as well as good fluidizing characteristics and mechanical strength characterized by low attrition losses. A fluidized version of PPCo's proprietary Z-SORB III sorbent was prepared by Phillips Research and Development. The sorbent used in this study had an average particle size of 175 μm, a particle size range of 50 to 300 μm and an apparent bulk density of 0.9 to 1.0 g/cc. The sorbent manufacturing process has been demonstrated for 100-lb batch sizes and is believed to be easily scaleable to commercial quantities.

After the initial chemical activity testing at PPCo, the sorbent was provided to RTI for testing in their bench-scale high-temperature, high-pressure (HTHP) semi-batch fluidized-bed reactor system. The reactor unit, shown in Figure 1, is described in detail elsewhere (Gupta and Gangwal, 1992). From initial thermogravimetric analyzer (TGA) tests, it was evident that this sorbent had high chemical reactivity for sulfur capture at operating temperatures of 482 to 538 °C (900 to 1,000 °F). Consequently, for the 50-cycle (sulfidation and regeneration) long-term testing of this sorbent, an absorption temperature of 538 °C (1,000 °F) was selected. Other test conditions are listed in Table 1, and the composition of simulated air-blown U-gasifier gas is included in Table 2. Testing was done in a 2-in. diameter reactor with 500 g of sorbent. Feed gases entered at the bottom of the reactor vessel and exited at the top. The detailed test procedure is described elsewhere (Gupta and Gangwal, 1993). The sorbent was subjected to alternating periods of sulfidation and regeneration. Sulfidation was accomplished by feeding simulated U-Gas composition produced by mixing of individual metered components upstream of the reactor. For regeneration, air was diluted with nitrogen. Initially, regeneration was initiated at 649 °C (1,200 °F) and 2.5 mol% oxygen in nitrogen.

Online analysis of the exiting gas was performed using a series of gas chromatographs (GCs). Concentrations of sulfurous gases (H_2S, COS, and SO_2) were measured every 5 minutes using a Varian flame photometric detector (FPD), while CO, H_2, N_2, CO_2, O_2, and CH_4 concentrations were measured every 25 minutes using a Carle thermal conductivity detector (TCD). During regeneration, the SO_2 concentration was monitored using a continuous SO_2 analyzer (Model 721AT2 from Western Research).

After 25 cycles of sulfidation (24 cycles of regeneration) the run was stopped, reactor unloaded, and 100 g (20 percent of total inventory) of sorbent was removed from the reactor for analysis and characterization. The

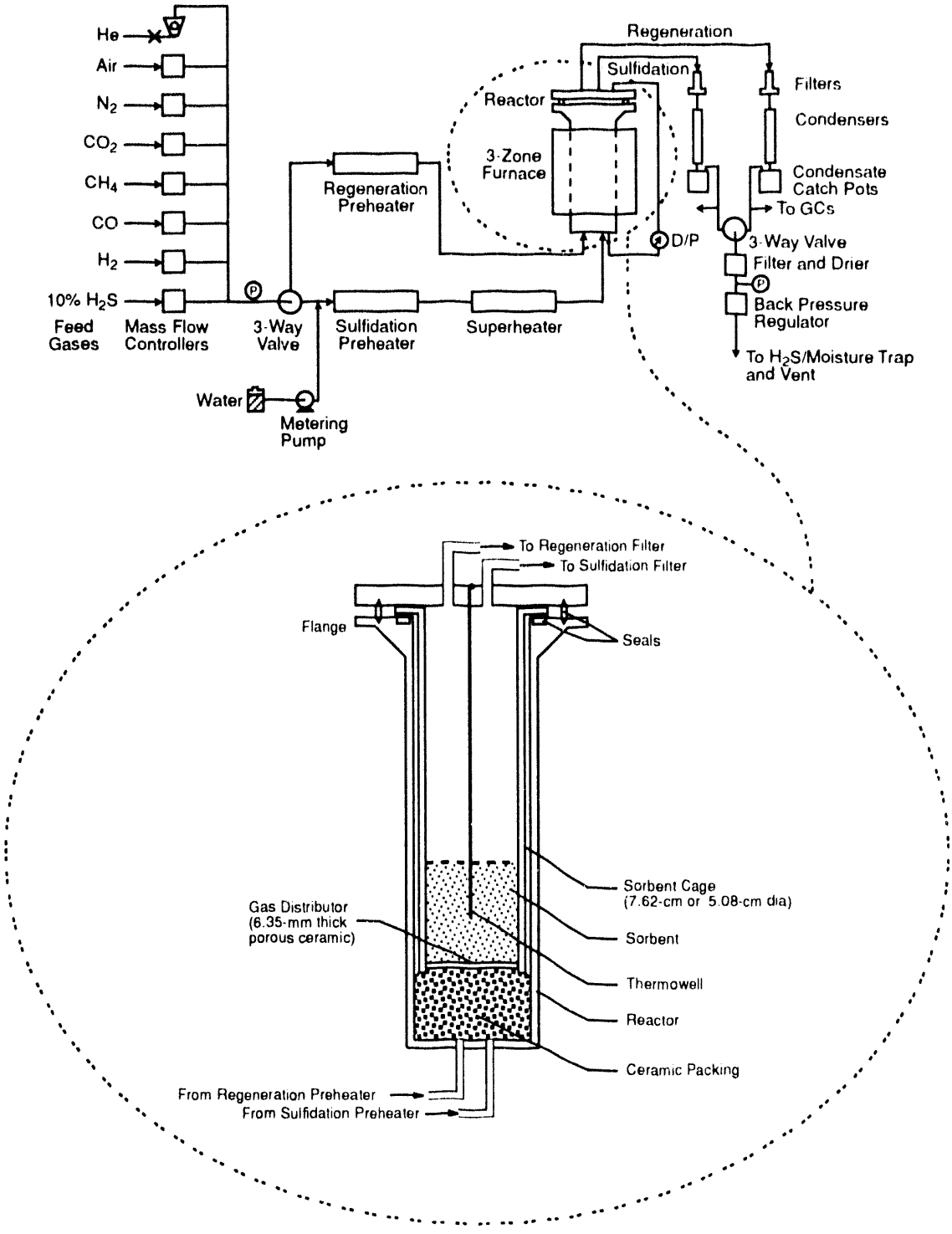


Figure 1. Bench-Scale Fluidized-Bed Sorbent Test Facility

Table 1. Nominal Test Conditions Used in 50-Cycle Test

Sulfidation	
Sorbent	Z SORB III
Temperature	538 °C (1,000 °F)
Pressure	20 atm (294 psia)
Sorbent particle size	100 to 300 μm (d_{50} = 174.3 μm)[a]
Sorbent inventory	500 g (Cycles 1 to 25)[b] 400 g (Cycles 26 to 51)[c]
Total gas flow rate	75 slpm (Cycles 1 to 25) 60 slpm (Cycles 26 to 35) 75 slpm (Cycles 36 to 51)
Sulfidation gas	Simulated U-Gas Gasifier Gas[d]
H_2S content of coal gas	5,000 ppmv (0.5 mol%)
Reactor tube diameter	5.08-cm (2 in.-ID)
Regeneration	
Initial temperature	580 to 650 °C (1,076 to 1,200 °F)
Maximum temperature	690 to 780 °C (1,274 to 1,436 °F)
Pressure	20 atm (294 psia)
Gas flow	Same as sulfidation[e]
Regeneration gas	2 to 2.5% O_2 in N_2

[a] d_{50} is the harmonic mean.
[b] Weight of uncalcined sorbent. On heating, sorbent lost 35 g weight due to evolution of 7 percent bound moisture.
[c] Weight of the sorbent in sulfided state containing 12.15 wt% S. The weight of regenerated sorbent would be 375.7 g.
[d] Complete gas composition is specified in Table 2.
[e] The same flow rates were used during regeneration as sulfidation (i.e., 75, 60, 75 slpm).

remaining 400 g of sorbent was reloaded to the reactor and regenerated before continuing to Sulfidation Cycles 26 to 50. The test program ended after the 50th sulfidation cycle. The reacted sorbent was subjected to a high-temperature exposure after the normal 50th regeneration cycle in an attempt to determine if excessive sulfates had been accumulated on the sorbent. Monitoring of SO_2 in the regenerator off-gas indicated minimum residual sulfate.

Table 2. Gas Composition

Component	Vol%
H_2	14.2
H_2S	0.5 (5,000 ppmv)
CO	23.1
CO_2	5.8
N_2	49.8
H_2O	6.6
Total	100.0

RESULTS

The sulfidation runs as indicated in Table 1 were carried out at 20 atm (294 psia) 538 °C (1,000 °F) using 5,000 ppmv (0.5 mol%) H_2S in the feed. The superficial gas velocity of about 9 cm/s was selected based on prior experimental and theoretical information to ensure complete fluidization of the sorbent. This resulted in a superficial gas residence time of 2.38 s based on a slumped bed of density at 72 lb/ft^3. Figure 2 shows the hydrogen sulfide breakthrough curves for selected cycles. The sulfur loadings were constant for the first ten cycles with breakthrough (500 ppm H_2S in effluent) occurring in 175 minutes. Estimation of sorbent utilization indicated that nearly 100 percent of the sorbent theoretical loading capacity was utilized over the first 10 cycles. Another interesting feature for this sorbent was its high efficiency for sulfur removal manifested in complete removal of H_2S (to nearly zero ppm) for the first 70 percent of each cycle prior to breakthrough.

During the first 10 cycles, the regenerations were very smooth, completing in about 60 minutes. Typically the regenerations were initiated at

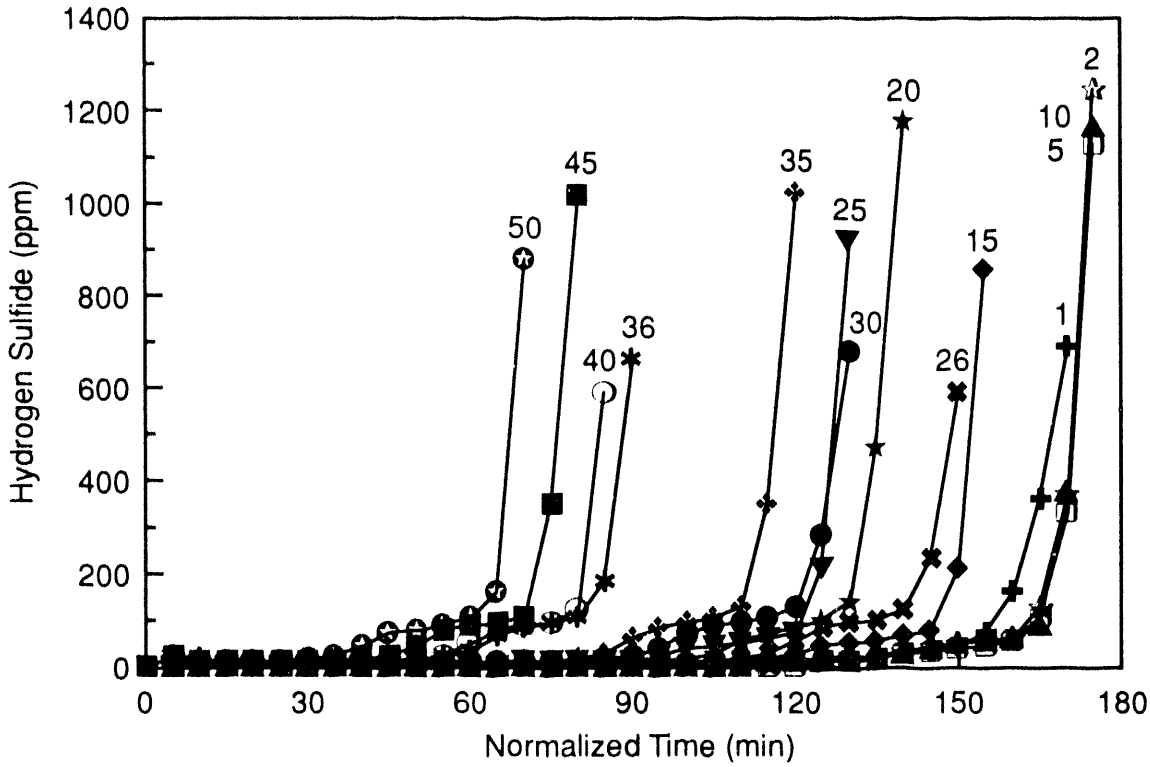


Figure 2. Breakthrough Behavior of Z-SORB III Sorbent U-Gas; 20 atm; 538 °C (1,000 °F)

649 °C (1,200 °F) leading to a peak temperature in the vicinity of 690 °C (1,275 °F). After the first ten cycles of operation, the sorbent suffered, as yet unexplained, exotherms during the start of regenerations resulting in undesired, uncontrolled temperature excursions up to 760 °C (1,400 °F). Breakthrough time declined by 30 percent in the first 25 cycles.

The sulfided sorbent removed from the reactor after 25 cycles was reloaded in the reactor after being stored for about 6 to 7 weeks to complete necessary analyses. The amount of sorbent reloaded was 20 percent less than the initial start-of-the-run loading; therefore, the feed gas flow rate was reduced by 20 percent for cycles 26 to 35, i.e., from 75.0 to 60.0 slpm to maintain the same gas residence time. The initial regeneration (No. 25) was successful and the sorbent reactivity in the 26th cycle was actually higher than what was observed prior to reactor unloading. After the next several cycles of operation, it became evident that the gas flow rate of 60 slpm was not quite enough to achieve a good quality fluidization of the sorbent; therefore, starting at Cycle 36 the gas flow rate was restored to 75 slpm. This change resulted in more smooth cycling.

The breakthrough curves presented in Figure 2 exhibit the sorbent performance for the entire test. It is quite noteworthy that the sorbent performance remained quite high after 50 cycles of operation. The sulfur capacities of the sorbent during Cycles 1 and 50 were 20.16 and 9.98 g S/100 g of sorbent, respectively, indicating about a 50 percent capacity utilization even after 50 cycles. In Figure 3, the sulfur capacity (g of S pickup per 100 g of sorbent) is plotted as a function of cycle number. Sulfur capacity is calculated using the concentration of H_2S in feed, breakthrough time of 500 ppmv H_2S in the effluent and the amount of sorbent used. Actual sulfur chemical analyses

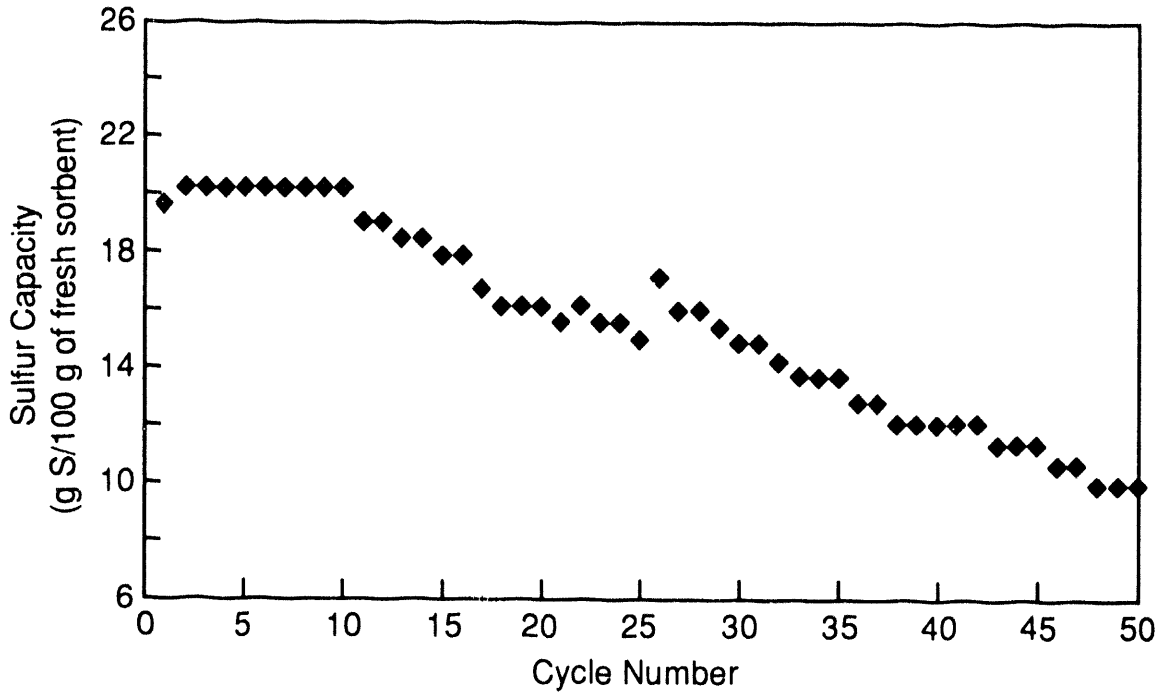


Figure 3. Sulfur Capacity of Z-SORB III Sorbent U-Gas; 538 °C (1,000 °F); 20 atm; 500 ppm Breakthrough.

after 25 and 50 cycles closely corroborated the calculated sulfur capacity.

As mentioned previously, the sorbent for the desulfurization application must have high chemical reactivity. The chemical reactivity is measured by the total sulfur loading capacity as well as the rate of sulfur absorption. In order to measure the latter, standard 1.5-cycle TGA reactivity tests described in Gupta and Gangwal (1992) were carried out for fresh and 25- and 50-cycle reacted sorbents. Figure 4 depicts both the saturation (indicated by the maximum weight gain during the second cycle) and the rate of sulfur pickup (indicated by the slope of the sulfidation curve). While this figure shows that saturation sulfur pickup decreases with increasing number of cycles as expected and observed for conventional desulfurization sorbents, it is important to note that the rate of sulfur pickup for 25- and 50-cycle reacted sorbent remained relatively constant even though the capacity had dropped.

Other notable findings of this test were that in the fluidized-bed reactor there was no evidence of the absorption exotherm that was previously observed in the fixed-bed reactor tests conducted at METC (Campbell et al., 1993) and attributed to methanation reaction promoted by nickel present in Z-SORB sorbent. GC analysis of the absorption effluent gas did indicate an occurrence of water gas shift reaction leading to higher concentration of hydrogen.

Sorbent Loss from the Reactor

The net sorbent loss during the entire 50 cycles was 0.5 percent of the original charge based on the weights of sorbent removed from the reactor and the material deposited on filters and lines. This is indicative of low attrition and high mechanical stability of Z-SORB sorbent. The total sorbent loss from the reactor itself was 2.5 percent.

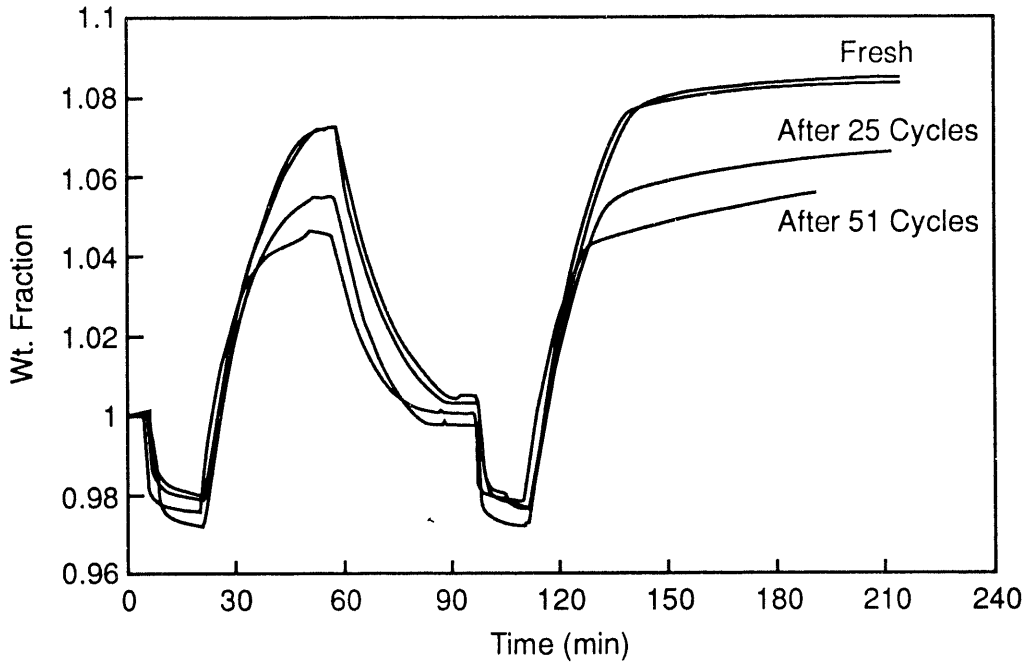


Figure 4. TGA Reactivity of Fresh and Reacted Z-SORB Sorbent

Selected Physical Properties of Fresh and Reacted Sorbents

Selected physical properties of the fresh and reacted sorbents were measured and are presented in Table 3. The average particle size of the sulfided sorbent after 25 and 50 sulfidations remained essentially the same within experimental error. These results corroborate the relatively small sorbent loss observed from the reactor, indicating good mechanical stability of the sorbent. The compacted bulk density of Z-SORB sorbent (66.5 lb/ft^3) increased about 8 percent after 25 cycles of operation, but then it remained essentially the same through the 50 cycles. This indicates that sorbent undergoes some sintering/ shrinking at the beginning, but then the density does not change further and remains relatively constant through the life-cycle test. Attrition tests performed in RTI's 3-hole airjet attrition tester indicated that the attrition resistance of the 25-cycle sulfided sorbent was lower than the fresh material. However, very little change in the attrition resistance was found between the 25-cycle sulfided and 51-cycle sulfided materials. It is realized that attrition data from an actual reactor environment is preferable to simulation using a 3-hole attrition test.

Table 3. Physical Properties of Fresh and Spent Sorbent

	Fresh	After 25th sulfidation	After 51st sulfidation
Average particle size (μm)	174.3	170.8	173.7
Compacted bulk density (lb/ft^3)	66.54	72.12	72.58

CONCLUSIONS

The 50-cycle data show that the fluidizable Z-SORB sorbent has high chemical reactivity and

mechanical durability for hot-gas desulfurization at 538 °C (1,000 °F). Z-SORB sorbent has very high efficiency for H_2S removal to essentially zero levels for a major portion of absorption cycle and a nearly constant rate of sulfur absorption whether fresh or reacted. The sulfur capacity of the sorbent at breakthrough (500 ppm H_2S in the reactor effluent) was 20.16 g S/100 g sorbent in Cycle 1 and 9.98 g S/100 g sorbent in Cycle 50. This sorbent can be easily regenerated at 649 to 704 °C (1,200 to 1,300 °F) with little evidence of sulfate accumulation. During the 50-cycle test only small changes were observed for such important sorbent physical properties as bulk density and particle size. Delineation of the capacity declines observed following Cycle 10 suggests additional research in this area. Definition of the required experiments is currently under assessment.

ACKNOWLEDGMENTS

The authors would like to thank Suresh Jain of METC and Gil Greenwood of PPCo for many helpful discussions.

REFERENCES

Brinkmeyer, F.M., and G.A. Delzer. 1990. Z-Sorb—A New Sulfur Removal Process. Presented at the National Meeting of the AIChE, Session 28, Tail Gas Treatment, Paper 28d, San Diego, August.

Campbell, W.M., J.J. O'Donnell, S. Katta, T. Grindley, G. Delzer, and G. Khare. 1993. Desulfurization of Hot Fuel Gas with Z-Sorb III Sorbent. In *Proceedings of the Coal-Fired Power Systems 93—Advances in IGCC and PFBC Review Meeting*. p. 179. DOE/METC-93/6131. NTIS/DE 93000289. Springfield, VA: National Technical Information Service.

Delzer, G.A., G.P. Khare, and G.J. Greenwood. 1993. "Z-Sorb Adsorbent for Hot Gas Desulfurization." Presented at the AIChE Annual Meeting, Symposium on Gas Purifications, Sessions 130. St. Louis, MO. November 7-12.

Gupta, R., and S.K. Gangwal. 1992. "Enhanced Durability of Desulfurization Sorbents for Fluidized-Bed Applications—Development and Testing of Zinc Titanate Sorbents." Topical Report to DOE/METC. Report No. DOE/MC/25006-3271. U.S. Department of Energy/Morgantown Energy Technology Center. Morgantown, WV. November.

Gupta, R., and S.K. Gangwal. 1993. "High-Temperature, High-Pressure Testing of Zinc Titanate in a Bench-Scale Fluidized-Bed Reactor for 100 Cycles." Topical Report to DOE/METC. Contract No. DE-AC21-88MC 25006. June.

Mei, J.S., L.D. Gasper-Galvin, C.E. Everitt, and S. Katta. 1993. Fixed Bed Testing of a Molybdenum-promoted Zinc Titanate Sorbent for Hot Gas Desulfurization. In *Proceedings of the Coal-Fired Power Systems 93—Advances in IGCC and PFBC Review Meeting*, p. 315. DOE/METC-93/6131. NTIS/DE 93000289. Springfield, VA: National Technical Information Service.

9a.4

Desulfurization Sorbent Development at the Morgantown Energy Technology Center

Ranjani V. Siriwardane
Ulrich Grimm
James Poston
Morgantown Energy Technology Center

Steven Monaco
EG&G Technical Services of West Virginia

OBJECTIVES

The overall objective of this project is to develop regenerable sorbents for hot gas desulfurization in IGCC systems. The major criteria for the development of novel sorbents included reasonable chemical reactivity and physical durability during repeated sulfidation and regeneration cycles.

BACKGROUND

Various formulations of zinc ferrite and zinc titanate in the form of extrudates and spherical pellets have been studied at the Morgantown Energy Technology Center (METC) for removal of sulfurous gases from coal gasification gas streams (Mei et al. 1993). Problems of decrepitation and spalling have occurred after sulfidation and regeneration of these sorbents. Z-Sorb, a proprietary sorbent developed at Phillips Petroleum Company, showed good physical durability during testing at METC, but there was a continuous decrease in reactivity during multiple cycle tests due to steam regeneration (Delzer et al. 1993). A series of novel sorbents containing zinc oxide have been developed at METC to address these problems. These METC-developed sorbents showed superior performance during a 20-cycle, high-pressure, fixed-bed test with steam regeneration conducted at METC.

PROJECT DESCRIPTION

Nine sorbents (METC1 through METC9) were prepared, but only some of these sorbents were selected for initial testing. The remaining sorbents will be tested in the future. Two of these sorbents (METC2 and METC6) have been tested both in the low-pressure and the high-pressure reactors. Results of the high-pressure testing of METC2 and METC6 and low-pressure testing of METC7 will be discussed in this paper. METC2 and METC7 were designed for fixed-bed or moving-bed applications, while METC6 was designed for fluid-bed applications. However, these three sorbents were tested in a fixed bed. Twenty (20) cycles of sulfidation reactions were completed for METC2 and 15 sulfidation cycles were completed for METC6 in the high-pressure reactor. Five sulfidations were completed with METC7 in the low-pressure reactor.

Sorbents were prepared at METC by a solid-state mixing method utilizing a mixer pelletizer. The sorbents contained about 50 wt% of zinc oxide. The sorbents were initially tested in a low-pressure (272 kPa/39.7 psia) reactor. This quartz reactor had a diameter of 5.7 cm

(2.2 inches) and a bed height of 15.2 cm (6 inches). Sorbents that showed promising results in the low-pressure unit were then tested in the high-pressure, bench-scale, hot gas desulfurization unit at 1034 kPa/150 psia, which contains a 5.5-cm (2.2-inch) inner diameter reactor system. The reactor is constructed of Incoloy 800HT alloy steel shell. Inside the shell there is a removable 316 stainless steel cage for easy loading and unloading of the sorbent. The sorbent cage is suspended from the top flange of the reactor shell. A gas distributor is fixed at the bottom of the cage to support the sorbent. The inside of the sorbent cage is Alon-processed to prevent corrosion of stainless steel by sulfur gases in the presence of steam. The reactor is housed inside a three-zone furnace equipped with separate temperature controllers for each zone. Quartz wool was installed on top of the sorbent bed to hold the sorbent as well as to capture particulates from the fixed bed for upflow operation. The details of this system are reported by Mei et al. (1993).

A 40.7-cm (16-inch) deep fixed bed of sorbent was subjected to alternating periods of sulfidation and regeneration. Sulfidation was accomplished by feeding a gas, which simulated the expected KRW fuel gas composition, in a downflow mode through the reactor at 538 °C (1000 °F). The sorbent regeneration was performed in the reverse direction (upflow), utilizing air diluted with nitrogen or nitrogen and steam in order to limit the regeneration exotherm and prevent overheating of the sorbent.

RESULTS

High-Pressure Testing

All the sulfidations in the high-pressure reactor were performed at 538 °C (1000 °F) and 1034 kPa (150 psia), utilizing a feed gas containing 800 ppmv hydrogen sulfide (H_2S). The superficial velocity for all sulfidations in the high-pressure reactor was maintained at 0.3 m/s (1.0 ft/s) and the space velocity was 1363 hr^{-1}. The outlet H_2S concentration was monitored using detector tubes and gas chromatography.

All regenerations in the high-pressure reactor were done at 170 kPa (24.7 psia), and the gas velocity was maintained constant at 0.3 m/s (1.0 ft/s). All dry regenerations were performed utilizing a multi-stage technique. With nitrogen as a diluent gas, the oxygen concentration was increased in discrete increments from 0.5 mole % to 21 mole %, while simultaneously increasing the bed temperature from 538 to 760 °C (1000 to 1400 °F). The exit gas was monitored for sulfur dioxide (SO_2) using detector tubes and gas chromatography. All regenerations were performed until the SO_2 concentration dropped to less than 50 ppmv.

Steam regeneration was conducted in four stages. The temperatures of the four stages were 538, 579, 621, 663 °C (1000, 1075, 1150, and 1225 °F). The steam concentration in all four stages was 50% with a varying concentration of oxygen and nitrogen. The oxygen concentration during the four stages was 0.5, 2.5, 4.0, and 7.0 % respectively.

Results of the METC2 Testing in the High-Pressure Unit

The results of the six sulfidation runs for METC2 performed utilizing dry regeneration in the high-pressure reactor are shown in Figure 1. There was a continuous increase in the sorbent sulfur capacity from sulfidation cycle 1 to cycle 5, after which the capacity stabilized. A comparison of the sulfidation breakthrough curves for METC2 and for a molybdenum-containing zinc titanate from General Electric Company tested under identical conditions is shown in Figure 2. For zinc titanate, there was a decrease in the sulfur capacity up to the third

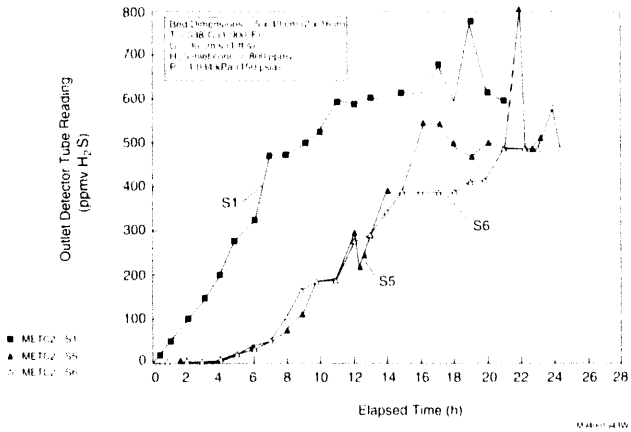


Figure 1. METC2 Sorbent Sulfidations 1 Through 6

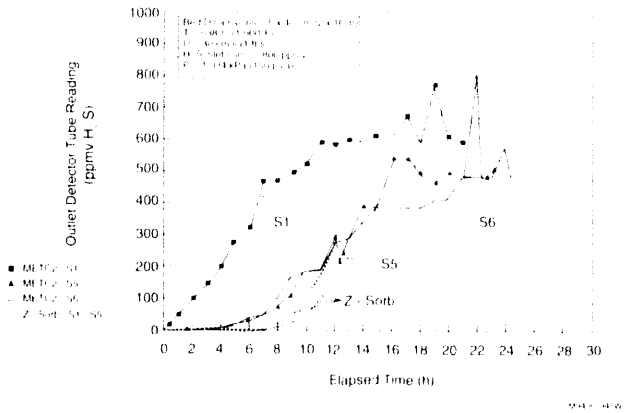


Figure 3. Sulfidations of METC2 Sorbent and Z-Sorb from Phillips Petroleum

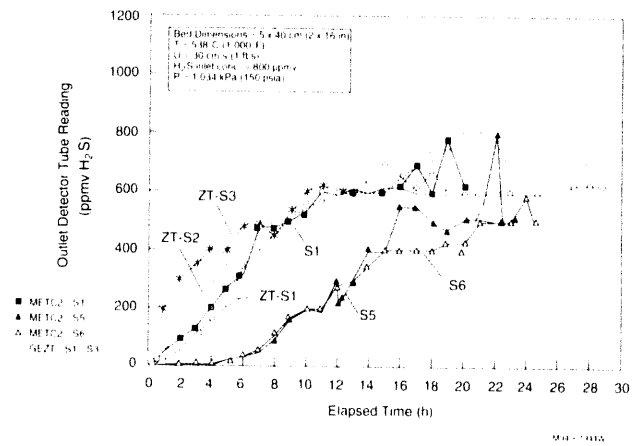


Figure 2. Sulfidations of METC2 Sorbent and GE Zinc Titanate

cycle, and the sorbent stabilized after the third cycle. The sulfur capacity of METC2 after it stabilized at cycle 5 was significantly better than that of the zinc titanate. A comparison of the sulfidation breakthrough curves for METC2 and Z-Sorb from Phillips Petroleum are shown in Figure 3. The sulfur capacity for METC2 after it stabilized at the fifth cycle is comparable to that of Z-Sorb.

In order to understand how steam regeneration would affect the performance of the METC2 sorbent, regenerations during cycles 6 through 19 were conducted utilizing steam. The sulfidation breakthrough curves from sulfidations 7 through 20 (which all follow steam regenerations) are shown in Figure 4. There was a slight decrease in the sulfur capacity between the sixth (last sulfidation following dry regeneration) and seventh sulfidation (first sulfidation following steam regeneration). However, the breakthrough curves for sulfidations 7 to 11 overlapped,

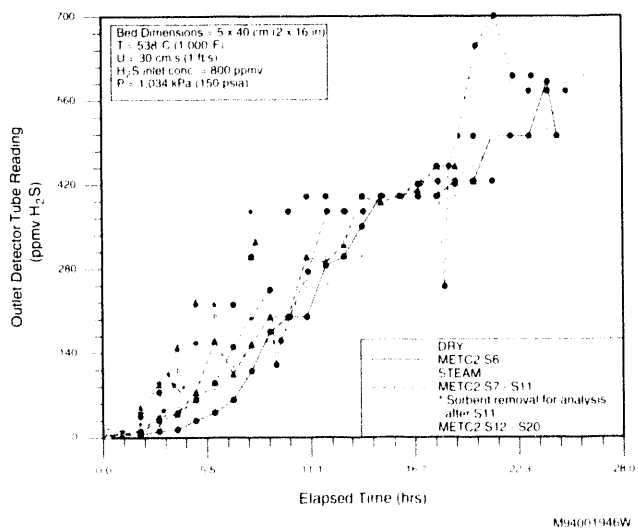


Figure 4. Effect of Steam Regeneration on on METC2 Sorbent During 20-Cycle Testing

indicating that the steam regeneration did not affect the sorbent.

After the eleventh sulfidation some of the sorbent was removed from the reactor for total sulfur analysis. The decrease in breakthrough time between sulfidations 11 and 12 is due to the removal of this material from the sorbent bed. The sulfidation breakthrough curves from cycles 12 to 20, which also follow steam regenerations, overlapped as well, indicating that the sorbent was stable during steam regeneration. The percent total sulfur content from the solid analysis of the sorbent after the 20th cycle was similar to that after the 11th cycle. This further confirmed that the decrease in sulfur capacity during the 11th and 12th cycles was due to the sorbent removal. There was no change observed in the sulfur absorption capacity caused by the steam regenerations in the 7th through 20th sulfidation cycles.

The visual examination of the sorbent after 20 sulfidations indicated that there was no spalling or any other physical deterioration of the sorbent. The crush strength of the sorbent after 20 cycles was higher than that of the fresh sample. Sieve analysis indicated that 92% of the material was unaffected after 20 cycles. This is even after dropping the sorbent in from the top of the reactor during the initial loading and utilizing a vacuum cleaner for sorbent removal from the bed. All of the condensates collected during the 20-cycle test were very clear, indicating that the sorbent did not decrepitate in the bed and that there was no powder lost from the sorbent as observed with zinc ferrite or zinc titanate. The zinc content detected in the condensates was negligible. The METC2 sorbent showed a superior level of performance during the 20-cycle, high-pressure, fixed-bed testing. It is spalling resistant, steam resistant, and had both excellent chemical and physical durability during the 20-cycle test.

Results of METC6 Testing in the High-Pressure Unit

The chemical formulation of METC6 was designed for fluid-bed applications, but the pellets were sized for the testing which was conducted in a fixed bed. Fifteen (15) sulfidation cycles were completed with METC6 in the high-pressure unit utilizing steam regeneration. This test series will be continued for up to a total of 20 sulfidation cycles. The sulfidation breakthrough curves of METC6 are shown in Figure 5. There was an increase in sorbent sulfur capacity between sulfidations 1 and 2, but the capacity decreased again at the third sulfidation cycle. The sulfidation breakthrough curves from the 3rd to 15th cycle overlapped, with a slight decline seen in cycles 14 and 15. This indicates that the sorbent was chemically stable during the 15 cycles of testing and was not affected adversely by the steam regeneration. The condensates collected from the reactor during this test series were very clear. Even though METC6 was formulated for fluid-bed applications, it performed very well with the bigger particle sizes required in fixed-bed testing.

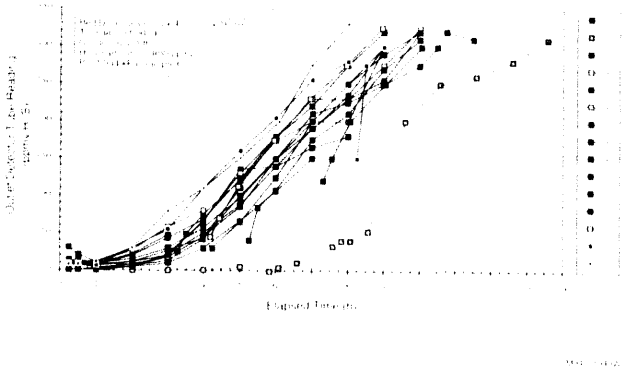


Figure 5. Sulfidations of METC6 Utilizing Steam Regeneration

Results of the METC7 Testing in the Low-Pressure Unit

All of the sulfidations in the low-pressure reactor were performed at 538 °C (1000 °F) and 260 kPa (38 psia), utilizing a feed gas containing 2000 ppmv H_2S. The superficial velocity for all sulfidations in the low-pressure reactor was maintained at 0.09 m/s (0.30 ft/s) and the space velocity was 2000 h^{-1}. The outlet H_2S concentration was monitored using detector tubes and gas chromatography.

All regenerations in the low-pressure reactor were done at 272 kPa (39.7 psia) and the gas velocity was maintained constant during each stage at 0.04 to 0.05 m/s (0.13 to 0.15 ft/s). The steam regenerations were conducted in three stages. The temperatures of the stages were 538, 593, and 649 °C (1000, 1100, and 1200 °F). The steam concentration in all three stages was 50%, with a varying concentration of oxygen and nitrogen. The oxygen concentrations during the three stages were 1.0, 2.5, and 3.5%, respectively.

The sulfidation breakthrough curves of METC7 in the low pressure unit are shown in Figure 6. There was an increase in sulfur capacity from sulfidation 1 to 2, but the sulfur capacity decreased in the third sulfidation. The sulfidation breakthrough curves overlapped after the third sulfidation, indicating sorbent stabilization at that point. As shown in Figure 6, the outlet hydrogen sulfide concentration was zero for about 15 hours, indicating that the efficiency of the sorbent was excellent. A comparison of METC6 and METC7 tested in the low-pressure unit is shown in Figure 7. It is clear that the sulfur capacity of METC7 is better than that of METC6. Since METC7 was the fixed-bed version of METC6, it was expected to have a better capacity in fixed-bed testing. Visual examination of the METC7 sorbent after the fifth cycle

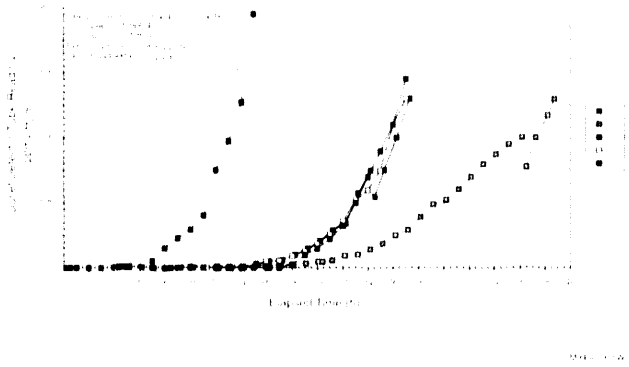


Figure 6. Sulfidations of METC7 Utilizing Steam Regeneration

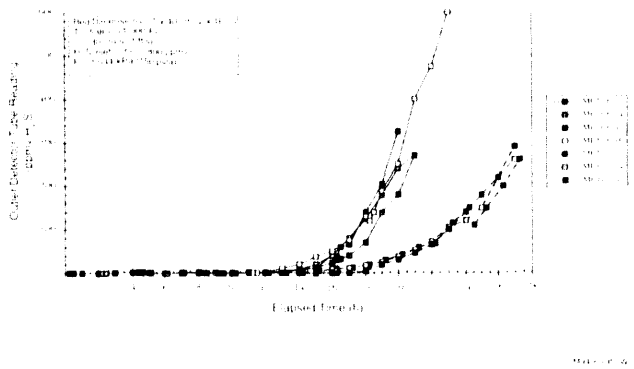


Figure 7. Sulfidations of METC6 and METC7

indicated that there was no spalling or any other signs of physical deterioration during the testing.

FUTURE WORK

1. The testing of METC6 in the high-pressure reactor will be continued for a total of 20 cycles.

2. METC2 will be tested using actual coal gas as the feed gas.

3. Other METC formulations will be tested in the thermogravimetric analysis (TGA) and in the low-pressure unit in order to optimize the formulations.

4. The sorbents will be tested in other types of reactors, such as a fluid-bed, moving-bed, or transport reactor.

5. A Cooperative Research and Development Agreement (CRADA) will be initiated.

6. The optimum sorbent may be tested in a Clean Coal Technology demonstration plant.

ACKNOWLEDGMENTS

The authors would like to acknowledge all the members of the Sorbent Development Cluster at the Morgantown Energy Technology Center (METC) for their contributions to this project as well as the members of EG&G, the prime support contractor at METC, who conducted the sorbent reactor testing.

REFERENCES

Mei, J.S., L.D. Gasper-Galvin, C.E. Everitt, and S. Katta. 1993. Fixed-Bed Testing of a Molybdenum-Promoted Zinc Titanate Sorbent for Hot Gas Desulfurization. In *Proceedings of the Coal-Fired Power Systems 93 -- Advances in IGCC and PPBC Review Meeting*, 315-325. DOE/METC-93/6131. NTIS/DE93000289. Springfield, Va.: National Technical Information Service.

Delzer, G.A., G.P. Khare, and G.J. Greenwood. 1993. *Z-Sorb Absorbent for Hot Gas Desulfurization*. AIChE Annual Meeting, St. Louis, Missouri. Symposium on Gas Purification, Paper No. 130f.

RSIRIW\1:940850

9a.5 Stabilization of Spent Calcium-Based Sorbent

CONTRACT INFORMATION

Contract Number	DE-AC21-91MC27233
Contractor	The M.W. Kellogg Company P.O.Box 4557 Houston, TX 77210-4557 (713) 753-3861
Contractor Project Manager	Philip J. Shires
Principal Investigators	Satyan Katta Gunnar B. Henningsen
METC Project Manager	Thomas P. Dorchak
Period of Performance	June 03, 1991 to October 03, 1994

OBJECTIVES

The overall objective of this project is to obtain experimental data on the reactions of calcium-based sorbents applicable to both air-blown coal gasification systems and second generation fluid bed coal combustion systems (partial gasification). The project is a 40-month effort. A key technical issue for the utilization of calcium sorbents in advanced coal technologies is the subsequent stabilization of the solid wastes (calcium sulfide/ash) produced by such systems.

More specifically, the project objectives are to:

- develop data on the kinetics of in-situ desulfurization reactions (Task 3);
- study the effect of calcium on the kinetics of carbon conversion rate (Task 4);
- study kinetics of oxidation of CaS to $CaSO_4$ and absorption of SO_2 (Task 5);
- develop and identify viable techniques to stabilize CaS;
- carry out further development work on most promising method for stabilization; and
- determine the commercial viability of calcium sulfide stabilization (Task 6).

BACKGROUND INFORMATION

A number of studies reported a catalytic effect on carbon conversion in the presence of calcium with attendant benefits in lowering capital and operating costs. Additionally, a number of researchers have demonstrated the feasibility of in-situ desulfurization using calcium-based sorbents in fluidized-bed and transport gasifiers

involving combustion or gasification operating at elevated pressures, thereby eliminating the need for conventional external desulfurization to control sulfur emissions. However, much of the previous experimental work on in-situ desulfurization research was performed at atmospheric pressure in contrast to the expected higher operating pressures of the advanced pressurized coal conversion processes.

The benefits to be derived from the utilization of in-situ calcium-based sorbents have led to a requirement for new approaches to solid waste disposal, LASHs and DASHs, (mixtures of coal ash with limestone and dolomite, respectively) due to incomplete conversion of CaS to environmentally acceptable $CaSO_4$. In addition, the solids need to absorb SO_2 in a sulfator/combustor. Prior studies have not produced a viable technique to minimize the reactive CaS in the solids without undesirable concurrent SO_2 evolution. Abbreviations and acronyms are defined at the end of the paper.

PROJECT DESCRIPTION

The project is a 40-month effort to investigate the complex influence of calcium-based sorbents on coal conversion. The work is broken into six tasks. Task 1 and Task 2 deal mostly with project related activities and preparation of test equipment. The experimental part of the project is separated into three separate tasks: Task 3 - studies on sulfidation of calcium-based sorbents, Task 4 - studies to obtain kinetic information and understand the mechanisms of calcium-catalyzed carbon gasification reactions, and Task 5 - studies on oxidation of CaS to $CaSO_4$ in order to identify and investigate different methods to oxidize the sulfide and to further develop a promising method. Task 6 is the economic evaluation of the most promising sulfation technique developed under this program.

EXPERIMENTAL

Description of Bench-Scale Reactor Unit (BRU)

The Bench-scale Reactor Unit (BRU), which is used primarily for sulfation studies, consists of a 2-inch I.D. reactor. Details of the BRU construction and the experimental procedures were described in a previous DOE paper[1]. Experimental conditions used in the BRU are given in Table 1.

Table 1. Experimental-BRU

Particle size Distribution	149 to 1000 μm for LASHs and DASHs 53 to 177 μm for TRTU LASH 105 to 210 μm for ground solids
Gas comp.	air
Temperature	1500-1700°F
Pressure	atmospheric

An online analyzer is provided for monitoring of SO_2 in the effluent gas of the BRU

Description of Quartz Reactor

The experimental apparatus for gas absorption studies consists of a horizontal quartz reactor containing a fixed bed (1.65-inch I.D. and 15-inch long), with a quartz fritted disc for gas distribution, that is contained in an electrical furnace. The length of the bed generally ranged from 10 to 12 inches. The wall temperature was monitored near the inlet, the middle, and the outlet locations of the bed. There is provision to measure the concentration of H_2S or SO_2 by means of Draeger tubes before the gas enters the bubblers. All the gas absorption experiments were done at atmospheric pressure.

If maldistribution of gas occurs during a test, the test is repeated, and only the results of the final test are considered. Experimental conditions used in the quartz reactor are given in Table 2.

Table 2. Experimental-Quartz Reactor

Particle size	177 to 1000 μm for pure sorbents 149 to 1000 μm for LASHs and DASHs
Gas comp.	1.5% SO_2, 3% O_2, balance N_2
Linear vel. at temperature	0.43 ft/s
Temperature	1600°F
Pressure	atmospheric

Description of ATGA

An atmospheric thermogravimetric analyzer (ATGA) was used to study the fundamental kinetics of oxidation of LASH at 1700°F in air. It consists of a DuPont 951 thermobalance, a DuPont 9000 console for controlling the heating rate and run time, a data acquisition system, and a personal computer for data storage, retrieval and analysis. Samples are placed in a platinum-mesh screen basket and suspended from the balance arm.

Description of PTGA

A pressurized thermogravimetric analyzer (PTGA), Cahn model TG-151 instrument, was used to study the CaO-SO_2-O_2 reaction producing $CaSO_4$. The PTGA is furnished with a sophisticated computerized data acquisition and control system. The PTGA is capable of operation to temperatures of 2012°F and 1832°F at ambient pressure and a pressure of 1000 psi, respectively. The experimental conditions used on the PTGA are given in Table 3.

Table 3. Experimental-PTGA

Particle size	707 to 1000 μm
Gas comp.	1.5% SO_2, 3% O_2, balance N_2
Gas flowrate	2.0 liter/min
Operating temp.	1600°F
Pressure	atmospheric

RESULTS

Summary and Conclusions

The results obtained on LASH oxidation in atmospheric pressure air at a temperature of 1700°F for a one hour residence time in the BRU fluidized bed can be summarized as follows:

- Higher sulfide conversions were obtained with KRW LASH compared to FW and TRTU LASHs. This may be attributed to the dolomitic limestone used in producing the KRW LASH.
- For the LASHs studied, the sulfide conversions ranged from about 22% to 80%. With alkali impregnation, the sulfide conversions increased to 90 to 95%.
- Slightly higher conversions were obtained for heavily-sulfided KRW LASHs than lightly sulfided KRW LASHs. Residual sulfide levels depend upon initial sulfide concentration.
- With Tampella and FW DASHs, 100% and 93% sulfide conversions were

achieved showing the advantage of using a dolomite over a limestone.

Fundamental kinetic studies conducted on the ATGA show:

- After about 20 to 50% sulfide conversion is achieved, the sulfide oxidation rate slows down substantially, possibly due to diffusional resistance in the $CaSO_4$ layer.

The results from the SO_2 absorption studies in the quartz reactor and the PTGA can be summarized as follows:

- The absorption of SO_2 in the presence of O_2 by pure sorbents was very good with breakthrough periods (outlet SO_2 concentrations of 100 ppm) of up to 12 hours.

- The absorption of SO_2 by pure limestones in the absence of O_2 was poor, possibly due to the absence of a stable product.

- The absorption of SO_2 by lightly-sulfided as well as heavily-sulfided Sierra Pacific and Greer limestones, and Plum Run dolomite was very good after exposing the sorbents to 10-21% O_2 for a period of time sufficient for the conversion of any CaS to $CaSO_4$ or after they were previously oxidized in a separate step.

- The absorption of SO_2 by KRW LASH, and KRW and Tampella DASHs was very poor. This may be attributed to the relatively high temperatures to which these solids were exposed during the gasification process.

- The absorption of SO_2 by FW DASH was very good, after converting any CaS to $CaSO_4$.

- The absorption of SO_2 by mixtures of LASHs and limestones was better than that expected based on the performance of individual solids. The absorption of SO_2 by a mixture of FW DASH and dolomite was about the same as that expected from individual solids.

- The absorption of H_2S by KRW LASH was as good as that observed for the Sierra Pacific and Greer limestones.

The physical characterization of the various solids by mercury porosimetry shows the following:

- Pores of about 0.05 to 0.5 micron in diameter, which were also found in pure sorbents, were present in FW DASH and TRTU LASH. The good SO_2 absorption capacity of these solids may be attributed to the presence of these larger diameter pores.

- Pores of about 0.05 to 0.5 micron in diameter were not present in the KRW LASH nor KRW and Tampella DASHs possibly contributing to poor SO_2 absorption capacity of these solids.

Recommendations

The following recommendations are made based on the results of this study:

- If complete oxidation of CaS is a requirement, consider using dolomite in the gasifier as it is likely to result in a higher degree of subsequent oxidation of CaS in the sulfator/combustor.

- Examine different options in the design of the gasifier (such as not feeding sorbent directly into the high-temperature jet) to

reduce sorbent exposure to high temperatures. Lower peak temperature exposure is likely to enhance the SO_2 absorption capacity of the sorbent in the sulfator/combustor.

- Consider addition of a portion of the fresh sorbent directly to the sulfator/combustor to reduce the leakage of SO_2.

Oxidation of LASHs

The effects of temperature, grinding the LASHs, and impregnating the ground and unground LASHs with an alkali on the oxidation of CaS were studied using both KRW and FW LASHs. These solids were formed from different sorbents operating at different gasification conditions. KRW LASH was formed in a fluidized bed with a central jet where the temperatures were substantially higher than in the FW carbonizer. The sorbents used to produce KRW and FW LASHs were New Enterprise(dolomitic type) and Longview limestones (high-calcium type), respectively. Thus, studies of these two LASHs are expected to show the effect of both differences on their oxidation characteristics. The TRTU LASH was produced using Longview limestone in Kellogg's Transport Reactor Test Unit under relatively mild conditions and starting with small ($<500\mu m$) particles of sorbent and coal.

The effect of temperature on the oxidation of LSCF KRW LASH was studied at atmospheric pressure over the temperature range of 1500 to 1700°F in air for an hour. An increase in sulfide conversion was obtained with an increase in temperature for both KRW and FW LASHs. Based on these results, 1700°F appeared to be the preferred temperature giving the highest level of oxidation. Hence, subsequent studies were conducted at these conditions. For heavily-sulfided materials, sulfide conversions to 80% were obtained. Table 4 shows a summary of sulfide conversions achieved for various LASHs and DASHs at 1700°F and atmospheric pressure in air for an hour. Conversions obtained during carbon burnoff in a muffle furnace (carbon-containing solids could not be processed in the BRU) are also shown and are included in the conversions reported for the various solids. The sulfide level (% of Ca as sulfide on a molar basis) in the as-received solids is given below.

HSAR KRW LASH	60
LSAR KRW LASH	33
HSAR FW LASH	42
LSAR FW LASH	21
TRTU LASH	55
FW DASH	55

The effect of impregnating the solids with 2 wt% Na_2CO_3 solution was studied using KRW, FW and TRTU LASHs. The impregnation of LASHs with the alkali increased the sulfide conversions to 90 to 95% for the three LASHs. In order to study the effect of grinding, samples were ground to a size distribution of 70x140 mesh. The combined effect of grinding and alkali-impregnation was also studied. For untreated samples of LASH, sulfide conversions ranged from about 22% to 80%. With alkali impregnation, the sulfide conversions increased to 90 to 95%.

Higher sulfide conversions were obtained for the KRW LASH compared to the FW and TRTU LASHs. This may be attributed to the dolomitic limestone used in producing the KRW LASH. Comparing the lightly-sulfided and heavily-sulfided KRW LASH, slightly higher conversions were obtained for the latter.

Oxidation of DASHs

The oxidation of FW and Tampella DASHs was studied at standard conditions. With the FW and Tampella DASHs, 93 and 100%

Table 4. Summary—Sulfide Conversions of LASHs and DASHs

LASH/DASH	Muffle*	UT	G	D	GD
CFHS KRW LASH	20	72	79	90	85
CFHS FW LASH	0	22	75	86	94
LSCF KRW LASH	20	58	65	94	-
LSCF FW LASH	0	33	-	-	-
HSCF KRW LASH	78	80	80	-	96
HSCF TRTU LASH	12	40	-	79	-
Tampella DASH	100	100	-	-	-
FW DASH	92	93	-	-	-

* sulfide conversion during carbon burnoff in a muffle furnace.

sulfide conversions, that are much higher compared to that of the LASHs, were achieved showing the advantage of using a dolomite over a limestone in the gasifier for subsequent oxidation.

Fundamental Kinetic Studies on the ATGA

The oxidation of CFHS FW and KRW LASHs was studied on the ATGA at atmospheric pressure to obtain rate information. These fundamental studies show that after a certain sulfide conversion is achieved, the rate slows down substantially, possibly as a result of diffusional resistance in the product layer. The results for the FW LASH are plotted to show the sulfide conversion as a function of time in Figure 1. The sulfide conversion profiles for the FW LASH show that much of the conversion occurred in less than 20 minutes. Similar results were obtained for the KRW LASH.

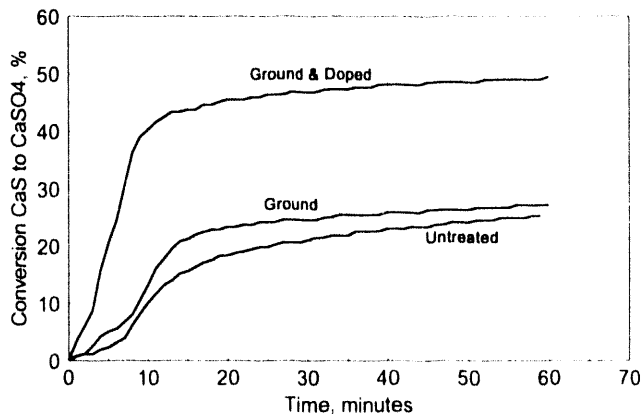


Figure 1. Effect of Grinding and Alkali Impregnation on Oxidation of FW LASH

Weathering Study on Oxidized KRW LASH

A study was conducted with CFHS KRW LASH, that was partially oxidized in the BRU at 1700°F and atmospheric pressure in air, to determine if "weathering" increases the level of oxidation of CaS present in the LASH. The alkali-impregnated and untreated LASH samples

were subjected to weathering by flowing saturated air through a fixed bed of solids for 60 days. The weathering of KRW LASH did not reduce the sulfide level. The LASH sample impregnated with Na_2CO_3 to 2 wt% showed a 32% sulfide conversion. The sulfide level (4.5%) in this sample may not be satisfactory.

Gas Absorption Studies

The objective of the gas absorption studies is to study the ability of various pure sorbents and KRW and FW LASHs to react with SO_2 over the temperature range of 1600 to 1800°F and at atmospheric pressure to enhance fundamental understanding of SO_2 absorption and to simulate the operation of a sulfator/combustor in an IGCC plant. The latter has to absorb the SO_2 evolved from the combustion of carbon as well as SO_2 that is present in the regeneration gas from an external desulfurizer if it is disposed of in the sulfator.

The absorption of SO_2 was studied to investigate the differences between pure sorbents and LASHs and to understand whether gasifier conditions contributed to any changes in the nature of LASHs.

The PTGA was used to study the CaO sulfation reaction with several sorbents and LASHs. The effect of bed weight and gas flowrate on the reaction rate was studied using Plum Run (P.R.) dolomite to establish the sample weight and gas flowrate required to get the true kinetic rate. At these conditions, the absorption of SO_2 on KRW DASH and KRW, FW, and TRTU LASHs was studied. Pure sorbents, LASHs and DASHs were characterized by means of mercury porosimetry to determine their pore characteristics.

SO_2 Absorption in the Quartz Reactor

The absorption of SO_2 by KRW LASH and KRW and Tampella DASHs was found to be very poor in the quartz reactor as determined from the breakthrough periods. This may be attributed to the relatively high temperatures at which these solids were processed in the gasifier. The use of a jetting fluidized bed to promote high solid circulation in a gasifier results in substantially higher temperatures in the jet due to the combustion of gases and solids in a confined region. This was substantiated by temperature measurements made in the KRW pilot plant[2]. Hence, the presence of a jet in both KRW and Tampella fluid bed gasifiers caused substantially higher temperatures in the jet than in the bed and exposed the sorbents to these temperature levels.

The absorption of SO_2 by FW DASH, after converting the CaS to $CaSO_4$, is very good reflecting the advantage of using a dolomite over a limestone in the FW carbonizer and the moderate temperatures that prevailed in the latter compared to the KRW and Tampella gasifiers.

The absorption of SO_2 by pure limestones in the presence of O_2 is very good with a maximum observed at 1700°F for Greer limestone[1]. The absorption of SO_2 by lightly-sulfided as well as heavily-sulfided Sierra Pacific and Greer limestones, and Plum Run dolomite is very good after exposing the sorbents to 10-21% O_2 for a period of time to supply enough O_2 for both oxidation of CaS and SO_2 absorption or after the sample is oxidized in a separate step. The absorption of SO_2 by pure limestones in the absence of O_2 is poor, possibly due to the absence of a stable product.

Kinetic Studies on the PTGA

The sample weight and gas flowrate required to obtain a true kinetic rate that is free from the gas film diffusional effect were established by studying the rate of CaO sulfation reaction at 1600°F and atmospheric pressure on a PTGA using P.R. dolomite (18x25 mesh) and these conditions were employed for all the subsequent tests. The reaction rate at any time is defined as the weight of CaO reacting per minute per unit weight of CaO present at this time. In the case of LASHs, DASHs and pure sorbents, the composition of the solids, as determined from gravimetric analysis, was used in calculating the reaction rate.

Sulfation Rate of KRW, FW and TRTU LASHs

The sulfation rate ($CaO-SO_2-O_2$ reaction) of the KRW, FW and TRTU LASHs was studied at standard conditions and the results are presented in Figures 2 and 3 showing the reaction rate as a function of CaO conversion and the latter as a function of time, respectively. For the various solids studied on the PTGA for reaction with SO_2, the PTGA results are in qualitative agreement with the results obtained in the quartz reactor.

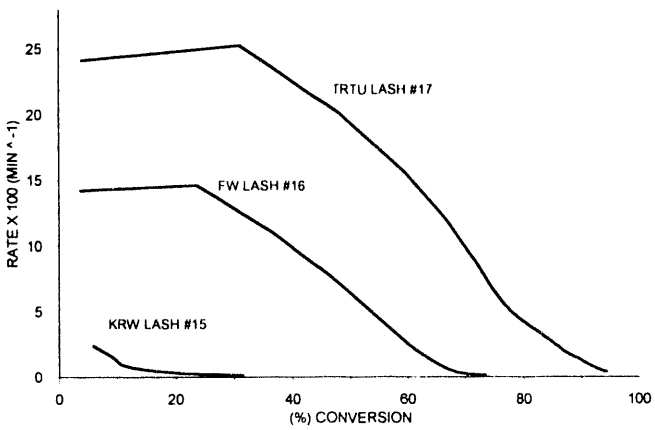


Figure 2. Sulfation of KRW, FW and TRTU LASHs—Rate vs. Conversion

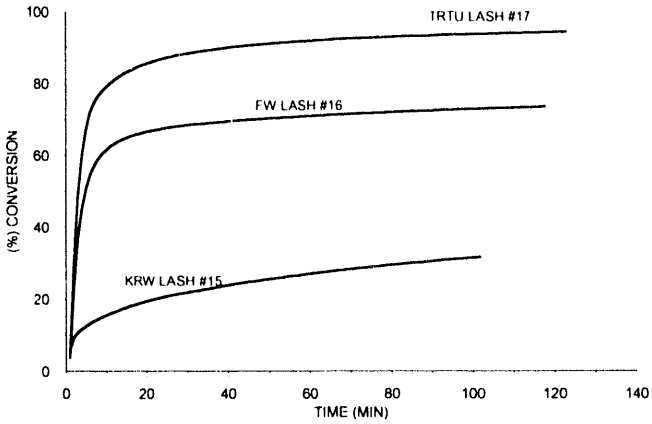


Figure 3. Sulfation of KRW, FW and TRTU LASHs—Conversion vs. Time

The reaction rate of TRTU LASH is much higher than that of the KRW and FW LASHs. This higher rate may be attributed to the mild conditions at which the TRTU LASH was prepared in the TRTU since the same sorbent was used in the preparation of FW LASH as well. Due to high solid circulation rate and the absence of a high-temperature jet in the TRTU, the LASH is not exposed to localized temperatures as high as in fluidized beds.

Sulfation Rate of FW, Tampella, and KRW DASHs

The sulfation rate of FW, Tampella, and KRW DASHs was studied at standard conditions. The results are presented in Figures 4 and 5 showing the reaction rate as a function of CaO conversion and the latter as a function of time. The poor reaction rates of KRW and Tampella DASHs corroborate the SO_2 absorption results obtained in the quartz reactor. The reaction rate of the KRW DASH is just as poor as that of the Tampella DASH and the KRW LASH.

Based on the qualitative agreement between the results obtained in the quartz reactor and in

the PTGA, it appears that, if a suitable model is developed, the SO_2 absorption capacity of a sorbent in either the quartz reactor or in a fluidized bed reactor can be predicted from the results of fundamental tests on the PTGA.

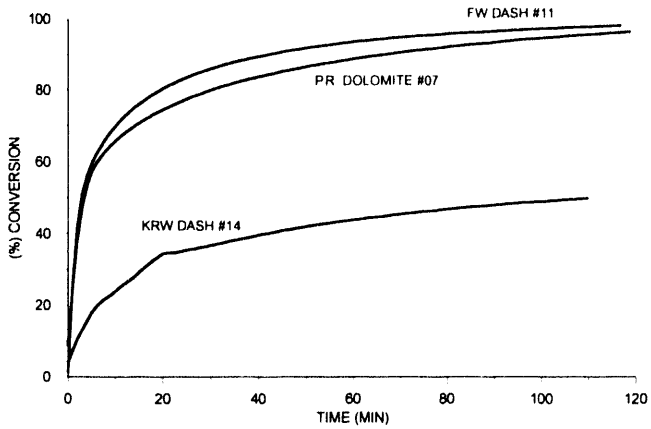


Figure 4. Sulfation of DASHs and P.R. Dolomite—Converson vs. Time

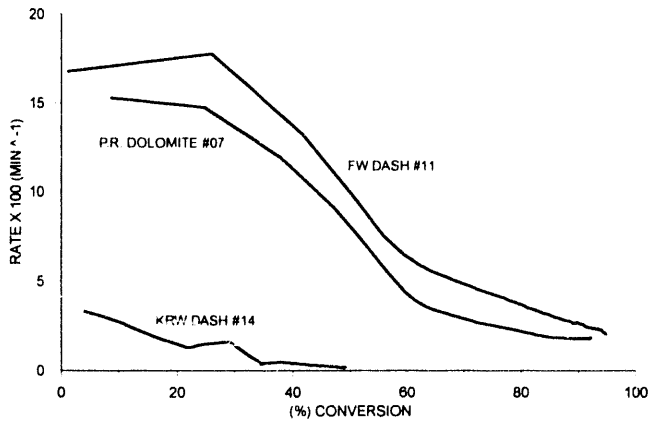


Figure 5. Sulfation of DASHs and P.R. Dolomite—Rate vs. Conversion

Effect of Heat Treatment Temperature on SO_2 Absorption

Pure sorbents were exposed to different temperatures in the range of 1600 to 2100°F and then their reactivities were studied on the PTGA at standard conditions. For exposure temperatures of about 2100°F, subsequent SO_2 absorption capacity was significantly reduced for both Longview limestone and Plum Run dolomite. The data on CaO conversion as a function of time for both of these solids are shown in Figures 6 and 7, respectively.

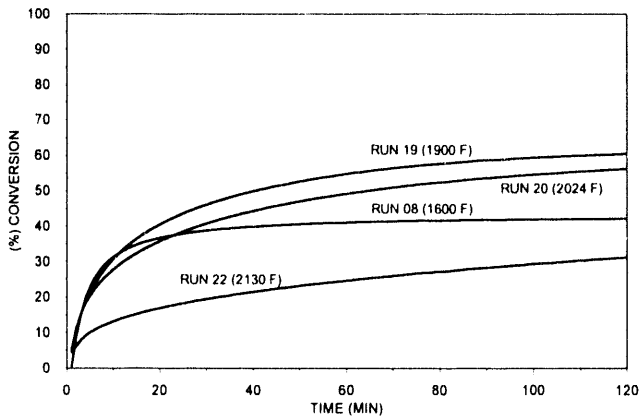


Figure 6. Effect of HTT on Sulfation of Longview Limestone

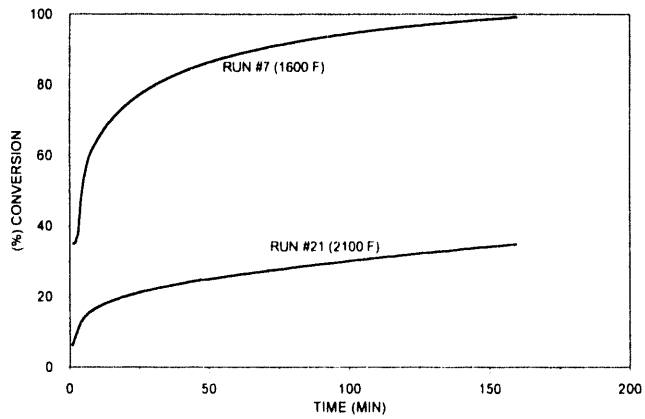


Figure 7. Effect of HTT on Sulfation of P.R. Dolomite—Conversion vs. Time

Characterization of Sorbents and LASHs and DASHs by Mercury Porosimetry

Calcined sorbents and carbon-free LASHs and DASHs were characterized by mercury porosimetry to measure the variation of pore surface area and pore volume as a function of pore size on a Micromeritics Autopore II 9220. The pressure was increased from 1.6 to 60,000 psia that covers pores from about 117μm to 0.003μm in diameter. Based on the SO_2 absorption capacity of the various solids and pore characteristics, no correlation appears to exist between either the total pore surface area or the total pore volume and SO_2 absorption capacity.

The differential pore volume divided by differential pore size for each incremental change in pressure, called differential intrusion, is plotted as a function of pore diameter in Figures 8 and 9. This type of plot appears to be the best in discerning the differences in SO_2 absorption capacity of the LASHs, DASHs and pure sorbents. A comparison of FW LASH and Longview limestone used in its production, given in Figure 8, shows a partial loss of pores of 0.05 to 0.5μm in diameter, while a comparison of KRW DASH and the P.R. dolomite, given in Figure 9, shows complete loss of these pores. Comparison of the pore characteristics of pure sorbents with KRW LASH, KRW and Tampella DASHs (not presented here), shows that in the case of the LASH and the two DASHs, larger pores present in the pure sorbents are not present in these solids and only pores smaller than about 0.01μm in diameter are present. This leads to the premise that larger pores beneficial for SO_2 absorption disappeared from the sorbents when they were processed in the KRW and Tampella gasifiers. The pore characteristics of FW DASH and TRTU LASH compare favorably with that of the pure sorbents, presumably due to lower processing temperatures in these gasifiers.

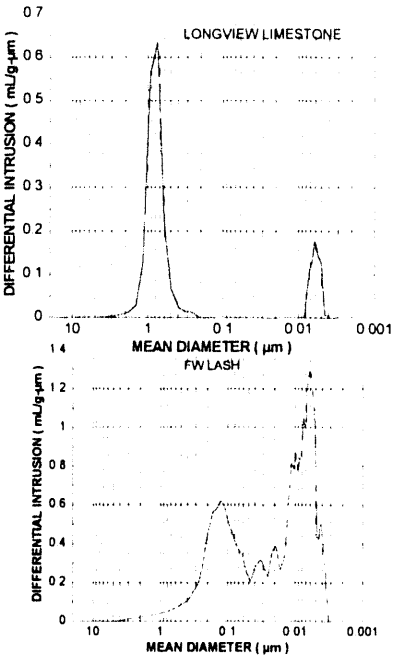


Figure 8. Characterization of Longview Limestone and FW LASH

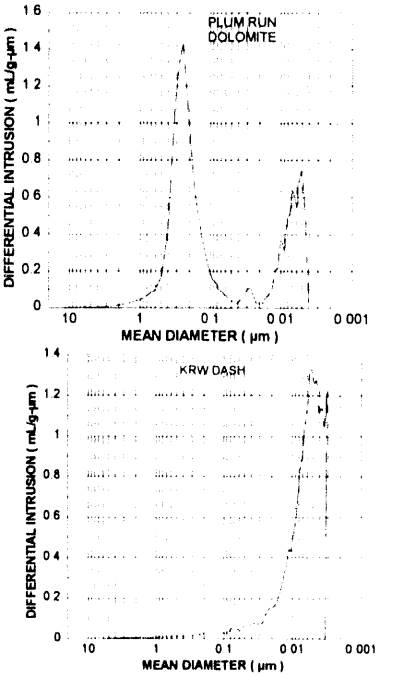


Figure 9. Characterization of P.R. Dolomite and KRW DASH

REFERENCES

1. Katta, S., G.B. Henningsen, and P.J. Shires, "LASH Oxidation, Waste Management," Proceedings of the Coal-Fired Power Systems 93 - Advances in IGCC and PFBC Review Meeting (June, 1993).

2. Katta, S., Principal Investigator, "Process Analysis Topical Report on Pressurized Ash-Agglomerating Fluidized-Bed Gasification System," FY-1984 & 1985, submitted by KRW Energy Systems to U.S. DOE, FE-21063-26 (1986).

FUTURE WORK

The effect of pressure at 150 psi, and a different O_2 partial pressure on the oxidation of KRW LASH at 1700°F, identified as the preferred temperature in this study, will be investigated. After completing Task 5, studies will be performed in support of Tasks 3 and 4.

ACKNOWLEDGEMENT

The guidance and support received from METC in the execution of this work is gratefully acknowledged. Foster Wheeler, Tampella, and Sierra Pacific supplied various materials for testing and their assistance is recognized.

ABBREVIATIONS

AR	As Received solids
ATGA	Atmospheric Thermogravimetric Analyzer
BRU	Bench-scale Reactor Unit
CF	carbon-free solids
CFHS	processed in the muffle furnace first to burn off carbon and then sulfided in the quartz reactor
DASH	mixture of dolomite and ash
DT method	Draeger Tube method to determine CaS content in solids
FW LASH	LASH produced in the Foster Wheeler carbonizer using Longview limestone
FW DASH	DASH produced in the Foster Wheeler carbonizer using Plum Run dolomite
HSAR	Heavily sulfided and as received (carbon-containing)
HSCF	Heavily sulfided and carbon free
HTT	Heat Treatment Temperature (maximum temperature to which the solids are exposed in processing)
IGCC	Integrated Gasifier Combined Cycle System
KRW LASH	LASH produced in the KRW pilot plant using New Enterprise limestone (a dolomitic limestone)
KRW DASH	DASH produced in the KRW pilot plant using Plum Run dolomite
LASH	mixture of limestone and ash
LSCF	lightly sulfided and carbon-free
LSAR	lightly sulfided and as received (carbon-containing)
P.R.	Plum Run
PTGA	Pressurized Thermogravimetric Analyzer
S.P.	Sierra Pacific-supplied
Tampella DASH	DASH produced in the Tampella pilot plant gasifier using a dolomite
TRTU	Transport Reactor Test Unit
TRTU LASH	LASH produced in the TRTU using Longview limestone

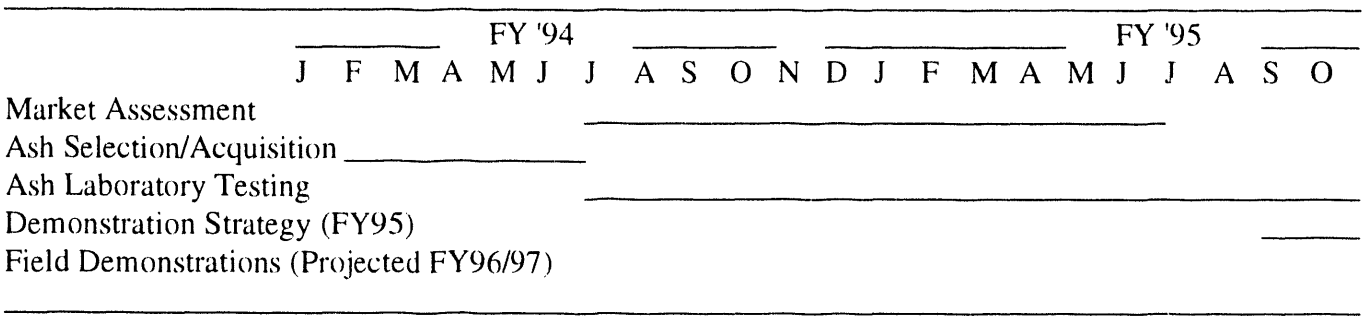
9a.6 Market Assessment and Technical Feasibility Study of PFBC Ash Use

CONTRACT INFORMATION

Cooperative Agreement Number	DE-FC21-93MC30127
Contractor	Western Research Institute 365 North 9th Street Laramie, WY 82071-3395
Contractor Project Manager	Verne E. Smith
Principal Investigators	Alan E. Bland - WRI Terry H. Brown - WRI Demetri N. Georgiou - JWA John Wheeldon - EPRI
METC Project Manager	Mary Beth Ashbaugh
Period of Performance	10/93 to 1/96

Schedule and Milestones

FY 94-95 Program Schedule



OBJECTIVES

The overall objectives of this study are to determine the market potential and the technical feasibility of using PFBC ash in high volume ash use applications. The information will be of direct use to the utility industry in assessing the economics of PFBC power generation in light of ash disposal avoidance through ash marketing. In addition, the research is expected to result in the generation of generic data on the use of PFBC ash that could lead to novel processing options and procedures. The specific objectives of the proposed research and demonstration effort are:

- define present and future market potential of PFBC ash for a range of applications (Phase I);

- assess the technical feasibility of PFBC ash use in construction, civil engineering and agricultural applications (Phase II); and
- demonstrate the most promising of the market and ash use options in full-scale field demonstrations (Phase III).

BACKGROUND INFORMATION

Market assessment studies for advanced SO_2 control wastes have concluded that the market potential for PFBC materials is promising (Baker, 1990). Potential markets and the projected market volumes include: road construction (high); structural fill (high); concrete (high); asphalt (medium); brick (medium); cement production (medium); and synthetic aggregate (medium). Table 1 shows the market assessment for these applications and others.

These markets have the potential to consume large volumes of PFBC ash. Unfortunately, the value of the market products and the availability of competing materials has restricted transportation distances. A number of competing materials are established in these markets, thereby offering substantial performance records. However, the disposal avoidance costs associated with a power plant may encourage the penetration of PFBC ash into these markets, if documented technical performance of uses can be made available.

Potential Ash Uses

Conventional power plant ashes and the new desulfurization residues have been used successfully in a number of industries, including building construction, road and highway construction, coal mining and reclamation, agriculture and recently environmental restoration industries. These industries consume enormous quantities of raw materials and fly ash has found acceptance in each of these industries.

Table 1.
Overall Marketability Projection for Advanced Coal Combustion By-Products

Utilization Market	Potential Market Volume	Marketability Projection*		Comments
		Short Term	Long Term	
Agricultural/Soil Amendment	Low	Good	Good	Seasonal
Asphalt	Medium	Fair	Fair	Abundance of inexpensive competing materials
Brick	Medium	Poor	Possible	Mine-mouth industry; unique contribution needed
Cement Production	Medium	Good	Good	
Concrete	High	Poor	Good	Current specifications may limit use
Grout	Low		Excellent	
Road Construction	High		Excellent	
Structural Fill	High		Excellent	
Synthetic Aggregate	Medium		Good	
Waste Stabilization	**		Possible	Liability issues must be resolved.

* Marketability projection for technically suitable coal ash assuming technical suitability is demonstrated.
** Presently indeterminate.
Source: Modified from Baker (1990) DOE/MC/25042-2872

An example of the market magnitude and potential of ash use can be seen in road and highway construction (Table 2). The road construction industry consumes a tremendous amount of raw materials including earth borrow, aggregates, portland cement, asphalt cement, and mineral fillers. Lesser amounts of lime are also used. Earthen borrow is used as a fill, backfill, or embankment material. Aggregates are used as subbase or base material, as well as in concrete and asphalt paving. Mineral fillers, such as rock fines and ash are used in asphalt paving mixtures. Lime is also used as a stripping agent in asphalt, as well as a stabilizing agent for soils and road subbases and bases. Ash has found its way into this industry/market at a level of 4 to 5 million tons per year.

The building industry has used fly ash as a raw material in cement production, cement replacement in concrete and concrete products, such as masonry units. Production of lightweight aggregate for concrete and concrete products has also been commercially practiced. Recently, FBC ash and FGD sludge have also use in the building materials industry, such as wall board production.

Conventional power plant ash and FBC residue use as an engineering and construction material have been investigated for over a decade. A summary of FBC ash use in construction applications was provided by Bland (1994). Construction applications include road and highway construction, airport runways, and dams and other earthen and concrete structures. Road construction has traditionally involved a number of techniques and materials, such as roller compacted concrete (RCC), soil stabilization, stabilized road subbases and bases, embankments and fills, engineered material for structural fills, synthetic construction aggregate production for concrete, asphalt paving, and road base construction.

Table 2.
Raw Materials Use in Road and Highway Construction Industry*

Materials Consumed	Potential PFBC Ash Uses	Road Bases/Subbases (million tons)	Asphalt Paving (million tons)	Concrete Paving, Bridges,etc (million tons)
Aggregate	Synthetic Aggregate			
Crushed Stone	from PFBC Ash	200	215	200-240 Crushed Stone
Sand and Gravel		150	100 to 125	& Sand and Gravel
Total		350	315 to 340	200-240
Cement	Replacement in Cement/Concrete & Soil Stabilization	1 (est.)		15 to 20
Lime	No Substitution	0.8	0.1	
Asphalt	No Substitution		25	
Mineral Filler	PFBC Ash as Filler		25	
Fly Ash	PFBC Fly Ash	0.5	0.1	3 to 4
Bottom Ash	PFBC Bed Ash	0.4 to 0.5		
Total Conventional Ash Production (1987) 68.9 million tons Total Conventional Ash Use (1987) 18.3 million tons				
*Does not include earthen materials used for fills and embankments, for which 2 million tons of fly ash used. (1987)				

Source: Compiled from data presented by Baker (1990) DOE/MC/25042-2872

The mining industry has used ash for a number of years as a reclamation and soil/spoil amendment, for subsidence control in underground mines, for haul road stabilization, and for numerous embankments and fills.

The agricultural industry is becoming a market for conventional ashes and FBC ashes. The ash is used as a lime and sulfate source, micro- and macro-nutrient source, soil texture modifier, and moisture barrier for root growth. FBC ash, in particular, is finding acceptance in a number of states in agricultural applications.

The use of conventional ashes and more recently FBC ash in these applications provides a basis for believing that PFBC ash can also penetrate these markets. The following provides a brief description of potential applications.

Cement Production. Approximately 82.5 million tons of cement were produced in the United States in 1992. Of that amount approximately 800,000 tons or approximately 1% of the conventional fly ash produced by power plants was used for clinker production. The fly ash is used as a raw material in the clinker production, as a source of silica and alumina; or as a material blended with ground clinker in the formulation of a blended Type P pozzolanic cement.

PFBC ash appears to show promise for this application. PFBC ash can also be used as a set retarder (normally gypsum or anhydrite is used) that is interground with the cement clinker. Competing materials for this application remain limestone and shales as well as conventional fly ashes. The use of dolomite as a sorbent in FBC can result in excess MgO, a detrimental (<4%) component in cement.

Replacement of Cement in Ready Mix Concrete and Concrete Products. In 1987, over 6 million tons of conventional fly ash were used as a cement replacement or portland cement in ready mix concrete and concrete products. This represented approximately 82% of all of the fly ash used in the United States. Approximately 42% of all ready mix concrete used fly ash at an average of 20% replacement of the cement.

The use of PFBC ash in concrete and concrete products relies on the pozzolanic property of the ash. Fly ash, including FBC ash is known to be a pozzolan, and therefore is used as a cement replacement (supplement) in portland cement concretes. However, ASTM requires that the SO_3 content of the ash can not exceed 5% if the ash is to be used as a pozzolan. This will restrict the use of certain PFBC ashes. Ashes from low-sulfur coal fired units (i.e., low sulfur subbituminous coals) will meet the specifications and represent excellent pozzolans (unpublished Western Research Institute data). Those from the combustion of high sulfur coal will not meet the SO_3 limits

No-Cement Concrete and Concrete Products. The use of FBC ash in the production of no-cement concrete and concrete products has also been the subject of extensive development in the United States and Canada during the 1980s (Minnick 1982; Bland et al. 1987, 1989, 1991a,b; Burwell et al. 1993). This material, originally developed as a material for subsidence control in underground mines, has been modified to have engineering properties comparable to portland cement concrete.

Bland et al. (1991a) concluded that AFBC concretes show promise as a construction material. The engineering properties of the concrete varies considerably due to the nature of the coal burned and the sulfur content which dictates the sorbent usage. Low-sulfur coal ash seems to exhibit the best durability characteristics, but may be short on unreacted sorbent, thereby limiting the strength

development. The AFBC no-cement concrete has been tested in field demonstrations as a road base material, including roller compacted concrete (RCC), as a ready mix concrete, and as masonry block mix.

PFBC ash may have potential in this application, when used in conjunction with lime. PFBC ash, unlike AFBC ash, is not expected to contain sufficient free lime for the required pozzolanic reactions to occur.

Soil and Road Sub-Base/Base Stabilization. The use of FBC residue for stabilization of soils has been proposed by a number of researchers. This application is similar to the cement stabilization of soils commonly applied in the construction industry. Soil stabilization is based on the lime treatment of clay soils and the self-cementing characteristics of the FBC ash. Unfortunately, the high-sulfate content of some FBC residue may create swelling due to the sulfate induced heaving of the soils. This is due to the formation of hydration products, such as ettringite and thaumasite in the soil/FBC residue mixture. Both of these mineral phases are known to cause expansion and swelling in cement or lime stabilization of high-sulfate soils. The use of relatively low-sulfate PFBC residue or the use of PFBC residue in low concentrations with the soil appear to show promise, although caution is warranted.

Bigham et al. (1993) has successfully demonstrated the application of FBC residue for the stabilization of cattle lots. In this application, the FBC residue is mixed into the soft cattle lot soils and allowed to cure. The FBC residue removes water from the cattle lot soil and hardens. The resultant cattle lots show improved stability and the cattle penetration into the soils is eliminated.

The largest stabilization area is related to the stabilization of subbases and bases for road and highway construction. There are essentially two forms of stabilized road bases: (1) stabilization of a base material as a soil cement application; or (2) production of a stabilized road base material in a form such as roller compacted concrete (RCC). Both of these road base materials have potential (Bland et al. 1989, 1991b). The first road base material form employs the principals of soil cement application and as such may be susceptible to dimensional instability for certain FBC residue compositions. On the other hand, roller compacted concrete, is a lean zero slump concrete mixture that resembles the texture of a damp aggregate. The RCC mixture is emplaced using typical asphalt paving equipment. The mixture is spread and compacted using roll compactors in lifts. The cured RCC mixture then has a wear surface placed on it in the case of road bases. RCC is used for other applications, such as dams and parking lots (Pitman, 1986).

RCC made from FBC ash has been demonstrated as part of the Tennessee Valley Authority (TVA)/Electric Power Research Institute (EPRI) sponsored research program (Bland et al 1989, 1991b; Hunsacker et al. 1987). FBC residue from the TVA 20 MW FBC facility in Paducah, Kentucky was used in a demonstration of RCC in McCracken County (Bland et al 1989, Hunsacker et al. 1987). PFBC ash is expected to be usable in this application, particularly in combination with controlled amounts of lime or cement.

Structural Fill and Embankments. The application of FBC residue as an engineered material for structural fills and embankments represents a large-scale use option. Structural fills and embankments are numerous in the road construction, mining and industrial construction industries. Structural fills and highway embankments using conventional ash materials

have been well documented through EPRI sponsored research and demonstration activities.

The application of FBC residue for these construction applications relies on the development of the stable properties of the ash. Ash Management Engineering and Jacques Whitford and Associates investigated the potential for the structural fill of a quarry using ash from the AES Barbers Point CFBC facility, Oahu, Hawaii (Georgiou et al. 1993). The study concluded that the construction of a structural fill using FBC ash was technically feasible and that the ash produced a fill with a high degree of strength and stability. However, the ash was a low-sulfate residue and the environmental conditions were warm temperatures and relatively low precipitation. Other high-sulfur residues may not produce a stable fill under these or more humid conditions.

A construction material has been produced by AES Barbers Point called 'Ash Rock', which can be used for structural fill applications. 'Ash Rock' material has not been able to meet the abrasion resistance requirements specified by ASTM or AASHTO for consideration as an aggregate material. Instead, this material is presently being produced as a structural fill material and has received designation as 'borrow' material on the island of Oahu.

PFBC ash is expected to be marketable in these applications. In fact, Bigham et al. (1993) have successfully used ash from the AEP Tidd PFBC facility in an embankment/fill application for a U.S. DOE-sponsored road field demonstration.

Synthetic Aggregate. The aggregate market in the United States is enormous. In 1992, approximately 1.2 billion tons of crushed stone and approximately 0.8 billion tons of sand and gravel were produced for a market valued in excess of $8 billion. The aggregate market encompasses conventional aggregate products, such as masonry units and ready mix concrete. Also with crushing, aggregates can be produced for use in asphalt paving, road base construction and even RCC. There is evidence that lightweight aggregate can also be produced from certain CFBC ashes.

Two CFBC ash pelletizing plants have been built in the United States at AES Thames and U.S. Generating Cedar Bay Cogeneration plants (Bland et al. 1993; Bland 1994). These plants have the capacity of pelletizing 500 to 800 tons/day, respectively. The pelletization of FBC ash was selected for ease of handling and for the possible subsequent use as a synthetic aggregate. Preliminary testing of the pelletized ash as an aggregate indicates that the material meets the strength, abrasion resistance, and other engineering requirements for its use as an aggregate (Bland et al. 1993).

Although the availability of free lime is not characteristic of PFBC ashes, this option still poses a major market for PFBC ashes, as well as a method for storage in the construction off-season.

Ash Use in Agricultural/Soil Amendment Applications. There are a number of benefits that result from the application of FBC residue to agricultural soils or mine spoils. The benefits include the modification of soil pH, supply of essential plant nutrients for crop production, increasing water infiltration, soil aggregation, and modification of texture of clay soils promoting root growth. This data base has resulted from years of research by universities and especially the U.S. Department of Agriculture (USDA).

Previous work has verified that the chemical composition of FBC residues includes compounds of interest in agriculture, such as lime and gypsum (Korcak 1980; Stout et al. 1988). This material has potential as both a soil amendment and a nutrient source. Greenhouse studies have

determined that the FBC residue was as effective as that of $Ca(OH)_2$ in increasing soil pH when the materials are applied in equivalent free lime amounts. The residue, when applied as a lime source, also increased the sulfur and manganese contents of tall fescue. The research to date indicates that application rates of FBC residue at 1 to 5 tons per acre to agricultural lands with acidic soils, soils high in heavy metals, or soils deficient in trace metals are beneficial.

The potential application of FBC residue as a soil amendment and nutrient source for revegetation of disturbed lands resulting from mining has received considerable attention (Bennett et al 1985; Stout et al. 1982; Sidle et al. 1978). The application of FBC residue to acidic soils and strip mine spoil can reduce the mobility of heavy metals through pH adjustment. Also beneficial micro- and macro-nutrients have been observed to move into the subsoil of infertile acidic soils and mine spoils after application of FBC residue, thereby promoting root penetration.

The application of FBC residue to agricultural lands has been commercially pursued in Hawaii for sugar cane applications (Sundstrom, personal communication); in New York at the Fort Drum facility (Tom Nickeson, personal communication) and in California at the Stockton facility (Lewnard 1991). Additional testing is ongoing at the USDA using FBC residue for orchard applications (Korcak, 1994, personal communication).

PFBC ash is expected to also meet the requirements for agriculture/soil amendment applications. Recent studies sponsored by the U.S. Department of Energy (DOE) using the ash from the AEP Tidd PFBC facility have examined the use of FBC residue in a variety of greenhouse studies. The technical feasibility of FBC ash use in agricultural applications was noted, but the potential of magnesium imbalance was also noted as a potential side-effect (Stehouwer and Sutton 1992; Bigham et al. 1993). This is specific to those units using dolomite as a sorbent.

PROJECT DESCRIPTION

The chemical characteristics of PFBC ash compared to AFBC ash has generated interest in the use of the PFBC ash for various construction and agricultural applications. However, before commercial entities are ready to commit to the concept of using PFBC ash, the performance of the ash in these high volume ash use applications must be documented. The first step must be a preliminary evaluation at the laboratory scale. If successful at that level, then full-scale demonstration projects will be required before acceptance is received by the contractors and regulatory agencies.

A research and development program composed of three phases is being conducted. Phase I focuses on an evaluation of the markets for PFBC ash. Phase II addresses the technical feasibility of PFBC ash use including chemical/physical characteristics, construction and civil engineering properties, and agricultural amendment properties. Phase III addresses the development of a strategy for demonstrating the most promising of the ash use applications defined in Phases I and II.

Phase I. Market Assessment of PFBC Ash

Potential market penetration of the existing markets will be assessed according to a protocol agreed to by DOE and EPRI. The market assessment will be an evaluation of the market potential in a number of areas including: **structural fill** as used in construction of highways, embankments and bridge abutments; **soil stabilization/road base material** used in building roads, parking lots, factory floors, etc.;

supplementary cementing material for concrete and concrete products; **bricks and blocks**; **synthetic aggregate** in concrete and asphalt paving of roads, etc.; and **agriculture/soil amendments** for agricultural and reclamation lands as a soil conditioner, liming and gypsum agents.

Each of these markets for PFBC ash are to be addressed and assessments of the magnitude of the market, competing materials and likely growth potential determined. The properties of the materials presently used in the markets will be determined and compared with known properties of PFBC ash to determine delimiting properties and/or required properties of the PFBC ash.

The market assessment will also provide an evaluation of the market trends and related opportunities, speculation about the market in the year 2000, and the nature of technical developments and marketing needed for market penetration by PFBC ash. A ranking of the potential applications for PFBC ash will be made, based on the results of the market assessment.

Phase II. Technical Feasibility of PFBC Ash Use

The scope of the proposed testing focuses on ash characterization and conditioning studies, geotechnical characteristics of the ash as related to stabilized fill applications, use of the PFBC ash as a supplementary cementing material, the production of a synthetic aggregate via pelletization of the ash, and the use of the ash in agricultural/soil amendment applications.

It is anticipated that two PFBC ashes will be evaluated as part of this study. Previous experience has indicated that the sulfur content of the coal is the primary controlling parameter affecting ash composition and resultant ash properties. Based on the use of ash from these coal sulfur content extremes, the determination of the range of technical performance of PFBC ash can be made.

The characterization of the ash includes both the chemical and the physical properties. The chemical characterization of the ash consists of the chemical analysis for the elemental composition of the ash, the identification of the phases present in the ash, and the leachate characteristics of the ash as a result of the standard Toxicity Characteristic Leaching Procedure (TCLP). Both the elemental concentration and the mineral phases are to be determined.

The geotechnical properties are the basis for evaluating the general feasibility of the ash for use in construction-related applications. In general, the geotechnical evaluation will determine those properties of the ash related to its use in **structural fill** applications.

The testing of the PFBC residue as a **supplementary cementing material** will consider both partial cement replacement and addition to standard portland cement mortar mixes. Applicable ASTM and AASHTO specifications and limits for (1) grouts and flowable fills, (2) ready mix or roller compacted concretes, and (3) soil-cement applications will be evaluated.

The production of **synthetic aggregate** from PFBC fly ash will be addressed through a series of laboratory tests and pelletizing trials and subsequent testing of the cured and hardened ash pellets. The pelletization trials will include the ash conditioning requirements, the water demand requirements for pelletizing, the curing requirements, and the definition of the engineering properties as related to materials handling.

The pellets produced from the pelletizing tests will be subjected to a series of standard ASTM

and AASHTO tests for aggregates to be used in concrete and masonry blocks, highway base construction, and asphaltic paving. The testing will determine the abrasion resistance, strength, and durability characteristics.

The use of PFBC ash as a **soil amendment** in reclamation and/or agricultural applications has potential due to the presence of macro and micro-nutrients and lime, calcium sulfate, and calcium carbonate in the ash, all of which could be beneficial to plant growth. Specifically, the available lime and sulfates are considered to be of value relative to replacement of fertilizers.

An evaluation of the potential of PFBC ash as a soil amendment will be made both in laboratory equilibration testing and in a greenhouse plant productivity study. The laboratory equilibration study will compare PFBC ash to agricultural lime in the treatment of two soil types with low pH. The greenhouse plant productivity testing will evaluate both the PFBC ash and the agricultural lime on several plant species of varying acid tolerances. The vegetation will be evaluated for elemental composition, production rates and root conditions.

Phase III. Ash Use Demonstration Strategies

Phase III will evaluate the results of the Phase I and II research in order to develop a strategy for the demonstration of the most promising of the PFBC ash uses in full-scale field demonstrations. The purpose of the Phase III activities is to develop a game plan for the implementation of Phase I and II results into field demonstrations with prospective commercial developers and or marketers.

The activities will identify potential developers and marketers as well as potential sites for field demonstrations. The details of Phase III activities are difficult to quantify until the results of the Phase I and II are complete. The detailed scope of work for this phase will be developed jointly with EPRI, DOE, and the others sponsors as the project progresses.

The results of the Phase III activities will lead to the implementation of one or more field demonstrations, under future funding opportunities. These field demonstrations will allow the developers, ash generators, ash management companies, and ash users to all participate and thereby develop confidence and the engineering data necessary to take these ash use options to a commercial business status.

RESULTS

The project is underway and ash sources for the technical feasibility study are being finalized. Ashes from the Ahlstrom Pyropower's Hans Ahlstrom Laboratory pilot PCFBC unit in Karhula, Finland are being made available for this study. The ashes represent the material from the combustion of low-sulfur Powder River Basin subbituminous coal with and without limestone sorbent. Sulfur capture of approximately 90 to 95% was achieved in the limestone sorbent tests. These tests are being conducted in support of the Des Moines Energy Center (DMEC) Clean Coal projects. The Powder River Basin coal (western U.S. subbituminous) and the Iowa Industrial Lime No. 1 are the proposed fuel and sorbent for the DMEC-1 PCFB demonstration project.

The Ahlstrom PCFBC pilot plant is of square cross-section. It is housed in an 11.8-ft (3.6-m) diameter pressure vessel. A high-pressure high-temperature, gas cleaning unit downstream of the PCFB exhaust is installed in a separate 8.5-ft. (2.6-m) diameter pressure vessel. The maximum plant operating pressure is 16 bar (232 psia). The fuel is fed as a slurry and the sorbent is also fed along

with the fuel. A separate dry sorbent feed system is also installed for trimming the sulfur oxides emissions during load swings. The plant has provisions for startup with gas and/or oil. A detailed description of the facility is provided in earlier papers (Isaksson et al. 1990; Sellakumar et al. 1993) and the design conditions is given in Table 3.

Table 3.
Summary of the Operating Conditions of the Ahlstrom Pyroflow PCFB Pilot Plant in Karhula, Finland

Heat Input	34 MM Btu/hr (10 MWth)
Max. Fuel Feed Rate	15870 lb/hr (2 kg/s)
Max. Air Flow Rate	43650 lb/hr (5.5 kg/s)
Operating Temperature	1616 °F (1153 °K)
Max. Operating Pressure	232 psia (16 bar)

FUTURE WORK

The project is just being initiated. The scope of the project as defined earlier will be conducted over the next three years.

REFERENCES

Baker/TSA, Inc., 1990, "Waste Disposal/ Utilization Study". U.S. Department of Energy, Morgantown Energy Technology Center, Morgantown, WV, DOE/MC/25042-2872, 335 p.

Bennett, O.L., J.L. Hern, R.L. Reid, H.D. Perry, W.L. Stout, and J.H. Edward, 1985, "Agricultural Uses of Atmospheric Fluidized Bed Combustion Residue (AFBCR) - A Seven Year Study". Unpublished Report, U.S. Department of Agriculture; Appalachian Soil and Water Conservation Research Laboratory, Beckley, WV.

Bigham, J., W. Dick, L. Forster, F. Hitzhusen, E. McCoy, R. Stehouwer, S.W. Traina, W. Wolfe, and R. Haefner, 1993, "Land Application Uses for Dry FGD By-Products; Phase I Report". U.S. Department of Energy, Morgantown Energy Technology Center.

Bland, A. E., C. E. Jones, J. G. Rose, and M. N. Jarrett, 1987. "Production of No-Cement Concretes Utilizing Fluidized Bed Combustion Waste and Power Plant Flyash", In *Proceedings of 9th International Conference on Fluidized Bed Combustion,* Boston, MA, May 3-7, 1987 p. 947-953.

Bland, A.E., C.E. Jones, J.G. Rose, and J.L. Harness, 1989, "Ash Management Options for AFBC". In *Proceedings of 10th International Conference on Fluidized Bed Combustion,* San Francisco, CA, April 30 - May 3, 1989, p. 323-333.

Bland, A.E., S.M. Burwell, and R.K. Kissel, 1991a, "Commercialization Potential of AFBC Concretes: Part 1. Mix Design and Engineering Properties". EPRI Project No. 2708-4, 1991., EPRI Report GS-7122.

Bland, A. E., R.K. Kissel, and G.G. Ross, 1991b, "Utilization of CFBC Ashes in Roller Compacted Concrete Applications". In *Proceedings of 11th International Conference on Fluidized Bed Combustion*, Montreal, Canada, April, 1991, p. 857-863

Bland, A.E., R. Cox, A. Rowen, and E.R. Lichty, 1993, "Pelletization as an Ash Management Option for CFBC Ash Handling and Utilization".

In *Proceedings of the 12th International Conference on Fluidized Bed Combustion*, LaJolla, CA, May, 1993, p. 1341-1350.

Bland, A. E., "Overview of Management Options for Residues from FBC Technologies". In *Proceedings of the EPRI 1994 Fluidized Bed Combustion Symposium*, Atlanta, GA, May, 1994.

Burwell, S.M., R.K. Kissel, A.E. Bland, and D.M. Golden, 1993, "Fluidized Bed Combustion Ash Concrete". In *Proceedings of the 12th International Conference on Fluidized Bed Combustion,* LaJolla, CA, May, 1993, p. 847-858.

Georgiou, D.N., A.E. Bland, and D. Sundstrom, 1993, " Laboratory Evaluation of a Low Sulfur Coal CFBC Residue as a Structural Fill". In *Proceedings of the 12th International Conference on Fluidized Bed Combustion*, LaJolla, CA, May, 1993, p. 629-639.

Hunsacker, D., G.W. Sharpe, J.G. Rose, and R.C. Deen, 1987, "Road Base Construction Utilizing Coal Waste Materials". In *Proceedings of the Eighth International Ash Utilization Symposium*, Washington, DC, October, p.22-1 to 22-15.

Isaksson, J., et al., 1990, Development of PYROFLOW* Pressurized Circulating Fluidized Bed (PCFB) Boilers for Utility Applications". In *Proceedings of Third International Conference on Circulating Fluidized Beds*, Nagoya, Japan, October 15-18, 1990.

Korcak, R. F., 1980, "Fluidized Bed Combustion Material as a Lime Substitute and Calcium Source for Apple Seedlings". J. Environmental Quality, vol. 9, p. 147-151.

Lewnard, J.J., 1991, "Agricultural Applications of CFBC Ashes from Western Coals". In *Proceedings of 1991 CANMET CFBC Ash Management Seminar*, July 2-3, 1991, Halifax, NS, p. 135-152.

Minnick, L.J., 1982, "Development of Potential Uses for the Residue from Fluidized Bed Combustion Processes". Final Report; Report No. DOE/ET/10415-T6, U.S. Department of Energy.

Pitman, D.W., 1986, "Construction of Roller Compacted Concrete Pavement". Transportation Research Board 1062, Washington, DC. p.1-6.

Sellakumar, K.M., Isaksson, J. and Tiensuu, J., 1993, "Process Performance of Ahlstrom Pyroflow PCFB Pilot Plant". In *Proceedings of the 1993 International Conference on Fluidized Bed Combustion*, LaJolla, CA, May 8-13, p. 423-429.

Sidle, R.C., W.L. Stout, J.L. Hern, and O.L. Bennett, 1978, "Leaching Experiments on Soil and Mine Spoil Treated with Fluidized Bed Combustion Waste". In *Proceedings of the Fifth International Conference on Fluidized Bed Combustion*, 1978, p. 821-831.

Stout, W. L., H. A. Menser, O. L. Bennett, and W. M. Winant, 1982, "Cover Establishment on an Acid Mine Spoil Using Composted Garbage Mulch and Fluidized Bed Combustion Residue". Reclamation and Revegetation Research, 1:, p. 203-211.

Stout, W.L., J.L. Hern, R.F. Korcak, and C.W. Carlson, 1988, "Manual for Applying Fluidized Bed Combustion Residue to Agricultural Lands". U.S. Department of Agriculture, Agr. Res. Ser., ARS-74.

Stehouwer, R., and P. Sutton, 1992, "Treatment of Acid Mine Spoil with Dry FGD By-Products: Leachate Quality and Plant Growth". In *Proceedings of Abandoned Mine Lands Conference*, Aug. 23-26, 1992, Chicago, IL.

9a.7

Co-Firing Waste Materials in an Advanced Pressurized Fluidized-Bed Combustor

CONTRACT INFORMATION

Contract Number	DE-AC21-89MC25177
Contractor	Gilbert/Commonwealth, Inc. P.O. Box 1498 Reading, PA 19603 (610) 775-2600
Contractor Project Manager	Lynn N. Rubow
Principal Investigators	Michael R. DeLallo Roman Zaharchuk
METC Project Manager	Donald L. Bonk Heather M. McDaniel
Period of Performance	August 26, 1992 to September 30, 1994

OBJECTIVES

A study has been undertaken to investigate the technical and economic feasibility of co-firing a pressurized fluidized-bed combustor (PFBC) with coal and municipal or industrial wastes. Focus was placed on the production of electricity and the efficient disposal of wastes for application in a central power station and distributed locations. Wastes considered for co-firing include municipal solid waste (MSW), municipal sewage sludge, and industrial de-inking sludge. Issues concerning waste material preparation and feed, PFBC operation, plant emissions, and regulations are addressed. This paper describes the results of the performance evaluation completed as part of this study, and provides recommendations for further evaluation.

BACKGROUND INFORMATION

The Environmental Protection Agency's (EPA) 1990 estimates place the amount of MSW generated in the United States at over 195 million tons per year, up approximately 44 million tons since 1980[1]. EPA estimates that 4.3 pounds of MSW are generated per person per day. Together with industrial process waste and municipal sewage sludge, the resultant burden on our capacity to dispose of these wastes, in a cost-effective and environmentally acceptable manner is an enormous management problem.

One method of waste management is through combustion or incineration with energy recovery. This alternative has been plagued with a legacy of inefficient, dirty, and poorly operated incinerators, resulting in environmental problems leaving communities searching for solutions. However, advanced power systems that can meet new stringent environmental regulations have been developed and operated successfully. Additionally, electric utilities and non-utility generators have shown significant interest in waste management through waste-to-energy facilities.

Co-firing waste with coal in a utility scale boiler has emerged as an effective approach to produce energy from waste. Fluidized-bed combustors are becoming a primary method of burning wastes. The fluidized-bed, with its stability of combustion and temperature, provides enhanced energy recovery and environmental control while achieving cost-effective waste management.

Waste Material Characteristics

The characteristics and analyses of the three waste fuels under consideration were obtained from facilities that presently co-fire these materials. The wastes are municipal solid waste, municipal sewage sludge, and industrial de-inking sludge

Municipal Solid Waste. Waste classified as MSW is extremely variable in composition both on a seasonal and location basis. To produce a fuel that can be fed to a PFBC, it must be processed to remove metal, glass, and other non-combustibles to produce what is called refuse derived fuel (RDF). Methods currently used process about 50 percent of MSW to RDF. A typical 3-inch shredded material is prepared by shredding, magnetic separation, and air classification. It can be burned as is, pelletized, or slurried. A representative RDF proximate and ultimate analysis is shown in Table 1.

Municipal Sewage Sludge. The incineration of sewage sludge has a long history in the United States. Initially, multiple hearth units were used; now the majority of new installations are FBCs.

Treatment plant sludges generally are less than 7 percent total solids (t.s.). Combinations of processes such as chemical addition, flocculation, thermal conditioning, gravity thickening, and centrifugation are used to thicken sludge prior to burning. Feed sludges range from 20 percent to 40 percent t.s., but 25 percent t.s. is a reasonable average.

Sludge analyses vary from plant to plant and from season to season in the same plant. The fibrous nature of sewage sludge greatly affects the fluidity. A 7 percent t.s. sludge has the consistency of wet cement. At 25 percent t.s., sludge can be conveyed "dry" on a conveyor belt. Table 2 is an ultimate analysis of a sludge that has 13.85 percent t.s. On a dry basis the Higher Heating Value (HHV) of sludge can be as high as 6,500 Btu/lb.

De-Inking Sludge. The amount of de-inking sludge produced is increasing as the use of recycled paper is gaining popularity. In the manufacture of newsprint, the repulping generates a large quantity of high ash sludge, which previously was disposed of in lagoons. Now incineration in fluidized-bed combustors is preferred since overall energy costs can be reduced and environmental requirements can be satisfied. The pulping process in a typical size facility produces 250 dry tons of de-inking sludge per day from a feed of 1,600 dry tons per day of old newsprint.

The sludge is concentrated from a 2 percent t.s. stream to 7 percent and is further de-watered to 45 percent t.s. using screw presses. The character of 45 percent sludge is such that storage bins are not used. The sludge is processed and conveyed directly to the boiler on conveyor belts. Table 3 shows a representative sludge analysis.

Design and Operation Issues

Although there is considerable data on the operation of PFBCs when feeding coal both dry and as a slurry, wastes have not been co-fired with coal. There is, however, considerable information on co-firing wastes in atmospheric fluidized-bed combustors (AFBC) that is relevant. Except for pressure, AFBCs have similar operational requirements. Feeding the wastes into the combustors has been the most common problem. This prompted an investigation as to what equipment is available to feed RDF and sludges into a PFBC.

Table 1. Representative RDF Analysis

Proximate Analysis As Received		Ultimate Analysis As Received	
Moisture	30.73 %	Moisture	30.73 %
Ash	11.59	Ash	11.59
Volatile	48.93	Sulfur	0.32
Fixed C	8.75	Nitrogen	0.61
	100.00 %	Carbon	28.30
		Hydrogen	4.20
Btu/lb, HHV	4,801	Oxygen	24.25
		Total	100.00 %

Table 2. Municipal Sewage Sludge Ultimate Analysis

Carbon	3.08 %
Hydrogen	0.46
Nitrogen	0.37
Sulfur	0.07
Ash	6.80
Oxygen	3.07
Moisture	86.15
Total	100.00 %
Btu/lb, HHV	464

Table 3. De-Inking Sludge Analysis

Proximate		Ultimate	
Moisture	55.00 %	Moisture	55.00 %
Ash	9.76	Ash	9.76
Volatile	28.74	Sulfur	0.11
Fixed C	6.50	Nitrogen	0.35
	100.00 %	Carbon	19.58
		Hydrogen	2.40
Btu/lb, HHV	3,562	Oxygen	12.80
		Total	100.00 %

The flow and handling characteristics of the waste materials considered in this study are affected by quality, moisture content, particle size, and extraneous contaminants. Feeding these materials into pressure vessels differs greatly from feeding into atmospheric processes due to pressure influences on the tension and compression strength of the feed material. Recently, there has been activity in developing pressurized feeders for biomass waste materials and both dry and slurry feeders have been tested. Dry feed systems include double lockhoppers, rotary valve feeders, piston feeders, screw feeders, and pneumatic systems. Slurry feeders include progressive cavity pumps, piston pumps, and rotary feeders. However, these options have not had substantial operating experience at PFBC conditions, but it is assumed that eventually a reliable system will be available. The slurry feeders have had the advantage based on experience feeding coal slurries, but there is a penalty effect on performance especially when feeding high moisture slurries. Table 4 presents some of the dry feeders evaluated.

PROJECT DESCRIPTION

Design and performance analyses were developed for PFBC advanced generation plant configurations with nominal ratings of 110 MWe and 250 MWe. Performance considerations were given to fuel handling, emission control, and residual solids handling. Thermal performance for all cases was calculated by using an Aspen/SP™ modular computer program. The program modeled the PFBC, gas turbine, heat recovery and steam generator, and the steam turbine cycle in a single, integrated calculation process. Plant material and energy balances were developed along with the net plant power, thermal efficiency, and net heat rate. Comparisons were made to firing with and without waste materials to define the effects on plant performance from waste co-firing.

RESULTS

The design and performance analyses for the PFBC power plant co-fired with RDF and/or sludge waste followed two application scenarios. The first assumed a utility base load application with electrical production in the 100 to 120 MWe range, and the second assumed a capacity of 240 to 250 MWe. Application specifics were then based on these scenarios including the definition of site and ambient conditions -- fuel, waste, and sorbent feedstock -- and method of fuel/waste handling. The PFBC 1.5-Generation plant configuration as presented in Figure 1 was the basis for this study and is used to establish the baseline performance. The study utilized defined plant boundary conditions including ISO ambient conditions, Pittsburgh 8 coal, Plum Run dolomite, and waste feedstock for each PFBC application analysis.

The ratio of coal-to-waste fuel was established on the following criteria: (1) an 80:20 coal-to-waste ratio on an as-received weight basis was used to define the maximum amount of co-fired waste products, and (2) co-fired amounts for municipal sewage sludge were based on the volume produced from a typical population center of 250,000, employing a typical sludge treatment process.

Design Review

Major subsystems specifically influenced by the waste material feedstock are fuel handling, emission control, and residual solids handling. Of particular concern to this study is the impact on system performance from variations in the fuel/waste handling process.

Table 4. Summary of Dry Feed Systems for High Pressure

Feeder Type	PSI Pressure (Max)	m3/h Capacity (Nominal)	Suitable For	Remarks
Lockhopper Gravity Feed	500	40	All Wastes	Unless double LH are used, compression gas use could be excessive.
Lockhopper Screw Feed	360	14	All Wastes	A larger capacity unit has not been designed.
Rotary Valve	175 to 350	200 to 280	All Wastes	Size should be <5 cm. Other Vendors offer <200 psi max. feeders.
Piston Feeders	333 to 2175	50 to 115	All Dry Wastes	Feeders are more suitable for dry fuels. Sludges would have to be tested.
Screw Feeders	250 to 1450	20 to 45	All Wastes	Expensive. Fibrous and abrasive materials are a problem.

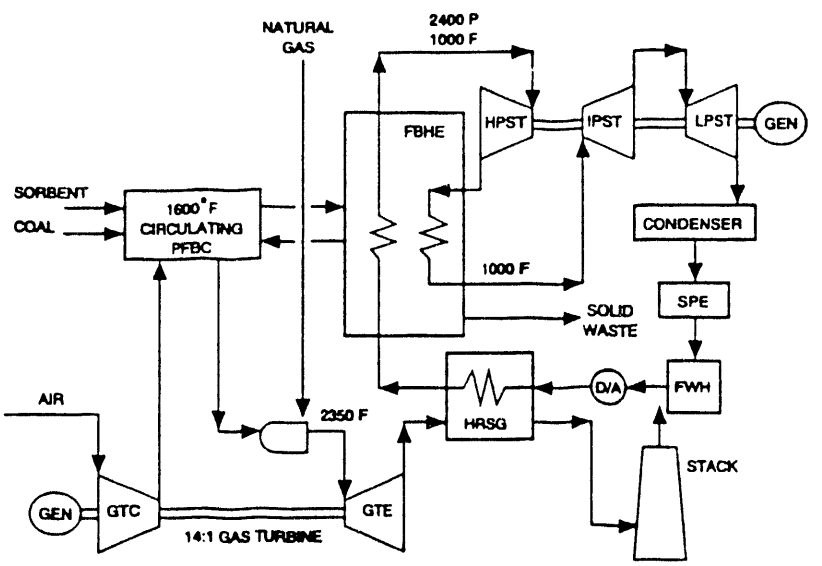


Figure 1. 1.5-Generation PFBC Cycle

Fuel Handling Options. The analyses investigated slurry processing of the coal and sorbent in either: (1) separate combustor feed of the coal/sorbent and waste streams, or (2) combined coal/sorbent and waste fired in a slurry media. As an alternative approach to slurry feeding, a sensitivity study of dry feeding of coal, sorbent, and the co-fired RDF was completed at the 250 MWe level. The analysis compared overall plant efficiency and cost-of-electricity to determine if an advantage exists in dry versus slurry feed. In the slurry feed approach, the coal and sorbent are transported via a water media at 75 percent total solids.

Waste Material Handling. For the 250 MWe system, RDF is fed to the PFBC as a slurry or pneumatically to determine which method proved higher system efficiency and lower economics of operation. For the slurry feed analysis, RDF is combined with coal and sorbent and slurried with water to 75 percent t.s. The slurry is then pumped into the PFBC. The inherent moisture of RDF was not considered to be used as part of the slurry water content.

In the case of dry feed, the RDF is fed to the PFBC via a screw conveyor. In this case, coal and sorbent are pneumatically conveyed to PFBC. Separate feed systems allow different fuel injection points in the combustor. In this manner the relatively light RDF material can be fed to the PFBC at a point to assure complete combustion.

For municipal sludge, it was assumed to be dewatered to 24 percent t.s. and fed in a separate flow stream to the combustor. A value of 24 percent t.s. corresponds to the industry achievable de-watering capability with conventional belt filter or screw press.

Based on a population value of 250,000 supplying the municipal sludge, a feed rate of 35,000 lb/day was assumed in both the 250 MWe and 110 MWe performance analysis. At this input rate, the coal-to-waste feed ratio, on an as received weight basis, is 95:5 and 91:9, respectively.

An additional case analysis examined the potential use of as-received municipal sludge at 6 percent t.s. as the slurry media for the PFBC fuel and sorbent. The limiting factor for this analysis was the requirement to maintain a 75 percent t.s. in the fuel and sorbent feed.

For the analysis of de-inking sludge, it was assumed that a 40 percent t.s. is fed to the PFBC via piston feeder. At this percent solids, de-inking sludge can not be pumped in a conventional fluid pump. A sludge total solids value of 40 percent was chosen to represent the industry standard in recycled newsprint facility operation. Separate feed systems for the coal/sorbent slurry and de-inking sludge allow for different fuel injection points. In this manner, the relatively light sludge material can be fed to the PFBC at a point that will inhibit rapid ascension of the sludge material assuring complete combustion. The coal-to-waste firing ratio of 80:20 was assumed, on a weight basis, and is based on as-received coal and "bone-dry" de-inking sludge.

Performance Analysis Assumptions

The design and performance analyses for a PFBC power plant co-firing RDF and/or sludge waste followed similar application scenarios. Operational conditions were established assuming a utility base load application located in the United States mid-Atlantic region.

The 250 MWe application includes the use of a Westinghouse 501D5 gas turbine with an 1800/1000/1000 steam turbine bottoming cycle. The performance for the 110 MWe is based on using a Westinghouse W251B12 gas turbine with a 1450/1000/1000 steam turbine bottoming cycle.

The PFBC combustor design parameters were assumed to follow the design assumptions defined in Gilbert/Commonwealth Report No. 2985[2]. The PFBC is a circulating bed with an operating temperature in the 1600^{O}F range. A 99.3 percent carbon conversion efficiency

was assumed for performance modeling along with a 93.3 sulfur removal.

The performance analysis for the various PFBC power plants co-fired with waste feedstocks were developed according to the application and waste material used.

The case profiles used to define the performance assumptions are as follows:

250 MWe Application

250 MWe with Pittsburgh 8 coal and municipal solid waste as RDF in a combined slurry feed at the 80:20 coal-to-waste ratio.

250 MWe Pittsburgh 8 coal and municipal solid waste as RDF as-received in separate dry feeds at the 80:20 coal-to-waste ratio.

250 MWe Pittsburgh 8 coal and municipal sewage sludge de-watered to 24 percent t.s. with separate feed at a waste feed volume based on a 250,000 population.

250 MWe Pittsburgh 8 coal and de-inking sludge de-watered to 40 percent t.s. with separate feed at the 80:20 coal-to-waste ratio.

110 MWe Application

110 MWe with Pittsburgh 8 coal and municipal solid waste as RDF in a combined slurry feed at the 80:20 coal-to-waste ratio.

110 MWe with Pittsburgh 8 coal and municipal sewage sludge de-watered to 24 percent t.s. with separate feed at a waste feed volume based on a 250,000 population.

110 MWe Pittsburgh 8 coal at 6 percent t.s. municipal sewage sludge to provide a combined slurry feed (coal, sorbent, and waste) at 75 percent t.s. with the slurry media supplied by the waste stream.

110 MWe Pittsburgh 8 coal and de-inking sludge de-watered to 40 percent total solids with separate feed at the 80:20 coal-to-waste ratio.

Performance Analysis Results

To further enhance the results of this study, performance comparisons were developed for the 1.5-Generation PFBC with and without co-firing of waste. The PFBC plant, as presented in Reference 2, is the basis for this study and was used to establish nominal performance without co-firing waste.

250 MWe Results. The performance for the 250 MWe PFBC plant without co-firing is shown in Table 6. Also shown are performance values for the same facility co-firing RDF as a slurry and in a dry form, co-firing municipal sewage sludge, and co-firing industrial de-inking sludge.

As indicated, an overall conversion efficiency of 41.38 percent was defined for the facility without co-firing of waste materials. With waste co-firing, conversion efficiencies decreased in the range of 1.0 percent to 2.7 percent depending on the waste co-fired and method of fuel handling. The lowest efficiency is attributable to the highest waste co-firing (industrial de-inking sludge), on a weight basis; thus a lower coal feed rate of approximately 13.6 percent.

In the comparison of alternative fuel and waste handling techniques, the pneumatic feed of coal, sorbent, and RDF had a slightly higher overall conversion efficiency of 40.98 percent compared to 40.39 percent for the slurried case. However, it was determined in follow-up work that the cost-of-electricity was also higher as a result of the required equipment capital cost for pneumatic feed.

110 MWe Results. The performance for the 110 MWe PFBC plant without co-firing is shown in Table 7. Performance values for the same facility co-firing RDF as a slurry, co-firing municipal sewage sludge, and co-firing industrial de-inking sludge are also presented for comparison.

Table 6. 250 MW PFBC Plant Performance Comparison

	W/O Waste Co-firing	RDF	(DRY) RDF	Municipal Sludge	De-Inking Sludge
ENERGY INPUT					
Coal Feed, lb/hr	128,861	118,313	117, 691	128,885	111,329
Coal HHV, Btu/lb	12,450	12,450	12,450	12,450	12,450
Natural Gas, lb/hr	19,257	19,635	19,251	19,553	19,710
Natural Gas HHV, Btu/lb	21,799	21,799	21,799	21,799	21,799
Waste Feed, lb/hr		29,578	28,367	6,076	69,581
Waste HHV, Btu/lb		4,103	4,103	804	3,166
Plant Energy Input, MW	595.181	592.713	588.256	596.628	596.710
ENERGY OUTPUT					
Gas Turbine, MW	87.501	98.882	89.139	96.908	103.182
Steam Turbine, MW	169.369	151.897	163.932	156.514	152.661
Auxiliaries, MW	10.590	11.407	12.030	10.166	10.583
Net Plant Power, MW	246.272	239.373	241.041	243.256	240.271
Thermal Efficiency, %	41.38	40.39	40.98	40.77	40.27
Net Heat Rate, (Btu/kWh)	8,246	8,449	8,327	8,369	8,474

As indicated, the overall conversion efficiency of 40.22 percent was defined for the facility without co-firing waste materials. With the additional waste co-firing, conversion efficiencies decreased in the range of 1.3 percent to 2.6 percent depending on the waste co-fired and method of fuel handling. As in the previous analysis, the lowest efficiency is attributable to the co-firing of industrial de-inking sludge.

The RDF co-fired analysis is based on a combined slurry feed system. As indicated, the overall conversion efficiency for the case of co-firing RDF was determined to be 39.29 percent, which represents a 2.3 percent decrease in thermal efficiency from the base case without co-firing.

Alternatives in co-firing municipal sewage sludge were investigated at the 110 MWe level. In the first analysis the coal was co-fired with municipal sewage sludge de-watered to 24 percent t.s. using a separate feed approach. A second analysis assumed a 6 percent t.s. municipal sewage sludge for use in providing a slurry media to transport the combined sludge, coal, and sorbent mixture at 75 percent t.s. This analysis was performed at the 110 MW nominal plant size to investigate the benefits of using the existing as-received municipal sludge as the transport media for the complete fuel, sorbent, and waste feedstock.

Table 7. 110 MW PFBC Plant Performance Comparison

	W/O Waste Co-firing	RDF	Municipal Sludge (24%)	Municipal Sludge (6%)	De-Inking Sludge
ENERGY INPUT					
Coal Feed, lb/hr	61,581	56,814	61,634	61,634	53,457
Coal HHV, Btu/lb	12,450	12,450	12,450	12,450	12,450
Natural Gas, lb/hr	7,781	7,853	7,902	7,890	7,880
Natural Gas HHV, Btu/lb	21,799	21,799	21,799	21,789	21,799
Waste Feed, lb/hr		14,200	6,076	24,306	33,410
Waste HHV, Btu/lb		4,103	804	201	3,166
Plant Energy Input, MW	275.345	274.550	276.844	276.767	276.434
ENERGY OUTPUT					
Gas Turbine, MW	38.107	43.760	43.491	44.025	44.735
Steam Turbine, MW	77.408	69.320	71.028	73.048	68.354
Auxiliaries, MW	4.774	5.204	4.608	7.039	4.806
Net Plant Power, MW	110.741	107.875	109.911	110.035	108.284
Thermal Efficiency, %	40.22	39.29	39.70	39.76	39.17
Net Heat Rate, (Btu/kWh)	8,484	8,684	8,594	8,582	8,711

As indicated in Table 7, there is no significant performance difference in the combined slurry approach over separate feed. However, a follow-up economic analysis indicated a savings in capital cost and lower cost-of-electricity with this approach. However, by combining the fuel, sorbent, and waste fuel streams, process control and combustor stability may be affected. Further data and analysis of the PFBC combustion parameters is required before accepting the benefits of the combined fuel feed approach.

FUTURE WORK

This study's objective was to investigate co-firing a pressurized fluidized-bed combustor with coal and refuse-derived fuel and/or sludges for the production of electricity and the efficient disposal of waste. Performance evaluation of the PFBC power plant co-fired with RDF and/or sludges showed only slightly lower overall thermal efficiency than similar sized plants without waste co-firing. Major contributors to the slightly lower performance include the waste material preparation and feed systems, and the additional water to support slurry feed of both the coal/sorbent and waste feedstock.

The results also indicate that there are no technology barriers to the co-firing of waste materials with coal in a PFBC power plant. The potential to produce cost-competitive electrical power and support environmentally acceptable waste disposal exists with this approach. However, as part of technology development, there remain several design and operational areas requiring data and verification before this concept can realize commercial acceptance.

Throughout the analysis, key issues concerning waste material preparation and feed, PFBC operation, plant emissions, and regulations were identified and addressed to the limits of available data. It is important to note that presently there are no known PFBC facilities co-firing coal and waste materials. Available information and performance data is limited to utility and municipal-owned facilities co-firing waste in AFBCs and private and government-funded research and development programs in PFBCs. Correlation of this data is difficult due primarily to the differences in operational parameters, combustion kinetics, and particulate removal temperature profiles. However, data on air/fuel distribution, primary emissions, and in-bed gas residence lend confidence to the use of existing AFBC operational information.

Specific R&D needs are listed below as major challenges.

Feeding waste materials against pressure using either dry feeders or slurry pumps,

waste material feed point spacing and location,

solids handling that includes circulating material and fly ash,

removal of tramp metal and other non-combustible material from the bed when feeding RDF,

corrosion effect of chlorine in waste materials,

levels of trace elements (organics and metals) in the gas and ash streams, and

storage of municipal sewage sludge and RDF at the power plant site.

In summary, the key issues for co-firing are feeding waste materials against system pressures (solids handling), materials concerns due to the addition of potentially corrosive constituents, and environmental impact of solid wastes and gaseous emissions. In order to address these issues, pilot-scale testing co-firing waste materials should be performed and the results used to predict commercial-scale performance. The testing should be performed in a facility of adequate size so that commercially representative fuel feed sizes and gas residence times can be evaluated.

REFERENCES

1. Franklin, W.E. and Franklin, M.A. "Putting the Crusade into Perspective" EPA Journal, Volume 18, No. 3 July/August 1992.

2. Gilbert/Commonwealth Report No. 2985, Conceptual Design and Optimization of a 1-1/2 Generation PFBC Plant, Draft Report, September 1993.

Session 9b

Membranes

9b.1 High Temperature Size Selective Membranes

CONTRACT INFORMATION

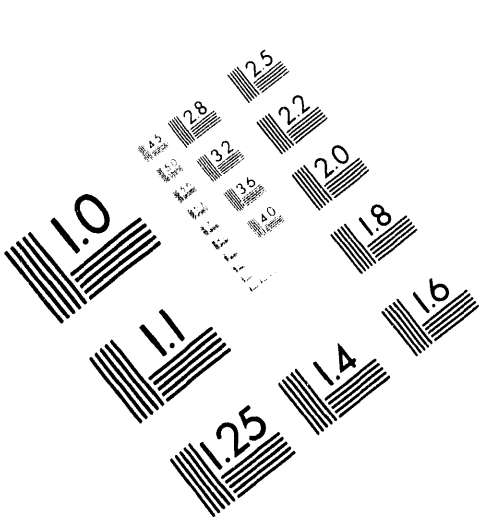
Contract Number	DE-AC21-92MC29245
Contractor	AlliedSignal, Inc. Box 5016 Des Plaines, IL 60017 (708) 391-3509
Contractor Project Manager	Stephen F. Yates
Principal Investigators	S. James Zhou David J. Anderson Alan E. van Til
METC Project Manager	Venkat K. Venkataraman
Period of Performance	September 19, 1992 to September 18, 1994

FY94 Program Schedule

	FY92								FY93								FY94							
	O	N	D	J	F	M	A	M	J	J	A	S	O	N	D	J	F	M	A	M	J	J	A	S
NEPA	___																							
Test Plan	___																							
Membrane Development	___	___	___	___	___	___	___	___	___	___	___	___	___	___	___	___	___	___	___	___	___	___	___	___

OBJECTIVE

The objective of this research is to develop a high temperature size selective membrane capable of separating gas mixture components from each other based on molecular size, using a molecular sieving mechanism. We are evaluating two concepts: a composite of a carbon molecular sieve (CMS) with a tightly defined pore size distribution between 3 and 4 Å, and a microporous supporting matrix which provides mechanical strength and resistance to thermal degradation, and a sandwich of a CMS film between the porous supports. Such a membrane would enable the separation of hydrogen

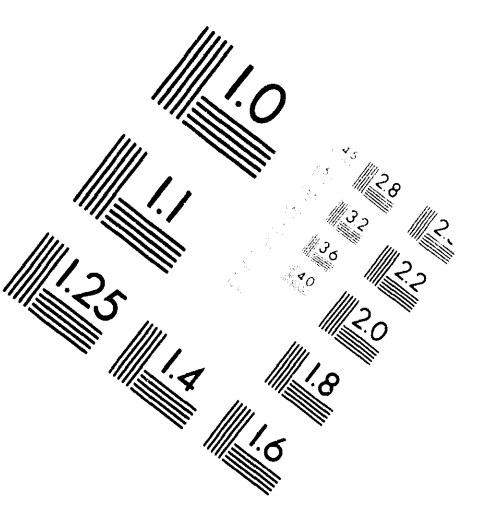


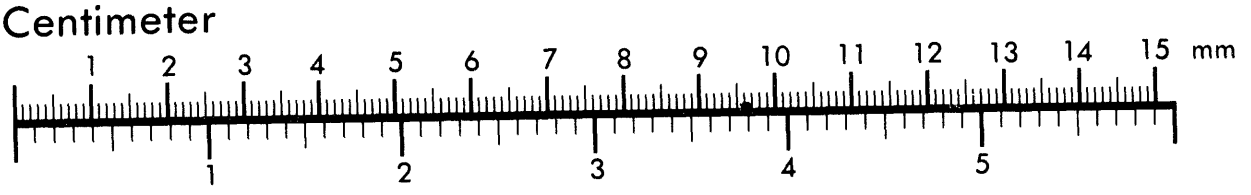
AIIM

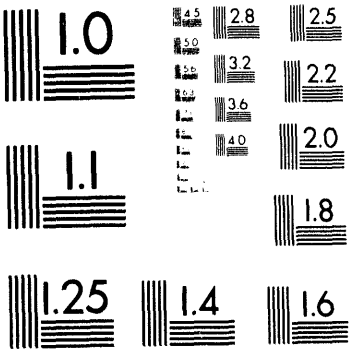
Association for Information and Image Management

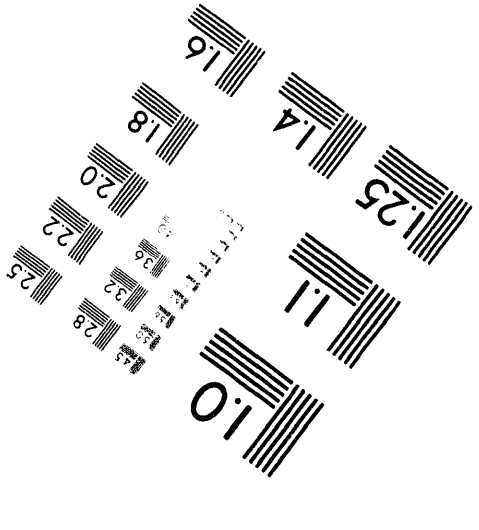
1100 Wayne Avenue, Suite 1100
Silver Spring, Maryland 20910

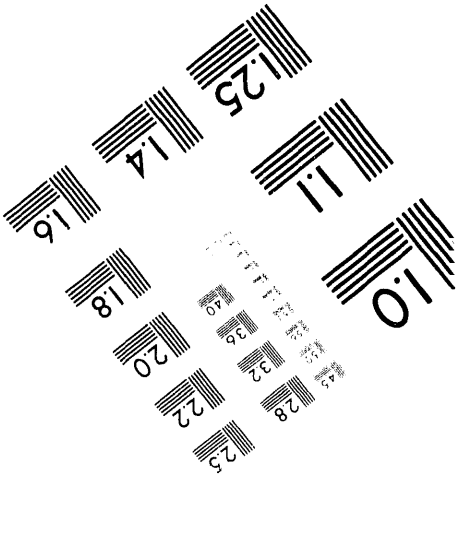
301/587-8202











MANUFACTURED TO AIIM STANDARDS
BY APPLIED IMAGE, INC.

3 of 3

from other gases.

BACKGROUND INFORMATION

Membranes that operate at temperatures higher than 100°C and still possess suitable selectivity and last for a few hundred to a few thousand hours are rare. However, the benefit of performing the separation at reactor temperatures in terms of energy cost, capital cost, and process simplicity has led many to work on developing such membranes. The high temperature membranes we are developing can be used to replace the current low-temperature unit operations for separating gaseous mixtures, especially hydrogen, from the products of the water gas shift reaction at high temperatures. Membranes that have a high selectivity and have both thermal and chemical stability would improve substantially the economics of the coal gasification process. These membranes can also improve other industrial processes such as the ammonia production and oil reform processes where hydrogen separation is crucial.

PROJECT DESCRIPTION

Our CMS membrane is composed of a thin layer of a size selective CMS supported by a microporous ceramic support. The separation of hydrogen from other gases is by a molecular sieving mechanism where the smaller hydrogen molecules (2.96Å) would pass through the pores while the larger molecules such as N_2, CO, and CH_4 are prevented from passing through.

The ceramic support is a fiber reinforced ceramic composite prepared from AlliedSignal's proprietary Blackglas™ resin. The reinforcing fibers can be carbon, glass, ceramic, or metal depending on the end use temperature. The Blackglas material in its resin form can be processed using the conventional polymer processing techniques such as lamination, infiltration, hot molding, casting, and injection molding. We have used hot molding, lamination, and infiltration techniques to make the fiber reinforced ceramic composite support. The Blackglas ceramic support has the potential for high temperature strength/stability with ease of fabrication because of the demonstrated chemical and thermal stability of Blackglas. The coefficient of thermal expansion of the support matches closely that of CMS. Such close match insures mechanical integrity and adhesion when the membrane is subjected to thermal cycles.

The CMS membrane is produced by controlled pyrolysis of polymeric precursors on the surface or in the pores of the support. Alternatively, a free standing CMS film can be made without the support and combined with a support structure in a later stage to form the membrane. The pore size of the CMS membrane can be modified by post-treatments.

The composite membrane will be tested for its permeation properties at 550°C or higher. Thermal, mechanical and chemical stability of the membrane will be assessed.

RESULTS

Supported Membrane

We have produced fiber reinforced ceramic microporous supports from Blackglas™ resin and carbon, glass, and ceramic fibers. The polymer composite is converted to a ceramic composite by pyrolysis under inert atmosphere (nitrogen). Repeated infiltration and pyrolysis steps are used to increase the density and decrease the porosity of the support. The resulting supports are tested for mechanical strength, pore size and pore size distribution at room temperature. The results are summarized in Tables 1 and 2.

Sample #	YIELD STRESS (psi)	YIELD STRAIN (%)	Modulus (psi)
1	1457	0.36	500500
2	3163	0.39	1031000
3	3709	0.29	1482000
4	5640	0.33	1984000

Table 1. Flexural Test Results

Sample #	MEDIAN PORE DIAMETER (μm)	POROSITY (%)
1	2.4077	23.8
2	1.1787	13.79
3	0.6216	7.02
4	0.2596	3.62

Table 2. Mercury Intrusion Results

The stress and strain results shown in Table 1 suggest that the supports are not only strong but also non-brittle as indicated by the yield strain of 0.3 to 0.4%. The pore size of the supports can also be changed to suit our needs as shown by the results presented in Table 2. The pore size distribution of the support is narrow.

SEM micrography of the porous ceramic support structure shows that the pores are formed by microcracks in the composite matrix. These microcracks come from the shrinkage associated with the pyrolysis of Blackglas resin. Thus, the pores generally have an elongated slit structure. Other pore size controlling techniques can also be used to modify the pore size and pore structure of the support.

We have also measured the flow rate of nitrogen through the support at room temperature. The results are given in Figure 1. This figure shows that the resistance of the support to gas flow is small even at room temperatures and that the flow rate is a function of the support pore size.

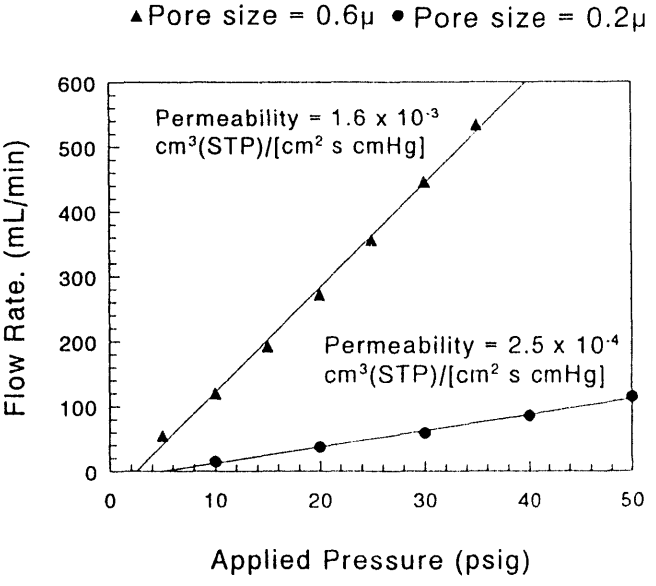


Figure 1. Nitrogen Flow Rate Through Porous Blackglas Supports

Our CMS membranes are prepared by a coating method where a CMS precursor polymer solution is coated on the microporous support and carbonized in nitrogen or helium. Repeated coating may be necessary to eliminate defects and cracks formed during carbonization because of the shrinkage of the polymer coating. The CMS is formed within the pores and on the surface of the porous support.

We have measured the flow rate and selectivity of nitrogen, hydrogen, and methane through the CMS membranes at both room temperature and at elevated temperatures up to 700°C and at pressures up to 60 psig. The results of these measurements are summarized in Figures 2

and 3. These figures show that the flow rate through the membrane (disk shape with effective diameter of 2.5 inches) increases with increasing temperature as expected. The ideal H_2/N_2 and H_2/CH_4 selectivities are not a strong function of temperature, and have values close to the Knudsen diffusion limit. These figures also show that the flux of all gases are high. The ideal selectivities obtained from the current study are comparable to those obtained by Koresh and Sofer [1,2] on un-supported CMS membranes prepared from cellulose material. The ideal selectivities reported are 20 and 8 for He/O_2 and O_2/N_2 before heat treatment and 2.8 and 0.92 after heat treatment, respectively. Hatori et al. [3] have also reported the following ideal selectivities for an unsupported carbon membrane made from Kapton polyimide: He/N_2 = 19.6, He/O_2 = 4.3, and He/CO_2 = 0.4. These results may suggest that the pore size of the current CMS membrane is still too large or simply that there are still defects in the membrane. Recently, SEM has confirmed the presence of micro defects on the surface of the CMS membranes we made. Moreover, the permeabilities of our CMS membrane is about two orders magnitude higher than those reported.

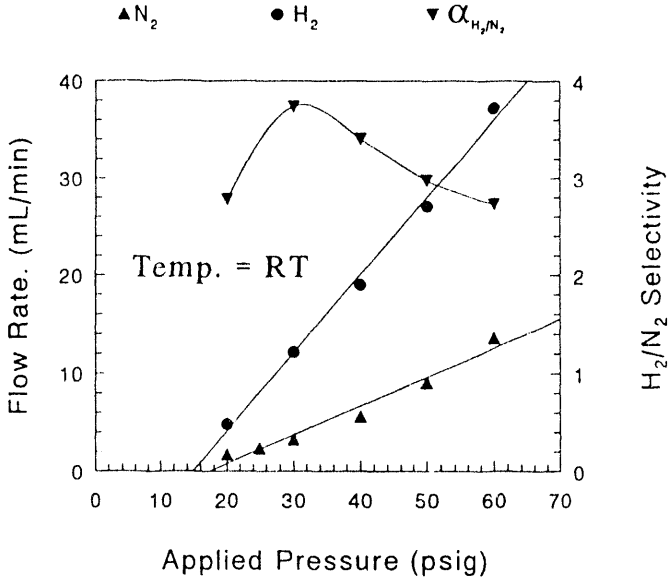


Figure 2. Nitrogen and Hydrogen Flow Rate and Selectivity at Room Temperature

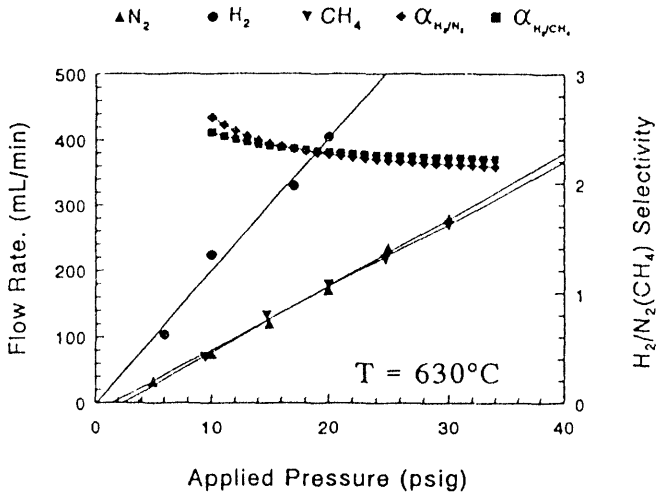


Figure 3. Nitrogen, Methane and Hydrogen Flow Rate and Selectivity at Elevated Temperature

Unsupported Carbon Film

We have developed methods for the carbonization of polymer precursor into continuous, defect-free, hydrogen impermeable, carbon films. During carbonization, the films lose 40% of their precursor weight and the isotropic shrinkage is 20%.

A carbon film prepared from the pyrolysis of 3 mil polymer precursor was sealed in epoxy and placed in a membrane test cell. A pressure of 320 psig of hydrogen was applied to one side of the membrane and a pressure of 290 psig of argon was applied to the other side. The static gas pressures were blocked off and allowed to remain for two hours. At the end of two hours the argon was collected and analyzed by gas chromatography for hydrogen. No hydrogen was observed and the limits of detection of the method used were 1000 ppm, which means that the maximum possible flux constant could not have exceeded about $2x10^{-10}$ [cm^3(STP) cm]/[cm^2 s cmHg]. In a similar experiment, a 5 mil film was configured such that a differential pressure of 60 psig of hydrogen was

applied to one side and allowed to stand for several hours. Flux exceeding 10^{-11} [cm^3(STP) cm]/[cm^2 s cmHg] was not observed.

We have developed a method for determining the B.E.T. surface area of materials using hydrogen as a probe gas at 19.7 K. The development of the hydrogen B.E.T. method resulted in part from recent developments in temperature control at the condensation temperature of hydrogen using a Janis Research Super Varitemp cryostat. The recently developed hydrogen B.E.T. method can be used in conjunction with the existing and well-established carbon dioxide B.E.T. method. By using both methods, we can directly compare the properties of surface interaction such as surface adsorption between hydrogen and carbon dioxide, the gases of principal interest in this project. In particular, we can study the effects of varying carbonization and activation conditions on the pore structure and it influence on the adsorption of the gases onto the carbon material. The ability to make direct comparisons between the two gases is a tool we can use to tune the pore structure and adsorption properties through variations in our synthetic procedures. Figure 4 shows a pore-size distribution determined with carbon dioxide as probe gas.

Surface areas depend on carbonization and activation. Variations in carbonization conditions can be used to control pore size and median pore diameter from 4.2 to 5.1 Å and pore volumes up to 0.20 cm^3/g. Surface areas as high as 400 m^2/g have been measured. The thickness of the polymer film influences the surface area. In particular, the thicker the polymer film, the lower the overall surface area. These observations strongly suggest that an impermeable, non-porous "dead" layer exists within the film. The overall composition of the film may be such that porosity exists in a higher concentration near the surface of the film. We anticipate that development of thinner carbon films may produce a hydrogen permeable material since a thinner film would have less or no dead layer material. Figure 5 shows the measured surface area as a function of precursor film thickness for both hydrogen and carbon dioxide probe gases. Also, activation has been shown to increase the surface adsorption selectively in such a way that the hydrogen pore volume (cc/g) increased from 0.10 to 0.19 but the carbon dioxide pore volume increased from 0.15 to 0.18.

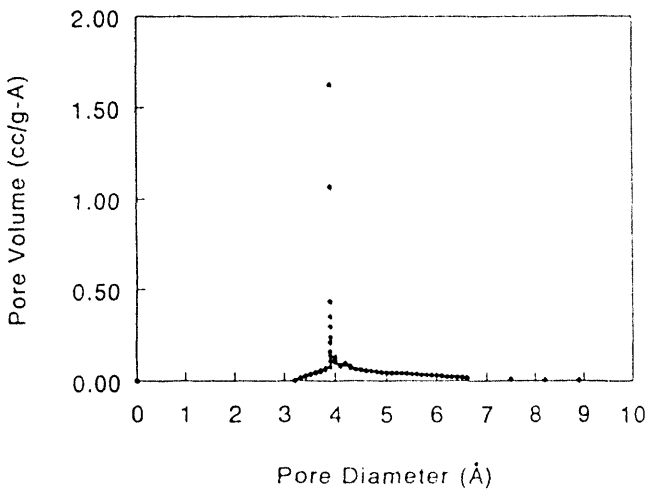


Figure 4. Pore-size Distribution of CMS Film Using CO_2 as Probe Gas

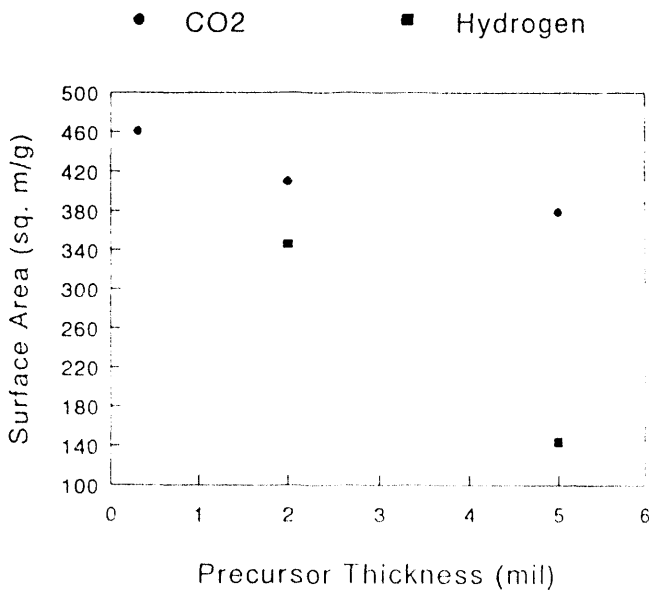


Figure 5. Surface Area vs. Precursor Thickness

FUTURE WORK

We are working on eliminating the micro defects on the CMS membrane surface to improve selectivity using several techniques. We are also putting efforts into making the CMS membrane just inside the pore mouth of the support, such that the CMS is constrained within the pores, eliminating any possible defects from the fabrication process and from late thermal cycling. The membranes made will be tested at high temperatures for gas permeability and selectivity. The surfaces and the interior of the membrane will also be examined by an SEM method to better understand the development of defects and ways of eliminating them. In addition to obtaining membrane permeabilities for the various gases, we will obtain information on the stability of the membrane for extended hours of operation at elevated temperatures in the reducing environment of the gases.

ACKNOWLEDGEMENT

The authors wish to thank Damyanti Patel for her efforts in performing the work discussed in this paper, Hayuta Zaffrir for her help in preparing and studying the porous supports. We also wish to express our thanks to Dr. Stephen Yates for his support and Dr. Xavier Pillai for his work on setting up the test rig and initial work on the CMS. Thanks are also due to the authors' colleagues Drs. Brian Bedwell, Robert Sedath, and Li Wang for many of their invaluable suggestions and discussions.

REFERENCES

1. J. E. Koresh and A. Sofer, "Molecular Sieve Carbon Permeselective Membrane. Part I. Presentation of a New Device for Gas Mixture Separation." **Sep. Sci. Technol., 18,** 723-734 (1983).

2. J. E. Koresh and A. Sofer, "Mechanism of Permeation through Molecular-Sieve Carbon Membrane," **J. Chem. Soc., Faraday Trans. 1, 82,** 2057-2063 (1986).

3. H. Hatori et al., "Carbon Molecular Sieve Film from Polyimide," **Carbon, 30,** 719-720 (1992).

9b.2 A Catalytic Membrane Reactor for Facilitating the Water-Gas Shift Reaction at High Temperature

CONTRACT INFORMATION

Contract Number DE-FG03-91ER81229

Contractor

Bend Research, Inc.
64550 Research Road
Bend, OR 97701-8599
(503) 382-4100

Contract Project Manager David J. Edlund

Principal Investigators David J. Edlund

METC Project Manager Venkat K. Venkataraman

Period of Performance March 31, 1992 to March 30, 1995

Schedule and Milestones

FY94 Program Schedule

J	J	A	S	O	N	D	J	F	M	A	M
Conduct Parametric Tests											
	Conduct Slip-Stream Tests										
		Construct Computer Model of Process									
					Evaluate Process Economics						
									Prepare Final Report		

OBJECTIVES

This program is directed toward the development of a metal-membrane-based process for the economical production of hydrogen at elevated temperature by the reaction of carbon monoxide with steam—i.e., the water-gas shift (WGS) reaction. Key to achieving this objective is the development of an inexpensive and durable metal-membrane module. The specific program objectives include the following:

- design, fabrication, and demonstration of prototype membrane modules;
- improving the membrane composition to increase the hydrogen flux;
- demonstrating that membrane lifetime ≥2 years is likely to be achieved; and
- conducting engineering and economic analyses of the process.

BACKGROUND INFORMATION

Currently, the gasification of coal incorporates conventional high- and low-temperature WGS reactors for the production of hydrogen, valued as a chemical feedstock (Figure 1). The cost and complexity of the conventional gas-processing technology, with associated heat exchangers and acid-gas scrubbers, has given rise to research directed at developing a more-efficient and less-expensive process.

PROJECT DESCRIPTION

The Proposed Membrane-Based Process

The proposed membrane-reactor process for producing hydrogen via the WGS reaction at elevated temperature is shown in Figure 2. This process is based on the principle that an equilibrium-limited reaction can be driven toward complete conversion of reactants to products if one of the products is removed from the reactor as it is formed. This operating characteristic of membrane reactors has led to numerous investigations of membrane reactors for a wide range of applications, in addition to facilitating the WGS reaction (Hsieh, 1991; Shu et al., 1991; Armor, 1989)

Essential to the successful development of this process is an affordable, durable, highly-selective membrane. A composite-metal membrane under development at Bend Research promises to meet these requirements. The composite-metal membrane (Figure 3) utilizes a coating-metal layer that is permselective for hydrogen, rejecting all other feed-stream components. The mechanical-support layer prevents the membrane from rupturing under high transmembrane pressures, and the intermediate-oxide layer prevents intermetallic diffusion between the coating-metal layer and the mechanical-support layer. Intermetallic diffusion between these layers leads to rapid flux decline and shortened membrane lifetime.

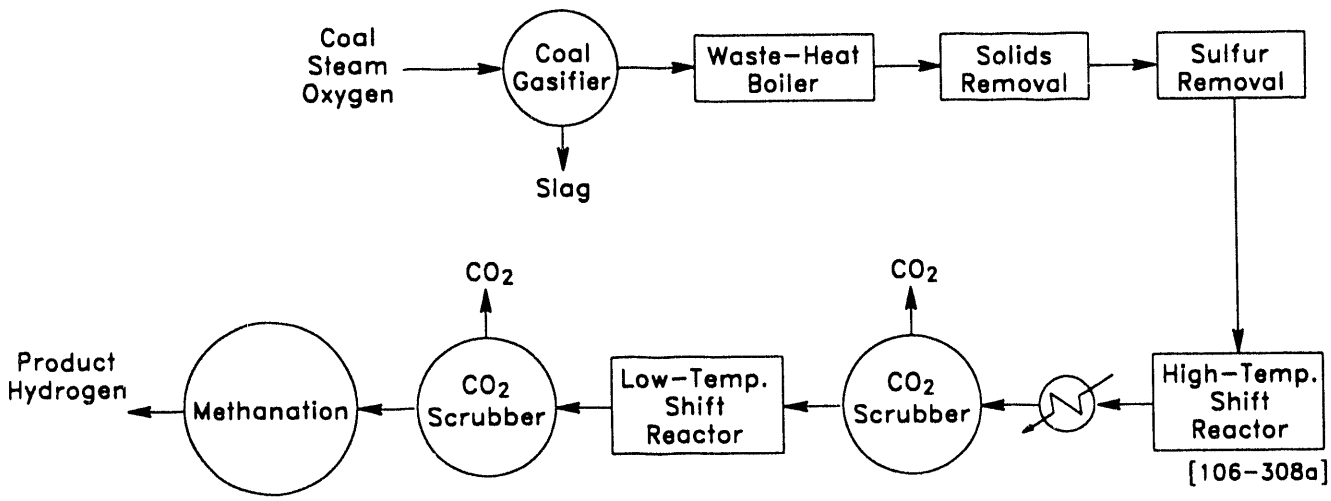


Figure 1. Conventional Process Scheme for the Production of Hydrogen

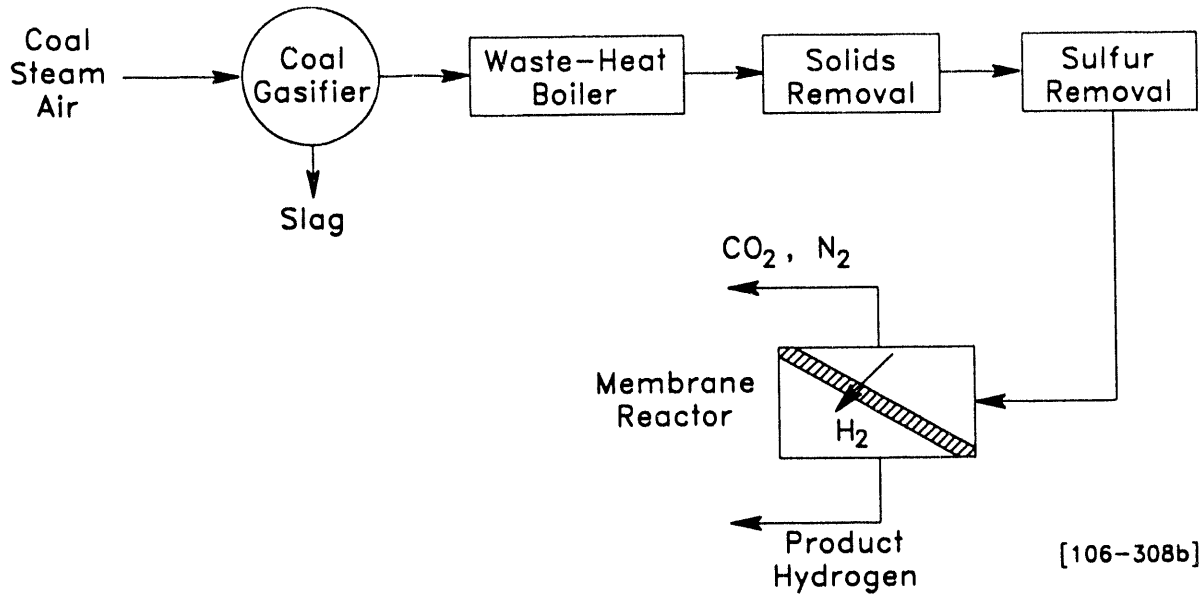


Figure 2. Proposed Membrane-Reactor Process For The Production Of Hydrogen

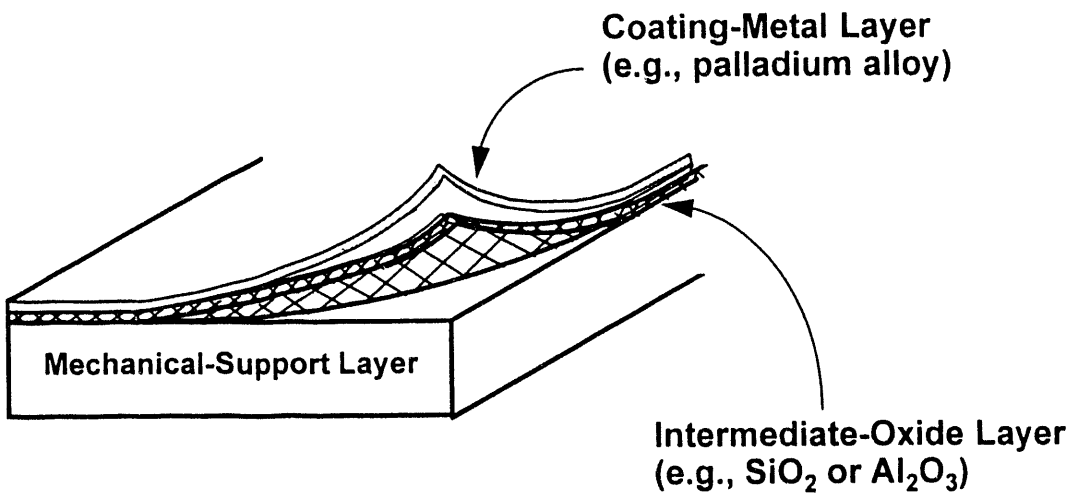


Figure 3. Key Elements Of The Bend Research Composite-Metal Membrane

The membrane composition shown in Figure 3 is sensitive to poisoning by sulfur compounds. Therefore, an absorbent bed prior to the membrane reactor will be necessary to remove sulfur compounds from the feed stream. However, since the membrane only permeates hydrogen, the gasifier can be air-blown without adversely affecting the hydrogen purity.

Hydrogen Production in a Membrane Reactor

We have previously demonstrated that the WGS reaction is driven toward completion in a small, laboratory-scale membrane reactor incorporating the Bend Research composite-metal membrane (Edlund, 1991). Greater than 90% conversion to hydrogen was achieved in these

initial experiments using a 2:1 steam:carbon monoxide ratio at 235 psia and 700°C (Figure 4).

As expected, the overall rate of conversion decreases with decreasing pressure (Figure 4) since both the chemical-reaction rate and the rate of hydrogen transport across the membrane are decreased at lower feed pressures.

The reaction time required to achieve maximum conversion shown in Figure 4 are relatively long, as no shift catalyst was used in these experiments (the rate of the non-catalyzed gas-phase WGS reaction is relatively slow even at 700°C). Incorporating a commercial shift catalyst (e.g., Haldor Topsoe SK-201) at the feed side of the membrane is expected to increase the overall rate of conversion significantly. Additional improvements in the process design might include multiple membrane stages and/or a condensable sweep stream (such as steam) over the permeate side of the membrane to achieve ≥95% hydrogen recovery while maintaining moderate permeate pressure (several atmospheres).

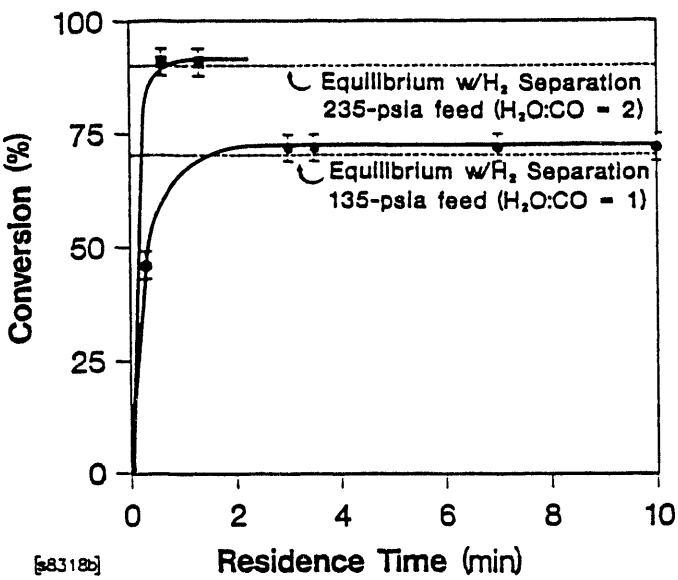


Figure 4. Conversion Versus Residence Time at 700°C in a Laboratory-Scale Membrane Reactor

RESULTS

Work in this program has focused on the first three program objectives listed above. Specifically, the following primary results have been obtained:

- Prototype plate-and-frame membrane modules containing up to 0.4 ft^2 of membrane have been designed, fabricated, and operated for up to 3 weeks. This represents a scale-up factor of about 100-fold relative to the laboratory-scale membrane samples that had been the focus of our testing. A patent application on the module design is being filed. The projected selling price of membrane modules is expected to be about \$275/ft^2.
- The membrane composition has been improved, resulting in a several-fold increase in hydrogen flux versus that obtained using earlier-generation membranes, while the overall cost of membrane materials has decreased seven-fold. Thus, the current-generation membrane delivers a hydrogen flux of 150 SCFH/ft^2 at 400°C and 100-psig hydrogen feed pressure, and 210 SCFH/ft^2 at 400°C and 100-psig hydrogen feed pressure.
- Small, laboratory-scale membranes have been operated for 6 months at 500°C without showing any flux decline, indicating that operational lifetimes of ≥2 years are likely to be achieved.

In addition, we have begun a collaboration with Teledyne Wah Chang (Albany, OR) to develop and market metal-membrane modules for a wide range of applications. It is anticipated that Teledyne Wah Chang will become the exclusive manufacturer of the membrane modules.

FUTURE WORK

We expect that the relatively high flux and low cost of the composite-metal membrane modules will lead to favorable process economics for producing hydrogen from coal. During the next year we will work toward completing an economic analysis of the membrane-reactor process. Parametric studies of conducting the WGS reaction within the membrane reactor will be completed. In these studies the prototype plate-and-frame modules will be used and a commercial shift catalyst will be placed within the reactor at the feed side of the membrane to ensure rapid chemical kinetics.

The parametric studies will be designed to determine the overall rate of conversion of reactants to hydrogen and carbon dioxide over a range of operating conditions. Furthermore, we will determine whether the catalyzed reaction kinetics or the rate of hydrogen removal from the feed side of the reactor is rate-limiting (the rate-limiting factor may vary with changing operating conditions). This information will serve as the basis for the design and optimization of the process.

Concurrent with the parametric studies, we plan to conduct a field test on a research-gasifier slip-stream in collaboration with the University of North Dakota Energy & Environmental Research Center.

REFERENCES

Armor, J.N., "Catalysis With Permselective Inorganic Membranes," *Applied Catal.*, 49(1989)1-25.

Edlund, D.J. et al., A Catalytic Membrane Reactor for Facilitating the Water-Gas Shift Reaction at High Temperature. Phase I Final Report to the U.S. Department of Energy, Grant No. DE-FG03-91ER81229, from Bend Research, Inc., 1992.

Hsieh, H.P., "Inorganic Membrane Reactors," *Catal. Rev.--Sci. Eng.*, 33(1991)1-70.

Shu, J. et al., "Catalytic Palladium-Based Membrane Reactors: A Review," *Canadian J. Chem. Eng.*, 69(1991)1036-1060.

DJE/jac
031:METC-PAP

9b.3 New Developments in Hydrogen Permselective Membranes

CONTRACT INFORMATION

Contract Number	DE-AC21-90MC26365
Contractor	California Institute of Technology 1201 E. California Blvd. Pasadena, CA 91125 (818) 395-6357
Contractor Project Manager	George R. Gavalas
Principal Investigator	George R. Gavalas
METC Project Manager	Richard A. Johnson Venkat K. Venkataraman
Period of Performance	January 9, 1990 to November 8, 1992

OBJECTIVES

The objectives of the original project was to develop silica hydrogen permselective membranes and evaluate the economic feasibility of these membranes in hydrogen production from coal gas. The objectives of the work reported here were to increase the membrane permeance by developing new precursors or deposition conditions, and to carry out fundamental permeability measurements of the membrane at different stages of pore narrowing.

BACKGROUND INFORMATION

In the work performed under the above referenced METC contract[1-3], the contractor developed hydrogen permselective membranes by chemical vapor deposition (CVD) of thin SiO_2 layers within the pores of Vycor tubes having mean pore diameter about 40 Å. The hydrogen permeance after CVD was about 0.35 cm^3/cm^2-min-atm versus about 0.5 for the original tube, both at 500°C, so that the resistance due to the deposit layer was 30% of the total resistance. To test their stability under conditions simulating the expected operating conditions in coal gas processing, the membrane tubes were heated under 3 atm of water vapor (and 7 atm N_2) at 550°C for up to 21 days. During this hydrothermal treatment the hydrogen permeance declined and stabilized to a value about 0.1 cm^3/cm^2-min-atm at 500°C. The stable membrane permeance represented 80% of the total resistance to hydrogen permeation. The H_2:N_2 selectivity after the hydrothermal treatment was in the range 500-1000.

To evaluate the economic feasibility of the silica membranes, KTI Inc. under subcontract to Caltech conducted a case study of an ammonia-from-coal process comparing a conventional process with a membrane-assisted process[2]. In the conventional process the coal gas was treated by catalytic water gas shift reaction followed by hydrogen separation by pressure swing adsorption (PSA). In the membrane-assisted process, hydrogen was separated simultaneously with the catalytic shift reaction, resulting in reduced consumption of steam and elimination of PSA. Although accurate capital costs for the hydrogen membrane were not available, approximate

estimates suggested that the membrane-assisted process would become competitive if the membrane permeance was increased from the then available 0.1 cm^3/cm^2-min-atm value to 0.3 cm^3/cm^2-min-atm.

In view of the results of the economic evaluation, a new project was undertaken to increase the hydrogen permeance of the silica membranes. This new project was supported by the DOE University Coal Research Program and by funds from internal Caltech sources (Gates-Grubstake Fund).

The obvious way to increase membrane permeance was to decrease the thickness of the silica deposit layer which represented about 80% of the resistance to permeation. The layer thickness depends on the penetration depth of the silica precursor within the pores of the tube wall. One way to decrease the penetration depth is to use silica precursors of higher reactivity. In our previous studies we used the silica precursors $SiCl_4$, $Cl_3SiOSiCl_3$, $Cl_3SiOSiCl_2OSiCl_3$. A literature survey revealed that one of the most reactive agents for liquid phase silylation is trimethylsilyl triflate ($(CH_3)_3SiOSO_2CF_3$). To grow a SiO_2 layer one would need to use the chloride analog $Cl_3SiOSO_2CF_3$. To this end we synthesized this analog and measured the reaction rate with Vycor glass in a thermogravimetric analyzer (TGA). It turned out that the reaction was too slow compared with the reactions of $SiCl_4$ and the other silylating compounds used previously. Evidently, reaction of the gaseous reagent with the pore surface is sterically hindered and also lacks the stabilization of the transition state afforded by the solvent in liquid phase reaction.

In view of the negative results the emphasis on different silica precursors was abandoned in favor of exploring different deposition conditions. The first modification was to use alternating rather than simultaneous reaction with $SiCl_4$ and H_2O. The second modification was to introduce carbon masks as means of decreasing the reactant penetration depth. These two techniques, and particularly the second one, resulted in dramatic improvements of membrane permeance as will be described in the following sections.

PROJECT DESCRIPTION

Alternating Reactants Deposition

Our previous membrane preparations[1-3] were carried out by one-sided CVD of SiO_2 on porous Vycor tubes using $SiCl_4$ (or some other related compound) and H_2O as the reactants. This standard deposition technique suffers from two disadvantages. The first is the development of nonuniform deposit layer thickness caused by depletion of $SiCl_4$ in the direction of flow. The second is formation of small clusters or particles in the gas phase by the direct reaction between $SiCl_4$ and H_2O, and subsequent deposition of these particles on the external surface of the support, causing additional thickening of the deposit layer. To avoid those two drawbacks of one-sided CVD we introduced the alternating reactants CVD. This new technique of membrane deposition entails two elements. The first element is the alternating rather than simultaneous contact of the support with the two reactants. The alternating contact completely eliminates formation of particles by gas phase reaction. The second element is the introduction of $SiCl_4$ into the evacuated reactor volume in discrete dosages rather than in continuous flow. Introduction of $SiCl_4$ into the evacuated volume eliminates or greatly reduces deposit layer nonuniformities. At the same time, limiting the dosage of $SiCl_4$ introduced in each cycle, reduces the penetration depth into the support.

The deposition reactor has been described in earlier publications. Briefly, it consists of an external quartz tube (11 mm ID) surrounding a concentrically placed porous Vycor tube (7 mm OD, 4.8 mm ID, 40 Å mean pore diameter) welded on both sections with nonporous quartz sections for convenient connection with inlet and outlet flows. The reactor is placed inside a split-tube electrical furnace. The reactant streams $SiCl_4$-N_2 and H_2O-N_2 were generated in bubblers at controlled temperatures. The $SiCl_4$-N_2 stream was stored in a large storage flask from which it was admitted intermittently into the reactor.

A membrane deposition experiment consisted of several consecutive silylation-hydrolysis cycles at reaction temperature 700-800°C. Each cycle entailed evacuating the reactor, admitting a dosage of $SiCl_4$-N_2 (the dosage being controlled by the

mol fraction of $SiCl_4$ in the storage flask) and allowing it to react for 1 minute, evacuating the reactor, and finally passing continuously a stream of H_2O-N_2 for 5 minutes. After each cycle, the permeance of N_2 was measured and when that permeance dropped below a preassigned level (lower by a factor 30-100 than the initial permeance), the deposition was terminated and the permeance of H_2 and N_2 were measured at several temperatures.

Selected membrane tubes were annealed at 500°C under 3 atm of H_2O (and 7 atm N_2) for several days to test their stability under expected operating conditions. After the hydrothermal treatment, the permeance of H_2 and N_2 were measured once more at several temperatures.

CVD Assisted by Carbon Barriers

A new technique developed in this project is the use of temporary carbon barriers to reduce the thickness of the deposit layer. The technique of carbon barriers involves first forming a thermosetting polymer inside the pores of the support, carbonizing the polymer, conducting SiO_2 deposition by one-sided or alternating CVD, and finally removing the carbon barrier by oxidation.

The polymer selected for these experiments was polyfurfuryl alcohol (PFA) which upon carbonization is known to undergo about 40% weight loss. The polymer was formed by polymerization of the furfuryl alcohol monomer (FA) using para-toluene sulfonic acid as the polymerization catalyst. After polymerization and cross-linking at 100°C for 24 hours, the support tube was heated slowly to 600°C to prepare it for CVD. Silica CVD was carried out by alternating deposition as described in the previous subsection. Finally, the carbon barrier was removed by oxidation with pure oxygen at 600°C for 18 hours. The permeance of H_2 and N_2 were measured after carbon deposition, after CVD and after the final oxidation step.

RESULTS

Alternating Deposition

Figure 1 shows the evolution of hydrogen and nitrogen permeance (based on the external diameter of the support tube) of two membranes formed by alternating CVD, one at 700°C and the other at 800°C. In each case the permeances were measured at the deposition temperature. Membrane 2 which was prepared at 800°C required a smaller number of cycles, had higher H_2:N_2 selectivity but somewhat lower H_2 permeance. These results can be attributed to a thinner but denser deposit layer at 800°C.

The two membranes shown in Figure 2 were heated at 500°C under 3 atm of H_2O (and 7 atm of N_2) for two weeks. Table 1 shows the change in the hydrogen and nitrogen permeances during this treatment. Table 2 shows the results of the same hydrothermal treatment in terms of the net permeance of the deposit layer, i.e. after subtracting the resistance of the bare support tube. Hydrothermal treatment decreases the permeances of the deposit layer by about 10% at 700°C and 50% at 450°C. The dependence of the reduction factor on temperature is due to the fact that hydrothermal treatment increases the activation energy. It is also seen that the membrane prepared at 800°C undergoes a slightly smaller change during hydrothermal treatment. These differences become more clear by looking at the activation energies for hydrogen permeation shown in Table 3. After deposition, membrane 2 has activation energy of 20.1 kJ/mol versus 17.3 of membrane 1. During hydrothermal treatment, however, the activation energy of both membranes increases and reaches a common level of 26 kJ/mol.

Comparison of the permeances shown in Tables 1-3 with the permeances of membranes prepared in our previous work by one-sided deposition reveals the following differences. The layers deposited by alternating reactants CVD have higher activation energies (17-20 kJ/mol vs. 10-12 kJ/mol) but approximately equal hydrogen permeances implying that the layers are thinner and denser. Upon hydrothermal treatment all layers are densified to the same final state with activation energy about 26 kJ/mol. As a result of this

densification, the permeance (at 600 K) declines by a factor 1.6 to 1.9 for the layers prepared by alternating deposition. The decline factor for the layers prepared by one-sided deposition is much higher, about 15. These large differences refer to the permeance of the deposit layer. The differences are much smaller for the permeance of the whole membrane tube because of the significant resistance of the support.

CVD Assisted by Carbon Barriers

Table 4 shows the H_2-permeance of a membrane prepared with the help of carbon barriers. The permeance for the whole tube and the net permeance of the deposit layer are listed. The activation energy for the permeance of the deposit layer is about 26 kJ/mol, essentially the same as that of layers prepared by one-sided deposition. Table 5 compares the permeance of layers prepared with and without the help of carbon barriers. Using the carbon barriers increases the deposit layer permeance by a factor of about 5.

FUTURE WORK

The practical result of using alternating deposition and carbon barriers is to increase the hydrogen permeance of the deposit layer by a factor of about 20 over the permeances obtained in our previous work. At 600 K the resistance to permeation due to the deposit layer is only 12% of the overall resistance, with 88% of the resistance residing on the support tube. To fully exploit the increased permeance of the deposit layer it is essential to use support tubes of lower resistance. One possibility is to use Vycor tubes of the same pore size as in the reported experiments but having smaller diameter and wall thickness. Reducing the wall thickness from 1.1 mm to 0.4 mm (corresponding to tubes with 0.2 mm ID) would increase the overall hydrogen permeance at 500 K from 0.68 to 1.26 $cm^3/cm^2/min$-atm, based on the inside diameter of the tube. Using as supports composite mesoporous/macroporous tubes like the ones marketed by US Filter, the overall permeance at 500 K can be increased to about 3.8 cm^3/cm^2-min-atm. These higher permeances are well above the economic viability threshold identified in the background section.

A number of issues need to be addressed in future work to demonstrate the commercial feasibility of the silica membranes. A critical need is the development of technology for fabrication of multitube modules. It is also important to demonstrate the preparation techniques using as supports smaller diameter Vycor tubes or composite mesoporous/macroporous tubes. Finally, the membranes should be tested for stability over longer periods of time.

REFERENCES

1. Tsapatsis, M., S. J. Kim, S. W. Nam and G. R. Gavalas. 1991. Synthesis of Hydrogen Permselective SiO_2, TiO_2, Al_2O_3, B_2O_3 Membranes from the Chloride Precursors. *IEC Research*, **30**, 2152-2159.

2. Gavalas, G. R. 1993. Hydrogen Separation by Ceramic Membranes in Coal Gasification, DOE/METC DE-AC21-90MC26365, Final Report.

3. Tsapatsis, M. and G. R. Gavalas. 1994. Structure and Aging Characteristics of Silica Membranes Prepared by CVD. *J. Membr. Sci.*, **87**, 281-296.

Table 1. Permeance of Membranes Deposited on the Inner Surface Before and After Hydrothermal Treatment for 15 Days at 550°C under 3 atm H_2 and 7 atm N_2. The Dosage of $SiCl_4$ per Cycle was 0.28 μmol/cm^2.

	Reaction T (°C)	Measurement T (°C)	Permeance (cm^3(STP)/min atm cm^2) After Deposition N_2	After Deposition H_2	After Treatment N_2	After Treatment H_2
Membrane 1	700	700	0.0039	0.38	0.00042	0.33
		600	0.0036	0.37	0.00015	0.30
		450	0.0019	0.33	0.000094	0.21
Membrane 2	800	800	0.0013	0.37	0.00033	0.34
		600	0.00046	0.34	0.00018	0.28
		450	0.00020	0.28	0.00015	0.19

Table 2. Permeance of Deposit Layers Excluding the Resistance of Vycor Tube. The Permeance is Given After Deposition and After 15 Days at 550°C under 3 atm H_2 and 7 atm N_2.

	Reaction T (°C)	Measurement T (°C)	Permeance (cm^3(STP)/min atm cm^2) After Deposition N_2	After Deposition H_2	After Treatment N_2	After Treatment H_2
Membrane 1	700	700	0.0041	1.74	0.00042	1.04
		600	0.0037	1.33	0.00015	0.70
		450	0.0019	0.82	0.000094	0.34
Membrane 2	800	800	0.0013	1.65	0.00033	1.16
		600	0.00046	0.99	0.00018	0.63
		450	0.00020	0.56	0.00015	0.29

Table 3. Activation Energy for H_2 Permeance of the Deposit Layers in Membranes 1 and 2 Before and After Hydrothermal Treatments for 15 Days at 500°C under 3 atm H_2O and 7 atm N_2

	Activation Energy (kJ/mol)	
	After Deposition	After Treatment
Membrane 1	17.3	25.8
Membrane 2	20.1	25.8

Table 4. Hydrogen Permeance of a Silica Membrane Prepared With Alternating CVD and Carbon Barrier With and Without the Resistance of the Support Tube

	H_2 Permeance, cm^3(STP)/cm^2-min-atm		
Temperature, °C	Support Tube Plus Deposit Layer	Support Tube	Deposit Layer
450	0.667	0.867	2.90
523	0.679	0.824	3.85
600	0.692	0.787	5.75
700	0.687	0.745	8.56

Table 5. Comparison of Deposit Layer Permeances of Membranes Prepared by Alternating CVD With and Without the Use of Carbon Barrier

	H_2 Permeance, cm^3(STP/cm^2-min-atm	
Measurement T °C	Membrane Prepared without Carbon Barrier	Membrane Prepared with Carbon Barrier
450	0.62	1.88
600	1.13	3.74
700	1.57	5.57

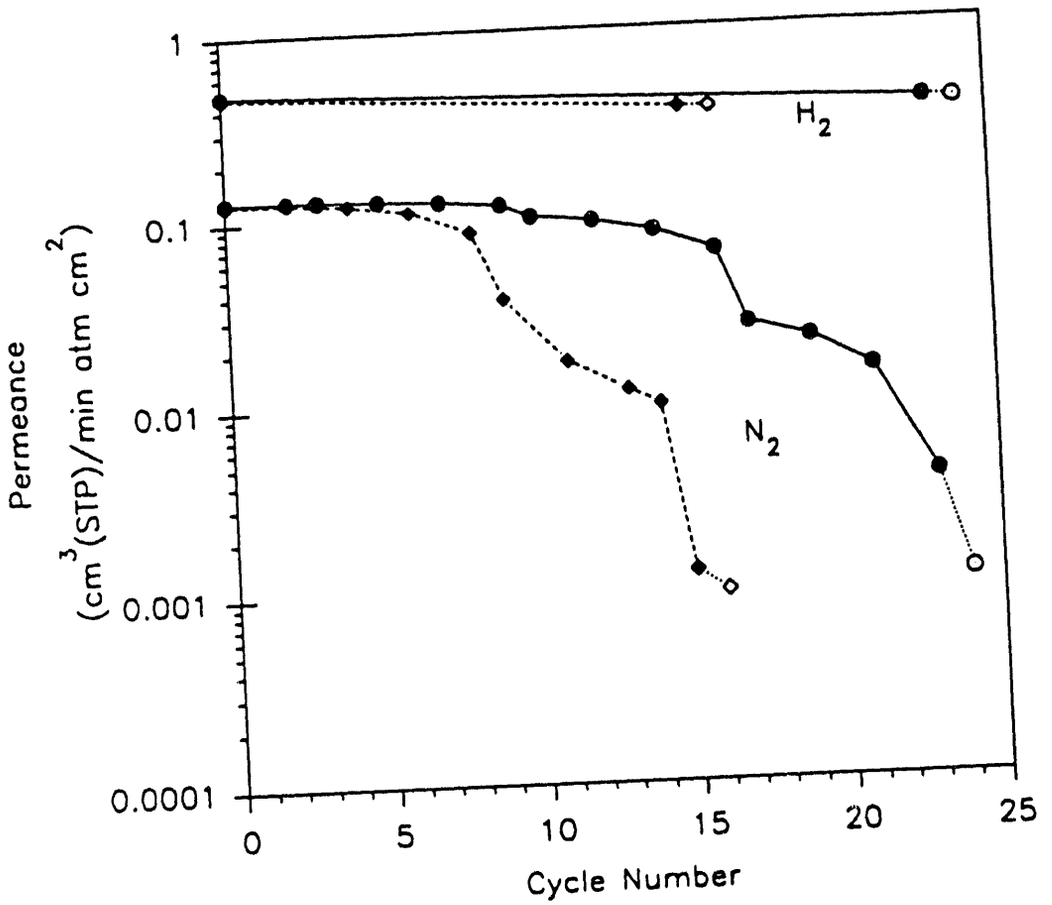


Figure 1. Permeances of H_2 and N_2 Versus Cycle Number for the Reaction at 700°C (Membrane 1. •) and 800°C (Membrane 2. ♦). Using $SiCl_4$ Dosage of 0.28 μmol/cm^2 per cycle. (◊) and (o) Indicate the Permeance Changes After 5 Days of Hydrothermal Treatment at 500°C under 3 atm H_2O and 7 atm of N_2.

9b.4 Preparation and Characterization of Composite Membrane for High Temperature Gas Separation

CONTRACT INFORMATION

Contract Number	DE-FG22-93MT93008
Contractor	North Carolina A&T State University Office of Research Administration Suite 305, Dowdy Administration Building Greensboro, NC 27411 (910) 334-7995
Contractor Project Manager	Shamsuddin Ilias
Principal Investigators	Shamsuddin Ilias Franklin G. King Nan Su
METC Project Manager	Venkat K. Venkataraman
Period of Performance	September 01, 1993 to August 31, 1996

OBJECTIVES

To develop a new class of permselective inorganic membranes, we have identified electroless plating as potential a route to deposit a thin metal film on porous substrate. Electroless plating is a controlled autocatalytic deposition of a continuous film on the surface of a substrate by the interaction of a metal salt and a chemical reducing agent. This method can give thin films of metals, alloys and composites on both conducting and nonconducting surfaces. The objective of this project is to develop thin film palladium membranes for separation of hydrogen in high temperature applications. We plan to use electroless plating to deposit thin palladium films on microporous ceramic and silver substrates and then characterize the membrane in terms of permeability and selectivity for gas separation. To accomplish the research objective, the project requires three tasks:

i. Development of a Process for Composite Membrane Fabrication

The work will involve the selection of methods for thin metal/metal-alloy film deposition on inorganic and ceramic microporous substrates. To assure reproducible film, optimization of the electroless deposition will be required. This step will involve determination of the optimum configuration of the plating bath, which consists of studying the effect of

parameters like pH, temperatures, concentrations, type of reducing agent and sensitizing solution on the rate of deposition of the film.

ii. Characterization of Composite Membrane

The work for this task will start with the fabrication of composite membranes. The membranes will be characterized by surface measurements and by evaluation of the physical properties of the composite (film composition by EDAX, film thickness by SEM). The measurements will also include hydrogen gas permeability, steady state diffusion and the effect of thermal cycling.

iii. Development of Theoretical Model For Hydrogen Gas Separation

The work for this task will be to find or develop a suitable model to describe the permeation of hydrogen gas through a thin palladium film on a porous support. Models developed in the literature deal only with the permeation of gases through a metal membrane. These models may or may not be applicable to composite membranes. The applicability of the model will depend on the role of the porous support in permeation of gases. It is well known that the permeability of gases through porous ceramics increases at higher temperatures. However, the behavior of hydrogen permeation through a palladium film is much more complex process. It is believed that the hydrogen molecule dissociates to hydrogen atoms on one side of the membrane, diffuses through the film and reassociates on the other side. A theoretical model will be developed to facilitate prediction and interpretation of data obtained in the permeation experiments. Permeation through the porous substrate will be analyzed in terms of Knudsen and binary gas diffusion as well as surface diffusion. In case of Pd/substrate composites, a model will be developed that accounts for the kinetics of hydrogen diffusion.

BACKGROUND INFORMATION

The development of high temperature membranes to recover hydrogen is a topic of considerable scientific interest. Since coal gasification and several high-temperature industrial processes generate hydrogen as a byproduct, the recovery of hydrogen is of significant commercial importance. Recently, there has been increased interest in developing inorganic and composite membranes for in-situ separation of product hydrogen to achieve equilibrium shift in a catalytic reactor [1]. However, the productivity of these membrane reactors is severely limited by the poor permeability of currently available membranes. Commercially available non-porous membranes are either thick film or thick walled tubes. Since permeability is inversely proportional to film thickness, a thick film membrane acts as a poor perm-separator. Thus, the major challenge lies in developing a permselective thin film, without compromising the integrity of the film. The availability of such a membrane for high temperature applications could open new areas of research in membrane reactor technology and gas separation. The success of membranes in these applications will largely depend on the availability of membranes with acceptable permselectivity and thermal stability. The polymeric membranes currently available are not suitable for high temperature applications (>180 °C) because of their thermal instability. In addition, inorganic membranes (mostly ceramic), although thermally stable, are also unsatisfactory as they lack permselectivity because of their porous nature.

To develop a new class of permselective inorganic membranes, we have identified electroless plating as a potential route to deposit a thin metal film on microporous substrate. Electroless plating is a controlled autocatalytic deposition of continuous film on the surface of a substrate by the interaction of a metal salt and a chemical reducing agent. This method can give thin films of metals, alloys and composites on both conducting and nonconducting surfaces. In this research, we are using electroless plating to deposit thin palladium films on microporous ceramic and silver substrates.

PROJECT DESCRIPTION

Electroless Plating of Ceramic Substrate

Microporous ceramic alumina membranes (6 cm diameter, open porosity 10-15%, average pore size 5 μm from Alfa/Johnson Mathey) were coated with a thin palladium film by electroless plating. Electroless plating is explained by a combination of the cathodic deposition of metal and the anodic oxidation of reductant at the immersion potential. Palladium deposition occurs as the result of the following simultaneous reactions:

Anodic Reaction:

$$N_2H_4 + 4OH^{-1} \rightarrow N_2 + 4H_2O + 4e^-$$

Cathodic Reaction:

$$2Pd[NH_3]_4^{2+} + 4e^- \rightarrow 2Pd^0 + 8NH_3$$

Autocatalytic Reaction:

$$2Pd[NH_3]_4^{2+} + N_2H_4 + 4OH^{-1} \rightarrow 2Pd^0 + N_2 + 4H_2O + 8NH_3$$

Electroless plating is a three step process involving pretreatment of the substrate, sensitization and activation of the substrate surface, and electroless plating. Typical electroless plating bath compositions given in Table 1. In electroless plating, pretreatment of the substrate is essential in order to deposit metals effectively. One of the common procedures is the two-step immersion sequence using an acidic stannous chloride solution followed by an acidic palladium salt solution. The first bath is referred to as the sensitizer (tin chloride solution), while the second bath is referred as the activator (palladium salt solution). The net result of the sequence is the formation of finely-divided palladium nuclei which initiate the autocatalytic plating process. The formation of the palladium metal nuclei is believed to be due to a redox reaction taking place between the adsorbed or absorbed stannous ions on the surface and the palladium ions in the activation solution. The sensitization and activation step can be described by the following reaction:

$$Sn^{2+} + Pd^{2+} \rightarrow Sn^{4+} + Pd^0$$

The sensitization process controls whether the final metallic film is uniform. The composition of the sensitization and activation solutions is given in Table 2.

Membrane Characterization

The membranes will be characterized by measurements and evaluation of physical properties of the composite (film composition by EDAX, film thickness by SEM and a weight gain method).
The measurements will also include permeability and steady state diffusion, and the effect of thermal cycling. A steady-state counter diffusion method, using gas chromatographic analysis, will be used to evaluate the permeability and selectivity of the composite palladium membrane for hydrogen separation. Composite membranes will be characterized by conducting permeability experiments with hydrogen, argon, nitrogen and carbon dioxide. The

membrane characterization work is now in progress.

Model for Hydrogen Permeation

The permeation of hydrogen through a palladium film is a complex process. The process begins with sorption of hydrogen molecules on the film surface and ends with hydrogen desorption from the ceramic substrate. It is believed that the hydrogen molecule dissociates into hydrogen atoms on one side of the film , diffuses through the film and reassociates on the other side [3]. Hydrogen permeation through palladium is thought to be taking place by the following mechanism:

Sorption on the surface → Formation of hydrogen atoms → Diffusion of hydrogen atoms through the lattice → Formation of hydrogen molecules at the other surface → Desorption.

The reaction kinetics of formation of hydrogen atoms from molecules and the reverse reaction are assumed to be very fast. The permeability can be considered as product of solubility and diffusivity. For isothermal, isobaric and plug flow conditions, the permeation rate of hydrogen can be given by [4]:

$$J_H = \frac{\overline{P}_H}{h}\left(p_1^n - p_2^n\right)$$

where J_H is the hydrogen flux, p_1 and p_2 are partial pressures of hydrogen on high and low pressure sides of the permeability cell. $\overline{P}_H$ is the hydrogen permeability at a given temperature and h is the thickness of the palladium film.

If diffusion through the bulk metal is the rate limiting step and hydrogen atoms form an ideal solution in the metal, then Sievert'law hydrogen solubility dependence holds and n is equal to 0.5. The hydrogen flux (J_H) is inversely proportional to the palladium film thickness (h) when the bulk diffusion is the rate limiting step. A value of n greater than 0.5 may result from several factors. For example, when the surface processes influence the permeation rate or when Sievert's law is not followed, a value of n greater than 0.5 may result. Leakage of hydrogen through defects in the metal film or through membrane seals may also increase the value of n.

With increasing temperature, the permeability coefficient increases and usually follows an Arrhenius type equation [5]:

$$\overline{P}_H = A_H \exp\left(-\frac{E}{RT}\right)$$

where A_H is the pre-exponential factor in the Arrhenius relationship for hydrogen permeability and E is the apparent activation energy of composite palladium-ceramic membrane. Here, it is assumed that the n in the hydrogen flux equation is essentially independent of temperature.

The above transport model will be used to facilitate the prediction and interpretation of data obtained in the permeability measurement experiments.

RESULTS

This is a three-year research grant. Currently we are at the first year of the project. Although we have started only recently, several key results have been obtained, including the following:

- Developed a three step procedure for electroless deposition of palladium on

ceramic substrate. The three steps are: (i) preparation of the substrate; (ii) sensitization and activation of substrate; and (iii) electroless plating. Now, we are in a position to coat palladium thin-films on ceramic substrates by electroless deposition. Palladium (Pd) plating rate on a ceramic substrate at room temperature is shown in Figure 1.

- Designed and assembled a diffusion cell to measure diffusivity and permeability of hydrogen at high temperature and pressure.

FUTURE WORK

During next two and half years, we will work on the following tasks:

- Design and build an experimental system to measure the permeability and diffusivity of hydrogen gas through palladium plated composite membrane. Also develop a method to measure the gas species composition by chromatographic method.

- Using SEM and EDAX, characterize composite ceramic-palladium membrane for film thickness and film composition.

- Evaluate the fabricated membrane for permeability and selectivity for hydrogen in presence of other gases, such as argon, nitrogen and carbon dioxide.

- Extend this work to investigate the silver-palladium composite membrane for separation of hydrogen.

REFERENCES

1. Itoh N., and Govind R., "Development of a Novel Oxidative Palladium Membrane Reactor," **AIChE Symposium Series 268**, **85**, 10 (1989).

2. Ilias S., and Govind R., "Development of High Temperature Membrane for Membrane Reactor: an Overview," **AIChE Symposium Series 268**, **85**, 18 (1989).

3. Lewis, F.A., **The Palladium Hydrogen System**, Academic Press, London, 1967.

4. Bohmholdt, G., and Wicke, E., "Diffusion of H_2 and D_2 in Pd and Pd-alloy," **Z. Physik. Chem.**, Neue Folge, 56, 133 (1967).

5. Barrer, R.M., **Diffusion In and Through Solids**, Cambridge University Press, London, 1941.

Table 1: Typical Composition of Electroless Plating Bath.

Components/Variables	Concentration
$PdCl_2$	5.4 g/l
Ammonium hydroxide (28 percent)	390 ml/l
EDTA	40 g/l
Hydrazine (1 molar soluition)	10 ml/l
pH	11
Temperature	25 °C

Table 2: Composition of Senistization and Activation Solutions.

Sensitization Soluition	Concentration
$SnCl_2$	1 g/l
HCl	0.2 N
Activation Solution	
$PdCl_2$	0.9 g/l
HCl	0.2 N

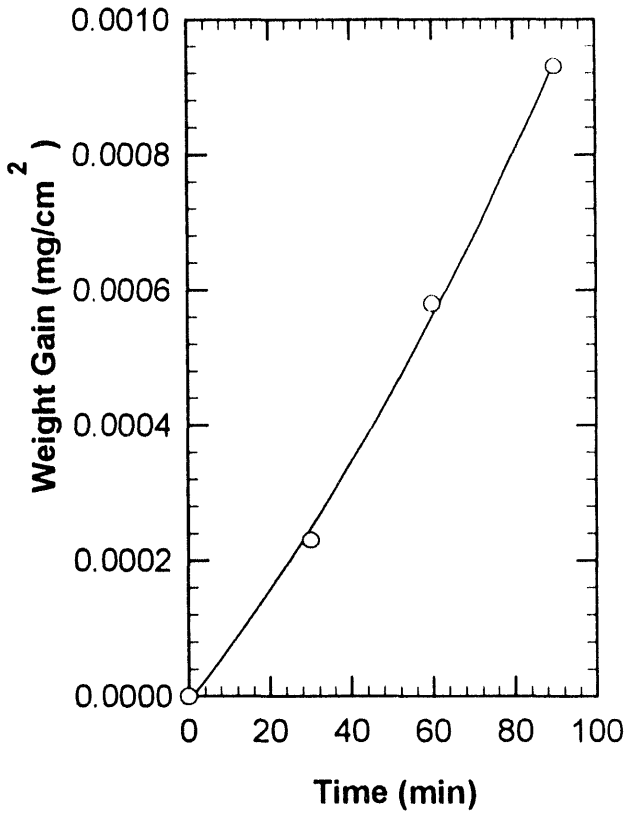


Figure 1: Palladium plating rate on ceramic substrate by electroless deposition at room temperature. Ceramic substrate is 6.0 cm in diameter, 7 mm thick, 10-15 % open porosity and 5 μm pore size.

9b.5 Development of Hollow Fiber Catalytic Membrane Reactors for High Temperature Gas Cleanup

CONTRACT INFORMATION

Contract Number	DE-AC21-89MC26372
Contractor	Chemical Engineering Department, Worcester Polytechnic Institute, 100 Institute Rd., Worcester, MA 01609
Contractor Project Manager	Dr. Y. H. Ma
Principal Investigators	Dr. Y. H. Ma Dr. W. R. Moser Dr. S. Pien Dr. A. B. Shelekhin
METC Project Manager	Dr. V. Venkataraman
Period of Performance	4/93- 3/94

FY94 Program Schedule

OBJECTIVES

The ***objective*** of this project was to develop economically and technically viable catalytic membrane reactors for high temperature, high pressure gaseous contaminant control in IGCC systems. These catalytic membrane reactors were used to decompose H_2S and separate the reaction products. The reactors were designed to operate in the hostile process environment of the IGCC systems, and at temperatures ranging from 500 to 1000 °C.

BACKGROUND INFORMATION

The technology employed in the Integrated Gasification Combined Cycle (IGCC) permits burning coals with a wide range of sulfur concentrations. Emissions from the process should be reduced by an order of magnitude below stringent federal air quality regulations for coal-fired plants. The maximum thermal efficiency of this type of process can be achieved by removing sulfur and particulates from the high temperature gas (e.g., 800 °C to 900 °C). High temperature sulfur removal can be accomplished with sorbents or by using membrane reactors. Catalytically active membrane reactors offer an inherent ability to combine reaction, product concentration and separation in a single unit operation. The conversion of H_2S is limited by the thermodynamic equilibrium of the reaction but can, in principle, be improved by the removal of products (e.g., H_2) during reaction. Here, selective removal of hydrogen could be provided by the membrane during reaction so that the reaction is continuously driven toward the product side. As the membrane is more

permeable to H_2, the reaction can be almost shifted to complete conversion.

PROJECT DESCRIPTION

The membrane reactor is an integrated process which includes membrane and reactor processes in a single unit operation. Therefore, to ensure a proper design of the membrane reactor several components of the process should be analyzed including:

* membrane gas permselectivity and thermal stability;
* hydrodynamics of gas flow at elevated temperatures;
* thermodynamics of H_2S decomposition;
* reaction rates of homogeneous and heterogeneous reactions of H_2S decomposition;
* membrane reactor design;
* H_2S decomposition in the membrane reactor at different operational parameters.

Based on experimental information on the H_2S conversion in the membrane reactor, a mathematical model was developed providing an adequate (within 5%) description of the process. The model provided information on the best operation parameters of the membrane reactor process.

RESULTS

Severe conditions encountered in the IGCC process (e.g., 900 °C, H_2S, CO_2 and H_2O) make it impossible to use polymeric membranes in the process. Therefore, inorganic membranes were used in the design of the membrane reactor - molecular-sieve glass membrane and Vycor glass porous membrane.

Membrane permselectivity

The molecular-sieve glass membrane acquired from PPG Industries Inc. was found far superior to polymeric counterparts in terms of the selectivity, permeability and thermal stability. Temperature dependencies of gas permeability in the molecular-sieve membrane is presented in Figure 1. Separation of gases in the microporous membrane occurs according to configurational diffusion mechanism developed in [1-4]. Even though the selectivity coefficients of the molecular-sieve glass membrane are very attractive for separation of H_2 at room temperature ($\alpha[H_2/H_2S] \approx 200$) the selectivity decreases with the temperature and at 800 °C is approximately 10. This selectivity is approximately two times higher than the selectivity coefficient for Knudsen diffusion mechanism. In addition, the porous structure of the membrane collapses at temperatures higher than 300 °C and gas permeability irreversibly decreases (Figure 2).

On the other hand, the permeability of the Vycor glass membrane remains unchanged up to a temperature of 850 °C. The selectivity factor in the Vycor glass membrane is independent of the temperature and is equal to $\alpha[H_2/H_2S]=4.1$. Even though the selectivity coefficient is lower than for the microporous glass membrane, the Vycor glass membrane was used for the design of the high temperature membrane reactor because of its thermal stability.

Experimental installation

A schematic diagram of the experimental installation used in this study is presented in Figure 3. Quartz tubes with OD/ID = 16/13 mm were used as the reactor shells. One end of the membrane was fixed to the quartz tube with epoxy resin Duralco 4525 (Cotronics) stable up to a temperature of 250 °C. The other end of the membrane was sealed with the same epoxy. The feed

gas mixture was supplied on the shell side of the membrane reactor. The furnace was 15 cm long. The porous glass membrane and the quartz tube were 30 cm long. The length of the permeable part of the membrane in the membrane reactor was equal to 22 cm. The temperature in the furnace was controlled by a thermocontroller. The gas composition on the shell and the tube sides of the membrane reactor was analyzed with a Hewlett Packard HP5890 GC. The pressure in the sampling loop was controlled with a specially designed vacuum gas sampling system to provide reliability and accuracy in a wide range of gas concentrations. The reactor ends were cooled by air flow to prevent overheating and decomposition of the epoxy resin. Flow rates on the feed and shell sides were measured with a bubble flowmeter. The pressure on the shell side of the membrane reactor was kept at either 2.36 atm or 7.8 atm while the pressure on the permeate side of the membrane was kept atmospheric. Before the experimental runs the system was kept at 800 °C in a feed gas flow for 24 hours.

Hydrogen concentration

The stage cut for the membrane reactor is similar to the stage cut for the conventional membrane reactor and is defined as the ratio of the permeate flow to the sum of the permeate and reject flows according to

$$Stage\ Cut = \frac{Permeate}{Permeate + Reject}$$

During the membrane reactor operation hydrogen produced during the reaction of H_2S decomposition was selectively removed through the Vycor glass membrane and concentrated on the permeate side (Figure 4). When the stage cut increased the concentration of H_2 on both the permeate and reaction sides decreased. At the stage cut equal to one the concentration of H_2 on the permeate side is equal to the equilibrium concentration of H_2 for the reaction of H_2S decomposition at 1 atm. Similarly, at stage cut equal to 0 the concentration of H_2 on the reaction side is equal to the equilibrium concentration of H_2 for the H_2S decomposition reaction at 7.8 atm. Similar dependencies of the H_2 on the stage cut were observed when 100%, 1%, and 500 ppm H_2S gas mixtures were used as a feed.

H_2S conversion

From the definition of the stage cut it follows that at the stage cut equal to 0 the effect of H_2 removal from the reaction gas mixture is negligible and cannot affect the total conversion in the membrane reactor. As the stage cut increased the effect of H_2 removal increased as well. At the stage cut equal to one, the total conversion in the membrane reactor is equal to the total conversion on the low pressure or permeate side of the membrane reactor (Figure 5).

Noteworthy, that even though the stripping of H_2 from the reaction side occurred in the membrane reactor the total conversion did not increase compared to the equilibrium conversion in the packed bed reactor. Therefore, the membrane with the Knudsen selectivity of gas separation appears to be not suitable for enhancement of the conversion in the membrane reactor.

Mathematical model

A mathematical model was developed to simulate the performance of the membrane reactor. Comparisons between theoretical predictions and experimental data are shown in Figure 4. A good agreement

between the experimental data and simulations was also observed for feed mixtures with a different content of H_2S.

The developed model was used to predict the optimum conditions at which the conversion of H_2S can be conducted to the highest degree of the conversion. When the membrane with selectivity coefficients higher than those of the Knudsen selectivity is used in the membrane reactor the conversion may be considerably higher than the conversion in the conventional packed bed reactor (Figure 6). The best results were obtained when the selectivity coefficients are equal to 500-1000 with respect to H_2 separation. Such high selectivity coefficients are difficult to get at temperatures equal to 800 °C even in the molecular-sieve membranes.

Additionally the effect of downstream pressure on the total conversion in the membrane reactor was analyzed. It was demonstrated that only when the absolute pressure on the permeate side is lowered down to 0.01 atm the high conversions (up to 90%) of H_2S can be achieved.

FUTURE WORK

A comprehensive analysis of the membrane reactor demonstrated that under certain conditions the membrane reactor may provide high conversions at low stage cuts. These conditions include high membrane selectivity (100 times the Knudsen selectivity) and low pressure on the permeate side (0.01 atm). it is not recommended to use sweep gas in any part of the membrane reactor because hydrogen in the permeate will be diluted and can not be utilized. The conversion in the membrane reactor can increase only if highly selective membrane is used such as Pd or Pt and low pressures on the permeate side are kept. The conversion can be further increased if simultaneously a higher pressure on the reaction side is applied to lower a pressure ratio (pressure ratio = downstream pressure/upstream pressure) and to improve the membrane separation performance.

The membrane reactor processes appears to be more appropriate for processes with high contents of the reactant material. It can be used in gas phase reactions whose components are difficult to separate. The membrane reactor unit operation in this case provides simultaneous reaction and separation in a single technological unit.

CONCLUSIONS

* Feasibility of the membrane reactor process for decomposition of hydrogen sulfide was demonstrated.
* Permeability and selectivity of molecular-sieve and Vycor glass membranes were studied at temperatures up to 1000 °C.
* Experimental study of hydrogen sulfide in the membrane reactor was completed.
* A generalized mathematical model was developed for the simulation of the high temperature membrane reactor.
* The efficiency of the membrane reactor process is probably lo for the high temperature clean-up of H_2S from the IGCC gas mixture.
* Knudsen selectivity is insufficient to yield an increase of the H_2S conversion in membrane reactor.

REFERENCES

1. M. Bhandarkar, A. B. Shelekhin, A. G. Dixon, Y. H. Ma, Adsorption, permeation and diffusion of gases in microporous membranes. I. Adsorption of gases on microporous glass membranes. J.Mem.Sci.,

75 (1992) 221-231

2. A. B. Shelekhin, A. G. Dixon, Y. H. Ma, Adsorption, permeation and diffusion of gases in microporous membranes. II. Permeation of gases in microporous glass membranes, J.Mem.Sci., 75 (1992) 233-244

3. A.B. Shelekhin, A. G. Dixon, Y. H. Ma, Adsorption, permeation and diffusion of gases in microporous membranes. III. Applications of percolation theory to interpretation of porosity, tortuosity, and surface area in microporous glass membranes, J.Mem.Sci., 83 (1993) 181-198

4. A. B. Shelekhin, A. G. Dixon, Y. H. Ma, Theory of gas diffusion and permeation in molecular-sieve membranes, AIChE J., In print 1994

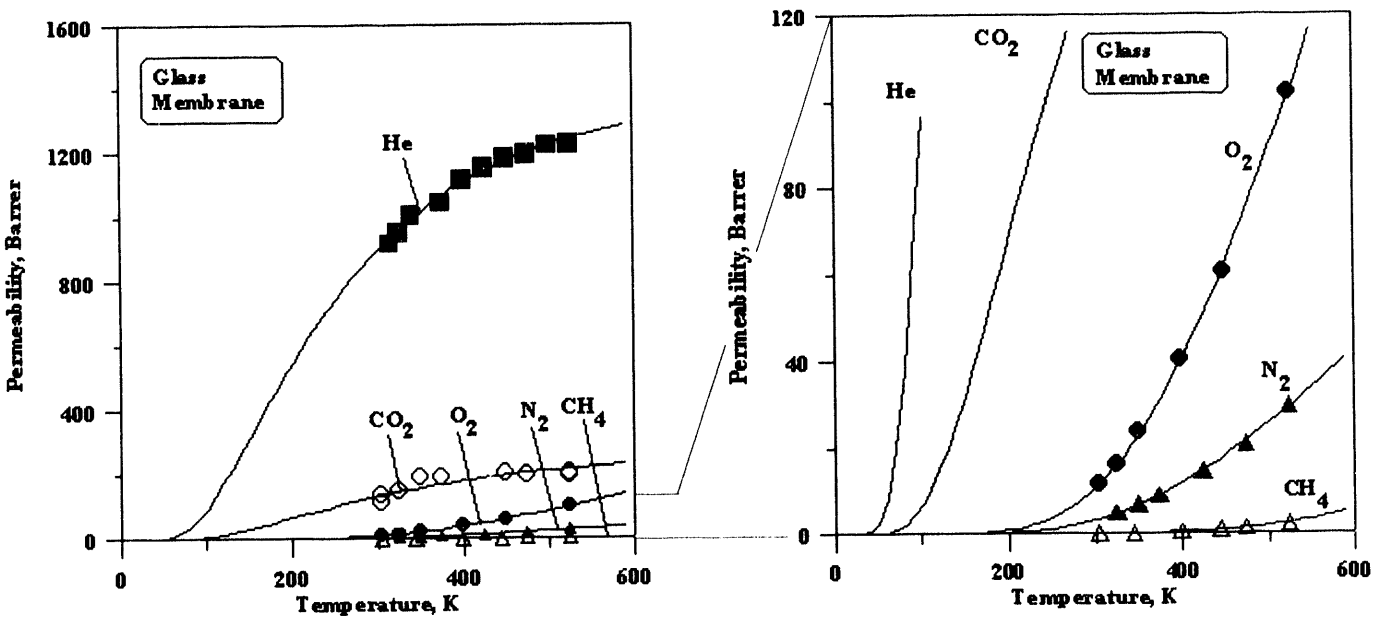


Figure 1 Permeability of molecular-sieve glass membrane.

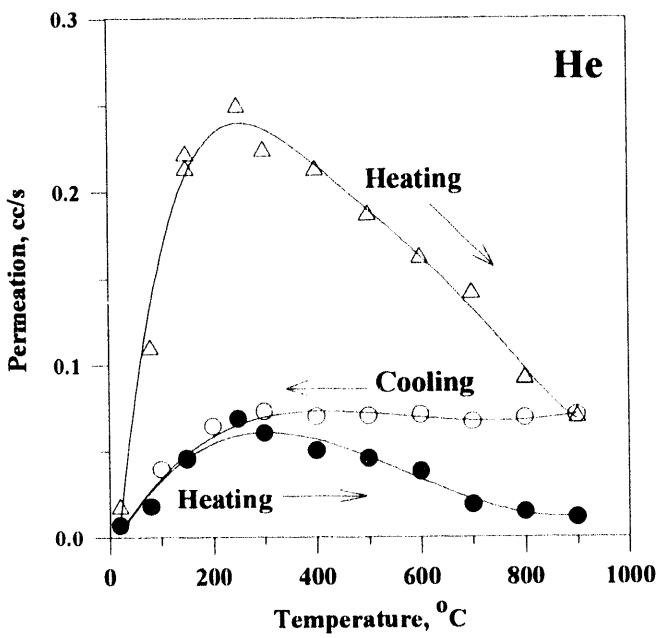
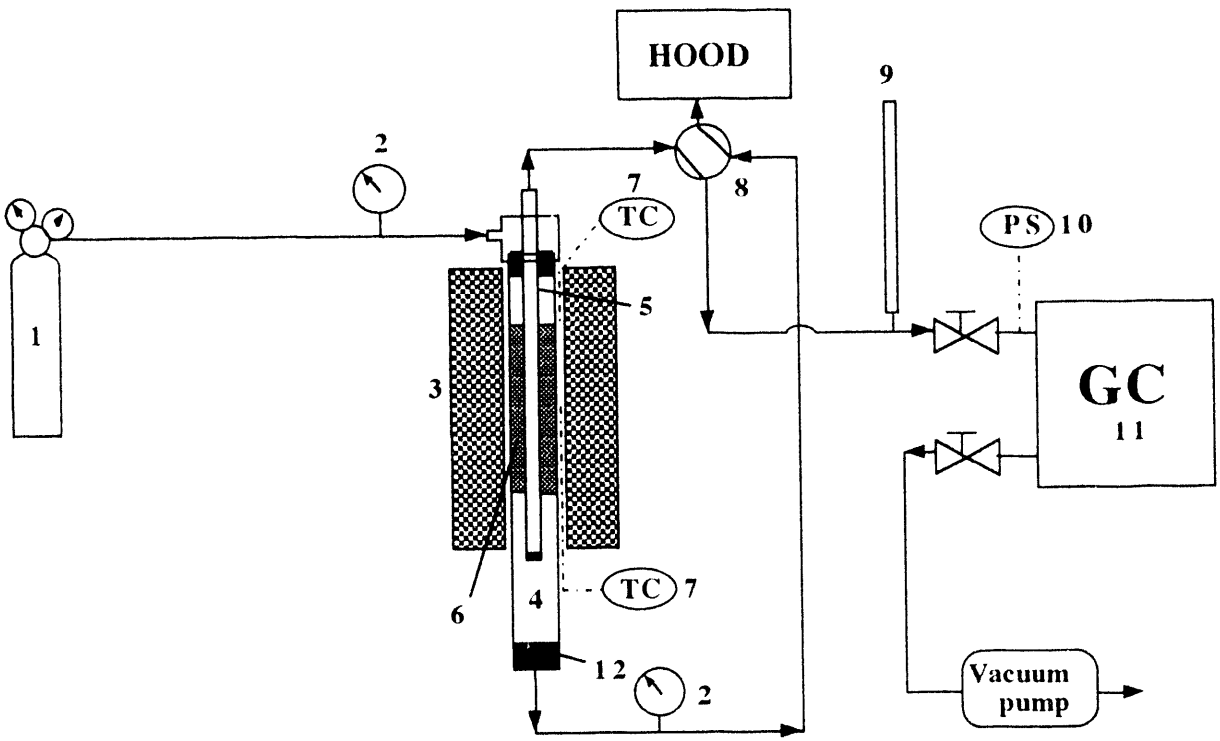


Figure 2 Temperature stability of molecular-sieve glass membrane.



1- Feed, 2- Pressure gage, 3- Furnace, 4- Membrane/packed-bed reactor, 5- Porous Vycor glass membrane, 6- Catalyst (MoS_2), 7- Thermocouple, 8- 4-way-valve, 9- Bubble flow meter, 10- Pressure sensor, 11- Gas chromatograph, 12- Epoxy resin.

Figure 3. The schematic diagram of the experimental installation.

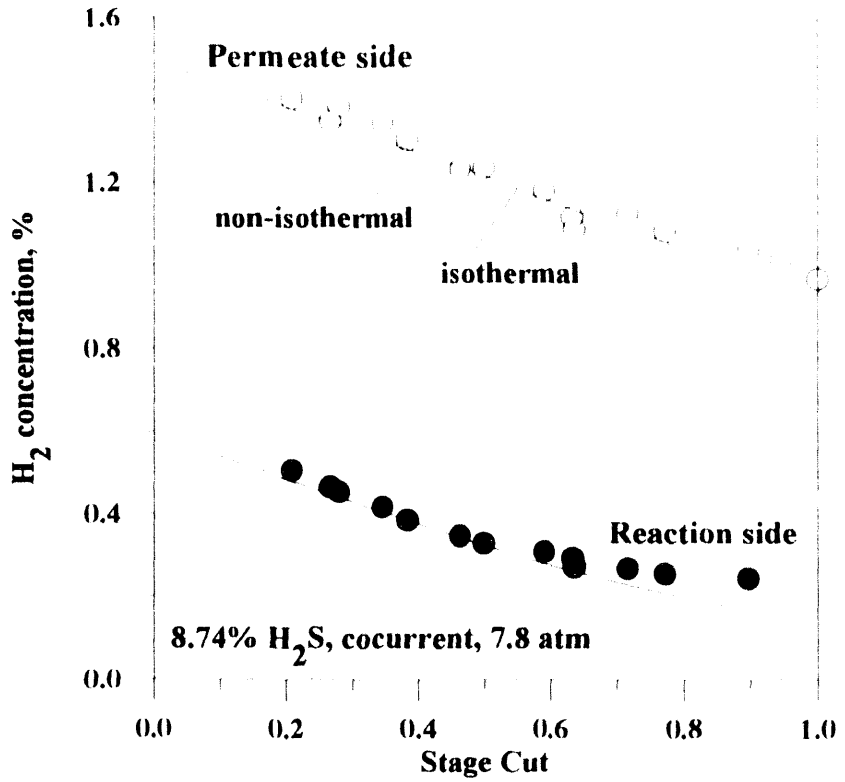


Figure 4 Concentration of hydrogen at the permeate and rejection side outlets in the membrane reactor.

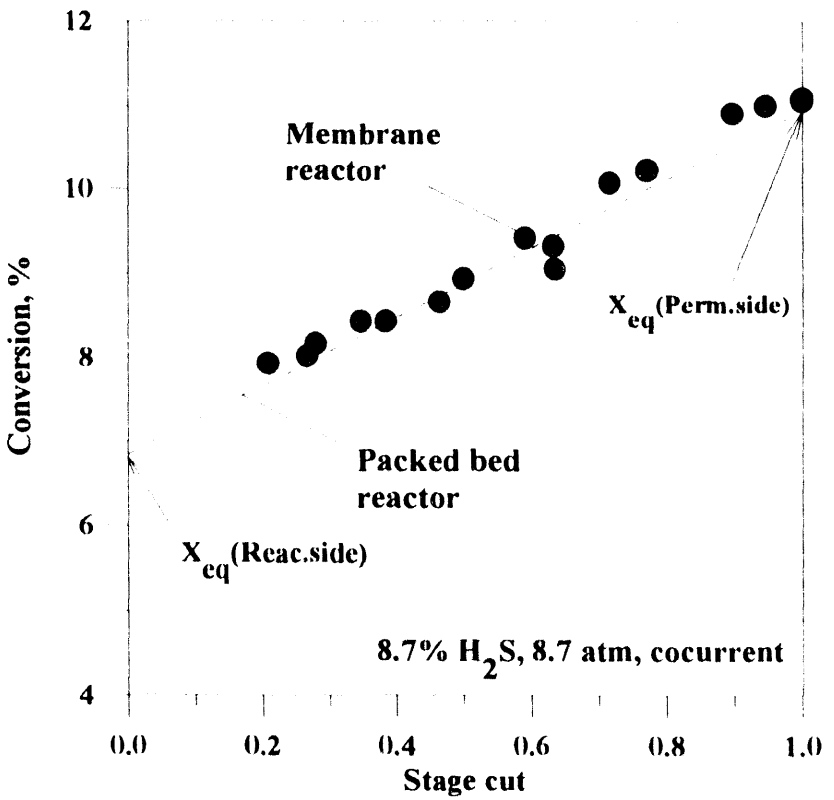


Figure 5 Total conversion of H_2S in the membrane reactor.

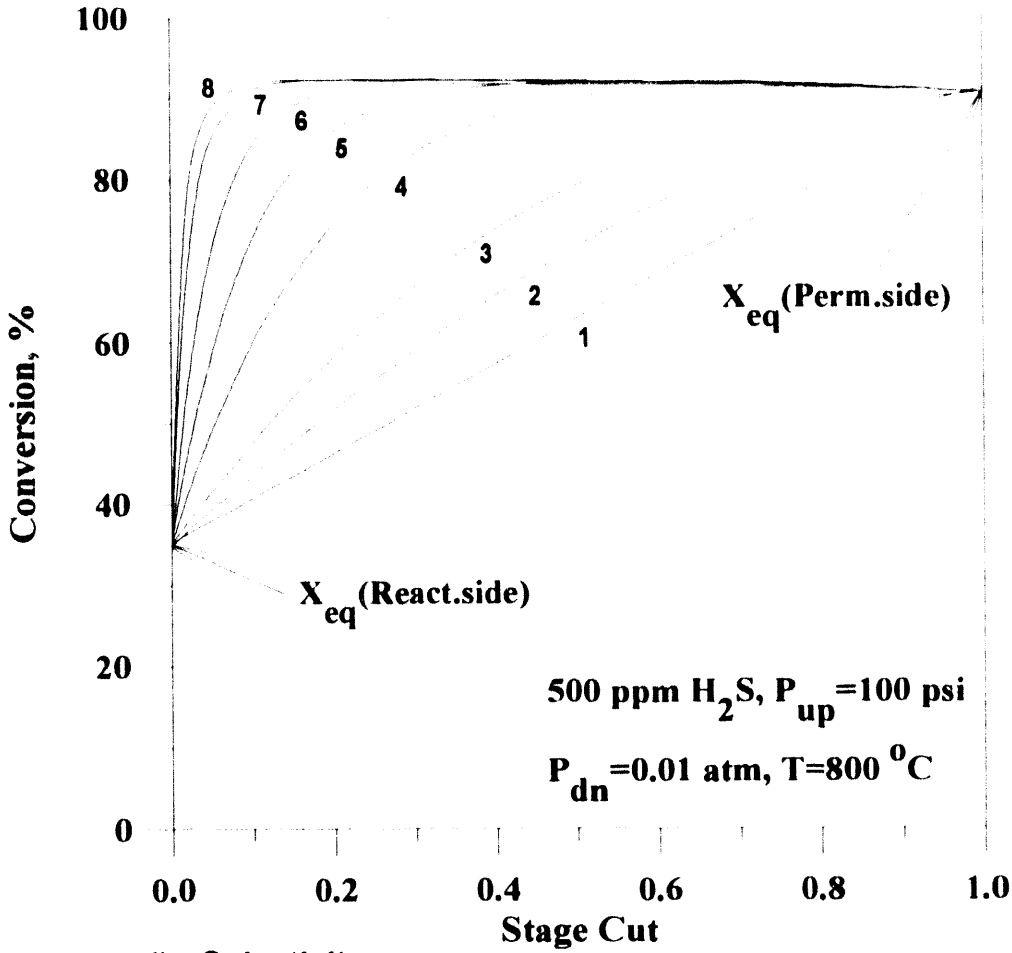


Figure 6. Effect of the membrane selectivity on the total conversion of H_2S in the membrane reactor.

9b.6 Thermal/Chemical Degradation of Inorganic Membrane Materials

CONTRACT INFORMATION

Contract Number DE-AC21-92MC28053

Contractor
SRI International
333 Ravenswood Avenue
Menlo Park, CA 94025
(415) 326-6200

Contractor Proj. Mgr. Gopala N. Krishnan

Principal Investigators
Gopala N. Krishnan
Angel Sanjurjo
Ashok S. Damle
Bernard J. Wood
Kai-Hung Lau

METC Project Manager Venkat K. Venkataraman

Period of Performance August 24, 1992 to December 19, 1994

Schedule and Milestones

FY94 Program Schedule

Task	S	O	N	D	J	F	M	A	M	J	J	A	S
Topical Report & Test Plan Development													
Experimental Testing													

OBJECTIVES

The overall objective of this program is to evaluate the long-term thermal and chemical degradation of inorganic membranes that are being developed to separate gaseous products produced by the gasification or combustion of coal in fixed-, fluidized-, and entrained-bed gasifiers, direct coal-fired turbines, and pressurized-fluidized-bed combustors. Specific objectives of this program are to (1) quantify the extent of the degradation process for the three most detrimental mechanisms by performing laboratory-scale experiments, and (2) develop a predictive model for membrane degradation under operating conditions.

BACKGROUND INFORMATION

Several impurities, such as H_2S, NH_3, SO_2, NO_x, and trace metal compounds are generated during the coal conversion process and they must be removed from the coal gas or the combustor flue gas to meet environmental standards. In an integrated-gasification combined-cycle plant, removal of such impurities from the gasifier product at high temperature increases the efficiency of electric power generation. Inorganic membranes are potentially attractive for such an application. They are also being considered as a means to separate from coal gas a high-value bulk component such as hydrogen. Hence, it is important to identify membrane materials that

possess the required characteristics of permeability, selectivity, and durability for use at high temperatures in a severe gaseous environment.

PROJECT DESCRIPTION

To achieve the overall objective, the program is divided into the following tasks:

1. Development of evaluation methodology
2. Evaluation of potential long-term degradation mechanisms
3. Submission of a topical report and a plan for experimental testing
4. Experimental testing
5. Model development.

In Task 2 which has been completed, Krishnan, et. al. (1993) evaluated potential inorganic membrane degradation mechanisms based upon an extensive literature search and theoretical calculations. Thermal sintering, hydrothermal attack, reaction with ash components, attack by vapor and solid phase alkali compounds, and deposition of carbon from the gas phase were identified as the likely degradation mechanisms for ceramic and metallic membranes.

The topical report describing this work was submitted in March 1994. Experimental testing of candidate materials (Task 4) is currently in progress. Task 5 is a separate option that may be exercised by the U.S. Department of Energy at the conclusion of Task 4.

CANDIDATE MEMBRANE MATERIALS

Micro-porous inorganic membranes, in which the separation process is based upon Knudsen diffusion, are available for commercial gas separation needs, but their selectivity is limited. A variety of developmental efforts are currently under way, many sponsored by U.S. Department of Energy (DOE), to improve the selectivity and flux characteristics of porous inorganic membranes (Liu, et. al., 1992; Goldsmith, et al., 1992; Gavalas, 1992; Yates, et. al., 1993). DOE is also sponsoring efforts to increase the applicability of metallic membranes (Edlund, 1993).

At present, no inorganic membranes are commercially available for application in the high-temperature, high-pressure (HTHP) gas environments encountered in integrated gasification combined cycle (IGCC), pressurized fluidized bed combustion (PFBC), and direct coal fired turbine (DCFT) applications. Most of the inorganic membrane developmental efforts have focused on hydrogen separation membranes which may be used in an IGCC system for maximizing hydrogen production from coal gas or to remove H_2S and NH_3 contaminants via thermal or catalytic decomposition of these contaminants.

The candidate inorganic membranes may be grouped as follows:

1) Dense Metallic Membranes. Both palladium and platinum membranes have been investigated for their hydrogen separation ability. Developmental work is presently underway to increase their tolerance to high temperature as well as sulfur species by combining platinum and palladium metal layers with base metal and barrier oxide layers.

2) Silica Based Membranes. Micro-porous silica/glass membranes have been commercially available with pore sizes down to 40 Å (e.g., Vycor glass). Efforts are underway to reduce the pore size of such membranes by CVD techniques.

3) Alumina Based Membranes. Micro-porous gamma alumina/alpha alumina composite membranes are commercially available with pore sizes down to 40 Å (e.g., membralox membranes). Efforts are underway to reduce the pore size of the alumina membranes by depositing additional nanopore layers.

4) Carbon Based Membranes - Carbon molecular sieves (CMS) have been extensively used in the chemical industry for gas separation applications. Efforts are presently underway to develop carbon/carbon composite CMS membranes, where a top layer of CMS is deposited on a porous carbon support.

EXPERIMENTAL TESTING

Three approaches are being used to evaluate the degradation of the membrane materials: (1) exposure of membrane materials to simulated coal gas streams under well-defined conditions, followed by characterization of the changes that

occur in their physical and chemical properties, (2) long-term testing of the permeation performance of membranes under representative conditions, and (3) exposure of the membrane materials to the hot coal gas stream of an operating coal gasifier, followed by examination and evaluation of durability.

RESULTS

Exposure Studies

The purpose of the exposure tests is to determine the changes in physical characteristics, chemical composition, and pore size distribution of the membrane materials as a result of exposure to simulated IGCC coal gas environments.

Figure 1 shows a schematic of the exposure test apparatus. For atmospheric pressure tests at temperatures up to 1000°C, a quartz exposure tube enclosed in a furnace is used. A movable quartz rack/platform, within the tube allows convenient placement of membrane samples. The desired gaseous environment is generated by mixing appropriate dry gases and adding steam and alkali vapors supplied from separate generation systems. The exhaust gas from the exposure tube is vented through a condenser into a fume hood. and a back pressure regulator which controls the exposure environment pressure to a desired level.

A similar apparatus has been constructed for experiments at elevated pressure. The exposure tube is made of an alloy steel and is equipped with flanged ends. Constant pressure is maintained in the tube by means of a back pressure regulator in the effluent stream.

To date, commercially available Vycor glass and γ-alumina membranes have been tested, in addition to platinum and palladium metal foils. The samples were exposed for various periods (24, 76, and 113 hours) to two coal gas compositions, at three temperatures (1000, 800, and 650°C), in separate, atmospheric-pressure experiments. The two gas compositions represent extremes in gasifier type. The gas simulating a fixed-bed, air-blown gasifier product contained 18% H_2, 9% CO, 12% CO_2, 1% H_2S, 30% H_2O and 30% N_2, whereas that from an entrained-bed, oxygen-blown gasifier contains 30% H_2, 10% CO_2, 0.5% H_2S, 15% H_2O and 44.5% CO.

The exposed membrane samples were analyzed by various techniques to determine changes in the physical and chemical characteristics of the membrane materials. The results are described below for each of the membrane materials.

Surface areas and average pore diameters of Vycor membrane samples were determined by the B.E.T. gas adsorption method. The results are summarized in Table 1. The surface area of Vycor decreased from a high of 188 m^2/g for an unexposed sample to a low of 1.9 m^2/g for a sample exposed for 24 h at 1000°C. Mean pore size increased from 4.1 nm to 11.7 nm after 76 h exposure at 800°C, but after 24 h exposure at 1000°C, all microporosity was lost.

X-ray diffraction was used to determine changes in the crystallinity of the exposed membrane samples. The unexposed Vycor membrane sample, which was transparent, was found to be completely amorphous. After exposure at 800°C, the sample turned opaque and developed a crystalline cristobalite phase. The sample exposed to 1000°C appeared fufsed and completely crystallized. Thus, temperatures greater than 650°C in the coal gas environment are found to be detrimental to the silica based membranes. These results are significant also for modifiied membranes based on the addition of silica layers to commercial Vycor and alumina membranes.

Table 1. Changes in Vycor Membrane Properties with Temperature

Membrane Sample	BET Surface Area (m^2/gm)	Mean Pore Diameter (nm)
Unexposed	188	4.1
Exposed at 650°C for 113 hrs	140	4.5
Exposed at 800°C for 76 hrs	33	11.7
Exposed at 1000°C for 24 hrs	1.9	---

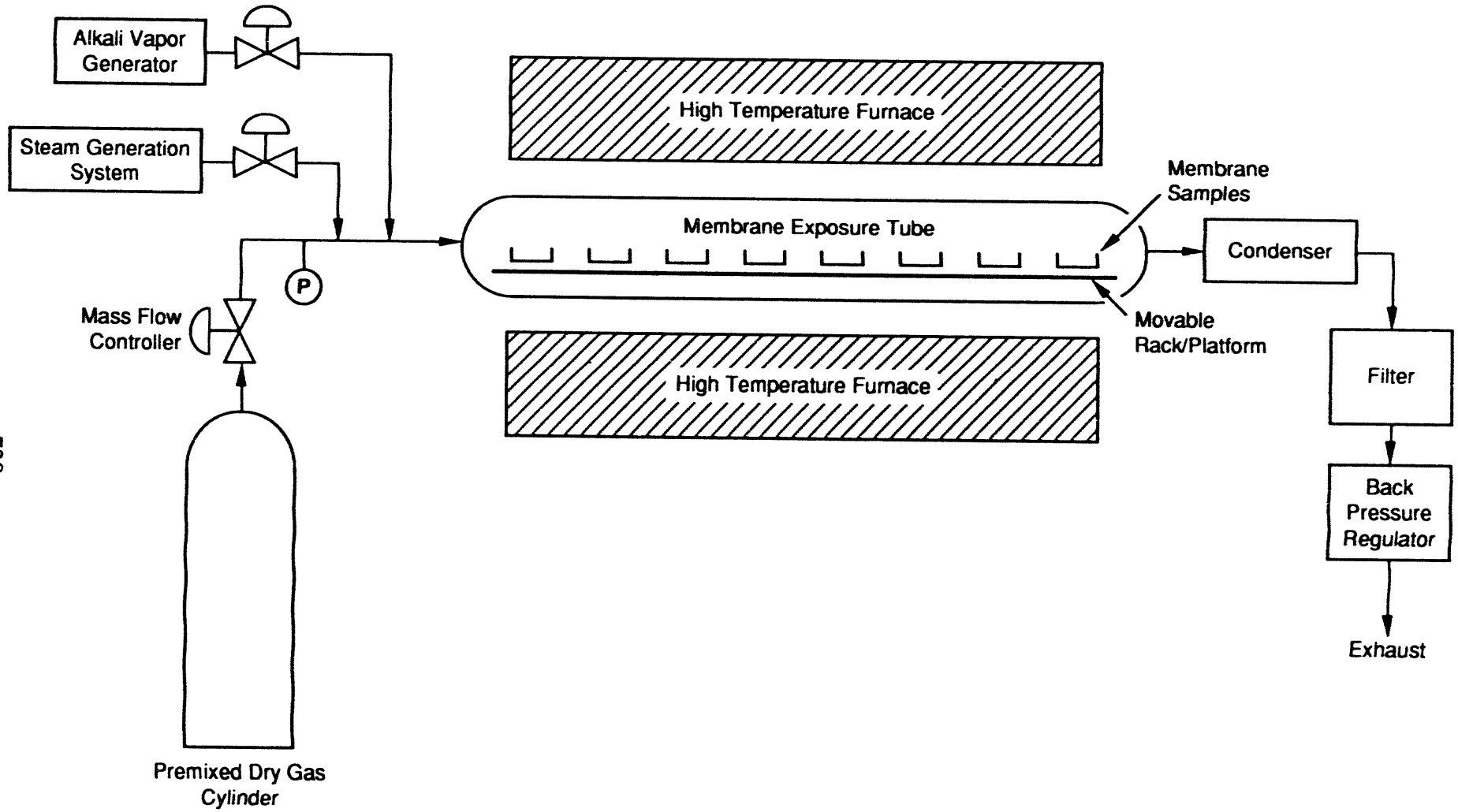


Figure 1. Schematic Diagram of the Reactor for Membrane Exposure Tests

The gamma-alumina membrane samples were also analyzed by X-ray diffraction (XRD) as well as by B.E.T. XRD identified α-alumina as the dominant bulk phase in the samples, but it failed to detect the γ-alumina phase present in the surface layers that is critical to the permselective character of the membrane. Refinement of this technique is necessary to determine the phase change in the thin γ-alumina layer due to high-temperature coal gas exposure. If phase changes in the surface layers occur, they would likely cause pore coarsening.

Nitrogen B.E.T. analysis of the alumina membranes indicated that a significant decrease in surface area occurred during exposure at all the temperatures studied (Table 2). The surface area of an unexposed sample was about 2.1 m^2/g. Exposure for 114 h at 650°C decreased the surface area to 0.9 m^2/g, and 76 h at 800°C reduced the surface area to 0.4 m^2/g. Exposure for 24 h at 1000°C decreased the surface area to 1.3 m^2/g. Because of these low values of surface area, these samples are being reanalyzed with an alternative adsorbent gas (krypton) to obtain greater accuracy. Both the exposure duration and temperature appear to affect the surface area reduction by mechanisms such as sintering and phase transformation.

Table 2. Surface Area Changes of an Alumina Membrane as a function of Temperature.

Test Conditions	BET Surface Area (m^2/g)
Unexposed	2.1
Exposed at 650°C for 113 hrs	0.9
Exposed at 800°C for 76 hrs	0.4
Exposed at 1000°C for 24 hrs	1.3

During exposure of the γ-alumina membrane samples at 800 and 1000 °C, vaporization of trace contaminants in the material occurred. Such vapor species reacted with silica material present in the exposure reactor causing them to crystallize. This vaporization behavior was studied by high temperature mass spectrometry, and the vapors were found to be CO_2, H_2O, Na (g), and Zn (g). Sodium vapor is detrimental to the operation of gas turbine components. Partial pressures of the N and Zn vapor species over a membrane sample are given in Table 3. In this experiment, the sample was heated slowly from room temperature. CO_2 evolution was observed at all temperatures whereas that of steam disappeared by 480°C. Significant evolution of elemental Na and Zn began at 480° and 1025°C respectively. The partial pressures of both species increased with temperatures. Sodium partial pressures were especially significant for coal gas exposure at 800 and 1000°C.

Table 3. Partial Pressure of Gaseous Species Evolved from an Alumina Membrane

	Partial Pressure (atm)	
Temperature (C)	Na Species	Zn Species
480	3.05E-10	< 1 E-10
545	1.15E-09	< 1 E-10
675	7.18E-09	< 1 E-10
780	3.25E-07	< 1 E-10
850	1.44E-06	4.71E-10
920	2.09E-06	5.52E-09
1025	1.20E-06	7.26E-09

Palladium foils exposed at 800° and 1000°C melted, presumably due to formation of PdS. Analysis of one of a resolidified sample by SEM/EDAX indicated bulk sulfidation of palladium. At 650°C the exposed Pd sample deformed extensively. This sample was also analyzed by Auger electron spectroscopy (AES) to determine the elemental sulfur content on its surface. Sulfur was not only a predominant component of the surface, but, upon depth profiling by argon bombardment, it was found at a high level within the bulk of the metal foil (Figure 2).

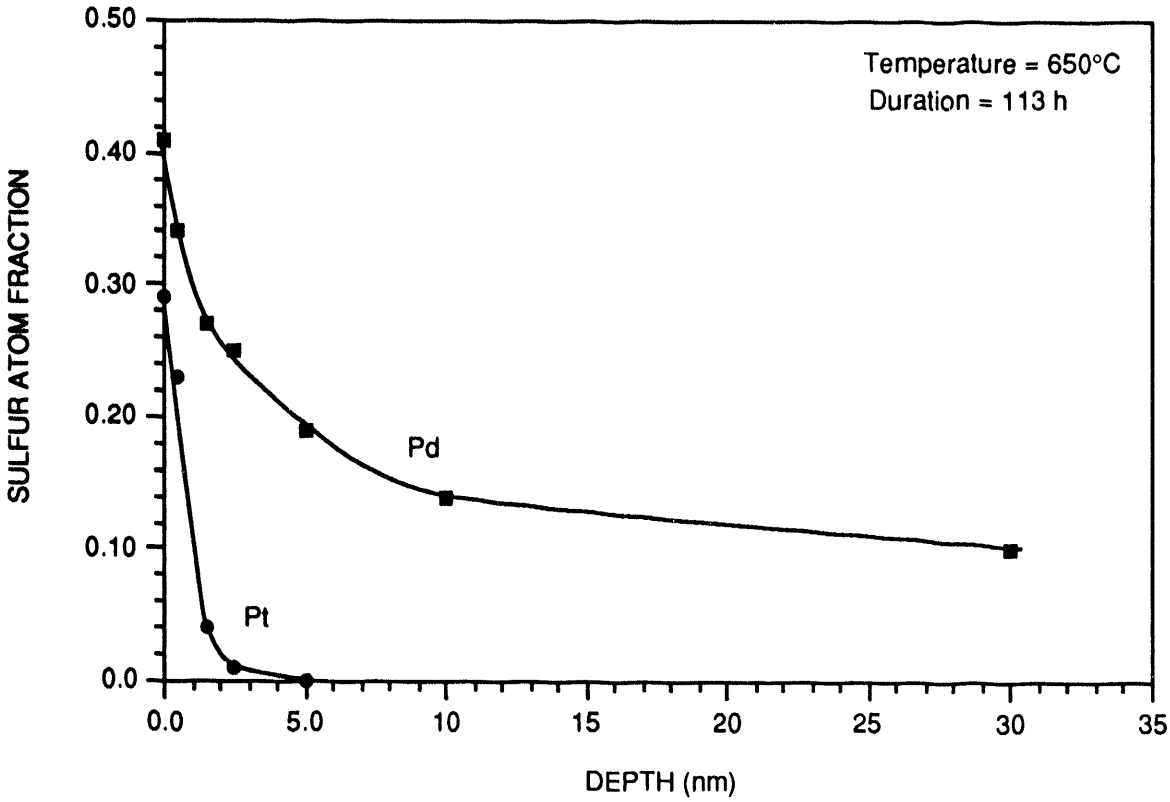


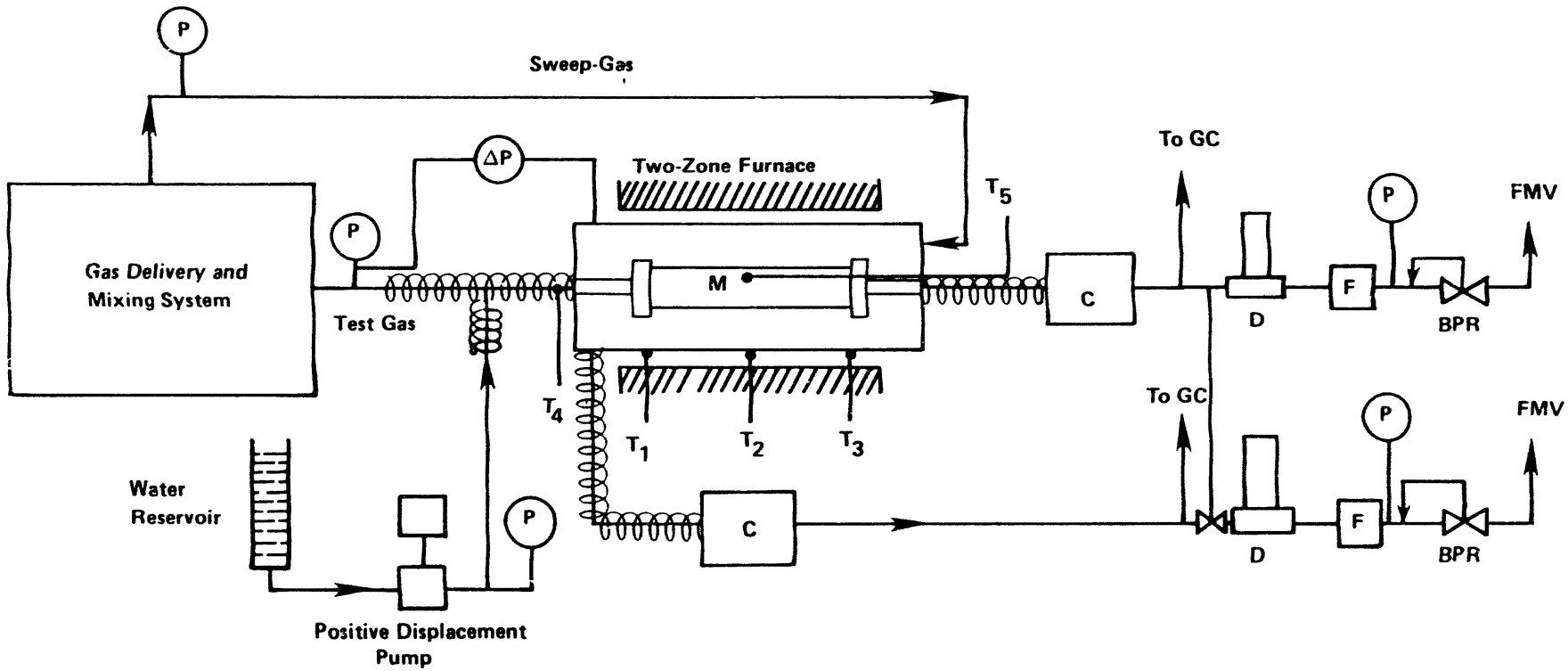
Figure 2. Incorporation of Sulfur on the Platinum and Palladium Membranes

Platinum foil samples exposed under all experimental conditions were unaffected visually. AES revealed a sulfur adlayer on the surfaces of all the samples, but the concentration decreased rapidly with argon sputtering and no sulfur was detected at depths about 5 nm beneath the foil surface. Thus, platinum sulfidation appears to be confined to the surface regardless of the exposure duration, temperature, and gas phase H_2S concentration.

Long-Term Membrane Permeation Testing

The purpose of long term testing of membrane permeation behavior is to quantify the changes in the membrane performance under controlled conditions. Specifically, changes in membrane permeation and selectivity characteristics will be determined as a function of time for a variety of operating conditions. The permeation measurements will also identify the key variables leading to loss of performance, if any, and will allow correlation of the observed degradation characteristics of the membrane materials with actual membrane performance under specified conditions of exposure.

Figure 3 is a schematic diagram of the test apparatus being assembled for long-term permeation testing. The system consists of mass flow controllers for mixing gases of known composition, a high temperature furnace, a gas chromatograph (GC), and a controlling computer that commands the GC and logs GC data. Steam will be supplied by using a high pressure pump to meter water into a vaporizer situated in the gas line. Alkali vapors will be generated in a high pressure vapor generation system similar to the one used in the exposure studies.



FMV: Flow Meter and Vent
M: Tubular Membrane Module
P: Pressure Gauge
ΔP: Differential Pressure Gauge
T_1-T_6: Temperature Measurement and Control
D: High Pressure Drier
BPR: Back Pressure Regulator
F: Filter

Preheater/Heated Lines
GC: Gas Chromatograph
C: Condensation and Liquid Separation System

Figure 3. Schematic Diagram of the Membrane Test System

The candidate membranes will be placed in appropriate membrane holders. The membranes will be exposed to typical gasifier product compositions on the feed side at realistic conditions of temperature and pressure. The flow rate and composition of the membrane feed gas, permeate gas, and feed reject gas will be monitored for an extended period of time, up to 60 days.

FUTURE WORK

Exposure studies will continue to determine changes in membrane characteristics in presence of fly ash and alkalis at high pressures, and for much longer durations. Modified Vycor and γ-alumina membrane samples will be included in these tests. Membrane permeation behavior will be determined in typical coal gas environments during long term tests. Also, selected membrane materials will be exposed to an actual hot coal gas stream at a pressurized fixed-bed gasifier facility, and the changes in the physical, chemical, and mechanical properties of the membrane that occur will be determined.

In Task 5, at the option of U.S. Department of Energy, the results from Task 4 and the data available in the literature will be used to develop a predictive model that can be used to estimate the long-term degradation of three selected inorganic membrane materials. Both theoretical and empirical approaches will be used in developing this model.

REFERENCES

Edlund, D. J., 1993. Catalytic Membranes for Facilitating the Water- Gas Shift Reaction. *Proceedings of the Coal-Fired Power Systems 93 -- Advances in IGCC and PFBC Review Meeting*, 233-237. DOE/METC-93/6131. NTIS/DE93000289. Springfield, Va.: National Technical Information Service.

Gavalas, G. 1992. Separation by Ceramic Membranes in Coal Gasification. *Proceedings of the Twelfth Annual Gasification and Gas Stream Cleanup Contractors Review Meeting*, 338-345. DOE/METC-92/6128. NTIS/DE93000229. Springfield, Va.: National Technical Information Service.

Goldsmith, R. L., R. J. Higgins, and B. A. Bishop. 1992. Low-Cost Ceramic Membranes and Supports for Gas Separation. *Proceedings of the Twelfth Annual Gasification and Gas Stream Cleanup Contractors Review Meeting*, 205-220. DOE/METC-92/6128. NTIS/DE93000229. Springfield, Va.: National Technical Information Service.

Krishnan, G. N., A. Sanjurjo, and B. J. Wood, 1993. Thermal/Chemical Degradation of Inorganic Membranes. *Proceedings of the Coal-Fired Power Systems 93 -- Advances in IGCC and PFBC Review Meeting*, 211-219. DOE/METC-93/6131. NTIS/DE93000289. Springfield, Va.: National Technical Information Service.

Liu, P. K. T., C. L. Lin, D. L. Flowers, J. C. S. Wu, and G. W. Smith. 1992. Gas Separations Using Ceramic Membranes. *Proceedings of the Twelfth Annual Gasification and Gas Stream Cleanup Contractors Review Meeting*, 351-361. DOE/METC-92/6128. NTIS/DE-93000229. Springfield, Va.: National Technical Information Service.

Yates, S. F., and A. X. Swamikannu, 1993. High Temperature Size Selective Membranes. *Proceedings of the Coal-Fired Power Systems 93 -- Advances in IGCC and PFBC Review Meeting*, 238-244. DOE/METC-93/6131. NTIS/DE93000289. Springfield, Va.: National Technical Information Service.

Appendices

Appendix A

Coal-Fired Power Systems 94 -- Advances in IGCC and PFBC Review Meeting

June 21- 23, 1994

AGENDA

TUESDAY, JUNE 21, 1994

7:30 a.m.		Registration/Coffee and Refreshments
8:15 a.m.		METC Site Tour
9:30 a.m.		*Opening Remarks* Harvey M. Ness Morgantown Energy Technology Center

SESSION 1 -- OPENING COMMENTARIES

Chairperson: Harvey M. Ness

9:40 a.m.	1.1	*The Future for Advanced Power Systems* Thomas F. Bechtel, Director Morgantown Energy Technology Center
10:10 a.m.	1.2	*Evolving Utility Business Structure and Impact on New Technology Application* J. Wayne Leonard Senior Vice President and Chief Financial Officer PSI Energy, Inc.
10:55 a.m.		BREAK

SESSION 2 -- CHANGES IN THE MARKET AND TECHNOLOGY DRIVERS

Chairperson: Rita A. Bajura

11:15 a.m.	2.1	*Overview of Global Utility Market for Advanced Coal-Fired Systems* Ronald Wolk Electric Power Research Institute

11:40 a.m.	2.2	*Overview of the Independent Power Producer (IPP) Market for Advanced Coal-Fired Systems* Dale Simbeck SFA Pacific, Inc.
12:05 p.m.	2.3	*The Search for Innovative Technology* C. Lowell Miller DOE Headquarters
12:30 p.m.		LUNCH -- METC ENERGIZER

SESSION 3 -- ADVANCED IGCC SYSTEMS

Co-Chairpersons: Justin L. Beeson and Dale K. Schmidt

1:30 p.m.	3.1	*IGCC System Analysis* Larry K. Rath Morgantown Energy Technology Center
1:55 p.m.	3.2	*Transport Reactor Development Status* William M. Campbell The M.W. Kellogg Company
2:20 p.m.	3.3	*Gasification Product Improvement Facility Status* Vijay B. Dixit CRS Sirrine Engineers, Inc.
2:45 p.m.		BREAK

SESSION 4 -- ADVANCED PFBC SYSTEMS

Co-Chairpersons: Donald L. Bonk and Randall J. Dellefield

3:10 p.m.	4.1	*PFBC System Studies* Michael E. Reed Morgantown Energy Technology Center
3:35 p.m.	4.2	*Second-Generation PFBC Systems Research and Development - Circulating Pressurized Fluidized Bed Combustor Test Results* Rich Conn Foster Wheeler Development Corporation

4:00 p.m.	4.3	*Status of the Advanced PFBC at the Power Systems Development Facility* Darrell L. Moore Southern Company Services, Inc.
4:25 p.m.		ADJOURN
6:30 p.m.		BARBECUE Lakeview Resort and Conference Center

WEDNESDAY, JUNE 22, 1994

7:30 a.m.		Coffee and Refreshments
8:00 a.m.		*Opening Remarks* Venkat K. Venkataraman Morgantown Energy Technology Center

SESSION 5 -- ADVANCED FILTER SYSTEMS

Chairperson: Richard A. Dennis

8:10 a.m.	5.1	*Status of the Morgantown Energy Technology Center's Particulate Cleanup Program -- Enabling Technology for Advanced Coal Based Power Systems* Richard A. Dennis Morgantown Energy Technology Center
8:20 a.m.	5.2	*Potential Industry Use of Continuous Fiber Ceramic Composites* Jill Jonkouski U.S. Department of Energy, DOE Chicago Operations Office Office of Energy Efficiency and Renewable Energy
8:45 a.m.	5.3	*Ceramic Fiber Ceramic Matrix Filter Development* Roddie R. Judkins Oak Ridge National Laboratory
9:10 a.m.	5.4	*Westinghouse Advanced Particulate Filter System* Thomas E. Lippert Westinghouse Electric Corporation
9:35 a.m.		BREAK

9:55 a.m.	5.5	*IF&P Fibrosic™ Filters* Paul Eggerstedt Industrial Filter & Pump Mfg. Co., Inc.
10:20 a.m.	5.6	*Multi-Contaminant Control Granular Bed Filter* John C. Haas Combustion Power Company
10:45 a.m.	5.7	*Westinghouse Standleg Moving Granular Bed Filter Status* Richard A. Newby Westinghouse Electric Corporation
11:10 a.m.		BREAK
11:30 a.m.	5.8	*MTCI Acoustic Agglomeration Particulate Control* Ravi R. Chandran Manufacturing and Technology Conversion International, Inc.

SESSION 6 -- DESULFURIZATION SYSTEMS

Chairperson: Ronald K. Staubly

11:55 a.m.	6.1	*METC Hot Gas Desulfurization Program Overview* Daniel C. Cicero Morgantown Energy Technology Center
12:05 p.m.	6.2	*Integrated Operation of a Pressurized Fixed Bed Gasifier, Hot Gas Desulfurization and Turbine Simulator System* David Najewicz GE Corporate R&D
12:30 p.m.		LUNCH -- METC ENERGIZER
1:30 p.m.	6.3	*Enviropower Hot Gas Desulfurization PDU* Jukka T. Konttinen Enviropower, Inc.
1:55 p.m.	6.4	*Slipstream Testing of the Direct Sulfur Recovery Process* Jeffrey W. Portzer Research Triangle Institute
2:20 p.m.	6.5	*METC Fluid-Bed Hot-Gas Desulfurization PDU* Larry A. Bissett Morgantown Energy Technology Center

2:45 p.m. BREAK

SESSION 7 -- TURBINE SYSTEMS

Chairperson: Darren J. Mollot

3:05 p.m. 7.1 *Development of Topping Combustor for Advanced Concept Pressurized Fluidized Bed Combustion*
Thomas E. Lippert
Westinghouse Electric Corporation

3:30 p.m. 7.2 *Development and Testing of Low Btu Fuel Gas Turbine Combustors*
Alan S. Feitelberg
GE Environmental Services, Inc.

3:55 p.m. 7.3 *Advanced Turbine Systems Program Overview*
Holmes A. Webb
Morgantown Energy Technology Center

4:10 p.m. POSTER SESSION

POSTER SESSION

P1 *High Temperature Electrochemical Separation of H_2S from Coal Gasification Streams*
Jack Winnick
Georgia Institute of Technology

P2 *Characterization and Fixed-Bed Testing of a Nickel-Based Hot Gas Desulfurization Sorbent*
Lee Gasper-Galvin
Morgantown Energy Technology Center
Kurt Hammerbeck
Oak Ridge Associated Universities

P3 *Pilot Gasification and Hot Gas Cleanup Operations*
John M. Rockey, Edwin Galloway, and Teresa A. Thomson
Morgantown Energy Technology Center
Jay Rutten and Alain P. Lui
EG&G Technical Services of West Virginia

P4 *Coal Ash Behavior in Reducing Environments*
Thomas A. Erickson
Energy and Environmental Research Center
University of North Dakota

P5 *Hot Coal Gas Desulfurization With Manganese-Based Sorbents*
Rachid Ben Slimane
University of Minnesota

P6 *A Calcium Oxide Sorbent Process for Bulk Separation of Carbon Dioxide*
Douglas P. Harrison
Louisiana State University

P7 *COMPCOAL™ -- A Stable, High-Btu Fuel from Western Coals*
Norman Merriam
Western Research Institute

P8 *Development of Biological Coal Gasification (MicGas Process)*
Radosvet J. Manolov
ARCTECH, Inc.

P9 *Simultaneous Removal of H_2S and NH_3 in Coal Gasification Processes*
K. Jothimurugesan and Adeyinka A. Adeyiga
Hampton University
Santosh K. Gangwal
Research Triangle Institute

P10 *Granular Filtration in a Fluidized Bed*
J. S. Mei, P.C. Yue, and J. S. Halow
Morgantown Energy Technology Center

P11 *Dust Cake Behavior in Filters with High Surface Area to Volume Ratios*
Douglas Straub, Ta-Kuan Chiang, and Richard Dennis
Morgantown Energy Technology Center

P12 *Computer Simulation of IGCC/PFBC Components*
Thomas O'Brien, Edward J. Boyle, and Lawrence J. Shadle
Morgantown Energy Technology Center
Madhava Syamlal and Suresh Venkatesan
EG&G Technical Services of West Virginia

P13 *Scaling of Pressurized Fluidized Beds*
Leon R. Glicksman
Massachusetts Institute of Technology

P14 *Evaluation of Options for CO_2 Capture/Utilization/Disposal*
Richard D. Doctor
Argonne National Laboratory

P15 *Absorption of Hydrogen Sulfide by Zinc Ferrite in the Temperature Range 315 to 538 °C (600 to 1000 °F)*
Thomas Grindley
Morgantown Energy Technology Center
C. Elaine Everitt
EG&G Technical Services of West Virginia

P16 *High Temperature Hydrogen Sulfide Removal with Stannic Oxide*
Robert J. Copeland
TDA Research, Inc.

P17 *Fossil Fuel Conversion - Measurement and Modeling*
Peter R. Solomon
Advanced Fuel Research, Inc.

P18 *CeraMem Filters for Removal of Particles from Hot Gas Streams*
Najib Khali
CeraMem Corporation

P19 *Development of Disposable Sorbents for Chloride Removal from High-Temperature Coal-Derived Gases*
Gopala Krishnan
SRI International

P20 *PyGas Design Support*
Lawrence J. Shadle
Morgantown Energy Technology Center

P21 *Chloride and Mercury Monitors for Air Toxics Measurements*
Glenn A. Norton
Ames Laboratory

P22 *Cooperative Research and Development Agreements at METC*
J. Christopher Ludlow
Morgantown Energy Technology Center

P23 *Optimal Design and Synthesis of Advanced Power Systems Under Uncertainty*
U.M. Diwekar and E.S. Rubin
Carnegie Mellon University

P24 *Development of a Radio Frequency Surface Contour Mapping System*
Warren E. Straszheim
Ames Laboratory

6:00 p.m. ADJOURN

THURSDAY, JUNE 23, 1994

7:30 a.m. Coffee and Refreshments

SESSION 8A -- FILTER TECHNICAL ISSUES

Chairperson: Theodore J. McMahon

8:15 a.m. *Opening Remarks*
Daniel C. Cicero
Morgantown Energy Technology Center

8:25 a.m. 8a.1 *Tidd PFBC Hot Gas Filter Operating Experience: July 1993 - April 1994*
John D. Hoffman
American Electric Power Service Corporation

8:50 a.m. 8a.2 *Karhula Hot Gas Cleanup Test Results*
Thomas E. Lippert
Westinghouse Electric Corporation

9:15 a.m. 8a.3 *Durability of Ceramic Filters*
Mary Anne Alvin
Westinghouse Electric Corporation

9:40 a.m. BREAK

10:00 a.m. 8a.4 *Properties of Ceramic Candle Filters*
Stuart Starrett
Southern Research Institute

10:25 a.m. 8a.5 *Results of Patch Tests*
Duane H. Pontius
Southern Research Institute

10:50 a.m. 8a.6 *PFBC Dust Cake Studies*
Richard A. Newby
Westinghouse Electric Corporation

11:15 a.m. BREAK

SESSION 8B -- HAZARDOUS AIR POLLUTANTS

Chairperson: Peter E. Botros

8:15 a.m. *Opening Remarks*
Heather M. McDaniel
Morgantown Energy Technology Center

8:25 a.m. 8b.1 *Comprehensive Assessment of Toxic Emissions From Coal-Fired Power Plants*
Thomas D. Brown
Pittsburgh Energy Technology Center

8:50 a.m. 8b.2 *Trace Element Emissions*
Steven A. Benson
Energy & Environmental Research Center
University of North Dakota

9:15 a.m. 8b.3 *HAP Sampling at Tidd PFBC*
Patrick A. Dal Porto
American Electric Power

9:40 a.m. BREAK

10:00 a.m. 8b.4 *Trace Species Emissions for IGFC*
A. Ed Pigeaud
Energy Research Corporation

10:25 a.m. 8b.5 *HAPs Sampling for Advanced Power Systems*
Robert M. Mann
Radian Corporation

10:50 a.m. 8b.6 *Instrumentation for Trace Emission Measurements*
William P. Chisholm
Morgantown Energy Technology Center

11:15 a.m. BREAK

SESSION 9A -- SORBENTS AND SOLID WASTES

Chairperson: Lee D. Gasper-Galvin

11:35 a.m.	9a.1	*Moving-Bed Sorbents* Raul E. Ayala GE Corporate Research and Development
11:55 a.m.	9a.2	*Fluid-Bed Sorbents* Raghubir P. Gupta Research Triangle Institute
12:15 p.m.	9a.3	*Fluidized Bed Desulfurizer Using Phillips Z-Sorb Sorbent* Gil J. Greenwood Phillips Petroleum Corp.
12:30 p.m.		LUNCH -- METC ENERGIZER
1:30 p.m.	9a.4	*Desulfurization Sorbent Development at the Morgantown Energy Technology Center* Ranjani V. Siriwardane Morgantown Energy Technology Center
1:55 p.m.	9a.5	*Stabilization of Spent Calcium-Based Sorbent* Satyan Katta The M.W. Kellogg Company
2:20 p.m.	9a.6	*Market Assessment and Technical Feasibility Study of PFBC Ash Use* Alan E. Bland Western Research Institute
2:45 p.m.	9a.7	*Co-Firing Waste Materials in an Advanced Pressurized Fluidized-Bed Combustor* Michael R. DeLallo Gilbert/Commonwealth, Inc.
3:10 p.m.		*Closing Remarks* William T. Langan Morgantown Energy Technology Center

SESSION 9B -- MEMBRANES

Chairperson: Susan K. Joines

11:35 a.m.	9b.1	*High Temperature Size Selective Membranes* S. James Zhou AlliedSignal, Inc.
12:00 p.m.	9b.2	*A Catalytic Membrane Reactor for Facilitating Water-Gas Shift Reaction at High Temperature* Dwayne Friesen Bend Research, Inc.
12:25 p.m.		LUNCH -- METC ENERGIZER
1:30 p.m.	9b.3	*New Developments in Hydrogen Permselective Membranes* George R. Gavalas California Institute of Technology
1:55 p.m.	9b.4	*Preparation and Characterization of Composite Membrane for High Temperature Gas Separation* Shamsuddin Ilias North Carolina A&T State University
2:20 p.m.	9b.5	*Development of Hollow Fiber Catalytic Membrane Reactors for High Temperature Gas Cleanup* Yi Hua Ma Worcester Polytechnic Institute
2:45 p.m.	9b.6	*Thermal/Chemical Degradation of Inorganic Membrane Materials* Gopala Krishnan SRI International
3:10 p.m.		*Closing Remarks* Harvey M. Ness Morgantown Energy Technology Center

Appendix B

Meeting Participants

Edwin W. Albers, President
CMP-Cativco International
1922 Benhill Avenue
Baltimore, MD 21226
410-354-1600, (FAX) 410-354-1604

Mary Anne Alvin, Senior Engineer
Westinghouse STC
1310 Beulah Road
Pittsburgh, PA 15235-5098
412-256-2066, (FAX) 412-256-2121

Mel Ambrose, Chemical Engineer
TVA
P.O. Box 1010
Muscle Shoals, AL 35660-1010
205-386-2461, (FAX) 205-386-3856

Bernard Anderson
Head, Coal-Fired Turbine Proj.
Herman Research Laboratory
677 Springvale Road
Mulgrave
Victoria, 3170
Australia
613-565-9822, (FAX) 613-565-9777

Gerald L. Anderson, Project Director
Benmol Corporation
1121 King Street
Alexandria, VA 22314
703-683-4288, (FAX) 703-683-4635

Jans Andries
Delft University of Technology
Mekelweg 2, P.O. Box 5037
Delft, 2622 CD
Netherlands
311-578-5410, (FAX) 311-578-2460

David H. Archer, Adjunct Professor
Carnegie Mellon University
114 Kentzel Road
Pittsburgh, PA 15237-2816
412-268-6808, (FAX) 412-268-3348

Raul E. Ayala, Chemical Engineer
GE Corporate R&D
P.O. Box 8
Bldg. K-1, ES 103
Schenectady, NY 12301
518-387-5850, (FAX) 518-387-7258

Devendra Barot
Sr. Process Engineer
Black & Veatch
10950 Grandview
Overland Park, KS 66210
913-661-6040, (FAX) 913-338-6425

Chris Benham
Director of Marketing
Brunswick Composites
1745 Jefferson Davis Hwy #410
Arlington, VA 22202
703-413-8050, (FAX) 703-412-6070

Steven A. Benson
Senior Research Manager
Energy & Environ. Research Center
P.O. Box 9018
Grand Forks, ND 58202-9018
701-777-5177, (FAX) 701-777-5181

Steve Bevan, Project Manager
GE Environmental Services
200 North 7th Street
Lebanon, PA 17046
717-274-7077, (FAX) 717-274-7060

Kenneth L. Bingaman
Sr. Engineer, IGCC Technology
GE Environmental Services
200 North 7th Street
Lebanon, PA 17046
717-274-7112, (FAX) 717-274-7060

Alan E. Bland
Program Manager, Solid Waste
Western Research Institute
365 North 9th Street
P.O. Box 3395
Laramie, WY 82071-3395
307-721-2443, (FAX) 307-721-2345

Alan E. Bogner, Principal Engineer
Stanton Energy Ind Consultants
R.D. #1, Liberty Court
New Stanton, PA 15672-9621
412-446-3300, (FAX) 412-446-1266

George S. Booras
Manager, Tech. Assessment
Electric Power Research Inst.
P.O. Box 10412
Palo Alto, CA 94303-0813
415-855-2471, (FAX) 415-855-2950

Daniel Boss, Research Scientist
BIRL/Northwestern University
1801 Maple Avenue
Evanston, IL 60201
708-491-3373, (FAX) 708-467-1022

Patrick Brauckmann
Director of Investor Relations
Minnesota Manganese Res. Company
P.O. Box 29205
Minneapolis, MN 55429
218-763-3759, (FAX) 218-763-3881

Jesse Brown, Professor
Virginia Polytechnic
301 Holden Hall
Blacksburg, VA 24061
703-231-6777, (FAX) 703-231-3028

Richard A. Brown, Project Manager
Electric Power Research Institute
3412 Hillview Avenue
Palo Alto, CA 94303
415-855-2216, (FAX) 415-855-2954

Thomas D. Brown, Project Manager
Pittsburgh Energy Technology Center
U.S. Department of Energy
P.O. Box 10940
Pittsburgh, PA 15236-0940
412-892-4691, (FAX) 412-892-4604

George Burris, Jr., Division Manager
American Electric Power
1 Riverside Plaza
Columbus, OH 43215
614-223-2470, (FAX) 614-223-2466

P. Vann Bush
Manager, Particulate Science
Southern Research Institute
2000 Ninth Avenue, South
Birmingham, AL 35205
205-581-2269, (FAX) 205-581-2448

Bill Buttermore
Director, Fossil Energy Program
Ames Laboratory
Iowa State University
280 Metals Development Building
Ames, IA 50011
515-294-3758, (FAX) 515-294-3091

W. M. Campbell
Manager, Clean Coal Technology
The M.W. Kellogg Company
P.O. Box 4557
Houston, TX 77210-4557
713-753-2184, (FAX) 713-753-6609

Steven C. Carlton, President and CEO
Minnesota Manganese Res. Company
P.O. Box 29205
Minneapolis, MN 55429
218-763-3759, (FAX) 218-763-3881

James Carr, Materials Engineer
U.S. Department of Energy
19901 Germantown Road
FE-72
Washington, DC 20585
301-903-6519, (FAX) 301-903-6350

R. D. Carson, Senior Project Director
CRS Sirrine Engineers, Inc.
1041 East Butler Road
P.O. Box 5456
Greenville, SC 29606-5456
803-676-5037, (FAX) 803-676-5033

Ravi Chandran, Lab Manager
MTCI
6001 Chemical Road
Baltimore, MD 21226
410-354-0420, (FAX) 410-354-0471

Prosenjit Chaudhuri, Graduate Student
Carnegie Mellon University
EPP Department, 129 Baker Hall
Pittsburgh, PA 15213
412-268-2940, (FAX) 412-268-3757

Daniel H. Chen, Associate Professor
Lamar University
P.O. Box 10053
Beaumont, TX 77710
409-880-8786, (FAX) 409-880-8121

Peter Cherish
Senior Engineering Consultant
The M.W. Kellogg Company
601 Jefferson Avenue
P.O. Box 4557
Houston, TX 77210-4557
713-753-4141, (FAX) 713-753-5353

Richard S. Chu, Assistant Manager
Ohio Coal Development Office
6566 Emco Place
Worthington, OH 43085
614-466-6538, (FAX) 614-466-6532

Nancy Cole, Manager
Oak Ridge National Laboratory
P.O. Box 2008
Oak Ridge, TN 37931-6153
615-574-4824, (FAX) 615-574-5118

Rich Conn, Research Associate
Foster Wheeler Development Corporation
12 Peach Tree Hill Road
Livingston, NJ 07039
201-535-2551, (FAX) 201-535-2242

John R. Cooper, Engineer R&D
Allegheny Power Service Corporation
800 Cabin Hill Drive
Greensburg, PA 15601
412-830-5688, (FAX) 412-830-5008

P. G. Cooper
Senior Process Engineer
Energy International Corporation
135 William Pitt Way
Pittsburgh, PA 15238
412-826-5359, (FAX) 412-826-5378

Robert J. Copeland, Principal Engineer
TDA Research, Inc.
12345 West 52nd Avenue
Wheat Ridge, CO 80033
303-940-2323, (FAX) 303-422-7763

Michele Corser, Research Engineer
Southern Company Services
P.O. Box 2625
Birmingham, AL 35202-2625
205-877-7633, (FAX) 205-868-5367

Patrick A. Dal Porto, Manager
Air Environment Section
American Electric Power
1 Riverside Plaza
Columbus, OH 43215
614-223-1267, (FAX) 614-223-1252

Ashok S. Damle, Research Chemical Engineer
SRI International
333 Ravenswood Avenue
Menlo Park, CA 94025
415-859-5458, (FAX) 415-859-2813

Ran K. Datta, Professor
Virginia Polytechnic
301 Holden Hall
Blacksburg, VA 24061
703-231-3577, (FAX) 703-231-3028

Hollice O. Davis
Vice President and Director R&D
Kaiser Aerotech
880 Doolittle Drive
San Leandro, CA 94577
510-562-2456, (FAX) 510-568-6420

Robert Dawson, Associate Scientist
Ames Laboratory
Iowa State University
273 Metals Development
Ames, IA 50011
515-294-1028, (FAX) 515-294-3091

Michael R. Delallo
DOE/Program Manager
Gilbert/Commonwealth, Inc.
P.O. Box 1498
Reading, PA 19603
610-775-2600, (FAX) 610-775-1584

Urmila M. Diwekar
Research Associate Professor
Carnegie Mellon University
129 Baker Hall, EPP Dept.
Pittsburgh, PA 15213
412-268-3003, (FAX) 412-268-3757

Vijay B. Dixit, Staff Engineer
Riley Stoker Corporation
45 McKeon Road
Worcester, MA 01610
508-792-4807, (FAX) 508-792-4817

Richard D. Doctor, Chemical Engineer
Argonne National Lab
9700 South Cass Avenue
Argonne, IL 60532
708-252-5913, (FAX) 708-252-9728

E. L. Doering, Engineering Consultant
Shell Oil Company
2234 Two Shell Plaza
P.O. Box 2099
Houston, TX 77252-2099
713-241-2693, (FAX) 713-241-1602

David A. Dulcey, Project Engineer
Sierra Pacific Power Company
P.O. Box 10100
Reno, NV 89520
702-689-3915, (FAX) 702-689-3047

Michael Durst
Director of R&D
Schumacher GMBH
P.O. Box 1562
Crailsheim D-74555
Germany
497-951-3020, (FAX) 497-951-21920

Dave Eckels, Assistant Scientist
Ames Laboratory
Iowa State University
5 Spedding
Ames, IA 50011
515-294-7943

Khanedra Edwards
Gas R&D Analyst
Northern Indiana Public Service
5265 Hohman Avenue
Hammond, IN 46320
219-647-4554, (FAX) 219-647-4321

Paul Eggerstedt
Vice President, Research
Industrial Filter and Pump
5900 Ogden Avenue
Cicero, IL 60650
708-656-7800, (FAX) 708-656-7806

Thomas A. Erickson, Research Manager
Energy & Environ. Research Center
P.O. Box 9018
Grand Forks, ND 58202-9018
701-777-5153, (FAX) 701-777-5181

William H. Eskridge, Process Engineer
Bechtel Power Corporation
9801 Washingtonian Boulevard
Gaithersburg, MD 20878-5356
301-417-4553, (FAX) 301-869-4078

Martin Fankhanel, Project Manager
The M.W. Kellogg Company
P.O. Box 4557
Houston, TX 77210-4557
713-753-2938, (FAX) 713-753-6323

Jack R. Farmer, Director
Center for Process Research
Research Triangle Institute
P.O. Box 12194
Research Triangle Park, NC 27709
919-541-8007, (FAX) 919-541-8000

Paul A. Farrell, Research Assistant
Massachusetts Institute of Tech.
77 Massachusetts Avenue
Room 7-008
Cambridge, MA 02139
617-253-7080, (FAX) 617-253-6152

Gabor Feher, Manager
IGCC Technology
Tampella Power
2600 Reach Road
Williamsport, PA 17701
717-327-3108, (FAX) 717-327-4450

Alan S. Feitelberg, Chemical Engineer
GE Corporate R&D
P.O. Box 8, K-1
ES Building, Room 103
Schenectady, NY 12301
518-387-5737, (FAX) 518-387-7258

Edward M. Fischer, Tech. Service Specialist
3M Ceramic Materials
3M Center
Building 207-1S-23
St. Paul, MN 55144
612-736-1005, (FAX) 612-733-0221

Harold Foster, Assistant Director
Coal Research Center
Southern Illinois University
Carbondale, IL 62901-4623
618-536-5521, (FAX) 618-453-7346

H. Christopher Frey
Assistant Professor
North Carolina State University
Department of Civil Engineering
Raleigh, NC 27695-7908
919-515-1155, (FAX) 919-515-7908

Dwayne Friesen
Director of Research
Bend Research, Inc.
64550 Research Road
Bend, OR 97701
503-382-4100, (FAX) 503-382-2713

Anthony H. Furman, Mechanical Engineer
GE Corporate R&D
P.O. Box 8
ES Building, Room 203
Schenectady, NY 12301
518-387-5849, (FAX) 518-387-7258

Eli Gal, Manager
Technology Development
GE Environmental Services
200 North 7th Street
Lebanon, PA 17046
717-274-7049, (FAX) 717-274-7074

Santosh K. Gangwal, Manager
Fuel Technology
Research Triangle Institute
P.O. Box 12194
Research Triangle Park, NC 27709
919-541-8033, (FAX) 919-541-8000

Charles Garrett, Program Manager
U.S. Department of Energy
FE-72
Washington, DC 20585
301-903-2819, (FAX) 301-903-8350

George R. Gavalas, Professor
California Institute of Tech.
Caltech 210-41
Pasadena, CA 91125
818-395-4152, (FAX) 818-568-8743

Philip M. Goldberg
Pittsburgh Energy Technology Center
Coal Utilization Division
P.O. Box 10940, MS 922H
Pittsburgh, PA 15236
412-892-5806, (FAX) 412-892-4604

Gary Grant
Senior Designer Drafter
Stanton Energy Ind Consultants
R.D. #1, Liberty Court
New Stanton, PA 15672-9621
412-446-3300, (FAX) 412-446-1266

Gil J. Greenwood
Senior Licensing Specialist
Phillips Petroleum Company
252 Patent Library Building
Bartlesville, OK 74004
918-661-3693, (FAX) 918-662-2007

Raghubir P. Gupta
Research Chemical Engineer
Research Triangle Institute
P.O. Box 12194
Research Triangle Park, NC 27709
919-541-8023, (FAX) 919-541-8000

John C. Haas
Principal Development Engineer
Combustion Power Company
2101 Webster St., #1700
Oakland, CA 94612
510-286-8820, (FAX) 510-286-8822

Wu Haifu, Senior Engineer
Central Coal Mining Research
H2PINGLI
Beijing
China

Douglas P. Harrison
Alumni Professor
Louisiana State University
Dept. of Chemical Engineering
Baton Rouge, LA 70803
504-388-3066, (FAX) 504-388-1476

Malcolm T. Hepworth, Professor
University of Minnesota
500 Pillsbury Dr., S.E.
Minneapolis, MN 55455-0220
612-625-6354, (FAX) 612-626-7750

Steve Higgins
Pennsylvania Electric Company
1001 Broad Street
Johnstown, PA 15907
814-533-8593, (FAX) 814-533-8591

John D. Hoffman, Senior Engineer
American Electric Power
1 Riverside Plaza
Columbus, OH 43215
614-223-1588, (FAX) 614-223-2466

Ed Holley, Senior Project Manager
Air Products & Chemicals, Inc.
7540 Windsor Drive
Allentown, PA 18195
610-481-8568, (FAX) 610-481-3228

John Holmgren, Interim Director
NRCCE
P.O. Box 6064
Morgantown, WV 26506-6064
304-293-2867, (FAX) 304-293-3749

R. Thomas Hower, Manager
Research and Development
Brunswick Composites
150 Johnston Road
Marion, VA 24354
703-783-9612, (FAX) 703-783-9671

Clayton L. Huber, Manager
Technical Marketing
Hope Gas, Inc.
Bank One Center West
P.O. Box 2868
Clarksburg, WV 26301
304-623-8668, (FAX) 304-623-8919

Ray V. Huff, Director
Technical Affairs
Minnesota Manganese Res. Company
P.O. Box 29205
Minneapolis, MN 55429
218-763-3759, (FAX) 218-763-3881

Ziaul Huque, Assistant Professor
Prairie View A&M University
Mechanical Engineering Department
P.O. Box 397
Prairie View, TX 77446-0397
409-857-4023, (FAX) 409-857-2222

John Hurley, Research Supervisor
Energy and Environ. Research
P.O. Box 9018
Grand Forks, ND 58202
701-777-5000, (FAX) 701-777-5181

Shahzeb I. Husain, Research Assistant
Morgan State University
2D Starwood Court
Baltimore, MD 21239
410-319-3139, (FAX) 410-319-3843

Shamsuddin Ilias, Assistant Professor
North Carolina A&T State University
Chemical Engineering Department
Greensboro, NC 27411
910-334-7564, (FAX) 910-334-7904

Daniel C. Itse, Chief Engineer
Powerserve
20 New England Business Center
Andover, MA 01810
508-689-0003, (FAX) 508-689-3232

Suresh Jain, Program Manager
U.S. Department of Energy
FE 231
Washington, DC 20585
301-903-0508, (FAX) 301-903-2406

Pang Jin, Senior Engineer
Central Coal Mining Research
H2PINGL1
Beijing
China

Eric Johnson, Professor
West Virginia University
P.O. Box 6106
Morgantown, WV 26506
304-293-3111

Mike Johnson, Consultant
Vortec Corporation
112 Windgate Drive
Wexford, PA 15090
412-935-2063

Tony Johnson
W. L. Gore
71 McMurray Road
Pittsburgh, PA 15241
412-854-4747, (FAX) 412-854-5096

Jill Jonkouski, Program Manager
U.S. Department of Energy
9800 S. Cass Avenue
Argonne, IL 60439-4899
708-252-2657, (FAX) 708-252-8649

K. Jothimurugesan, Assistant Professor
Hampton University
Department of Engineering
Hampton, VA 23668
804-727-5817, (FAX) 804-727-5189

Roddie R. Judkins, Manager
Fossil Energy Program
Martin Marietta Energy Systems
P.O. Box 2008
Oak Ridge, TN 37831-6084
615-574-4572, (FAX) 615-574-5812

Trina Karolchik
Assoc. Director of NRCCE
West Virginia University
P.O. Box 6064
Evansdale Campus
Morgantown, WV 26506
304-293-2867

Hendrik Kathrein, Applications
Development Manager
Research and Development
Miles, Inc.
Mobay Road
Pittsburgh, PA 15205-9741
412-777-5349, (FAX) 412-777-7626

Satyan Katta, Principal Engineer
The M.W. Kellogg Company
601 Jefferson Avenue
Houston, TX 77210
713-492-5847, (FAX) 713-492-5832

Najib Khalil, Project Engineer
Ceramem Corporation
20 Clematis Avenue
Waltham, MA 02154
617-899-0467, (FAX) 617-899-1227

Jacob H.A. Kiel, Branch Manager
Energy Research Foundation
P.O. Box 1
Petten 1755 ZG
Netherlands
312-246-4590, (FAX) 312-246-3489

David L. Kinsinger, Licensing Specialist
Phillips Petroleum Co.
Research & Development
261 Patent Library Bldg.
Bartlesville, OK 74004
918-661-1244, (FAX) 918-662-2007

Michael Klosky, Vice President
Engineering
Enertech Environmental
430 10th Street, N.W.
Suite N-104
Atlanta, GA 30318
404-892-9440, (FAX) 404-892-8816

Bernard J. Koch, Director
Project Development
Consol, Inc.
4000 Brownsville Road
Library, PA 15129
412-854-6612, (FAX) 412-854-6613

Jukka T. Konttinen, Research Engineer
Enviropower, Inc.
33701 Tampere
Finland

Jacob Korenberg, Vice President
Energy Systems
Donlee Technologies, Inc.
693 North Hills Road
York, PA 17402
717-755-1081, (FAX) 717-755-0020

Gopala Krishnan, Program Manager
SRI International
333 Ravenswood Avenue
Menlo Park, CA 94025
415-859-2627, (FAX) 415-859-2111

Reijo Kuivalainen, Assistant Director
Research and Development
Ahlstrom Pyropower, Inc.
8925 Rehco Road
San Diego, CA 92121-3269
619-458-3066, (FAX) 619-458-3190

Lee Lamarre
Project Engineering Manager
Foster Wheeler USA
1965 Duncan Drive
Scotch Plains, NJ 07076
908-232-9493, (FAX) 908-730-4570

Leonard N. Lapatnick
Environmental Research Engineer
Public Service Electric and Gas Co.
80 Park Plaza, T17C
Newark, NJ 07101
201-430-8129, (FAX) 201-642-0859

Seong W. Lee, Assistant Professor
Morgan State University
Cold Spring Lane & Hillen Rd.
Baltimore, MD 21239
410-319-3137, (FAX) 410-319-3843

Sheldon H. D. Lee, Chemical Engineer
Argonne National Laboratory
9700 South Cass Avenue
Argonne, IL 60439
708-252-4395, (FAX) 708-252-4176

Wayne Leonard
Senior V.P. and Chief Fin. Officer
PSI Energy
1000 E. Main Street
Plainfield, IN 46168
317-838-2096, (FAX) 317-838-2208

Jack Lewnard, Senior Process Engineer
Air Products & Chemicals, Inc.
7540 Windsor Avenue
Allentown, PA 18195
610-481-6932, (FAX) 610-481-3228

Joann Linder
Business Development Manager
GE Corporate R&D
P.O. Box 8, Building KW-C258A
Schenectady, NY 12301-0008
518-387-6141, (FAX) 518-387-5449

Thomas E. Lippert, Manager
Advanced Fossil Energy
Westinghouse STC
1310 Beulah Road
Pittsburgh, PA 15235-5098
412-256-2440, (FAX) 412-256-2121

Alain P. Lui, Chemical Engineer
EG&G/TSWV
P.O. Box 880, MS M02
Morgantown, WV 26507-0880
304-291-4008, (FAX) 304-291-4403

Scott Lynn, Professor
University of California
201 Gilman Hall
Dept. of Chemical Engineering
Berkeley, CA 94720
510-642-1634, (FAX) 510-642-4778

Yi Hua Ma, Professor
Chemical Engineering
Worcester Polytechnic Inst.
100 Institute Road
Worcester, MA 01609
508-831-5398, (FAX) 508-831-5867

Greg Mack, Control Systems Engineer
Lawrence Livermore National Lab
P.O. Box 808, L-369
Livermore, CA 94550
510-423-1905, (FAX) 510-423-7040

Robert M. Mann, Senior Staff
Radian Corporation
P.O. Box 201088
Austin, TX 78720-1088
512-454-4797, (FAX) 512-454-8807

Radosvet J. Manolov, Research Scientist
Arctech, Inc.
14100 Park Meadow Drive
Suite 210
Chantilly, VA 22021
703-222-0280, (FAX) 703-222-0299

Momtaz Mansour, President
MTCI
6001 Chemical Road
Baltimore, MD 21226
410-730-0445, (FAX) 410-997-6980

John J. Marano, Senior Engineer
Burns and Roe Services Corp.
P.O. Box 18288
Pittsburgh, PA 15236
412-892-4845, (FAX) 412-892-4736

Mario Marrocco, Section Manager
American Electric Power
1 Riverside Plaza
Columbus, OH 43215
614-223-2460, (FAX) 614-223-2466

Jim McClung, APFBC Manager
Foster Wheeler Development Corp.
12 Peach Tree Hill Road
Livingston, NJ 07039
201-535-2315, (FAX) 201-535-2242

Chuck McMenamy, Program Manager
Donlee Technologies, Inc.
693 North Hills Road
York, PA 17402
717-755-1081, (FAX) 717-755-0020

Ray Mello, Principal Engineer
Stanton Energy Ind Consultants
R.D. #1, Liberty Court
New Stanton, PA 15672-9621
412-446-3300, (FAX) 412-446-1266

Aubrey Miller, Assistant Professor
West Virginia University
P.O. Box 6101
Morgantown, WV 26506
304-293-2111

C. Lowell Miller
Assoc. Deputy Asst. Secretary
U.S. Department of Energy
FE 22/GTN
Washington, DC 20585
301-903-9451, (FAX) 301-903-9438

Wahab Mojtahedi
Senior Research Scientist
Enviropower, Inc.
Tekniikantie 12
Espoo 02150
Finland

Darrell Moore
Senior Research Engineer
Southern Company Services
P.O. Box 2625
Birmingham, AL 35202-2625
205-868-5584, (FAX) 205-868-5367

David J. Najewicz, Manager
Energy & Environment
GE Corporate R&D
P.O. Box 8, K-1
Engineering Systems Building
Schenectady, NY 12301
518-387-6427, (FAX) 518-387-7258

Robert Ness, Research Manager
Energy & Environ. Research Center
P.O. Box 9018
Grand Forks, ND 58202
701-777-5000, (FAX) 701-777-5181

Richard A. Newby, Fellow Engineer
Westinghouse STC
1310 Beulah Road
Pittsburgh, PA 15235-5098
412-256-2210, (FAX) 412-256-2121

Grady Nichols
Southern Research Institute
2000 9th Avenue, South
Birmingham, AL 35205
205-581-2361, (FAX) 205-581-2448

Ion Nicolaescu, Sr. Process Engineer
GE Environmental Services
200 North 7th Street
Lebanon, PA 17046
717-274-7139, (FAX) 717-274-7074

P. E. Hojlund Nielsen, Senior Scientist
Haldor Topsoe A/S
55 Nymollevej
Lyngby DK-2800
Denmark
454-527-2457, (FAX) (45) 45272999

Glenn A. Norton, Associate Chemist
Ames Laboratory
Iowa State University
281 Metals Development
Ames, IA 50011
515-294-1035, (FAX) 515-294-3091

William S. O'Brien, Associate Professor
Southern Illinois University
Mech. Engineering and Energy Process
Carbondale, IL 62901-6603
618-453-7017, (FAX) 618-453-7455

Ralph P. Overend
Principal Research Scientist
National Renewable Energy Lab
1617 Cole Boulevard
Golden, CO 80401-3393
303-231-1450, (FAX) 303-275-2905

David Painter, Environmental Engineer
U.S. EPA
Industrial Studies Branch, MD-13
Research Triangle Park, NC 27711
919-541-5515, (FAX) 919-541-5600

William Partanen, Vice President
Engineering Power Generating, Inc.
P.O. Box 2251
W. Scarborough, ME 04074
207-883-3052, (FAX) 207-885-0964

Don W. Pfennig
Custom Products Specialist
United Catalysts, Inc.
P.O. Box 32370
Louisville, KY 40232
502-634-7248, (FAX) 502-637-3732

A. (Ed) Pigeaud, Senior Scientist
Energy Research Corporation
3 Great Pasture Road
Danbury, CT 06813
203-792-1460, (FAX) 203-798-2945

Timothy Pinkston
Senior Research Engineer
Southern Company Services
P.O. Box 2625
Birmingham, AL 35202-2625
205-877-7042, (FAX) 205-868-5367

Donald E. Pless, Project Manager
Tampa Electric Company
P.O. Box 111
Tampa, FL 33601
813-228-1332, (FAX) 813-228-4802

Duane Pontius, Director
Particulate Science
Southern Research Institute
2000 9th Avenue, South
Birmingham, AL 35205
205-581-2268, (FAX) 205-581-2448

Jeffrey W. Portzer
Research Chemical Engineer
Research Triangle Institute
P.O. Box 12194
Research Triangle Park, NC 27709
919-541-8025, (FAX) 919-541-8000

Neil Prosser, Consultant
Praxair, Inc.
P.O. Box 44
Tonawanda, NY 14151-0044
716-879-2662, (FAX) 716-879-7091

Michael T. Quandt, Project Manager
Foster Wheeler Energy Corporation
Perryville Corporate Park
Clinton, NJ 08809-4000
908-236-1156, (FAX) 908-236-1119

Predrag T. Radulovic
Research Associate Professor
Brigham Young University
75B CTB
Provo, UT 84602
801-378-3097, (FAX) 801-378-3831

Adrian S. Radziwon, Senior Engineer
BRSC
P.O. Box 18288
Pittsburgh, PA 15236
412-892-4672, (FAX) 412-892-4736

Massood Ramezan, Principal Engineer
Burns and Roe Services Corp.
P.O. Box 18288
Pittsburgh, PA 15236
412-892-6451, (FAX) 412-892-4736

C. John Rawley, Jr.
R&D Program Consultant
Texas Utilities
400 N. Olive Street, L.B. 81
Dallas, TX 75201
214-812-4459, (FAX) 214-812-8967

Maria Redipath, Engineer
EG&G/TSWV
P.O. Box 880, MS M02
Morgantown, WV 26507-0880
304-291-4140

Young-Woo Rhee, Associate Researcher
Korea Institute of Energy Research
P.O. Box 5
Daeduk Science Town
Taejeon 305-343
Korea

Donna Riley, Graduate Student
Carnegie Mellon University
Engineering and Public Policy Dept.
129 Baker Hall
Pittsburgh, PA 15213
412-268-5618, (FAX) 412-268-3757

Robert E. Riley, Pilot Plant Manager
United Catalysts, Inc.
P.O. Box 32370
Louisville, KY 40232
502-634-7316, (FAX) 502-637-3732

Archie Robertson, Research Associate
Foster Wheeler Develop. Corporation
12 Peach Tree Hill Road
Livingston, NJ 07039
201-535-2328, (FAX) 201-535-2242

Paul D. Rodebaugh, Supervising Engineer
Florida Power and Light Company
700 Universe Boulevard
P.O. Box 14000
Juno Beach, FL 33408
407-691-2620, (FAX) 407-691-2695

Edward S. Rubin, Professor
Carnegie Mellon University
128-A Baker Hall
Pittsburgh, PA 15213
412-268-5897, (FAX) 412-268-3757

Brian Runge, Research Engineer
Energy & Environ. Research Ctr.
P.O. Box 9018
Grand Forks, ND 58202
701-777-5000, (FAX) 701-777-5181

Richard Sadowski, Director
Advanced Technology
CRS Sirrine Engineers, Inc.
1041 E. Butler Road
Greenville, SC 29606-5456
803-676-5082, (FAX) 803-676-5087

J. A. Salter, Staff Research Engineer
Shell Development Company
P.O. Box 1380
Houston, TX 77251-1380
713-544-7718, (FAX) 713-544-7705

Angel Sanjurju
SRI International
333 Menlo Park
Menlo Park, CA 94025
415-859-5215, (FAX) 415-859-2111

Carl E. Schenone, Principal Engineer
Stanton Energy Ind Consultants
R.D. #1, Liberty Court
New Stanton, PA 15672-9621
412-446-3300, (FAX) 412-446-1266

Hermann J. Schloemer, Professor
University of Saarland
P.O. Box 151150
Saarbrucken 66041
Germany

Michael R. Schmid, Director
Tamco Power Partners
Tampella Power
2600 Reach Road
Williamsport, PA 17701-0308
717-327-4457, (FAX) 717-327-4450

John H. Schwartz, President
Stanton Energy Ind Consultants
R.D. #1, Liberty Court
New Stanton, PA 15672-9621
412-446-3300, (FAX) 412-446-1266

Kumar M. Sellakumar
Assistant R&D Manager
Ahlstrom Pyropower, Inc.
8970 Crestmar Drive
San Diego, CA 92121-3222
619-450-2604, (FAX) 619-552-8296

Vijay Sethi
Sr. Research Staff Engineer
Western Research Institute
P.O. Box 3395
Laramie, WY 82070
307-721-2376, (FAX) 307-721-2233

Philip T. Seymour, President
Schumacher Filters America
P.O. Box 8040
Asheville, NC 28814
704-252-9000, (FAX) 704-253-7773

Walter Shelton, Chemical Engineer
EG&G/TSWV
P.O. Box 880, MS M02
Morgantown, WV 26507-0880
304-291-4209, (FAX) 304-291-4403

Suhas D. Shelukar
Research Triangle Institute
P.O. Box 12194
Research Triangle Park, NC 27709
919-541-8042, (FAX) 919-541-8000

Phil J. Shires, Project Manager
The M.W. Kellogg Company
P.O. Box 4557
Houston, TX 77210-4557
713-753-3861, (FAX) 713-753-6609

Karl Siebert, Environmental Engineer
Air Products & Chemicals, Inc.
7540 Windsor Drive
Allentown, PA 18195
610-481-3996, (FAX) 610-481-3228

Reijo Silvonen, Project Manager
Tampella Power
2600 Reach Road
Williamsport, PA 17701
717-327-4458, (FAX) 717-327-4450

Dale R. Simbeck
Vice President, Technology
SFA Pacific, Inc.
444 Castro Street, Suite 920
Mountain View, CA 94041
415-969-8876, (FAX) 415-969-1317

Rachid Ben Slimane
Graduate Research Assistant
University of Minnesota
500 Pillsbury Drive, S.E.
Minneapolis, MN 55455-0220
612-625-3071, (FAX) 612-626-7750

Robert G. Smith, Senior Research Specialist
3M Ceramic Materials
3M Center, Building 203-1-01
St. Paul, MN 55144-1000
612-733-2564, (FAX) 612-737-5484

Nelson Sobel, Senior VP Technical Director
Pall Corporation
Route 281
Cortland, NY 13045
607-753-6041, (FAX) 607-753-8525

Peter R. Solomon, President
Advanced Fuel Research, Inc.
87 Church Street
East Hartford, CT 06108
203-528-9806, (FAX) 203-528-0648

H. Stuart Starrett, Director
Mechanics Research Department
Southern Research Institute
2000 Ninth Avenue, South
Birmingham, AL 35205
205-581-2452, (FAX) 205-581-2414

Robert J. Steffen, Project Manager
Stanton Energy Ind Consultants
R.D. #1, Liberty Court
New Stanton, PA 15672-9621
412-446-3300

Warren Straszheim, Associate Scientist
Ames Laboratory
270 Metals Development Building
Ames, IA 50011
515-294-8187, (FAX) 515-294-3091

Daniel W. Sutherland, Sr. Design Engineer
Pall Trinity Micro
3643 Route 281, P.O. Box 2030
Cortland, NY 13045-0930
607-753-6041, (FAX) 607-756-1862

Madhava Syamlal, Engineer
EG&G/TSWV
P.O. Box 880, MS M02
Morgantown, WV 26507-0880
304-291-4685, (FAX) 304-291-4403

Bruce Thomson, Manager
Business Development
Textron Specialty Materials
2 Industrial Avenue
Lowell, MA 01851
508-454-5619, (FAX) 508-934-7593

Robert Travers, Program Manager
U.S. Department of Energy
FE-232
Washington, DC 20585
301-903-6166, (FAX) 301-903-2406

Tero Vaaranen, Performance Engineer
Tampella Power
2600 Reach Road
Williamsport, PA 17701
717-327-4417, (FAX) 717-327-4450

Don C. Vymazal, Manager
Government and Contract Admin.
Air Products & Chemicals, Inc.
7540 Windsor Drive
Allentown, PA 18195
610-481-3687, (FAX) 610-481-2762

Richard A. Wagner, Principal Engineer
Babcock & Wilcox
P.O. Box 11165
Lynchburg, VA 24506-1165
804-522-5697, (FAX) 804-522-6196

Daman S. Walia, President and CEO
Arctech, Inc.
14100 Park Meadow Drive
Chantilly, VA 22021
703-222-0280, (FAX) 703-222-0299

Robert Weber, Associate Scientist
Ames Laboratory
280 Metals Development Building
Ames, IA 50010-3020
515-294-8187

Robert F. Weimer, Chief Engineer
Air Products & Chemicals, Inc.
7201 Hamilton Boulevard
New Process Technology
Allentown, PA 18195
610-481-7626, (FAX) 610-481-5084

Harvey Weisenfeld, Vice President
Energetics, Inc.
7164 Gateway Drive
Columbia, MD 21046
410-290-0370, (FAX) 410-290-0377

Paul S. Weitzel, Technical Consultant
Babcock & Wilcox
20 S. Van Buren Avenue
Barberton, OH 44203
216-860-1655, (FAX) 216-860-2348

James Welshimer, Manager
Technical Service
National Lime and Stone
P.O. Box 120
Findlay, OH 45839
419-422-4341, (FAX) 419-422-3952

Thomas P. Wendahl
Project Development Manager
Air Products & Chemicals, Inc.
7201 Hamilton Boulevard
Allentown, PA 18104
610-481-7025, (FAX) 610-481-5444

James K. Wessel, Director
Cooperative Research and Development
DOW Corning
1800 M. Street, N.W.
Suite 325, South
Washington, DC 20036
202-785-0585, (FAX) 202-785-0421

Gerald Wheeler, Program Manager
U.S. Department of Energy
FE-231
Washington, DC 20585
301-903-3511, (FAX) 301-903-2406

Charles White, Engineer
EG&G/TSWV
P.O. Box 880, MS M02
Morgantown, WV 26507-0880
304-291-4344, (FAX) 304-291-4403

Keith Wilson, Program Manager
Combustion Power Company
2101 Webster Street, No. 1700
Oakland, CA 94612
510-286-8820, (FAX) 510-286-8824

William G. Wilson, President
Gas Desulfurization Corporation
820 Harden Drive
Pittsburgh, PA 15229
412-364-1822, (FAX) 412-367-1254

Jack Winnick, Professor
Georgia Tech
Dept. of Chemical Engineering
Atlanta, GA 30332
404-894-2839, (FAX) 404-894-2866

David C. Wolfe, R&D Manager
United Catalysts, Inc.
P.O. Box 32370
Louisville, KY 40232
502-634-7349, (FAX) 502-637-3732

Ronald H. Wolk, Director
Advanced Fossil Power
Electric Power Research Inst.
3412 Hillview Avenue, P.O. Box 10412
Palo Alto, CA 94304
415-855-2509, (FAX) 415-855-2954

Steve R. Wright, Vice President
Research and Development
Micro Composite Materials Corp.
4608-D Industry Lane
Durham, NC 27713-5414
919-361-3535

Thomas Wright
TVA
1101 Market St.
Chattanooga, TN 37402-2801
615-751-6120, (FAX) 615-751-8384

Beth Wrobel
Principal Corp. R&D
Northern Indiana Public Serv.
5265 Hohman Avenue
Hammond, IN 46320
219-647-4320, (FAX) 219-647-4321

Meng Xiande, Project Coordinator
Central Coal Mining Research
Hepingli
Beijing 100013
861-421-2752, (FAX) 861-421-9234

Xie Ke Yu, Deputy Director
Coal/Chemistry
Central Coal Mining Research
Hepingli
Beijing 100013
861-421-4931, (FAX) 861-421-9234

Jianren Zhou, Assistant Professor
Prairie View A&M University
P.O. Box 397
Prairie View, TX 77446-0397
409-857-4023, (FAX) 409-857-2222

S. James Zhou
Research Chemical Engineer
Allied Signal Research & Tech.
50 E. Algonquin Road
Des Plaines, IL 60017
708-391-3459, (FAX) 708-391-3750

Yu Zhufeng, Engineer
Central Coal Mining Research
Hepingli
Beijing 100013
China
861-421-4931, (FAX) 861-421-9234

Appendix C

METC Participants

Morgantown Energy Technology Center
P.O. Box 880
Morgantown, WV 26507-0880

Femi Adesanya, ORAU
304-285-5461, MS L08

Rodney Anderson, Physical Scientist
304-285-4709, MS B05

Rita A. Bajura, Director
Product & Strategic Management Division
304-285-4109, MS D01

Thomas F. Bechtel, Director
Morgantown Energy Technology Center
304-285-4511, MS C02

Justin L. Beeson, Chemical Engineer
304-285-4671, MS C04

Larry A. Bissett, General Engineer
304-285-4266, MS N04

Don Bonk, Project Manager
304-285-4889, MS C04

Peter Botros, Mechanical Engineer
304-285-4162, MS C04

Edward J. Boyle, Chemist
304-285-4000, MS N05

John W. Byam, Jr., Manager
Global Business Development
304-285-4064, MS B06

Cliff Carpenter, Project Manager
304-285-4041, MS D06

Ta-Kuan Chiang, Mechanical Engineer
304-285-4406, MS N05

Bill Chisholm, Research Chemist
304-285-4730, MS A04

Daniel Cicero, Project Manager
304-285-4826, MS C04

Floyd Crouse
Deputy Director, PPMD
304-285-4535, MS D01

Kamalendu Das, Physical Scientist
304-285-4065, MS C05

Randy Dellefield
Product Manager, PFBC
304-285-4725, MS D01

Richard A. Dennis, Project Manager
304-285-4515, MS C04

Thomas P. Dorchak, Project Manager
304-285-4305, MS C04

Dan Driscoll, Physical Scientist
304-285-4717, MS B05

Mark Freier, Project Engineer
304-285-4759, MS E01

Edwin Galloway, Mechanical Engineer
304-285-5429, MS C03

Lee Gasper-Galvin, General Engineer
304-285-4832, MS N04

Madhav R. Ghate, Director
Tech. Base Project Management
304-285-4135, MS C05

Leonard E. Graham, Director
Fuel Resources Management
304-285-4714, MS E06

Thomas Grindley, Chemical Engineer
304-285-4286, MS N04

Hugh D. Guthrie, General Engineer
304-285-4632, MS B06

Jack Halow, Director
Combustion/Cleanup Division
304-285-4114, MS N06

Kurt Hammerbeck, ORAU
304-285-4163, MS N04

Norman Holcombe, Project Manager
304-285-4829, MS C05

Benjamin Hsieh, Project Engineer
304-285-4254, MS E01

William Johansen, Graduate Student
University of Wyoming
304-285-4076

Richard Johnson, Project Manager
304-285-4564, MS C04

Susan K. Joines, Project Manager
304-285-4063, MS C05

Thomas W. Keech, Jr.
Deputy Director, Power Systems Tech.
304-285-4285, MS D04

Margaret Kotzalas, Chemical Engineer
304-285-5426, MS C05

K. C. Kwon
ORAU Summer Faculty Research
304-285-4076, MS L08

Wu K. Lan, Project Manager
304-285-4044, MS C05

William Langan, Director
Power Systems Technology
304-285-4519, MS D04

Patrick H. Le, Mechanical Engineer
304-285-4324, MS E01

George T. Lee, Chemical Engineer
304-285-4824, MS E01

H. P. Loh, Chemical Engineer
304-285-4546, MS E01

James Longanbach, Project Manager
304-285-4659, MS C04

Chris Ludlow, General Engineer
304-285-4608, MS B05

Ken Markel, Deputy Associate Director
Office of Product Technology
Development
304-285-4364, MS A03

Manville J. Mayfield
Product Manager, Fuel Cells
304-285-4847, MS D01

Heather M. McDaniel, Mechanical
Engineer
304-285-5430, MS C04

Ted McMahon, Project Manager
304-285-4865, MS C04

Mike McMillian, Project Engineer
304-285-4669, MS N04

Daniel Mei, HBCU Faculty
304-285-4076, MS L08

Joseph S. Mei, Mechanical Engineer
304-285-4409, MS N05

Darren Mollot, Project Manager
304-285-5447, MS C04

Harvey Ness, Chief
Power Systems Technology
304-285-4172, MS C04

Daniel Nguyen, Chemical Engineer
304-285-4668, MS E01

Stephen Noel, Electrical Engineer
304-285-4441, MS A04

John Notestein, Chief Engineer
304-285-4232, MS A05

Tom O'Brien, Research Chemist
304-285-4571, MS N05

Leland E. Paulson, Project Manager
304-285-4074, MS E03

Lawrence K. Rath, Chief
Process & Project Engineering
304-285-4094, MS E01

Michael E. Reed, Chemical Engineer
304-285-4860, MS E01

John M. Rockey, Chemical Engineer
304-285-4711, MS N04

Robert R. Romanosky, Director
Technology Support Projects Division
304-285-4721, MS A04

Louis A. Salvador
Associate Director, OPTM
304-285-4147, MS B06

Dale Schmidt
Product Manager, IGCC
304-285-4359, MS D01

Larry Shadle, Research Chemist
304-285-4647, MS N04

Ranjani Siriwardane, Research Chemist
304-285-4513, MS N04

Ron Staubly, Project Manager
304-285-4991, MS C04

Doug Straub, Mechanical Engineer
304-285-5444, MS N05

Larry Strickland
Division Director, Gas Cleanup
304-285-4494, MS N04

Fred Sudhoff, Chemical Engineer
304-285-4560, MS E01

Teresa Thomson, Student Intern
304-285-4163, MS N04

George Trapp, Professor
West Virginia University
304-285-4076, MS L07

Venkat K. Venkataraman, Project Manager
304-285-4105, MS C05

Mike Vermeersch, Associate Professor
University of North Dakota
304-285-4199, MS L07

Holmes A. Webb
Product Manager, Heat Engines
304-285-4724, MS D01

Gary L. White
ORAU, Visiting Faculty
304-285-4799, MS L08

Paul R. Wieber
Associate Director, OTBD
304-285-4544, MS B05

John S. Wilson, Deputy Director
Morgantown Energy Technology Center
304-285-4529, MS A05

Paul Yue, Physicist
304-285-4062, MS A04

Charles M. Zeh, Product Manager
Environmental & Waste Management
304-285-4265, MS D01

DATE
FILMED
11/9/94
END